

Conversion of waste high-density polyethylene into liquid fuels

A Thesis Submitted in Partial Fulfillment for the Award of the Degree

Of

DOCTOR OF PHILOSOPHY

In

CHEMICAL ENGINEERING

By

Sachin Kumar

Under the guidance of

Prof. (Dr.) R. K. Singh



**Department of Chemical Engineering
National Institute of Technology
Rourkela-769008**

Dedicated to

My Parents



**Department of Chemical Engineering
National Institute of Technology
Rourkela 769008 (ORISSA)**

CERTIFICATE

This is to certify that the thesis entitled “**Conversion of waste high-density polyethylene into liquid fuels**” being submitted by **Sachin Kumar** for the award of Ph.D. degree is a record of bonafide research carried out by him at the Chemical Engineering Department, National Institute of Technology, Rourkela, under my guidance and supervision. The work documented in this thesis has not been submitted to any other University or Institute for the award of any other degree or diploma.

Supervisor

Dr. R. K. Singh

Professor and Head

Department of Chemical Engineering,
National Institute of Technology,
Rourkela - 769008

ACKNOWLEDGEMENT

This study would have never been accomplished without the support, assistance, and motivation provided by those around me.

In particular, I would like to thank my supervisor Prof. (Dr.) R. K. Singh for his help and guidance during the period of research. I feel indebted to my supervisor for giving abundant freedom to me for pursuing new ideas. The experience of working with him, I strongly believe, will have far-reaching influence in my future life.

I express my deep sense of gratitude to the members of my Doctoral Scrutiny Committee Prof. S. Murugan of Mechanical Engineering Department, Prof. K. C. Biswal of Civil Engineering Department and Prof. A. Sahoo of Chemical Engineering Department for thoughtful advice during discussion sessions. I express my gratitude and indebtedness to Prof. K. C. Biswal, Prof. P. Rath, Prof. S. K. Agarwal, Dr. Madhusree Kundu, Dr. Susmita Mishra, Dr. Basudeb Munshi, Dr. Santanu Paria, Dr. S. Khanam, Dr. Arvind Kumar, Dr. Pradip Chowdhury and Dr. Sujit Sen of Chemical Engineering Department, for their valuable suggestions and instructions at various stages of the work. My special thanks to Mr. R. Prakash and other supporting staffs of I. C. Engine lab, Mechanical Engineering Department for their help. I also thank to staff members of Chemical Engineering Department for their constant help throughout the work.

This work also would not have been possible without the help of all the research group members. I would like to express my gratitude to my research group senior Dr. Achyut Kumar Panda for his assistance in my research work. I am also thankful to my other research colleagues Dr. Nihar Ranjan Biswal, Dr. Gaurav Kumar, Dr. Rajiv Ghosh Chaudhuri, Mr. Sandip Mandal, Mr. Shailesh Dewangan, Ms. Debalaxmi Pradhan, Ms. Namrata Kumari and Mr. Tanmaya Rout for their support and good wishes.

Finally, I express my humble regards to my parents for their immense support, sacrifice and their unfettered encouragement at all stages.

(Sachin Kumar)

CONTENTS

Chapter No.	Title	Page No
	ABSTRACT	x-xi
1.	INTRODUCTION	1-7
1.1	General background	1
1.2	Origin of the problem	3
1.2.1	Scarcity of fossil fuels	3
1.2.2	Solid waste management	4
1.2.3	Environment impacts of waste plastics recycling	5
1.3	Objective of present work	6
1.4	Organization of thesis	7
2.	LITERATURE REVIEW	8-57
2.1	Plastics	8
2.1.1	High-Density Polyethylene	9
2.1.1.1	Structure and physical chemistry of HDPE	10
2.1.1.2	Uses of HDPE	12
2.1.1.3	HDPE-World demand	12
2.2	Plastics waste recycling	15
2.2.1	Primary recycling	15
2.2.2	Secondary recycling	16
2.2.3	Tertiary recycling	16
2.2.3.1	Chemolysis/Solvolysis	17
2.2.3.1.1	Hydrolysis	17
2.2.3.1.2	Alcoholysis	17
2.2.3.1.3	Glycolysis and methanolysis	17
2.2.3.2	Gasification or Partial oxidation	18
2.2.3.3	Cracking	18

2.2.3.3.1 Thermal cracking	18
2.2.3.3.2 Catalytic cracking	19
2.2.3.3.3 Hydro cracking	20
2.2.4 Quaternary recycling	21
2.3 Pyrolysis of HDPE	22
2.3.1 Thermal pyrolysis	22
2.3.2 Catalytic pyrolysis	24
2.4 Mechanism and kinetics of pyrolysis	38
2.4.1 Investigative methods for polymer degradation	40
2.4.2 Reaction Mechanism of polymer degradation	45
2.4.3 Reaction kinetics of polymer degradation	52
2.5 Performance and emission analysis of waste plastics oil in CI engine	57
3. EXPERIMENTAL	58-66
3.1 Materials	58
3.1.1 Virgin and waste high-density polyethylene	58
3.1.2 Catalysts	59
3.1.2.1 Kaolin	59
3.1.2.2 Silica alumina	60
3.1.2.3 Mordenite	61
3.2 Methods	62
3.2.1 Catalyst modification	62
3.2.2 Catalyst characterization techniques	62
3.2.2.1 X-Ray fluorescence	62
3.2.2.2 X-Ray diffraction	62
3.2.2.3 Fourier transformed infrared spectroscopy	62
3.2.2.4 Thermogravimetric/differential thermal analysis	63
3.2.2.5 Sorptometric studies	63
3.2.2.6 Scanning electron microscope	63
3.2.2.7 Temperature programmed desorption (Ammonia)	63

3.2.3 Pyrolysis setup	63
3.2.4 Pyrolysis experimental procedure	65
3.2.5 Analysis of pyrolysis oil	65
3.2.5.1 Physical properties of pyrolysis oil	65
3.2.5.2 Chemical properties of pyrolysis oil	65
3.2.5.2.1 FT-IR analysis	65
3.2.5.2.2 GC-MS analysis	66
4. THERMAL DEGRADATION OF VIRGIN HIGH-DENSITY POLYETHYLENE TO LIQUID FUEL	67-79
4.1 Introduction	67
4.2 Experimental programme	68
4.3 Result and discussion	68
4.3.1 Proximate and ultimate analysis of virgin HDPE	68
4.3.2 TGA and DTG analysis of virgin HDPE sample	69
4.4 Effect of temperature on product distribution	71
4.5 Effect of temperature on reaction time	72
4.6 Characterization of liquid product	73
4.6.1 FT-IR of the oil sample obtained at 450 °C	73
4.6.2 GC-MS the oil sample	74
4.6.3 Physical properties of oil sample	76
4.7 Conclusion	79
5. THERMO-CATALYTIC DEGRADATION OF WASTE HIGH-DENSITY POLYETHYLENE TO LIQUID FUEL	80-132
5.1 Introduction	80
5.2 Materials and methods	81
5.3 Result and discussion	82
5.3.1 Characterization of raw material	82
5.3.1.1 Proximate and ultimate analysis of waste HDPE	82
5.3.1.2 TGA and DTG of waste HDPE	82
5.3.2 Effect of temperature on product distribution	84

5.3.3 Effect of temperature on reaction time	85
5.3.4 Effect of holding time on liquid yield	86
5.3.5 Characterization of liquid product	87
5.3.5.1 FT-IR analysis of oil sample	87
5.3.5.2 GC-MS analysis of oil sample	89
5.3.5.3 Physical properties of oil sample	91
5.3.6 Effect of different catalysts on product yield and reaction time at a temperature 450 °C	92
5.3.6.1 Effect of kaolin catalyst on yield and reaction time at a temperature 450 °C	92
5.3.6.2 Effect of mordenite catalyst on yield and reaction time at a temperature 450 °C	94
5.3.6.3 Effect of silica-alumina catalyst on yield and reaction time at a temperature 450 °C	95
5.3.6.4 Effect of different catalysts on liquid product yield and reaction time at a temperature 450 °C and 1:4 catalyst to plastic ratio	97
5.4 Preparation and characterization of acid and alkali treated kaolin clay	98
5.4.1 Introduction	98
5.4.2 Experimental programme	100
5.4.3 Results and Discussion	100
5.4.3.1 XRF analysis	100
5.4.3.2 XRD analysis	101
5.4.3.3 FTIR analysis	102
5.4.3.4 TG-DTA analysis	105
5.4.3.5 BET surface area and pore volume	107
5.4.3.6 SEM analysis	108
5.4.3.7 TPD (ammonia) analysis	110
5.5 Catalytic conversion of waste high-density polyethylene to liquid fuel using acid and alkali treated kaolin clay	112

5.5.1 Introduction	112
5.5.2 Experimental programme	113
5.5.3 Results and Discussion	113
5.5.3.1 Effect of catalysts on reaction time and yield of liquid fuel	113
5.5.3.2 Compositional analysis of waste HDPE pyrolysis oil using acids and alkaline treated kaolin	115
5.5.3.1.2.1 FTIR analysis of waste HDPE pyrolysis oil using acids and alkaline treated kaolin	115
5.5.3.1.2.1.1 FTIR analysis of waste HDPE pyrolysis oil using hydrochloric acid treated kaolin	115
5.5.3.1.2.1.2 FTIR analysis of waste HDPE pyrolysis oil using acetic acid treated kaolin	117
5.5.3.1.2.1.3 FTIR analysis of waste HDPE pyrolysis oil using nitric acid treated kaolin	118
5.5.3.1.2.1.4 FTIR analysis of waste HDPE pyrolysis oil using phosphoric acid treated kaolin	119
5.5.3.1.2.1.5 FTIR analysis of waste HDPE pyrolysis oil using sodium hydroxide treated kaolin	120
5.5.3.1.2.2 GC-MS analysis of waste HDPE pyrolysis oil using acids and alkali treated kaolin	121
5.5.3.1.2.2.1 GC-MS analysis of waste HDPE pyrolysis oil using hydrochloric acid treated kaolin	121
5.5.3.1.2.2.2 GC-MS analysis of waste HDPE pyrolysis oil using acetic acid treated kaolin	123
5.5.3.1.2.2.3 GC-MS analysis of waste HDPE pyrolysis oil using nitric acid treated kaolin	124
5.5.3.1.2.2.4 GC-MS analysis of waste HDPE pyrolysis oil using phosphoric acid treated kaolin	126

5.5.3.1.2.2.5 GC-MS analysis of waste HDPE pyrolysis oil using sodium hydroxide treated kaolin	127
5.5.3.1.3.3 Physical properties of liquid fuel obtained by catalytic pyrolysis of waste HDPE using nitric acid treated kaolin clay	129
5.6 Conclusion	131
6. OPTIMIZATION OF PROCESS PARAMETERS BY RESPONSE SURFACE METHODOLOGY (RSM) FOR CATALYTIC PYROLYSIS OF WASTE HDPE TO LIQUID FUEL	133-149
6.1 Introduction	133
6.2 Experimental programme	134
6.2.1 Optimization study	134
6.3 Result and discussion	136
6.3.1 Characterization of raw material and catalyst modification	136
6.3.2 Optimization study of liquid fuel yield	138
6.3.3 Residual plots of optimization	140
6.3.4 Surface plots and contour plots of optimization	141
6.3.5 Characterization of liquid fuel	144
6.3.5.1 FT-IR of the oil sample	144
6.3.5.2 GC-MS of the oil sample	145
6.3.5.3 Physical properties of oil sample	147
6.4 Conclusion	149
7. PERFORMANCE AND EMISSION ANALYSIS OF BLENDS OF WASTE PLASTIC OIL OBTAINED BY CATALYTIC PYROLYSIS OF WASTE HDPE WITH DIESEL IN A CI ENGINE	150-169
7.1 Introduction	150
7.2 Experimental programme	151
7.2.1 Experimental set up of CI engine and test detail	151
7.3 Result and discussion	153
7.3.1 Characterization of raw material and catalyst preparation	153

7.3.2 Characterization of waste plastic oil	155
7.3.2.1 FT-IR of the oil sample	155
7.3.2.2. GC-MS of the oil sample	156
7.3.2.3 Physical properties of oil sample	158
7.3.3 Performance analysis of blends of waste plastic oil with diesel	159
7.3.3.1 Brake thermal efficiency	159
7.3.3.2 Exhaust gas temperature	160
7.3.3.3 Brake specific energy consumption	161
7.3.3.4 Mechanical Efficiency	162
7.3.4 Emission analysis of blends of waste plastic oil with diesel	163
7.3.4.1 Oxides of nitrogen	163
7.3.4.2 Unburned hydrocarbon	165
7.3.4.3 Carbon monoxide	166
7.3.4.4 Carbon dioxide	167
7.4 Conclusion	168
8. KINETIC STUDY OF WASTE HIGH-DENSITY POLYETHYLENE PYROLYSIS USING THERMOGRAVIMETRIC ANALYSIS	170-177
8.1 Introduction	170
8.2 Experimental programme	171
8.2.1 Non-isothermal kinetic study using TGA	171
8.3 Result and discussion	172
8.3.1 Characterization of waste HDPE sample	172
8.3.2 TGA and DTG analysis	173
8.3.3 Kinetic study using TGA under non-isothermal conditions	175
8.4 Conclusion	177
9. CONCLUSIONS AND FUTURE RECOMMENDATIONS	178-180
9.1 Summary and conclusions	177
9.2 Recommendations for future	180
REFERENCES	181-195

LIST OF FIGURES	196-198
LIST OF TABLES	199-202
LIST OF PUBLICATIONS	203-205
BIOGRAPHY	206

ABSTRACT

The present work involves the experimental studies for the production of liquid fuel by thermal and catalytic pyrolysis of waste high-density polyethylene in a laboratory batch reactor.

Thermal pyrolysis of virgin HDPE was performed at a temperature range from 400 °C to 550 °C and heating rate of 20 °C/min. The liquid yield is highest 50 wt. % at temperature 450 °C. Reaction time decreases with increase in temperature. Maximum oil yield in thermal pyrolysis of waste HDPE was 50.8 wt. % at optimum condition of temperature, which is improved to 58.8 wt. %, in kaolin catalyzed degradation under optimum condition of temperature and feed ratio. The rate of reaction, oil yield and quality of oil obtained in the catalytic pyrolysis are significantly improved as compared to thermal pyrolysis.

The catalytic activity of kaolin is further enhanced by treating it with four different acids and one base (acetic acid, phosphoric acid, nitric acid, hydrochloric acid and sodium hydroxide). Acid treatment increased the surface area, acidity and also alters the pore volume distribution of kaolin, which support the cracking reaction. The maximum yield of oil in the acid treated kaolin catalyzed pyrolysis of waste HDPE was 79% under optimum conditions. The composition of the oil was analyzed by FTIR and GC-MS. The oil obtained from the catalytic pyrolysis of waste HDPE mostly contains aliphatic hydrocarbons. The fuel properties of the oil obtained from the catalytic pyrolysis of waste HDPE is similar with that of petro-fuels. So they can directly be used as an engine fuel after fractionation or as a feedstock to petroleum refineries.

Response surface methodology (RSM) was used to optimize the catalytic pyrolysis process of waste high-density polyethylene to liquid fuel over modified catalyst. The reaction temperature, acidity of the modified catalysts and mass ratio between modified catalysts to waste high-density polyethylene (HDPE) were chosen as independent variables. Optimum operating conditions of reaction temperature (450 °C), acidity of catalyst (0.341) and catalyst to waste HDPE ratio (1:4) were produced with respect to

maximum liquid product yield of 78.7 %. The polynomial model obtained fits well to predict the response with a high determination coefficient of R^2 (0.995).

The diesel blended plastic oil obtained by the catalytic pyrolysis of waste HDPE has been tested for its performance and emission in a CI diesel engine. Engine was able to run with maximum 40% waste plastic oil- diesel blends. The engine vibrates at and above this blend. Brake thermal efficiency of the waste HDPE oil blend is lower to diesel at all loads. This may be due to lower calorific value of Waste HDPE Oil-diesel blend than diesel. The BSEC increases with the increasing WPO blend ratio at all engine loads and decreases with increase in engine load. Mechanical efficiency increases with increasing brake power for all fuel blends. The NO_x emission increases with increase in percentage of waste plastic oil in blends and decreases with increase in engine load. The unburnt hydrocarbon emission is decreasing with increase in the engine load and increases with increase in percentage of waste plastic oil in blends. The CO emission increases with the increasing WPO blend ratio and engine load. The carbon dioxide emission for the blends is lower than diesel for almost all loads and all blends.

The thermo gravimetric analysis of waste HDPE at 10 °C/min, 20 °C/min and 40 °C/min in the N_2 atmosphere was studied and kinetic parameter (activation energy) was determined by using thermogravimetric curves. When the heating rate increases, the activation energy and degradation temperature of the waste HDPE also increases. The activation energy values of waste HDPE have been calculated as 207.43, 268.22 and 473.05 kJ/mol at 10, 20 and 40 °C/min heating rates respectively. Reasonable fits of data to straight lines in kinetic study plot indicate that the assumption of first-order kinetics for thermal degradation of waste HDPE is acceptable.

Key words: Waste plastics, High-density polyethylene, Pyrolysis, Liquid fuel, Batch reactor, Kaolin clay, Acid treatment, FT-IR, GC-MS, Aliphatic hydrocarbons, Petro-fuels, Optimization, Response surface methodology (RSM), ANOVA, Diesel blended waste plastic oil, CI diesel engine, Brake thermal efficiency, Brake specific fuel consumption, Exhaust gas temperature, Mechanical efficiency, NO_x , CO, HC, CO_2 emissions, Thermogravimetric kinetics, Activation energy.

CHAPTER 1

Introduction

INTRODUCTION

1.1 General background

Plastics have become an indispensable ingredient of human life. They are non-biodegradable polymers of mostly containing carbon, hydrogen and few other elements as chlorine, nitrogen etc. Plastics are used in our daily lives in a number of applications, from greenhouses, mulches, coating and wiring, to packaging, films, covers, bags and containers. After food waste and paper waste, plastic waste is the major constitute of municipal and industrial waste in cities. Rapid growth of the world population led to increased demand of commodity plastics. This increase has turned into a major challenge for local authorities, responsible for solid waste management and sanitation. Due to lack of integrated solid waste management, most of the plastic waste is neither collected properly nor disposed of in appropriate manner to avoid its negative impacts on environment and public health and waste plastics are causing trashing and chucking of sewerage system. High density polyethylene (HDPE) is the third largest commodity plastic material in the world, after polyvinyl chloride and polypropylene in terms of volume. HDPE has accounted for a major share of ethylene consumption in the recent years. The demand for HDPE has increased drastically in the recent years. The increased demand and production of waste HDPE has led to the accumulation of large amount of its waste in the final waste stream due to its low useful life.

Plastic waste recycling can provide an opportunity to collect and dispose of plastic waste in the most environmental friendly way and it can be converted into a resource. Plastics recycling include four categories, these are: primary (mechanical reprocessing into a product with equivalent properties), secondary (mechanical reprocessing into products requiring lower properties), tertiary (recovery of chemical constituents) and quaternary (recovery of energy). Primary recycling is often referred to as closed-loop recycling, and secondary recycling as downgrading. Tertiary recycling is either described as chemical or feedstock recycling and applies when the polymer is de-polymerized to its chemical constituents. Quaternary recycling is energy recovery, energy from waste or valorization. Biodegradable plastics can also be composted, and this is a further example of tertiary

recycling, and is also described as organic or biological recycling. Chemical or feedstock recycling has the advantage of recovering the petrochemical constituents of the polymer, which can then be used to re-manufacture plastic or to make other synthetic chemicals. However, while technically feasible it has generally been found to be uneconomic without significant subsidies because of the low price of petrochemical feedstock compared with the plant and process costs incurred to produce monomers from waste plastic. This is not surprising as it is effectively reversing the energy intensive polymerization previously carried out during plastic manufacture.

Waste plastics are one of the most promising resources for fuel production because of its high heat of combustion and due to the increasing availability in local communities. The conversion methods of waste plastics into fuel depend on the types of plastics to be targeted and the properties of other wastes that might be used in the process. Additionally the effective conversion requires appropriate technologies to be selected according to local economic, environmental, social and technical characteristics. Polyethylene has been targeted as a potential feedstock for fuel (gasoline) producing technologies. PE thermally cracks into gases, liquids, waxes, aromatics and char. The relative amounts of gas and liquid fraction are very much dependent on the type of polymer used. Thus, higher decomposition was observed in PP, followed by LDPE and finally HDPE.

Thermolysis is the treatment in the presence of heat under controlled temperatures without catalysts. Thermolysis processes can be divided into advanced thermo-chemical or pyrolysis (thermal cracking in an inert atmosphere), gasification (in the sub-stoichiometric presence of air usually leading to CO and CO₂ production) and hydrogenation (hydrocracking). Thermal degradation processes allow obtaining a number of constituting molecules, combustible gases and/or energy, with the reduction of landfilling as an added advantage. The pyrolysis process is an advanced conversion technology that has the ability to produce a clean, high calorific value gas from a wide variety of waste and biomass streams. The hydrocarbon content of the waste is converted into a gas, which is suitable for utilization in either gas engines, with associated electricity generation, or in boiler applications without the need for flue gas treatment.

This process is capable of treating many different solid hydrocarbon based wastes whilst producing a clean fuel gas with a high calorific value. Solid char is also produced from the process, which contains both carbon and the mineral content of the original feed material.

Pyrolysis provides a number of other advantages, such as (i) operational advantages, (ii) environmental advantages and (iii) financial benefits. Operational advantages could be described by the utilization of residual output of char used as a fuel or as a feedstock for other petrochemical processes. An additional operational benefit is that pyrolysis requires no flue gas clean up as flue gas produced is mostly treated prior to utilization. Environmentally, pyrolysis provides an alternative solution to landfilling and reduces greenhouse gas (GHGs) and CO₂ emissions. Financially, pyrolysis produces a high calorific value fuel that could be easily marketed and used in gas engines to produce electricity and heat. Several obstacles and disadvantages do exist for pyrolysis, mainly the handling of char produced and treatment of the final fuel produced if specific products are desired.

1.2 Origin of the problem

1.2.1 Scarcity of fossil fuels

The rate of petroleum consumption is increasing very rapidly in the world. Although this rate of increase may appear to be mild, it must be noted that petroleum resources are finite (coal reserve 984453 Million Tonnes, oil reserve 1147 Billion Barrels and natural gas reserve 176 Trillion m³ at the end of 2003) and can be depleted over years. Estimation of the years for which petroleum can be supplied and consumed at the current consumption rate has often been made by professionals and policymakers, but the numbers have been inconsistent and fluctuating from year to year. This uncertainty comes from the difficulty of estimating the future recoverable amount of petroleum from all the proved and unproved reserves. Currently, transportation, fuel, and petrochemical industries depend very heavily upon petroleum-based feedstocks. Therefore, alternative fuels replacing petrochemical feedstocks and supplementing petroleum derived materials must be developed and utilized more. Necessary infrastructure also needs to be developed

and changed to make a transition from the current petroleum economy. Mankind has to rely on the alternate/renewable energy sources like biomass, hydropower, geothermal energy, wind energy, solar energy, nuclear energy, etc. Waste plastic to liquid fuel is also an alternate energy source path, which can contribute to depletion of fossil fuel as in this process liquid fuel with similar fuel properties as that of petro fuels are obtained.

1.2.2 Solid waste management

Waste management was once a down-to-earth technical problem, to be solved under thrifty, yet environmentally 'acceptable' and hygienic conditions and preferably performed by unskilled labor. Most waste was disposed of in landfills, except in densely populated regions, where volume reduction by incineration was a practical necessity. The recovery of heat, distributed in district heating systems or converted into electrical power was a means of cooling flue gases prior to their cleaning, but barely contributes to cost reduction, especially since a deep cleaning of flue gases became mandatory. But, at present time, waste management has turned into a fashionable legislation-driven business, a responsibility of top management, as part of the environmental profile of each corporation, and requiring expert knowledge in Law, Ethics, Politics and Sustainable Development. Operators belong to the world's largest service companies. The European Union waste management policy focuses on waste hierarchy, giving great priority to waste prevention or reduction (elimination of technical or economic impediments and distortions that encourage the over-production of wastes) followed by re-use, recycling, recovery and residual management. Such a strategy includes an integrated approach to waste management with emphasis on material recycling that is preferred over energy recovery. Pre-consumer plastic wastes are generated during the manufacture of virgin plastics from raw materials (oil, natural gas, salt, etc.) and from the conversion of plastics into plastic products. Such waste streams are soiled (floor sweepings, skimmings from wastewater treatment, crusts from polymerization reactors), mixed (laboratory testing), or off-specifications. Both production and conversion waste are easily identified and collected and handled by professional scrap dealers that discover and develop applications and market outlets that allow the use of secondary resins with less stringent

and less defined specifications. The amount of plastic waste generated is still considerably less than that of plastics produced: in numerous applications (building, furniture, appliances) plastics meet long term requirements before their disposal and therefore do not yet occur in the waste stream in big quantities. The majority of plastic wastes are found in municipal solid waste (MSW), as well as in waste streams arising in distribution, agriculture, construction and demolition, furniture and household ware, automotive, electronic and electrical, or medical applications. The alternatives for available waste management are source reduction, reuse, recycling, and recovery of the inherent energy value through waste-to-energy incineration and processed fuel applications. Production of liquid fuel would be a better alternative and is carried out by pyrolysis process, occur in absence of oxygen at high temperatures.

1.2.3 Environmental impacts of waste plastics recycling

The production and disposal of waste plastic products contributes significantly to their environmental impact. Most plastics are non-degradable and take longer time to break down when land filled. With the increased use of plastics in modern life, the landfill space required by plastics waste is a matter of serious concern. Furthermore, plastic production requires significant quantities of primarily fossil fuels for both as a raw material and to deliver energy for the manufacturing process. It is estimated that 4% of the world's annual oil production is used as a feedstock for plastics production and an additional 3-4% during manufacture. The overall environmental impact of waste plastics varies according to the type of plastic used and the production method employed. The production of plastics also involves the use of potentially harmful chemicals under the name of stabilizers or colorants. Many of these stabilizers/additives have not undergone environmental risk assessment and their impact on human health and the environment is currently uncertain and doubtful. Waste disposal contributes towards climate change, for example through the release of methane from landfill sites or the burning of fossil-fuel-based plastics. Human toxicity is a measure of the potential risk to health from a plant. Like incineration, pyrolysis and gasification produce emissions: Air emissions include acid gases, dioxins and furans, nitrogen oxides, sulfur dioxide, particulates, cadmium,

mercury, lead and hydrogen sulfide; solid residues include inert mineral ash, inorganic compounds, and any remaining unreformed carbon.

1.3 Objective of present work

The overall objective of this work is to study the thermal and catalytic pyrolysis of waste high-density polyethylene in a semi batch reactor with an objective to optimize the liquid product yield by changing different parameters such as temperature, catalyst and catalyst to plastic ratio. The specific objectives of this study are:

- To study the thermal and catalytic pyrolysis of waste high-density polyethylene (HDPE) to liquid fuel/chemicals using mordenite, silica alumina and kaolin catalyst.
- To study the effect of acid and alkali treatment on the physicochemical characteristics of kaolin and its catalytic behavior in the waste HDPE pyrolysis.
- To optimize the process variables of catalytic degradation of waste HDPE by Response Surface Methodology (RSM) method.
- To characterize the liquid fuel for its composition and fuel properties for its suitability as fossil fuel substitute.
- To study the engine performance and emission analysis of waste plastic oil obtained by the catalytic pyrolysis of waste HDPE.
- To study the kinetics of waste HDPE pyrolysis using thermogravimetric analysis.

1.4 Organization of Thesis

The thesis has been organized in twelve chapters. The present chapter, chapter-1 is an introductory chapter. Chapter-2 contains literature review for high-density polyethylene pyrolysis (HDPE) along with some statistics of HDPE production and consumption and the different methods of recycling of waste plastics. Chapter-3 presents the materials selection for the experiments and their characterization techniques, methods of pyrolysis experiments, and analysis of liquid product obtained by this process. Chapter-4 presents the thermal pyrolysis of virgin HDPE and characterization of the liquid product. Chapter-5 presents the thermal pyrolysis of waste HDPE, characterization of the liquid product and effect of different catalysts on waste HDPE pyrolysis, preparation and characterization of acid and alkali treatment of kaolin clay, catalytic pyrolysis of waste HDPE with acid and alkali treated kaolin clay and characterization of the liquid product. Chapter-6 presents the optimization of process variables of catalytic degradation of waste HDPE by Response Surface Methodology (RSM). Chapter-7 presents the engine performance and emission analysis of the waste HDPE pyrolysis oil obtained by acid treated kaolin catalyzed pyrolysis of waste HDPE blends with diesel in a CI diesel engine. Chapter-8 presents the non-isothermal kinetic study of waste HDPE pyrolysis by integral method. Chapter-9 presents the summary of the work and some suggestions for further study and finally the references used in this work.

Chapter 2

Literature Review

LITERATURE REVIEW

2.1 Plastics

Plastics are a generic group of synthetic or natural materials, composed of high-molecular chains whose sole or major element is carbon. In common usage the terms plastics, polymers and resins are roughly equivalent. A plastic material is a large group of materials consisting wholly or in part of combinations of carbon with oxygen, hydrogen, nitrogen, and other organic or inorganic elements which, while solid in the finished state, at some stage in its manufacture is made liquid, and thus capable of being formed into various shapes, most usually through the application, either singly or together, of heat and pressure. Plastics are manufactured from monomers, i.e. a repeatable molecular unit and building block, by means of various chemical processes. Every day, people use plastics in various applications. Over the last 50 to 60 years, the uses for plastic have expanded to infiltrate virtually every aspect of life. Because of how versatile the material is, and how affordable it can be, it has taken the place of other products including wood and metals. The properties of the various types of plastics make it beneficial for manufacturers to use. Consumers like it because it is easy to use, lightweight and easy to maintain ([What are plastics](#)).

Plastics can be synthesized via the polymerization (polyaddition or polycondensation) of small molecules and are in general classified into two groups i.e. thermoplastics and thermoset plastics. Thermoplastics are linear chain macromolecules where the atoms and molecules are joined end-to-end into a series of long, sole carbon chains. The bi-functionality necessary to form a linear macromolecule from vinyl monomers can be achieved by opening the double bond and reaction proceeds by a free radical mechanism. Such type of polymerization is known as addition polymerization, polyethylene and polypropylene are the examples. On the other hand, thermoset plastics are formed by step-growth polymerization under suitable conditions allowing bi-functional molecules to condense inter-molecularly with the liberation of small by-products such as H_2O , HCl , etc. at each reaction step. In this class, the monomers undergo some chemical changes

(condensation) on heating and convert themselves into an infusible mass irreversibly (Singh B et al. 2008).

2.1.1 High-Density Polyethylene

High density polyethylene (HDPE) or Polyethylene high density (PEHD) is a polyethylene thermoplastic made from petroleum. It takes 1.75 kilograms of petroleum (in terms of energy and raw materials) to make 1kilogram of HDPE. HDPE is commonly recycled and has the no. “2” as its recycling symbol (HDPE).

Up until the 1950’s the only type of polyethylene produced was low density polyethylene. Low Density polyethylene was being produced at extremely high pressures. This high-pressure polymerization created polyethylene with many branches; the branches are created due to intermolecular and intramolecular chain transfer during polymerization. The utility of low-density polyethylene are limited due to high number of branches leading to poor strength properties and requirement of extreme pressure condition for its production.

Karl Ziegler, a German scientist, made the greatest contribution to produce high-density polyethylene while preparing polyethylene using a catalyst at atmospheric pressure. However, at first, this process did not go very smoothly. At first, Ziegler reacted aluminum triethyl, a metal alkyl, with ethylene gas at atmospheric pressure. The reaction only yielded polyethylene with a molecular weight of 4,000. The reason for this is due to the displacement reaction where the aluminum-carbon bond displaces into a double bond. Ziegler realized the problem was due to the reactivity of aluminum triethyl. After that, Ziegler reacted aluminum triethyl, a metal alkyl, with titanium tetrachloride, an organometallic. He hoped the reaction of the two compounds would create an active site where polymerization would occur. When the two compounds were placed in a reactive vessel the precipitate titanium trichloride forms along with small amounts of unreacted aluminum triethyl. The titanium trichloride has a lower valence state than titanium tetrachloride, thus, making it more reactive than titanium tetrachloride in the presence of the monomer ethylene. When ethylene was introduced to the precipitate along with an inert solvent, polyethylene with a high molecular and very little branching was formed.

This polymerization took place at atmospheric pressure and 100 °Celsius (Singh B et al. 2008).

The difference in high-density polyethylene and low-density polyethylene is the degree of branching. The mechanical properties change drastically when comparing high-density polyethylene to low density polyethylene. In general, the degree of branching in polyethylene determines its mechanical properties. For example, high-density polyethylene is more crystalline than low-density polyethylene because it contains fewer branches.

2.1.1.1 Structure and physical chemistry of HDPE:

High-density polyethylene (HDPE) is a thermoplastic material composed of carbon and hydrogen atoms joined together forming high molecular weight products. Methane gas is converted into ethylene, then, with the application of heat and pressure, into polyethylene. The polymer chain may be 500,000 to 1,000,000 carbon units long. HDPE has a linear structure, with little or no branching. Short and/or long side chain molecules exist with the polymer's long main chain molecules. The longer the main chain, the greater the number of atoms, and consequently, the greater the molecular weight. The molecular weight, the molecular weight distribution and the amount of branching determine many of the mechanical and chemical properties of the end product. High-density polyethylene resin has a greater proportion of crystalline regions than low-density polyethylene. The size and size distribution of crystalline regions are determinants of the tensile strength and environmental stress crack resistance of the end product. Figure 2.1 is a schematic diagram of high density polyethylene structure.

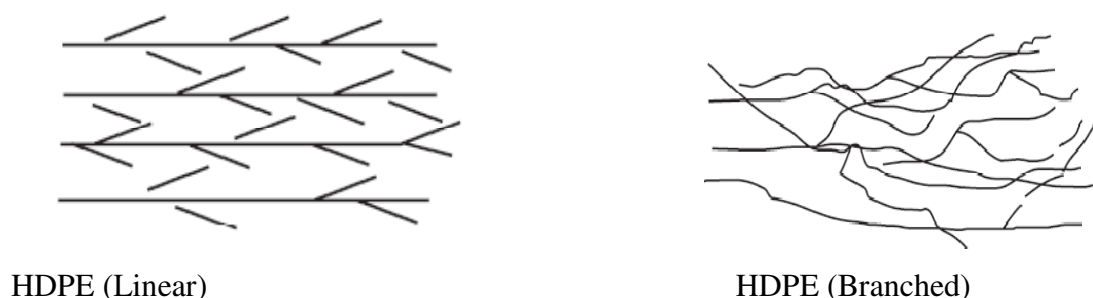


Figure 2.1 Schematic of linear and branched arrangements

HDPE has little branching, giving it stronger intermolecular forces and tensile strength than lower-density polyethylene. It is also harder and more opaque and can withstand somewhat higher temperature. High-density polyethylene, unlike polypropylene cannot withstand normally-required autoclaving conditions. The lack of branching is ensured by an appropriate choice of catalyst. HDPE contains the chemical elements carbon and hydrogen. Physical, mechanical, electrical and thermal properties of high density polyethylene are summarized in table 2.1, 2.2, 2.3, 2.4 (Plastics Data).

Table 2.1 Physical properties of HDPE (Plastics Data)

Tensile Strength	0.20 - 0.40 N/M ²
Notched Impact Strength	No Break
Thermal Coefficient Of Expansion	100 - 200×10 ⁻⁶
Max. Continued Used Temperature	65 ⁰ C
Melting Point	126 ⁰ C
Density	0.941 - 0.965 G/Cm ³

Table 2.2 Mechanical properties of HDPE (Plastics Data)

Hardness, Shore D	62
Tensile Strength, Ultimate	30 MPa
Tensile Strength, Yield	21.9 MPa
Elongation At Break	840%
Tensile Modulus	0.86 GPa
Flexural Modulus	0.928 GPa
Coefficient Of Friction	0.28

Table 2.3 Electrical properties of HDPE (Plastics Data)

Electrical Resistivity	1e – 0.17 Ohm Cm
Surface Resistance	1e + 0.17 Ohm
Dielectric Constant	2.3
Dissipation Factor	0.0003

Table 2.4 Thermal properties of HDPE (Plastics Data)

Melting Point	130 °C
Softening Point	120 °C
Glass transition temperature	-120 °C
Brittleness Temperature	-86.2 °C

2.1.1.2 Uses of HDPE

HDPE is resistant to many different solvents and has a wide variety of applications, including: Telecom Ducts, Containers, Laundry Detergent bottles, Milk jugs, Fuel tanks for vehicles, Plastic lumbers, Folding tables, Folding chairs, Storage sheds, Portable basketball system bases, Plastic bags, Containment of certain chemicals, Chemical-resistant piping systems, Heat-resistant fireworks display mortars, Geothermal heat transfer piping systems, Natural gas distribution pipe systems, Water pipes for domestic water supply, Coax cable inner insulators (Dielectric insulating spacer), Root barrier, Corrosion protection for steel pipelines, Bottles suitable for use as refillable bottles, Ballistic plates etc. HDPE is also used for cell liners in sanitary landfills, wherein large sheets of HDPE are either extrusion or wedge welded to form a homogeneous chemical-resistant barrier, with the intention of preventing the pollution of soil and ground water by the liquid constituents of solid wastes. One of the largest uses for HDPE is wood plastics composites and composite wood, with recycled polymers leading the way. HDPE is also widely used in the polytechnics trade. HDPE mortars are preferred to steel or PVC tubes because they are more durable and more importantly they are much safer compared to steel or PVC (CEH Report).

2.1.1.3 HDPE-World demand

HDPE is the third-largest commodity plastic material in the world, after polyvinyl chloride and polypropylene in terms of volume. According to a British market-research consulting agency, “Merchant Research & Consulting Ltd.” High density polyethylene (HDPE) has accounted for a major share of ethylene consumption structure over the

recent years. The demand for HDPE has increased 4.4% in a year to 31.3 million MT in 2009.

The countries and regions primarily responsible for the growth are as follows: China (+8.5%), other Asian countries (+5%), Latin America (+5.9%). Below average consumption growth will be demonstrated by North America (+3.1%) and Europe (+2.8%).

HDPE is the main polyethylene type in the Russian market. In 2007, polyethylene consumption in Russia was broken down in the following way: HDPE - 51%, LDPE - 42%, LLDPE - 7%. Russia features traditional polyethylene consumption structure: tare and package (30%), consumer and household commodities (22%), polyethylene films (19%), pipes and pipeline fittings (9%), insulation and cable insulation (8%), industrial-purpose items and other related products (10%) ([Plastics Production](#)).

China is most attractive market for polyethylene in the world and will be principal driver for global polyethylene demand to 2020 as per 'Global Markets Direct'. The Chinese polyethylene market size was US\$13865 millions in 2008 and is forecast to grow by more than 8%, accounting for nearly 17% of the global polyethylene demand in 2020. China has emerged as the principal manufacturing and export location for low value plastic products in the world due to low cost manpower and significant government support. The rapid increase in downstream processing capacity additions, primarily geared towards export markets, will be the main driver of polyethylene demand in the future. With over 40% of the demand dependent on imports, China will continue to remain the largest importer of polyethylene in the world despite the many polyethylene capacity additions expected to come on-stream in the next few years. As a result of the growth of the HDPE industry in China and the Middle East, a considerable share of HDPE production is now switching from traditional established economies in North America, Western Europe and Japan to production centers in Iran, Qatar and Saudi Arabia ([Plastics Data](#)).

In 2008, these emerging regions accounted for a combined 21% of world production and by 2013 will account for 31% of world production. On the demand side, China and the

rest of Asia, excluding Japan, represented 16% of world demand in 2008 and by 2013 will represent almost 38% of world demand. Blow molding, injection molding, and film and sheet account for approximately 66% of the world market for HDPE, most of it being packaging, with the exclusion of blow-molded car gas tanks. Construction represents 10–15%, while another 10–15% is distributed among a myriad of consumer and industrial applications. These markets are influenced by business cycles and fluctuate in tandem with the economy. Future growth in world HDPE consumption will be driven by the status and progress of regional economies, continued substitution of traditional materials (e.g., glass, wood, concrete, paper) by HDPE, and avoidance and obsolescence of HDPE in some traditional applications. This latter factor will be more evident in the developed regions of the world, where continued improvements in polyolefin processes and catalyst technologies should allow for the production of very broad ranges of products and grades that will increase the utility of HDPE in the market. HDPE will also face competition, not just from traditional materials such as other existing thermoplastics, but also from emerging polymers brought into the marketplace via new technologies such as metallocene catalysts ([Plastics Data](#)).

The India Petrochemicals Report Q4 2009 recently published by Business Monitor International, London, England (BMI), forecasts that India's petrochemicals industries will double production capacity by 2014-15. Production capacity of high-density polyethylene (HDPE) is forecast to reach 750,000 tons per year, in the third quarter of 2009. China is India's biggest rival in this sector. Industry experts have observed that in the short term, India's production capacity of ethylene, which is presently much lower than that of China, is not expected to increase. India also lags behind China in per-capita polymer consumption. India consumes about 5.2 kilograms per capita compared to China's per-capita consumption of 30 kilograms. India's consumption of polymers is about 6.2 million tons, which is only around 3 percent of the global consumption of 200 million tons. The Indian government forecasts domestic polymer demand reaching 11mn tonnes in 2015, up from 5.8mn tonnes in 2008. This implies that India will remain a net polymer exporter. However, BMI is doubtful that India will come close to increasing the

value of its production from the current US\$15-18bn to US\$30-35bn by 2012-2014, a level that the Tata Strategic Management Group (TSM) says is necessary to cover the rate of domestic demand growth. By 2013, BMI estimates that per capita polymer consumption will reach 13kg. While relatively modest by international levels, it will be far higher than 4.7kg in 2007, which represented 20% of the global average. Moreover, it will make India the world's third-largest plastics consumer after the US and China (ASTM D-5033-90).

2.2 Plastic waste recycling

Plastic materials comprise a steadily increasing proportion of the municipal and industrial waste going into landfill. Owing to the huge amount of plastic wastes and environmental pressures, recycling of plastics has become a predominant subject in today's plastics industry. Development of technologies for reducing plastic waste, which are acceptable from the environmental standpoint and are cost-effective, has proven to be a difficult challenge, because of the complexities inherent in the reuse of polymers. Establishing optimal processes for the reuse/recycling of plastic materials thus remains a worldwide challenge in the new century. Plastic materials find applications in agriculture as well as in plastic packaging, which is a high-volume market owing to the many advantages of plastics over other traditional materials. However, such materials are also the most visible in the waste stream, and have received a great deal of public criticism as solid materials have comparatively short life-cycles and usually are non-degradable.

There are four main approaches for recycling of plastic wastes; these are primary, secondary, tertiary and quaternary recycling (Warren LM et al. 1988).

2.2.1 Primary recycling: This is the recycling of clean, uncontaminated, single-type waste, and it remains the most popular as it ensures simplicity and low cost, especially when done 'in-plant' and fed with scrap of controlled history. In this type of recycling, conversion of waste plastic into products having performance level comparable to that of original products made from virgin plastics. The recycled scrap or waste is either mixed with virgin material to assure product quality or used as second-grade material. Primary

recycling is very simple without any precautions except the proper and clean collection of waste in the plant (Horvat N et al. 1999).

2.2.2 Secondary recycling: In this type of recycling, conversion of waste plastics into products having less demanding performance requirements than the original material. There are two main approaches to secondary recycling. One approach is to separate the plastics from their contaminants and then segregate the plastics into generic types, one or more of which is then recycled into products produced from virgin or primary recycled material. The other approach is to separate the plastics from their associated contaminants and re-melt them as a mixture without segregation. The treatment of the plastics-containing waste streams may include a series of material recycling methods such as: size reduction by granulators, shredders or crumbler; separation of plastics from other waste materials and from one another; cleaning; drying; and compounding. The actual order and number of operations in a particular treatment system depends on the waste being processed and the desired quality of the final material (Waste Care).

2.2.3 Tertiary recycling: Tertiary recycling includes chemical recycling. The terms ‘chemical recycling’ and ‘feedstock recycling’ of plastics are sometimes collectively referred to as ‘advanced recycling technologies’ (figure 2.2). In these processes, solid plastic materials are converted into smaller molecules as chemical intermediates through the use of heat and/or chemical treatment. These chemical intermediates, usually liquids or gases, but sometimes solids or waxes, are suitable for use as feed stocks for the production of new petrochemicals and plastics (Ullmann F 2003a).

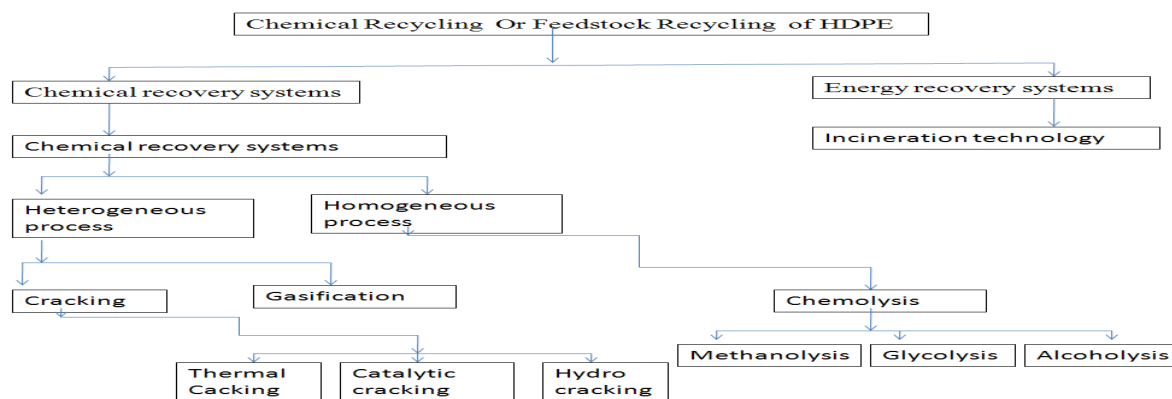


Figure 2.2 The different routes of chemical recycling

2.2.3.1 Chemolysis/Solvolysis

Individual plastics are chemically treated or depolymerized and turned back into monomers. Chemolysis uses chemical agents as catalysts for complete depolymerisation of plastic resins. Chemolysis includes a range of processes such as glycolysis, hydrolysis, methanolysis, and alcoholysis.

2.2.3.1.1 Hydrolysis

Hydrolysis leads to direct recovery of the original raw materials by targeted reaction of water molecules at the linkage points of the starting materials. All hydrolysable plastics such as polyamides, polyesters, polycarbonates, polyureas, and polyurethanes are resistant to hydrolysis under normal conditions of use. Hydrolysis of polyurethanes foams is particularly interesting since they have a very low density (30kg/m^3) and thus take up considerable storage space. Product yields are outstanding. Almost 100% of the polyether and 90% of amine can be recovered. The regenerated materials can be reused directly, together with fresh starting material, for the same foam material. Raw material in the waste can thus be fed back again to the same production process and the environment is thus not burdened by that quantity of waste material (Ullmann F 2003b).

2.2.3.1.2 Alcoholysis

Chemical degradation polyurethanes can also be achieved by alcoholysis to give a polyhydroxy alcohol and small urethane fragments formed by transesterification. Carbon dioxide is not formed in this reaction. If a diol is used as the alcohol, then the urethane fragments also contain terminal hydroxyl groups. These polyhydroxy alcohols can be converted directly to polyurethane foam following the addition isocyanates and varying proportions of new polyhydroxy alcohols (Garforth AA et al. 2004).

2.2.3.1.3 Glycolysis and methanolysis

The degradation of polymers in the presence of glycol such as ethylene glycol or diethylene glycol is known as glycolysis and the degradation of polymers in the presence of methanol is known as methanolysis and this is also an example of transesterification.

2.2.3.2 Gasification or Partial oxidation

The direct combustion of polymer waste, which has a good calorific value, may be detrimental to the environment because of the production of noxious substances such as light hydrocarbons, NO_x, sulfur oxides and dioxins. Partial oxidation (using oxygen and/or steam), however could generate a mixture of hydrocarbons and synthesis gas (CO and H₂), the quantity and quality being dependent on the type of polymer used. A waste gasification and smelting system using iron-making and steel making technologies has been developed to produce a dioxin-free and high calorie purified gas. Hydrogen production efficiency of 60-70% from polymer waste has been reported for a two-stage pyrolysis and partial oxidation process. Co-gasification of biomass with polymer waste has also been shown to increase the amount of hydrogen produced while the CO content reduced. The production of bulk chemicals, such as acetic acid, from polyolefins via oxidation using NO and/or O₂, is also possible ([Garforth AA et al. 2004](#)).

2.2.3.3 Cracking

2.2.3.3.1 Thermal cracking

Thermal cracking, or pyrolysis, involves the degradation of the polymeric materials by heating in the absence of oxygen. The process is usually conducted at temperatures between 500- 800°C and results in the formation of a carbonized char and a volatile fraction that may be separated into condensable hydrocarbon oil and a non-condensable high calorific value gas. The proportion of each fraction and their precise composition depends primarily on the nature of the plastic waste but also on process conditions.

In pyrolytic processes, a proportion of the species generated directly from the initial degradation reaction are transformed into secondary products due to the occurrence of inter and intramolecular reactions. The extent and the nature of these reactions depend both on the reaction temperature and also on the residence of the products in the reaction zone, an aspect that is primarily affected by the reactor design.

In addition, reactor design also plays a fundamental role, as it has to overcome problems related to the low thermal conductivity and high viscosity of the molten polymers.

Several types of reactors have been reported in the literature, the most frequent being fluidized bed reactors, batch reactors and screw kiln reactors.

Characteristics of thermal degradation of heavy hydrocarbons can be described with the following items;

1. High production of C_1 s and C_2 s in the gas product.
2. Olefins are less branched.
3. Some diolefins made at high temperature.
4. Gasoline selectivity is poor; that is, oil products are a wide distribution of molecular weight.
5. Gas and coke products are high.
6. Reactions are slow compared with catalytic reactions.

2.2.3.3.2 Catalytic Cracking

Many researchers have searched for ways of improving light oil and oil quality from waste plastics because the addition of catalyst in the pyrolysis process has many advantages. A number of experimental studies have been carried out by various researchers with the objective of improving liquid hydrocarbons yield from plastics pyrolysis by introducing suitable catalysts, Common plastics such as PE and PP have already been tested extensively; the catalysts tested were mainly those used in the petrochemical refinery industry. The laboratory experimental set-up in these studies was a mostly flow reactor; it may be useful to distinguish between two modes of catalyst usage: 'liquid phase contact' and 'vapor phase contact'. In 'liquid phase contact', the catalyst was contacted with melted plastics and acted mainly on the partially degraded oligomers from the polymer chains; in 'vapor phase contact', the polymer was thermally degraded into hydrocarbon vapors which are then contacted with the catalyst.

The cracking reactions of heavy hydrocarbons using a catalyst such as solid acid and bifunctional catalyst, etc. have been explained with the difference of simple thermal degradation of the polymer (Buekens G et al. 1998). In the depropagation of the polymer chain using the catalyst, the molecular weight of the main polymer chains might be rapidly reduced through successive attacks by acid sites on the catalyst, yielding a high

fraction of low-molecular product. Also, the carbonium ion intermediates in the catalytic reaction progress could undergo rearrangement by hydrogen or carbon atom shifts with producing the isomers of high quality and could undergo cyclization reactions, by means of the intramolecular attack on the double bond of an olefinic carbonium ion. In the case of a bifunctional catalyst playing different active site roles, this catalyst consisted of both acidic and metal material as reforming catalyst. The metallic sites catalyze hydrogenation/dehydrogenation reactions, while the acidic sites on the support catalyze isomerization reactions. This catalyst can promote the isomerization of straight-chain paraffins into branched-chain molecules, the dehydrocyclization of straight-chain paraffins into cycloparaffins and also the dehydrogenation of naphthenes into aromatics. These reactions improved the octane numbers of light hydrocarbons. However, this catalyst was very expensive. Thus, its use in oil recovery from waste plastics containing contaminated material must be taken into careful consideration.

Characteristics of catalytic degradation of heavy hydrocarbons can be described with the following items:

1. Decrease in the reaction time and degradation temperature.
2. High production of C_3 s and C_4 s in the gas product
3. Olefins are the primary product and more branched by isomerization
4. Gasoline selectivity is high; that is, oil products contains components in the $C_5 - C_{10}$ range
5. Aromatics are produced by naphthene dehydrogenation and olefin cyclization
6. Larger molecules are more reactive
7. Pure aromatics do not react
8. Paraffins are produced by H_2 transfer
9. The product distribution over the catalytic degradation can be controlled by the selection of a suitable catalyst and its modification

2.2.3.3.3 Hydro cracking

A process by which the hydrocarbon molecules of petroleum are broken into simpler molecules, as of gasoline or kerosene, by the addition of hydrogen under high pressure

and in the presence of a catalyst. Hydrocracking of polymer waste typically involves reaction with hydrogen over a catalyst in a stirred batch autoclave at moderate temperatures and pressures (typically 423–673 K and 3–10 MPa hydrogen). The work reported, mainly obtaining a high quality gasoline starting from a wide range of feeds. Typical feeds include polyethylene, polyethylene terephthalate, polystyrene, polyvinyl chloride and mixed polymers, polymer waste from municipal solid waste and other sources, co-mixing of polymers with coal, co-mixing of polymers with different refinery oils such as vacuum gas–oil and scrap tyres alone or co-processed with coal. To aid mixing and reaction, solvents such as 1-methyl naphthalene, tetralin and decalin have been used with some success. Several catalysts, classically used in refinery hydrocracking reactions, have been evaluated and include transition metals (e.g., Pt, Ni, Mo, Fe) supported on acid solids (such as alumina, amorphous silica–alumina, zeolites and sulphated zirconia). These catalysts incorporated both cracking and hydrogenation activities and although gasoline product range streams had been obtained, little information on effect of metal and catalyst, surface areas, Si/Al ratio or sensitivity to deactivation was quoted (Panda AK et al. 2010).

2.2.4 Quaternary recycling: Quaternary recycling includes the recovery of the energy content of plastic wastes. Owing to a lack of other recycling possibilities, incineration (combustion) aimed at the recovery of energy is currently the most effective way to reduce the volume of organic material. This may then be disposed of to landfill. Plastics, either thermoplastics or thermosetting, are actually high-yielding energy sources. For example, one liter of heating oil has a net calorific value of 10,200 kcal, whereas 1 kg of plastics releases 11,000 kcal worth of energy; for comparison, it should be added that 1 kg of briquettes (blocks of pressed coal dust) has a net calorific value of 4,800 kcal. It has been estimated that, by burning 1 ton of organic waste, approximately 250 liters of heating oil could be saved (Maraghi R 1993). Clean incineration of municipal solid waste (MSW) is widely accepted in countries like Sweden and Germany (50% of total MSW), Denmark (65%), Switzerland (80%) and Japan (70%) (Burkle D 1992). Although there are very stringent emissions regulations, more than 50 refuse incineration units are

working in Germany. The energy that can be recovered from the incineration of plastics depends on the type of plastic. It has been estimated (in kcal/kg) as: 18,720 for PE; 18,343 for PP; 16,082 for PS; 13,179 for phenol-formaldehyde; 11,362 for foamed polyurethane (PU); 10,138 for Nylon; 8,565 for polyvinyl acetate (PVA); 7,516 for PVC; and 7,014 for PU. This energy is on average 10,000 kcal/kg. Each ton will release about 10^7 kcal. However, plastics emit some objectionable compounds such as polynuclear aromatics hydrocarbons (PAHs) and soot. Thus, recovering energy from plastic waste is not acceptable. The main goal must be to avoid the formation of these hazardous compounds by the correct construction of incinerators and by considering all proper means to avoid pollution. Incineration plants should be designed and operated to produce the least amount of pollution. The use of incineration plants is mandatory for plastic wastes from hospitals and similar institutions, which is considered as a potential source of disease. Incinerators do not emit ethane gas, as this gas is completely combusted into CO_2 and water, even at low temperature. However, incinerators have often been associated with dioxin and furan emissions, which are avoided in modern ones by working at temperatures that are high enough to decompose such chemicals and prevent them from reaching the ecosystem. So quaternary recycling is also called the process of recovery energy from waste plastic by incineration.

2.3. Pyrolysis of HDPE: The pyrolysis of HDPE has been studied by different researchers. In the degradation of waste plastics, the quality and quantity of different product fractions such as liquid, gas and solid change depending on various factors such as the degradation temperature, presence of catalyst, nature of catalyst used, type of reactor used etc. The results of both thermal and catalytic pyrolysis of HDPE carried out by different researchers are summarized below.

2.3.1 Thermal Pyrolysis

The effect of temperature and the type of reactor on the pyrolysis of waste HDPE has been studied and some of the results are reviewed.

Wallis et al. (Wallis MD et al. 2007) have done the thermal degradation of high density polyethylene in a reactive extruder at various screw speeds with reaction temperatures of

400⁰C and 425⁰C. A continuous kinetic model was used to describe the degradation of the high density polyethylene in the reactive extruder. It was found that purely random breakage and a scission rate which had a power law dependence on molecular size of 0.474 best described the experimental data. The greatest discrepancy between the model prediction and the experimental data was the large molecular size region at short residence times; however this only accounted for a very small percentage of the total distribution and was attributed to the presence of fast initiation reaction mechanism that was only significant at low conversions.

Conesa et al. ([Consea JA et al. 1994](#)) studied the production of gases from polyethylene (HDPE) at five nominal temperatures (ranging from 500⁰C to 900⁰C) using a fluidized sand bed reactor. HDPE primary decomposition and wax cracking reactions take place inside the reactor. Yields of 13 pyrolysis products (methane, ethane, ethylene, propane, propylene, acetylene, butane, butylenes, pentane, benzene, toluene, xylenes and styrene) were analyzed as a function of the operating conditions. From the study of HDPE pyrolysis in a fluidized sand bed reactor, they have found that yield of total gas obtained increased in the range 500⁰C – 800⁰C from 5.7 to 94.5%, at higher temperatures, the yield of total gas decreased slightly, the formation of methane, benzene and toluene was favored by high residence times, but ethane, ethylene, propane, propylene, butane, butylenes and pentane undergo cracking to different extents at increasing residence times and/or temperature, the maximum yield of total gas obtained at 800⁰C from HDPE pyrolysis was 94.5% with the following composition: 20% methane, 3.8% ethane, 37% ethylene, 0.2% propane, 4.7% propylene, 0.3% butane, 0.4% butylenes, 2.2% pentane, 24% benzene, 2.1% toluene, 0.01% acetylene and 0.02% xylenes and styrene.

Walendziewski et al. ([Walendziewski J et al. 2001](#)) reported the thermal degradation of polyethylene in the temperature range 370–450⁰C. In the case of thermal degradation of polyethylene, an increase in degradation temperature led to an increase of gas and liquid products, but a decrease of residue (boiling point >360⁰C). However, the increase of gas was not too large as compared to the sharp decrease of residue with increase of temperature. Similar results were obtained in the catalytic degradation and hydro

cracking process. The result of analysis of gas products obtained by the pyrolysis of polyethylene at 400 °C is summarized in the Table 2.5.

Table 2.5 Composition of gas products obtained from pyrolysis of polyethylene at 400 °C (Marcilla A et al. 2001)

Component	Thermal	Catalytic	Hydro cracking
Methane	22.7	12.4	21.1
Ethane	27.4	20.4	21.2
Ethylene	1.4	2.3	0.1
C3	26.6	30.4	23.7
C4	11.0	20.3	20.7
C5	6.9	5.6	7.3
C6	2.1	3.3	3.8

2.3.2 Catalytic Pyrolysis

The thermal degradation of waste HDPE can be improved by using suitable catalysts in order to obtain valuable products. The most common catalysts used in this process are; zeolite, alumina, silica–alumina, FCC catalyst, reforming catalyst etc.

The desired chemical and physical properties of catalyst used for plastic degradation are;

- The catalysts should consist of Lewis and Bronsted acid sites, which is an important factor in determining the catalytic activity and product selectivity. This is because Bronsted acid sites play a proton addition role and Lewis acid sites involve hydride abstraction, which leads to different reaction pathways in the cracking of hydrocarbons.
- Al content per unit cell or Si/Al ratio of catalyst (related to the density of acid site), which also has a marked influence on the cracking reaction. The acid sites are generated by Al species in the catalyst consisting of silica and alumina. High acid site density favors the cracking reaction of hydrocarbons, but promotes undesired reactions such as coke formation. Thus, in order to design the catalysts with a high activity and also high selectivity of desired product, the acid site

density of the catalyst is controlled by preparation methods and various pretreatment methods such as steam or acid/base solution treatment, etc.

- c) In addition to the chemical properties of the catalyst, the physical properties are also very important in determining the catalytic activity and product selectivity. These parameters are the surface area, pore size, pore volume, pore size distribution, pore structure, etc. As an example, the zeolite has a micropore crystalline structure with pore size below 1.0 nm, whereas alumina and amorphous silica–alumina are mesoporous materials with a wide distribution of large pore size. Various natural or synthetic zeolites have relatively high surface area, but small pore size and also small pore volume. The narrow distribution of zeolite having a pore size below 1.0 nm allows different molecules to control a limited diffusion inside the pores, known as shape selectivity, which is selectively reacted on active sites within pores. Also, other advantages of zeolites are high acid strength, high stability and low coke formation, etc. Accordingly, zeolites such as zeolite Y and ZSM-5 have been extensively used for catalytic cracking of heavy hydrocarbons in many commercial processes. However, the catalytic degradation of waste plastics using zeolite may be a difficult problem due to a limited diffusion of big molecules into zeolite pores, which can be overcome with small crystal size and also high external surface area due to the use of a fine powder. Also, activated carbon impregnated with transition metals is a micropore material with a high surface area, which promotes hydrogen transfer reactions during decomposition of hydrocarbons like the reforming catalyst. On the contrary, alumina and amorphous silica–alumina have relatively low surface area, but big pore size and large pore volume, due to their mesopore structure. They have low acid strength compared with zeolites. However, they have a sufficient diffusion of heavy hydrocarbon having large kinetic diameter through the pores, without control of different molecules. A similar catalyst is MCM-41, although it has high surface area, has a uniform mesopore structure. The utility of its high surface area and uniform mesopore in catalytic degradation of polyolefin has

recently studied by several researchers (Marcilla A et al. 2001, Stefanis AD et al. 2001, Sakata Y et al. 1999, Serrano DP et al. 2004). Also, sulfated zirconia known as a super acid solid can be used as a catalyst in catalytic reaction of hydrocarbons (Ono Y 2003, Zhou Z et al. 2003). FCC catalyst has been developed for the cracking of heavy hydrocarbon molecules into gasoline range hydrocarbons. The catalyst consists of silica–alumina with a mesopore structure and zeolite with a micropore structure, which can be well cracked by step-by-step diffusion of heavy molecules in the catalyst of different pore structure. FCC catalyst has been found to have a significant effect in the pyrolysis of thermoplastics (Marcilla A et al. 2003, Puente DLG et al. 2002).

However, the catalytic pyrolysis method suffers from several drawbacks. The catalysts are deactivated by the deposition of carbonaceous residues and Cl, N compounds present in the raw waste stream. Furthermore, the inorganic material contained in the waste plastics tends to remain with the catalysts, which hinders their reuse. These reasons necessitate a relatively high purity of waste plastics, containing very low concentrations of a contaminant. Thus, various pretreatments are required to remove all the components that may negatively affect the catalyst.

The effects of various catalysts on the pyrolysis of HDPE studied by different investigators are summarized below.

Beltrame et al. have studied polyethylene degradation over silica, alumina, silica–alumina and zeolites in a small Pyrex vessel reactor without stirring, in the temperature range 200–600⁰C. Thermal degradation and degradation catalyzed by alumina or silica leave the residue amount, even at 600⁰C. However, at this temperature the gas and distillate yield obtained in the presence of these two catalysts was much higher than that in the thermal degradation. For the silica–alumina with higher activity, the degradation gave much more gas and distillate fraction at 400⁰C, but at temperatures lower than 400⁰C, it did not reach completion (Beltrame PL et al. 1989).

The catalytic upgrading of the pyrolysis gases derived from the pyrolysis of polyethylene over zeolite in the temperature range 400–600⁰C has been investigated by Bagri et al. as

the zeolite bed temperature was increased, the gas yield increased with a decrease in oil and coke yield (Bagri R et al. 2002). Venuto et al. also showed that as the catalyst temperature was increased from 480 to 590⁰C, coke formation in the zeolite catalytic cracking of petroleum was reduced and also alkene gases in gas product increased (Venuto PB et al. 1979).

Sharratt et al. carried out the catalytic degradation of high-density polyethylene using ZSM-5 zeolite. As the reaction temperature was increased from 290 to 430⁰C, the gas yield was increased, whereas the oil yield was decreased. The oil obtained in the thermal pyrolysis of polyethylene contained a low concentration of aromatic compounds. After it was catalyzed, there was a marked increase in the concentration of aromatic compounds in the oil, which further increased with the increase in catalyst bed reactor temperature (Sharratt PN et al. 1997).

The liquid-phase catalytic degradation of waste polyolefinic polymers such as HDPE, LDPE, PP over spent fluid catalytic cracking (FCC) catalyst was carried out at atmospheric pressure in a stirred semi-batch operation by Lee et al. It was concluded that the initial rate of degradation of waste HDPE was linearly increased with catalyst amount, while that was exponentially increased with reaction temperature. The reaction temperature had a great influence on the initial rate of degradation of waste plastics using spent FCC catalyst than the catalyst amount (Lee KH et al. 2003a).

The difference in the product yields between thermal and catalytic degradation using spent FCC catalyst of waste HDPE in a stirred semi-batch reactor on a laboratory scale was studied by Lee et al. (Lee KH et al. 2003b). The results are shown in Table 2.6.

Table 2.6 Yields of gas, liquid and residue obtained from thermal and catalytic degradation of waste HDPE at 430 °C (Lee KH et al. 2003b)

Types of degradation	Gas (%)	Liquid (%)	Residue (%)
Thermal degradation	20.0	75.5	4.5
Catalytic degradation	19.4	79.7	0.9

As compared with thermal degradation, the catalytic degradation showed an increase of liquid yield whereas that of residue was reduced, due to the decomposition of heavier

residues into lighter oil product. The difference of cumulative yield distribution in liquid product between thermal and catalytic degradation of waste HDPE was clearly apparent. The catalytic degradation produced initial liquid product with more rapid, higher degradation rate into liquid product and also much more liquid yield in comparison with thermal degradation. It was supposed that if waste plastic in the thermal degradation process was subject to short residence time in a continuous stirred tank reactor, partial degradation of plastic can occur, while the rest of the feed could produce high-viscosity product, such as wax. In the case of thermal degradation, paraffin and olefin components are the main products and aromatic compounds hardly appear, without change by increase of reaction time. On the other hand, the catalytic degradation using spent FCC catalyst showed about 80% olefin products as the main product. Again, the paraffin products were decreased, whereas aromatic compounds were increased, compared with those of thermal degradation. Spent FCC catalyst improved the fraction of liquid olefin and aromatic components with comparatively high octane number. Molecular weight distribution of liquid product obtained at a similar reaction time was compared over thermal and catalytic degradation of waste HDPE. In the case of thermal degradation, both paraffin and olefin as a main liquid product were distributed in a wide molecular weight range, between 80 and 400, whereas naphthene products with cyclic structure showed a narrow molecular weight distribution. On the other hand, the catalytic degradation produced mainly light olefin products in the range of gasoline with molecular weight below 200. Spent FCC catalyst could be supplied from commercial FCC process, which was very cheap and retained with adequate activity. Thus, it could be used as an alternative catalyst in liquid-phase catalytic degradation of polyolefin.

Miskolczi et al. have done the catalytic degradation of waste high density polyethylene with three different catalysts (equilibrium FCC, HZSM-5 and clinoptilolite). Catalysts differ basically in their costs and activity due to differences of micro and macroporous surface areas and furthermore the Si/Al ratio and acidities are also different. Mild pyrolysis was used at 430⁰C and the reaction time was 45 min in each case in a pyrex batch reactor. The effects of catalysts on the properties of degradation products were

investigated. It was found that waste polymer could be converted into lighter fractions at 430⁰C during 45 min with yields of 40-50% depending on the catalysts. HZSM-5 increased both the yields of gaseous (C₁-C₄) and liquid (C₅-C₂₃) products, while FCC and clinoptilolite catalysts increased rather the yield of liquid. Using catalysts of 2% the structure of products were significantly modified, because hydrocarbons got rather branched and the position of olefinic double bonds also changed in case of thermo catalytic cracking. The degradation of HDPE was well followed via the decrease of average molecular weight of heavier residue fractions (C₂₄+). Liquid hydrocarbons and residues were of low sulphur and nitrogen content from additives of raw material therefore they might be favorable for energy production or for raw materials of the petrochemical industry (Miskolczi N et al. 2008).

Seo et al. studied the catalytic degradation of waste high density polyethylene to hydrocarbons by ZSM-5, zeolite-Y, mordenite and amorphous silica-alumina in a batch reactor and investigated the cracking efficiency of catalysts by analyzing the oily products including paraffins, olefins, naphthenes and aromatics with gas chromatography/mass spectrometry (GC/MS). From this study it was found that catalytic degradation of HDPE with zeolite-Y, mordenite and silica-alumina yielded oil ranging from 71 to 81 wt% which mostly comprises C₆-C₁₂ hydrocarbons. Relative to catalytic degradation products, thermal degradation of HDPE also produced 84 wt% oil, but the oil contained much longer hydrocarbons, leading to solidification from the bottom of container during storage. Both all zeolites and silica-alumina increased olefin content in oil product, particularly ZSM-5 and zeolite-Y enhanced the formation of both aromatics and branched hydrocarbons simultaneously. ZSM-5 showed the greatest catalytic activity on cracking of heavy hydrocarbons to small gaseous hydrocarbons and formation of aromatics. Mordenite produced the greatest amount of coke among all catalysts, and much greater fraction of C₁₁-C₁₃ paraffins due to its bottleneck crystalline structure. Amorphous silica-alumina showed a great activity on cracking heavy hydrocarbons. It generated a pronouncedly high yield of lighter olefins due to strong acidity, but was far inferior to zeolites in the formation of aromatics and branched hydrocarbons because of

amorphous structure (Seo YH et al. 2003). The yields of gas, liquid and residue are illustrated in Table 2.7(a) and the PONA distribution in liquid products is shown in Table 2.7(b).

Table 2.7(a) The distribution of gas, liquid and residue fractions from thermal and catalytic degradation of HDPE with various catalysts at 450 °C (Seo YH et al. 2003)

Type of pyrolysis	Yields of products			Liquid (wt %)		
	Liquid (wt %)	Gas (wt %)	Coke (wt %)			
				C ₆ -C ₁₂	C ₁₃ -C ₂₃	≥ C ₂₄
Thermal cracking only	84.00	13.00	3.00	56.55	37.79	5.66
ZSM-5 (Powder)	35.00	63.50	1.50	99.92	0.08	0
Zeolite Y (Powder)	71.50	27.00	1.50	96.99	3.01	0
Zeolite (Pellet)	81.00	17.50	1.50	86.07	11.59	2.34
Modernite (Pellet)	78.50	18.50	3.00	71.06	28.67	0.27
Silica-Alumina (Powder)	78.00	21.00	1.00	91.31	8.69	0
Alumina (Powder)	82.00	15.90	2.10	53.02	43.27	3.71

Table 2.7(b) PONA distribution in oil products from thermal and catalytic degradation of HDPE with various catalysts at 450 °C (Seo YH et al. 2003)

Type of pyrolysis	Total Paraffin	Individual Paraffin		Total olefin	Naphthene	Aromatics	Others
		n- paraffin	i- paraffin				
Thermal Cracking	40.75	40.47	0.28	39.93	18.50	0.68	0.14
ZSM-5 (Powder)	1.63	1.51	0.12	16.08	23.55	58.75	0.01
Zeolite Y (Powder)	5.39	0.00	5.39	79.92	7.68	7.01	0.00
Zeolite Y (Pellet)	25.10	20.68	4.42	49.28	12.05	8.43	5.14
Modernite (Pellet)	31.07	30.89	0.18	57.07	11.51	0.13	0.22
Si-Al (Powder)	0.20	0.20	0.00	91.62	5.62	0.39	2.17
Alumina (Powder)	32.57	32.57	0.00	50.19	14.99	1.14	1.11

The liquid-phase catalytic degradation of HDPE over BEA, FAU, MWW, MOR and MFI zeolites with different pores in a batch reactor at 380 °C or 410 °C had been studied by Park et al. Among zeolites, high activity was obtained with BEA and MFI zeolites, because of their bent pore structure suppressing carbon deposit, whereas MOR zeolite showed low activity, due to the rapid blocking of the linear pore structure even by a small amount of carbon deposit. Large three-dimensional pores of FAU enhanced mass transfer, resulting in a high yield of liquid product and also the slow diffusion of cracked

product in MWW zeolite brought about much more cracking into small hydrocarbons. Accordingly, the pore shape of the zeolites was very important in determining the activity and product distribution in the degradation of polymers (Park JW et al. 2002).

Sharratt et al. had done the pyrolysis of high density polyethylene over HZSM-5 catalyst using a specially developed laboratory fluidized bed reactor operating isothermally at ambient pressure. The influence of reaction conditions including temperature, ratios of HDPE to catalyst feed, and flow rates of fluidizing gas was examined. A fluidized-bed reactor had been developed and demonstrated to be particularly suitable to obtain hydrocarbon products from the catalytic pyrolysis of HDPE polymer in the temperature range from 290 to 520⁰C. HZSM-5-catalyzed degradation resulted in much greater amounts of volatile hydrocarbons compared with degradation over silicalite. In the presence of the HZSM-5 catalyst at 360⁰C, conversion to volatile hydrocarbons in the catalytic fluidized-bed reactor was more than 90 wt % of feed in 15 minutes, while silicalite yielded less than 6 wt % of feed after 60 min. The systematic experiments carried out with HZSM-5 showed that the use of catalyst reduced the required reaction temperature, improves the yield of volatile products, and provides selectivity in the product distributions. The selectivity could be further influenced by changes in reactor conditions; in particular, olefins and *i*-olefins were produced by low temperatures and short contact times. The catalytic pyrolysis of polymer in the fluidized bed reactor was a useful method for the production of potentially valuable hydrocarbons. It was concluded that under appropriate conditions the resource potential of polymer waste could be recovered (Sharratt PN et al. 1997).

Manos et al. studied the catalytic degradation of high density polyethylene to hydrocarbons over different zeolites. The product range was typically between C₃ and C₁₅ hydrocarbons. Distinctive patterns of product distribution were found with different zeolites structures. Over large-pore ultrastable Y, Y, and β zeolites, alkanes were the main products with less alkenes and aromatics and only very small amounts of cycloalkanes and cycloalkenes. Medium-pore mordenite and ZSM-5 gave significantly more olefins. In the medium-pore zeolites secondary bimolecular reactions were sterically hindered,

resulting in higher amounts of alkenes as primary products. The hydrocarbons formed with medium-pore zeolites were lighter than those formed with large-pore zeolites. The following order was found regarding the carbon number distribution: (lighter products) ZSM-5 < mordenite < β < Y < US-Y (heavier products). A similar order was found regarding the bond saturation: (more alkenes) ZSM-5 < mordenite < β < Y < US-Y (more alkanes) (Manos G et al. 2000).

The catalytic pyrolysis of high density polyethylene was studied at different times using different types of reactors: a pyroprobe apparatus, where the volatile residence time was in the range of few milliseconds, and a fluidized bed reactor, where the secondary reactions took place in a larger extension. The catalyst used in this study was HZSM-5. It was observed that the effect of HZSM-5 was more evident at low residence times. Compounds such as propane, isobutene, isobutene and isopentane increased their yield significantly at low residence time in the presence of HZSM-5, showing an increase in the range 15-200 times the thermal value, in the pyroprobe equipment. At high residence times, secondary cracking reactions tend to equalize the yields obtained in catalytic cracking. In this way, propene only showed an increase of 1.6 times the thermal yield at a value $V/m = 1500$. In the case of isostructures, this increment was in the range 4-10 times at the same V/m value. In the presence of HZSM-5, together with C_1 - C_3 hydrocarbons, the yield of other heavier compounds such as butadiene, n-hexane, n-heptane, and benzene increased with residence time. The results obtained clearly showed the different effect of catalyst on the product evolution, depending on the residence time of the volatiles in the reactor. The contact effectively between polymer and catalyst during the degradation process was another parameter related to the type of reactor which had a significant influence not only on the percentages of each fraction obtained, but also on the product distribution. Thus, a better contact favored the gas fraction and the formation of lighter hydrocarbons and low contact effectivity reduced the gas fraction (Hernandez MR et al. 2006).

Garforth et al. studied the catalytic pyrolysis of high density polyethylene in a laboratory fluidized bed reactor operating in the 290 °C-430 °C range under atmospheric pressure.

The catalysts used were HZSM-5, Silicalite, HMOR, HUSY and SAHA and the yield of volatile hydrocarbons (based on the feed) was typically HZSM-5>HUSY≈HMOR>SAHA. The results obtained from this work stated that although the initial cracking of HDPE must be confined to the external surface and pore mouths of the zeolite catalysts, the resultant initial cracked were then degraded further within the zeolite. Clearly both acidity and diffusion constraints within individual micropores of each zeolite may play significant roles in the observed product distribution from HDPE cracking. The acidic zeolites catalysts, HZSM-5, HMOR, and HUSY were more effecting in converting the polymer to volatile hydrocarbons than the less acidic amorphous SAHA. SAHA showed the lowest conversion and generated an olefin rich product, predominantly between C₃-C₈, whereas HUSY yielded a saturate rich product with a wide carbon number distribution and substantial coke levels. Greater product selectivity was observed with HZSM-5 and HMOR as catalysts with over 80% of the product in the C₃-C₅ range and HMOR generating the highest yield of *i*-C₄ for all catalysts studied. Both the larger pore zeolites (HUSY and HMOR) showed deactivation in contrast to the more restrictive HZSM-5. The less acidic catalyst, SAHA, was less reactive and did not appear to deactivate under the reaction conditions. Thus the use of a catalyst significantly reduced the required reaction temperature and improves the yield of volatile products as well as providing better selectivity in the product distributions. The catalytic degradation of polyethylene performed in fluidized bed reactor was also found to be a useful method for the production of potentially valuable hydrocarbons (Garforth AA et al. 1998).

The catalytic degradation of high density polyethylene (HDPE) under nitrogen using a laboratory fluidized bed reactor operating at 360⁰C with catalyst to polymer feed ratio of 2:1 and at 450 °C with catalyst to polymer feed ratio of 6:1 under atmospheric pressure was studied. The catalysts used in this study were ZSM-5, US-Y, ASA, fresh FCC (fluid catalytic cracking) commercial catalyst (Cat-A) and equilibrium FCC catalysts with different levels of metal poisoning were studied. This study showed the use of catalysts in the pyrolysis of polymer waste significantly reduced the required reaction temperature and improves the yield of volatile products as well as provides better selectivity in the

product distribution. The use of catalytic recycling process based on equilibrium catalysts would lower the operating temperature and produce more valuable feed stocks. The degradation of HDPE over equilibrium catalysts yielded a predominantly olefinic stream in the range of C₃-C₈ similar to that of ASA (Ali S et al. 2002).

Mastral et al. studied the catalytic degradation of high density polyethylene in a laboratory fluidized bed reactor at mild temperatures, between 350 °C to 550 °C. The catalyst used was nanocrystalline HZSM-5 zeolite. The use of nanocrystalline HZSM-5 allowed greater yields of gas fractions at mild temperatures and a higher selectivity to the products obtained than those achieved by thermal cracking. Polyethylene first cracked over the acid sites on the external surface of zeolite. A part of the compound produced can then diffuse into the internal active surface through the zigzag pores and over crack giving lighter compounds. Due to size restrictions of pores, gases were produced mainly in the pores while waxes were the result of external cracking. The temperature affected the gas and wax yields. Gas production increased as temperature rised. However, when the temperature exceeded 500 °C, some HDPE was cracked thermally, increasing the wax yield and varying the wax and gas compositions. If the catalytic pyrolysis temperature was too low (350 °C-400 °C), the polymer was not fully cracked and a solid residue was produced in the reaction bed. The gases were mainly composed of olefins. Cracking reactions (β - scission) controlled the reaction mechanism inside the pores. Due to their small dimensions, HZSM-5 pores inhibit bimolecular reactions, which were a source for paraffin production. Terminal olefins were not produced in significant quantities because of the strong effect of isomerization reactions. The waxes obtained had very high concentrations of compounds between C₁₀ and C₂₀. This composition did not change over a wide temperature range (350 °C-500 °C). As with the gas distribution, the wax composition changes at temperatures exceeding 500 °C. Typical thermal pyrolysis products such as heavy olefins, cycles and aromatics were detected at 550 °C. The polymer to catalyst ratio also affects the product yields. This influence was especially noticeable when the ratio was high. In these cases, the number of acid sites per gram of polyethylene was not sufficient to degrade the entire polymer, resulting in a lower gas

production and altering the product distribution. It had been resulted that thermal pyrolysis produces lower gas yields than catalytic pyrolysis, and that this fraction was largely composed of heavier compounds (C_5 - C_7). The chain reaction mechanism and radical species involving the thermal degradation of polyethylene produce olefinic gases, as in the catalytic mechanism, but they also allowed methane formation which had not previously been produced. The most important compositional change was observed in the waxes which increased their olefinic and cycle contents as the HDPE/Cat ratio increased. This also resulted that the most suitable temperature and HDPE/Cat ratio for the process are 450 °C and 1.41 respectively. In these conditions no solid residue was formed and the wax obtained did not contain olefins and cyclics which were environmentally and operationally dangerous (Mastral JF et al. 2006).

Lin et al. studied the pyrolysis of high density polyethylene over various catalysts using a laboratory fluidized-bed reactor operating isothermally at ambient pressure. Both catalyst acidity and diffusion constraints within individual pores of each catalyst may play significant roles in the observed product distribution from HDPE cracking. HZSM-5 catalyzed degradation resulted in much more amounts of volatile hydrocarbons compared with degradation over non-zeolitic catalysts (MCM-41 and SAHA). Both MCM-41 and SAHA yielded a saturate-rich stream with a wide carbon number distribution and substantial coke levels. Some valuable hydrocarbons of olefins and *i*-olefins were produced for mixed catalysts when HZSM-5 was used as a co-additive. The larger pore structure of the MCM-41 and SAHA catalysts showed deactivation in contrast to the more restrictive HZSM-5. So they had concluded that under appropriate reaction conditions and suitable catalysts could have the ability to control both the product yield and product distribution from polymer degradation, potentially leading to a cheaper process with more valuable products (Lin YH et al. 2004).

Karagoz et al. studied the conversion of high density polyethylene in vacuum gas oil to fuels in absence and presence of catalyst. The blend containing 20% HDPE was co-processed in the presence of hydrogen at the temperatures of 435 °C and 450 °C. Five kinds of metal supported on active carbon catalysts (M-Ac) and acidic catalysts {HZSM-

5 and DHC (Distillate Hydro Cracking-8)} were tested. The effects of metal type on the product distribution from co-processing were investigated. The cracking ability of M-Ac catalysts was also compared with two acidic catalysts. And the quality of liquid fuel from co-processing was also compared for M-Ac catalysts and acidic catalysts. They have concluded that the type and the concentration of metal on the active carbon surface effected both product distribution and the quality of liquid product at low co-processing temperature. Metal supported on active carbon catalysts showed hydrodesulphurization effect beside its hydro cracking effect so the type of metal affected the sulphur amount in liquid product. At low temperature, cobalt on activated carbon (Co-Ac) produced more amount and lighter liquid than commercial hydrocracking catalysts (DHC-8). Although HZSM-5 showed good cracking activity in co-processing, it gave the liquid containing highest amount sulphur. As a consequently, metal loaded active carbon especially can be taken into consideration in co-processing of polymers with heavy petroleum fractions (Karagoz S et al. 2003).

Jan et al. studied the degradation of waste high density polyethylene thermally and catalytically using MgCO_3 at 450 °C into liquid fraction in a batch reactor. Different conditions like temperature, time and catalyst ratio were optimized for the maximum conversion of HDPE into liquid fraction. Thermal degradation of waste HDPE converted it into wax and the wax is further degraded at 450 °C into liquid, while with catalytic degradation 92% of the liquid was obtained at 450 °C in a single step. Therefore the catalytic process was superior to thermal process. The liquid products from thermal and catalytic degradation of HDPE could be considered a as mixture of heavy naphtha ($\text{C}_7\text{-C}_{10}$), gasoline ($\text{C}_8\text{-C}_{10}$) and diesel oil ($\text{C}_{10}\text{-C}_{20}$) and had the potential for commercialization (Jan MR et al. 2010a).

Jan et al. studied the thermal and catalytically degradation of waste high-density polyethylene (HDPE) using BaCO_3 as a catalyst under different conditions of temperature, cat/pol ratio and time. The oil collected at optimum conditions (450 °C, 0.1 cat/pol ratio and 2 h reaction time) was fractionated at different temperatures and fuel property of the fractions and parent oil was evaluated by their physicochemical

parameters for fuel tests. The results were compared with the standard values for gasoline, kerosene and diesel oil. Boiling point distribution (BPD) curves were plotted from the gas chromatographic study of the samples and compared with that of the standard gasoline, kerosene and diesel. The oil samples were analyzed using GC/MS in order to find out their composition. The physical parameters and the composition of the parent oil and its fractions supported the resemblance of the samples with the standard fuel oils. The light fractions best match with gasoline, the middle fractions match with kerosene and the heavier fractions matched with diesel oil in almost all of the characteristic properties (Jan MR et al. 2010b).

Waste high-density polyethylene (HDPE) was catalytically degraded using CaCO_3 as a basic catalyst by Jan et al. Various parameters like temperature, catalyst to polymer ratio (cat/pol) and reaction time were explored in order to find out optimum reaction conditions. Total conversion of 97.20% was achieved with 52.33% oil yield and 53.84% oil selectivity. Sufficient quantity of the oil product was collected for further physicochemical study. The oil obtained was fractionated at different temperatures and physical parameters were studied for all the fractions including parent catalytic oil. The ASTM distillation study of the catalytically derived oil showed that its 40% fraction was in the boiling point range of light naphtha, 24% fraction was in the range of heavy naphtha and 36% fraction was in the boiling point range of middle distillate. The oils obtained were analyzed by GC/MS to find out its composition. Major constituent hydrocarbons were found to be in the range of C_7 – C_{28} distributed in various fractions derived at different temperatures. Different fractions showed varied compositions with constituents common to two or more sample fractions showing overlap of the distillation ranges. Comparing the physical parameters of the sample oils with standard fuels it was observed that the collected fractions were either in the range of gasoline, kerosene or diesel oil (Jan MR et al. 2013).

2.4 Mechanism and kinetics of pyrolysis

The degradation of polymer may be considerably different based on the way in which reaction is carried out: heat (thermal degradation), heat and catalyst (thermo catalytic

degradation), oxygen (oxidative degradation), heat and oxygen (thermo-oxidative degradation), radiation (photochemical degradation), radiation and oxygen (photo-oxidative degradation), chemicals (chemical degradation), etc. The common characteristic of these methods is that they cause irreversible changes in the structure of polymers. The decomposition of the framework of polymers results in decreasing molecular weight and significant changes of physical and chemical properties. The widely known and thoroughly studied methods are thermal and thermo catalytic degradation, which are referred as chemical recycling in the literature. Chemical recycling and chemical degradation are not the same, because chemical degradation means degradations caused by chemicals (acids, solvents, alkalis, etc.) Several reports have described the thermal and catalytic cracking of waste polymers. Two types of polymers have been widely investigated: polyethylene and polypropylene, because they represent 60–65% of all plastic wastes. The degradation of plastics means heating to high temperatures where macromolecules break into smaller fragments in which valuable mixtures of hydrocarbons (gas, liquid and residue) are obtained (Pinto F et al. 1999, Miskolczi N et al. 2004, Kim JS et al. 2003, Masuda T et al. 1999, Uddin MA et al. 1997, Seddegi ZS et al. 2002). The structure of the hydrocarbons produced can be modified by the use of catalyst. Catalytic cracking consumes less energy than the non catalytic process and results in formation of more branch-chain hydrocarbons. On the other hand the addition of the catalyst can be troublesome, and the catalyst accumulates in the residue or coke. There are two ways to contact the melted polymer and catalysts: the polymer and catalyst can be mixed first, and then melted, or the molten plastics can be fed continuously over a fluidized catalyst bed. The usually employed catalysts are US-Y, and HZSM-5. It was found that the HZSM-5 and FCC catalysts provided the best possibility to yield hydrocarbons in the boiling range of gasoline (Sakata Y et al. 1997, Grieken RV et al. 2001, Jalil PA 2002, Hwang EY et al. 2002).

The kinetics and mechanism of these reactions have been elucidated by several physical and chemical methods using different analytical techniques.

2.4.1 Investigative methods for polymer degradation

It must be said at the onset that no single method of investigation is appropriate to cover all pyrolysis phenomena. This is because three extreme categories of pyrolysis behaviour can be defined, and each presents a different investigative problem:

- (1) Cross linking or other reactions within the polymer leading to the formation of infusible resins, or coke/char precursors.
- (2) Chain scissions and other processes leading to decrease in the average molecular weight of the sample.
- (3) The formation of significant yields of small molecular weight materials, which may be monomeric, oligomeric, or which may originate from substituents on the chain backbone.

It is very likely that more than one of these categories of behavior will be occurring simultaneously, in which case it will be desirable to pursue several experimental approaches, and to coordinate the results ([Lehrle RS 1987](#)).

Categories (1) require the study of changes in the original polymer or the residue from it. This behaviour is generally studied by the methods of thermal analysis (thermogravimetric analysis, differential thermal analysis, and differential scanning calorimetry); which may indicate the overall energetics of the processes occurring, but cannot give direct details of the chemistry of the processes involved ([Lehrle RS 1987](#)). Thermogravimetry (TG) is a thermal analysis method in which the mass change of a sample subjected to a controlled temperature programme is measured. The use of isothermal and dynamic TG for the determination of kinetic parameters in polymeric materials has raised broad interest during recent years. Although TG cannot be used to elucidate a clear mechanism of thermal degradation, dynamic TG has frequently been used to study the overall thermal degradation kinetics of polymers because it gives reliable information on the activation energy, the exponential factor and the overall reaction order. Consequently, the corresponding differential TG (DTG) curves exhibit multiple peaks or asymmetric peaks with more or less pronounced shoulders. Except when the mass losses corresponding to each decomposition step occur in different

temperature ranges, TG does not provide clear information on thermal degradation mechanisms because of its insufficient ability to analyse the evolved gas mixture. In general, any changes in physical properties may be used to assess category (1) behaviour, but again this approach does not directly provide any information about the molecular behaviour. The capacity to obtain such molecular information with any reliability depends upon the extent to which spectroscopic methods can be applied to study the polymer residue. Any possibility of using such methods should be explored. If all else fails, an attempt may be made to further degrade the infusible residue under conditions so drastic that fragmentation of the structure occurs; it may then be assumed optimistically that the fragments obtained are sufficiently characteristic of the original residue to permit proposals about its structure. The simplest way to achieve such drastic degradation is to heat the sample to temperatures exceeding 1000⁰C, but unfortunately most of the products obtained in this way are small molecules or radicals which are not helpfully characteristic of the overall structure. The best way to obtain large characteristic fragments is to use a technique such as fast ion bombardment or fast atom bombardment; if this is carried out in the source region of a mass spectrometer, mass analysis of the resulting fragments can be performed in situ ([Pieliowski K et al. 2005](#)).

Category (2) behaviour is more amenable to study; in particular, viscometry and any of the recognised techniques of polymer molecular weight measurement can be considered, and liquid chromatographic methods, especially gel-permeation chromatography are now widely used. The latter technique is especially useful since the results provide information about changes in molecular weight distribution; such changes may provide mechanistic clues ([Lehrle RS 1987](#)).

However, the study of polymeric residues and partially degraded solid polymers [i.e. categories (1) and (2)] presents numerous experimental problems. The sensitivity of the available techniques is also very less for the accurate assessment. This means that mechanistic information derived from measurements on solid samples or residues is generally less reliable than that derived from measurements on volatiles, as discussed in the following paragraphs ([Lehrle RS 1987](#)).

Behaviour leading to the formation of small molecular-weight materials [category (3)] will be evidenced by the fact that such materials are generally volatile at the elevated temperatures used for pyrolysis. They may be condensed on a cold surface or in a cold trap, and subsequently analysed, though this approach is not recommended because of the high probability of secondary reactions occurring when the frozen condensate is heated to recover the products for analysis. When this occurs it can give a very misleading idea of degradation processes occurring within the sample. Another method of estimating the yield of volatiles is in terms of the pressure they create in a continuously pumped system (“thermal volatilization analysis”) but this method is of only moderate sensitivity, and becomes cumbersome when there are several pyrolysis products (Lehrle RS 1987).

The techniques of gas-liquid chromatography (GLC) and mass spectrometry (MS), either individually or in combination (GLC-MS) have been used on the assessment of volatiles. In either case the pyrolysis (Py) may be performed in situ, and the resulting techniques of Py-GLC and Py-MS both have the distinct advantage that pyrolysis products are not only analysed, but removed from the pyrolysis zone as they are formed, so that secondary reactions are minimized. In Py-MS the pyrolysis zone is within or close to the continuously- pumped source of the mass spectrometer; in Py-GLC the pyrolysis products are swept away by the inert carrier gas as they are formed. In many respects these two techniques are complementary. Py-MS is rather less sensitive, and the results may be difficult to interpret if there are several pyrolysis products, because their MS cracking patterns will be superimposed. However, mass spectra are much more specific for characterizing volatiles than are chromatographic peaks. Py-GLC is extremely sensitive when detectors such as flame ionization detectors are used, and chromatograms of pyrolysis products are much simpler than mass spectra. The combined technique of Py-GLC-MS uses a suitable interface to pass the gas chromatographic effluent into a mass spectrometer so that each GLC peak is mass analysed. This is the most useful approach for initially characterizing the products from the pyrolysis (Lehrle RS 1987).

Recently, the development of a TG-MS and TG-FTIR interface design has made a significant breakthrough in thermal degradation investigations. The combination of TG

and FTIR provides a very useful tool for the determination of the degradation pathways of a polymer, copolymer or the combination of one of these with an additive. The TG is normally coupled to the FTIR spectrometer *via* a glass-coated transfer line. This transports the volatile products evolved during the decomposition of the sample to the gas cell of the FTIR spectrometer. Both the transfer line and the gas cell are heated to prevent condensation of the decomposition products. The FTIR spectrometer measures the spectra of the gases in the cell rapidly at frequent intervals. TG-FTIR makes it possible to assign the volatile components under investigation to the decomposition stages detected by TG during an experiment. Based on the measurements conducted, it is possible to achieve a simultaneous quantitative and qualitative characterization of the materials investigated. TG-MS is a useful ‘hyphenated’ technique combining the direct measurement of weight loss as a function of temperature with the use of a sensitive spectroscopic detector. The TG is coupled to the MS via a heated metal or quartz glass capillary tube. One end of the capillary is positioned close to the sample in the thermo balance. Part of the evolved gases is sucked into the capillary by the vacuum in the MS. The MS repeatedly measures the entire mass spectrum or monitors the intensity of characteristic fragment ions (m/z , the mass-to-charge ratio). TG-MS features are high sensitivity and high resolution, which allow extremely low concentrations of evolved gases to be identified, together with overlapping weight losses that can be interpreted qualitatively. In addition to the weight-loss information, MS permits temporal resolution of the gases that are evolved during thermal or thermo oxidative degradation of a polymer in controlled atmospheric conditions. The characteristics of a broad variety of TG-MS instrumental solutions that depend partly on the sample characteristics and the desired conditions of thermal degradation are normally considered in relation to polymer characterization ([Pielichowski K et al. 2005](#)).

Py-GC is mainly employed in structure analysis that includes the exploration of monomer arrangement in the (co) polymer system, such as the number-average sequence length and stereoregular distributions. In addition to the traditional post-pyrolysis derivatisation, pre-

pyrolysis derivatisation has been developed in order to reselect degradation pathways effectively.

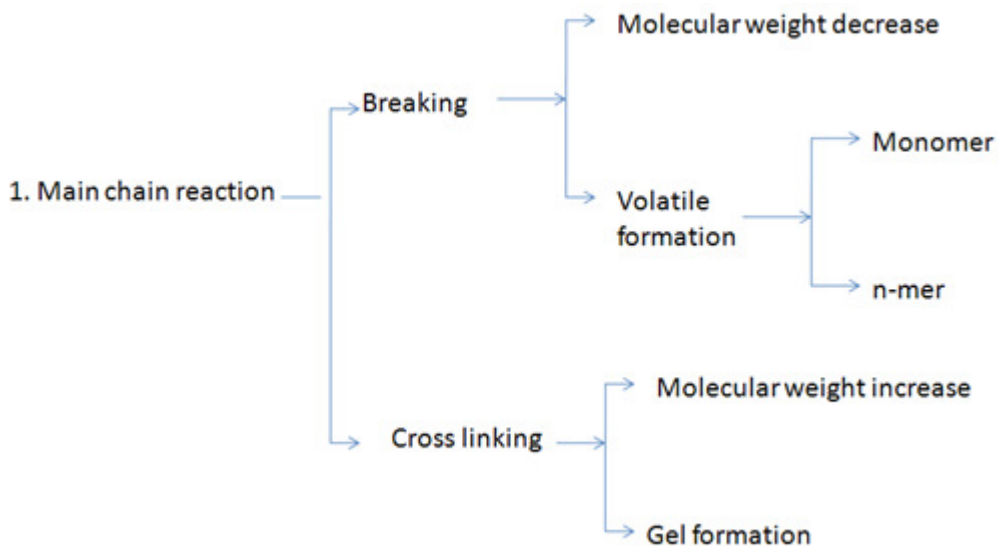
Pyrolysis is carried out either outside or inside the identification instrument. In the outside mode, the thermal degradation is carried out by a pyroprobe connected to the injection port of a GC using a selected technique—time-programmed or flash pyrolysis. GC-separated individual pyrolysates can be identified with different equipment connected to the GC, e.g., Py-GC-MS, Py-GC-FTIR or Py-GC-AED (atomic emission detector) (Pielichowski K et al. 2005).

Direct pyrolysis–mass spectrometry (Py-MS) is applied to determine the primary structure of macromolecules and to investigate selective thermal degradation mechanisms. This technique allows the thermal decomposition products of the polymer sample to be observed directly in the ion source of the mass spectrometer, so that the evolving products are ionised and continuously detected by repetitive mass scans almost simultaneously with their formation. Since pyrolysis is accomplished under high vacuum, the thermal fragments are readily removed from the hot zone, and because of the low probability of molecular collisions and fast detection the occurrence of secondary reactions are reduced. Therefore, primary pyrolysis products bearing the structure of the decomposing materials are mainly detected (Pielichowski K et al. 2005).

In recent years pyrolysis–gas chromatography–mass spectrometry (Py-GC-MS) has been widely used for the separation and identification of the volatile pyrolysis products of polymers and can be considered as the most convenient method to detect simultaneously the presence of decomposition products qualitatively and quantitatively. Evolved gas analysis (EGA) performed by using a GC coupled with a mass-selective detector offers a number of advantages for the decomposition study. The number of peaks seen in the total ion chromatogram (TIC) represents the number of compounds detected by GC-MS. The relative intensity of each peak corresponds to the relative concentration of each compound. The identification of each decomposition product can also be confirmed either by using model compounds and/or by comparing the spectrum with those in a GC-MS library (Pielichowski K et al. 2005).

2.4.2 Reaction Mechanism of polymer degradation

As a matter of fact the cracking of C–C bonds takes place as the result of competition between reactions initiated by thermal and catalytic effects of thermo catalytic degradation. It means that thermal and catalytic reactions do not separate from each other, therefore in discussing thermo catalytic cracking of polymers one has to touch upon both the thermal and catalytic degradation reactions. It is well known, that the thermal (non catalytic) cracking of plastics occurs by a radical mechanism, wherein the initiating radicals are formed by the effect of heat. A diagram of the most probable reactions involved in thermal degradation of polymers is given in figure 2.3. It must be emphasized, however, that the instability of macromolecules under heat treatment is often due to the presence of anomalous weak links in the polymer. In these cases, low molecular weight models of the normal chain unit are much more stable than the polymer.



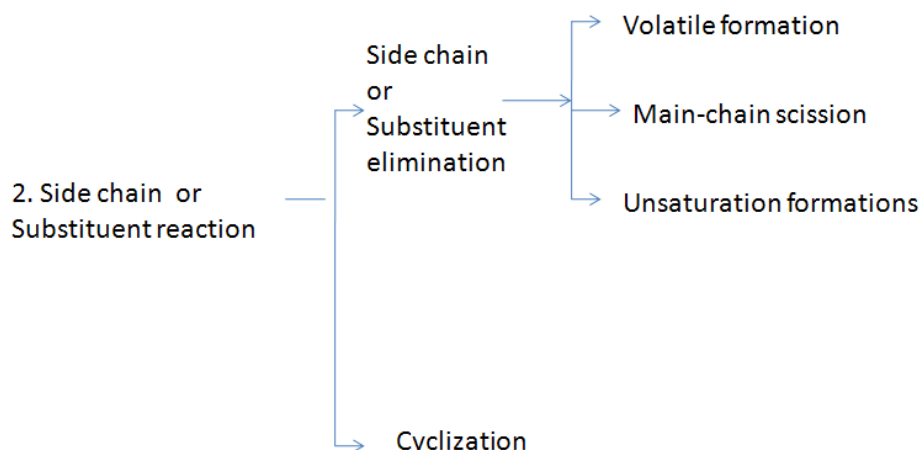


Figure 2.3 Most probable reactions involved in thermal degradation of polymers

On the other hand, catalytic cracking generally proceeds through carbenium ions, which are considered to be produced by the abstraction of hydride ion from the polymer (when the catalyst acts as Lewis acid) or the addition of proton to the polymer (when the catalyst acts as Bronsted acid) macromolecule in the initial reaction step. Fragments formed in the first cracking reactions cracked further into lower molecular weight hydrocarbons on the active sites of the catalyst. Unstable primary fragments are cracked in further decomposition reactions. The following elemental reactions take place both in thermal and thermo-catalytic cases:

(a) Initiation

(b) Formation of secondary radicals

- Depolymerization, formation of monomers;
- Favorable and unfavorable hydrogen transfer reactions;
- Intermolecular hydrogen transfer (formation of paraffins and dienes);
- Isomerization via vinyl groups;

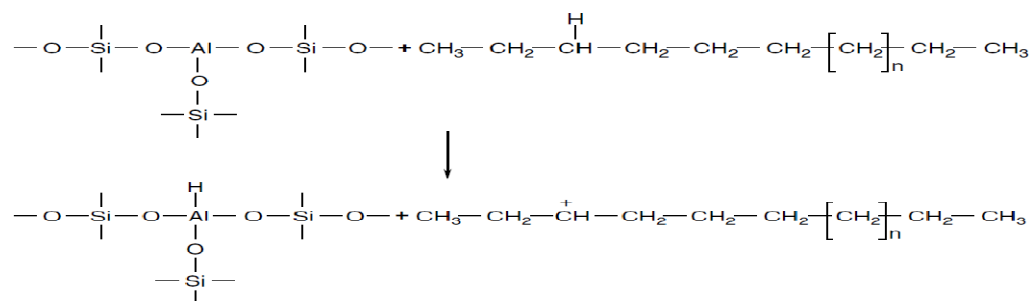
(c) Termination by disproportionation or recombination of radicals

In the presence of catalysts, heterogeneous catalytic cracking occurs on the surface interface of the melted polymer and solid catalysts. The main steps of reactions are as follows: diffusion on the surface of catalyst, adsorption on the catalyst, chemical reaction, desorption from the catalyst, diffusion to the liquid phase. The reaction rate of catalytic reactions is always determined by the slowest elementary reaction. The dominant rate

controlled elementary reactions are the linking of the polymer to the active site of catalyst. But the selectivity of catalysts on raw materials and products might be important. The selectivity is affected by molecular size and shape of raw materials, intermediates and products (Takuma K et al. 2000).

(a) Initiation:

The mechanism of initiation is partly radical in thermo catalytic degradation. The cracking of C–C bonds occurs by homolytic cracking of C–C bonds, at regions with structural faults or distortion of the electron cloud. Thermal decomposition of HDPE initially proceeds essentially by random scission mechanism. But, catalytic cracking generally proceeds through a carbenium ion, which is considered to occur by the abstraction of hydride ion from polymer or the addition of proton on the polymer macromolecule in the initial step of the reaction (Chan JH et al. 1997) which is as shown below.



Bond dissociation energy of C–C and C–H bonds is 347 kJ/mol and 413 kJ/mol, respectively. The cracking of C–C bonds has lower energy consumption, than that of C–H, because it has lower bond energy, by 40–60 kJ/mol, than the C–H bond. Thus, C–C bond dissociation is the more probable initiation step, since it is weaker of the two. The framework of waste polymers might be cracked at C–C bonds at low temperature and both at C–C and C–H bonds at high temperature. Hence, random scission to unstable hydrocarbon radicals is the initiation step in thermal degradation (Wiley J 1966).

Table 2.8 shows the activation energies of elemental reactions in the case of polymer degradation. It is noticeable the initiating reactions have the highest potential barrier. This

potential barrier can be decreased by the use of catalysts and it results a decrease of 50–100 kJ/mol in activation energy (Moriya T et al. 1999).

Table 2.8 Energies of elementary steps in polymer degradation (Moriya T et al. 1999)

Elementary steps	Activation energy (kJ/mol)
Initiation	284-336
Depropagation	21-77
Termination by disproportionation or recombination	4-10
Diffusion in molten state	27
Diffusion in solid state	41

In the presence of catalysts the beginning of cracking of C–C bonds of macromolecules of polymer occurs at a lower temperature than in the absence of catalysts. This phenomenon could be explained by the acidic sites of the catalysts which assist the formation of greater number of unstable molecular fragments at lower temperature. Volatile products are formed from polymers with suitable yields only above 450 °C without catalysts, but at 300–400 °C using catalysts. On the other hand, some noncatalytic cracking takes place at 400–450 °C (Takuma K et al. 2000, Wiley J 1966, Moriya T et al. 1999), because the preferred compounds are aliphatic ones. It is well known that above 450–460 °C the possibility of reactions of cyclization, aromatization and polycondensation increases considerably and these results growing concentrations of naphthenes and aromatics. If waste polyolefins (LDPE, HDPE, PP) have to be converted into aliphatic olefins and paraffins the low temperature is a key parameter.

Another important parameter is the catalyst concentration. Thermo catalytic cracking of HDPE and MDPE over HZSM-5 and Y-zeolite catalysts was carried out in a cycled spheres reactor. It was found that the required temperature of cracking could be decreased by 2% using a low concentration of catalysts, and by 16–20% in the case of greater catalyst concentration because the reaction rate increased with increasing catalyst concentration (Schirmer J et al. 2001).

Smaller differences were found between thermal and thermo catalytic degradations in respect to yields and structure of products at higher temperatures (450–500 °C), than at lower temperatures (400–420 °C).

(b) Formation of secondary unstable compounds

Unstable molecular fragments (radicals and ions) formed in the initiating reaction take part in further decomposition reactions with un cracked macromolecules of polymer or radicals and ions, resulting, among others, in secondary instable compounds of lower molecular weight.

In thermal pyrolysis, the different radicals thus formed from random scission are capable of stabilizing themselves either by hydrogen abstraction or β -scission, all of which form a stable molecule. The reaction that would be favored for stabilization depends on temperature. At (200–300 °C), where sufficient energy is not available for termination of radicals, abstraction is the preferred route for radical stabilization leading to higher hydrocarbons at these low temperatures. However as temperature increases, the increase in H^+ radicals somewhat slows down this reaction. Therefore, abstraction is probably not favored at high temperature. At high temperatures (300 °C), other reactions viz., intermolecular and intramolecular H-transfer, β -scission, etc. become important. Mostly, at higher temperature intermolecular hydrogen transfer takes place followed by β -scission, which justifies the formation of more amounts of lighter hydrocarbons beyond 300 °C. Again, 1,5-hydrogen transfer is important in producing products such as dimers, trimers, tetramers, pentamers etc. At 400–500 °C, β -scission and/or depolymerization is responsible to produce lower molecule (Hujuri U et al. 2011).

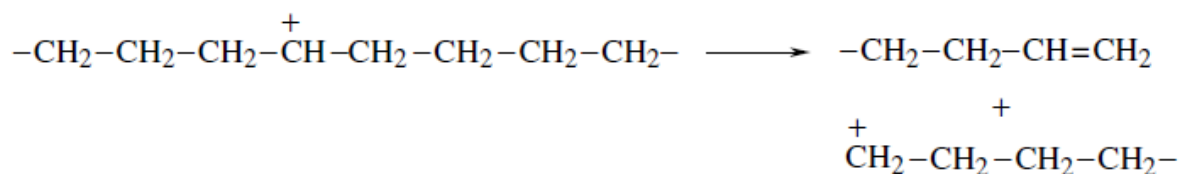
Although, the thermal degradation of PE has been generally classified as “random scission” from the analysis of the degradation products (Seeger M et al. 1975, Seeger M et al. 1977) not all the degradation pathways are random scissions. For example, Murata et al. measured the scission products of PE and PS at various temperatures and pressures and reported that there were two scission pathways from a macroscopic viewpoint. One is the random scission, and other is the chain-end scission (Murata K et al. 2002, Murata K et al. 2004). From a microscopic viewpoint, the chain end radicals are active, which

causes a depolymerization reaction and abstraction of hydrogen from the main chain. Other researchers have reported that six-membered ring formation was the most stable for the radical transfer process (Kiran E et al. 1976).

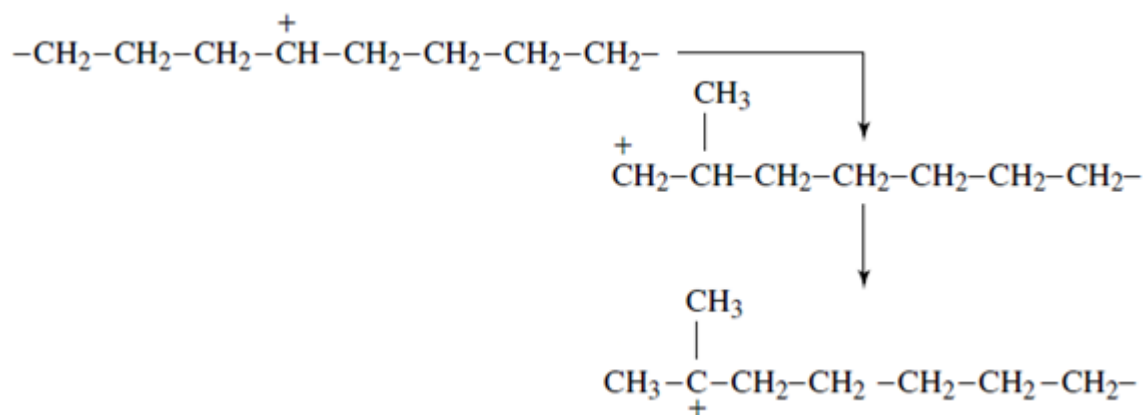
Ueno et al. have studied the degradation pattern of PE at higher temperature to quantify the different session at different temperatures. They found, the amount of scission products does not depend on the carbon number at 590 °C, while the amount of smaller compounds was larger than that of larger chemicals at 800 °C. This indicates that polyethylene decomposes only by primary decomposition at 590 °C while it decomposes through secondary decomposition at 800 °C. The characteristic distribution observed in lower molecular weight could be explained by direct scission and one to five-step radical transfer scission. These results showed that chain-end scission increased along with the temperature. In particular, the direct scission and one-step-radical transfer increased along with the temperature, which indicate that β -scission occurs on the chain end before the radical transfer because the rate of β -scission become faster as the temperature rises (Ueno T et al. 2010).

In addition, at higher temperature the polymer chain cracked to a greater degree; therefore the primary unstable fragments react with alkanes. It is important to note that the probability of formation of aromatics by Diels–Alder reactions is greater. In these reactions, e.g. polyenes might be the precursors of benzene at higher temperature. In the olefins it is found that the double bond moves toward the end of the framework in the case of non branched structures, and that of tertiary carbons of branched structures. Terminal double bonds turn into internal ones in the case of catalytic cracking, but this is not typical in thermal cracking. The different reactions that occur in second step are given below.

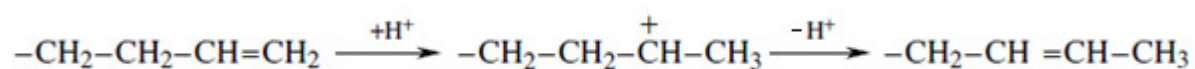
(A) β -scission



(B) Isomerization of carbon framework

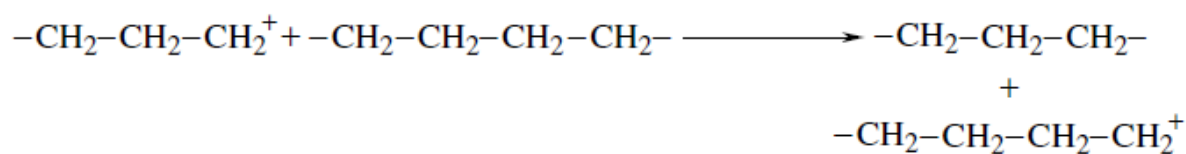


Isomerization of double bond

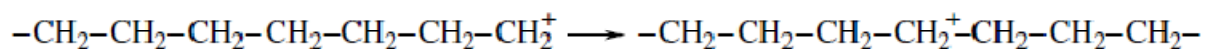


(C) Hydrogen transfer reactions

Intermolecular hydrogen transfer reactions



Intramolecular hydrogen transfer reactions



Generally the concentration of iso-paraffins and olefins increased with decreasing temperature because the increase in further degradation of branched hydrocarbons is

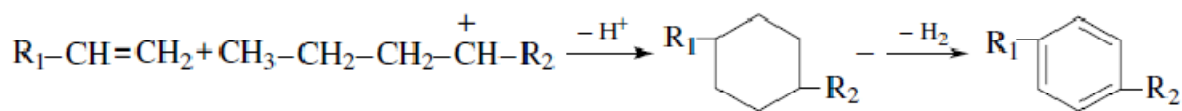
greater, than that of non-branched with increasing temperature. A similar phenomenon could be observed in the case of catalysts possessing a weak hydrogenation property accompanied by considerable acidity, because the olefin intermediates formed are isomerized in greater ratio on the acidic sites of catalysts. On the other hand not only the probability of isomerization, but catalyst activity is decreases with decreasing of the acidity of catalysts.

(c) Termination with recombination or disproportionation:

Primary and secondary unstable molecular fragments formed in the cracking reactions could be stabilized in several ways. Recombination or disproportionation of unstable fragments is one simple way. As a result of recombination the molecular weight and branching of products might be significantly increased. It is important to note that both recombination and disproportionation are second-order reactions according to reaction kinetics.

Cyclization, aromatization or polycondensation are other ways of termination. Basically cyclic alkenes, alkenes, mono and polynucleararenes or coke are formed in these reactions. Termination reactions are principally controlled by the properties of polymers and the temperature.

Cyclization and aromatization



2.4.3 Reaction kinetics of polymer degradation

The description of decomposition reactions during degradation of polymer is quite difficult, because they are very complex in chemical structure. And there are considerable differences between thermal degradation of waste plastics in the absence and presence of catalysts, but the type of reactor or the amount of plastics used for degradation is also important. Degradation in presence of catalysts is called thermo-catalytic degradation.

Cracking experiments are done in batch reactors in 95% of polymer degradation studies (Seo YH et al. 2003, Miskolczi N et al. 2004, Kim JS et al. 2003, Masuda T et al. 1999, Uddin MA et al. 1997, Seddegi ZS et al. 2002, Sakata Y et al. 1997, Grieken RV et al. 2001, Jalil PA 2002, Hwang EY et al. 2002) and within it the thermogravimetric analysis connected with different techniques (e.g. TG, DTG, DSC, TG-MS, etc.) is predominant (Gonzalez J et al. 2001, Garforth A et al. 1997, Marcilla A et al. 2003a, Marcilla A et al. 2003b, Fernandes VJ et al. 1997, Breen C et al. 2000). Only a few researchers have investigated the cracking of waste polymers under continuous or semi-continuous conditions (Mastral FJ et al. 2003, Sharrath PN et al. 1997, Garforth AA et al. 1998, Ali S et al. 2002). One reason for this is that considerable amounts of wastes are needed for continuous cracking and difficulties emerge caused by the geometry of the reactor and greater amounts of materials (e.g. Circulation, heat transfer, coking fouling, etc.) or the feeding of catalysts, their separation from products and regeneration.

Some kinetic models for thermal or catalytic polymer degradation have been proposed. The commonly used approach is first-order kinetics to investigate the characteristics of degradation (Equation 1). In this approach at first the weight loss curve of polymers during the decomposition is determined and overall rate constants are calculated (Gonzalez J et al. 2001, Marcilla A et al. 2003, Fernandes VJ et al. 1997, Lin YH et al. 2001, Gao Z et al. 2003, Yang J et al. 2001, Bate DM et al. 1996). The objectives of experiments are the determination of the apparent activation energies and other reaction kinetic parameters (reaction rate, pre-exponential constant, etc.) of degradation resulting volatile products (gases and liquids). Besides the development of kinetic models the prediction of the yields or main properties of products in the knowledge of properties of the raw material are also important. The principal problem in this case is the derivation of reaction rate constant because some factors significantly affect the conversion of degradation (physical, geometrical, steric, etc.). Usually a constant value of reaction rate is postulated and first-order kinetic equation together with the Arrhenius equation is used. Relations become more difficult when considering autocatalytic reactions. Some correlations exist to calculate reaction kinetic parameters under dynamic circumstances

(Manchado ML et al. 2002, Ballice L et al. 2002). The activation energy and the pre-exponential constant are determined from the logarithmic form of the Arrhenius equation (Equation 2).

$$-\frac{dm}{dt} = km^n \text{-----(1)}$$

$$k = Ae^{\frac{-E}{RT}} \text{-----(2)}$$

Where n is the reaction order, k is the reaction rate coefficient, m is the weight of residue, t is the time of degradation, E is the activation energy and A is the pre-exponential constant.

Relations can be simplified by using thermogravimetric and connected methods, but a new parameter i.e. the heating rate is to be introduced. Table 2.9 shows some of the approaches used for the determination of kinetic parameters (Cho YS et al. 1998, Chan JH et al. 1997, Navarro R et al. 2003).

Table 2.9 Summery of approaches for the determination of kinetic parameters (Ballice L et al. 2002, Chan JH et al. 1997)

Method	Equation	Nomenclature
Flynn-Wall	$\Delta \ln \beta = -1052 \left(\frac{E}{R} \right) \Delta \left(\frac{1}{T} \right)$	E Thermal decomposition activation energy (kj/mol)
Friedmann	$\ln \left(\frac{d\alpha}{dt} \right) = \ln \left\{ A(1-\alpha)^n \right\} - \frac{E}{RT}$	R Gas constant (8.314 j/mol k)
Kissinger	$\ln \left(\frac{\beta}{T_m^2} \right) = \ln \frac{AR}{E} + \ln \left[n(1-\alpha)^{n-1} \right] - \frac{E}{RT}$	T Temperature
Ozawa	$\ln \beta = -0.4567 \frac{E}{RT} + \left(\log \frac{AE}{R} - \log F(\alpha) - 2.315 \right)$ Where, $F(\alpha) = \int_0^\alpha \frac{d\alpha}{(1-\alpha)^n} = \frac{A}{\beta} \int_{T_a}^T \exp \left(\frac{-E}{RT} \right) dT$	β Heating rate ($^0C/min$) α Conversion (extent of reaction) da/dt Rates of weight loss n Order of reaction T_m Temperature corresponding to the maximum reaction rate

Horowitz-Metger	$\ln \ln \left\{ \frac{1}{(1-\alpha)} \right\} = \frac{E\theta}{RT_s^2}$	A Pre-exponential factor T _s is the temperature at which 1- α=1/exp=0.368 θ=T-T _s
-----------------	--	--

When comparing the equations in table 2.9, it is found that the equations of Flynn–Wall, Horowitz–Metger and Friedmann gave excellent correlation in the case of degradation of polypropylene (Cho YS et al. 1998, Chan JH et al. 1997a). Others created software to calculate the reaction kinetic parameters using the first-order kinetic equation based on these equations. Key parameters were calculated with the minimization of differences between calculated and experimental results obtained directly by a thermogravimetric apparatus (Ballice L et al. 2002). Good correlation between data was observed in case of HDPE and PS by using this software.

The main problem in case of thermo-catalytic cracking of polymers is the activity loss of catalysts; therefore first-order kinetics is applicable only with some simplifications in thermo-catalytic cases. On the other hand there is a relation modeling the fluid catalytic cracking taking into consideration the catalyst deactivation in refineries [91]:

$$\eta = \exp[-\alpha C(c)] \text{ --- (3)}$$

Where η is the activation loss of catalyst, C(c) is the coking of catalyst and α is a constant depending on the type of catalyst.

Equation (3) was used to model the thermo-catalytic degradation of waste polyethylene and polypropylene (Lin YH et al. 2001). In this case researchers had to calculate η for each catalyst. On the other hand it is complicated; therefore researchers disregard the change of reaction rate and order caused by deactivation of catalysts in most experiments. The reaction rates and other reaction kinetic parameters are given in table 2.10 (Miranda R et al. 2001).

Table 2.10 The reaction rates and other reaction kinetic parameters of degradation of waste polyethylene (Miranda R et al. 2001)

Kinetic Model	Equation	E _a (kJ/mol)	n	A (min ⁻¹)
$\text{HDPE} \xrightarrow{k_t} \text{V} + \text{R}$ V: volatile products; R: Residue products	$\frac{d[\text{HDPE}]}{dt} = -Ae^{\frac{-E}{RT}} [\text{HDPE}]^n,$ E =Thermal decomposition activation energy (kJ/mol), R= Gas constant (8.314 j/mol k), T =Temperature, n= Order of reaction	250	0.65	1.71×10^{17}

There are also some empirical equations for describing the yields of products formed in the cracking reactions of polymers. One of them is the Atkinson and McCaffrey kinetic model, which derives the weight loss of polymer for their initial degree of polymerization, weight of sample and reaction rate. As a matter of fact the reaction rate constant is calculated by using a first-order kinetic equation (Horvat N et al. 1999, Caffrey WCM et al. 1995).

The temperature significantly affects the conversion of thermo-catalytic degradation besides the characteristic of catalysts. The time–temperature superposition describes the dependence of reaction rate from temperature. The conversion can be increased both with degradation temperature and time. It means that the cracking time which is needed to achieve the same degree of conversion decreases with increasing temperature. The shift factor is the quotient of cracking times at different temperatures or the quotient of temperatures at different cracking times. The value of the shift factor is affected by the characteristics of the polymer and by the cracking conditions. There are two methods to derive the shift factors: the Arrhenius equation and the Williams–Landel–Ferry (WLF) equation. Chan et al. calculated the value of shift factors in case of polypropylene degradation (Chan JH et al. 1997b). It was found that the product of reaction rate coefficients and cracking times at different temperatures is nearly constant. The shift

factors and constants of the WLF equations can be calculated by the use of these similarities.

2.5 Performance and emission analysis of waste plastics oil in CI engine

The properties of waste plastic oil was compared with the petroleum products and found that it can also be used as fuel in compression ignition engines (Mani M et al. 2009a). Most of the research work has been done by mixing oil developed from waste plastic disposal with heavy oil for marine application. The results showed that waste plastic disposal oil when mixed with heavy oils reduces the viscosity significantly and improves the engine performance. However, very little has been done to test their use in high-speed diesel engines.

Mani et al. used waste plastic oil as an alternate fuel in a DI diesel engine without any modification and studied the performance, emission and combustion characteristics of a single cylinder, four-stroke, air-cooled DI diesel engine. The experimental results showed a stable performance with brake thermal efficiency similar to that of diesel. Carbon dioxide and unburned hydrocarbon were marginally higher than that of the diesel baseline. The toxic gas carbon monoxide emission of waste plastic oil was higher than diesel. Smoke reduced by about 40% to 50% in waste plastic oil at all loads (Mani M et al. 2009b).

Mani et al. experimentally investigated the influence of injection timing on the performance, emission and combustion characteristics of a single cylinder, four stroke, direct injection diesel engine using waste plastic oil as a fuel. Tests were performed at four injection timings (23°, 20°, 17° and 14° bTDC). When compared to the standard injection timing of 23° BTDC the retarded injection timing of 14° bTDC resulted in decreased oxides of nitrogen, carbon monoxide and unburned hydrocarbon while the brake thermal efficiency, carbon dioxide and smoke increased under all the test conditions (Mani M et al. 2009a).

Chapter 3

Experimental

EXPERIMENTAL

3.1 Materials

3.1.1 Virgin and Waste high-density polyethylene: HDPE pellets (2.5 mm in size) obtained from Reliance industries limited, India with density 0.945 g/cc^3 , Melt Flow Index (MFI) value $0.2\text{-}15 \text{ g/10 min}^{-1}$ (at 190°C and 2.16 kg load) and melting point 133°C were used for experiments. These plastic pellets were used directly in the thermal pyrolysis reaction. Waste HDPE (used mobil oil containers) was collected from the National Institute of Technology Rourkela, Orissa, India campus waste yard and used in this experiment. The plastic waste was cut into small pieces (approx. 1 cm^2) and used in the pyrolysis experiments (Figure 3.1). The waste HDPE sample is identified by determining melting temperature and glass transition temperature from DSC curve of the sample (Figure 3.2). The melting point of the waste sample is found to be 137°C which ensures the samples to be high-density polyethylene. Thermo gravimetric analysis of the virgin and waste HDPE samples were carried out with a SHIMADZU DTG-60/60H instrument. A known weight of the samples were heated in a silica crucible at a constant heating rate of 20°C/min operating in a stream of nitrogen with a flow rate of 40ml/min from 32°C to 700°C . The proximate analysis of HDPE pellets and waste HDPE was done by ASTM D3173-75 and ultimate analysis was done using CHNS analyzer (ELEMENTAR VARIO EL CUBE CHNSO). Calorific value of the raw materials was found by ASTM D5868-10a.



Figure 3.1 Virgin HDPE, Used mobil oil containers, Small pieces of used mobil oil containers

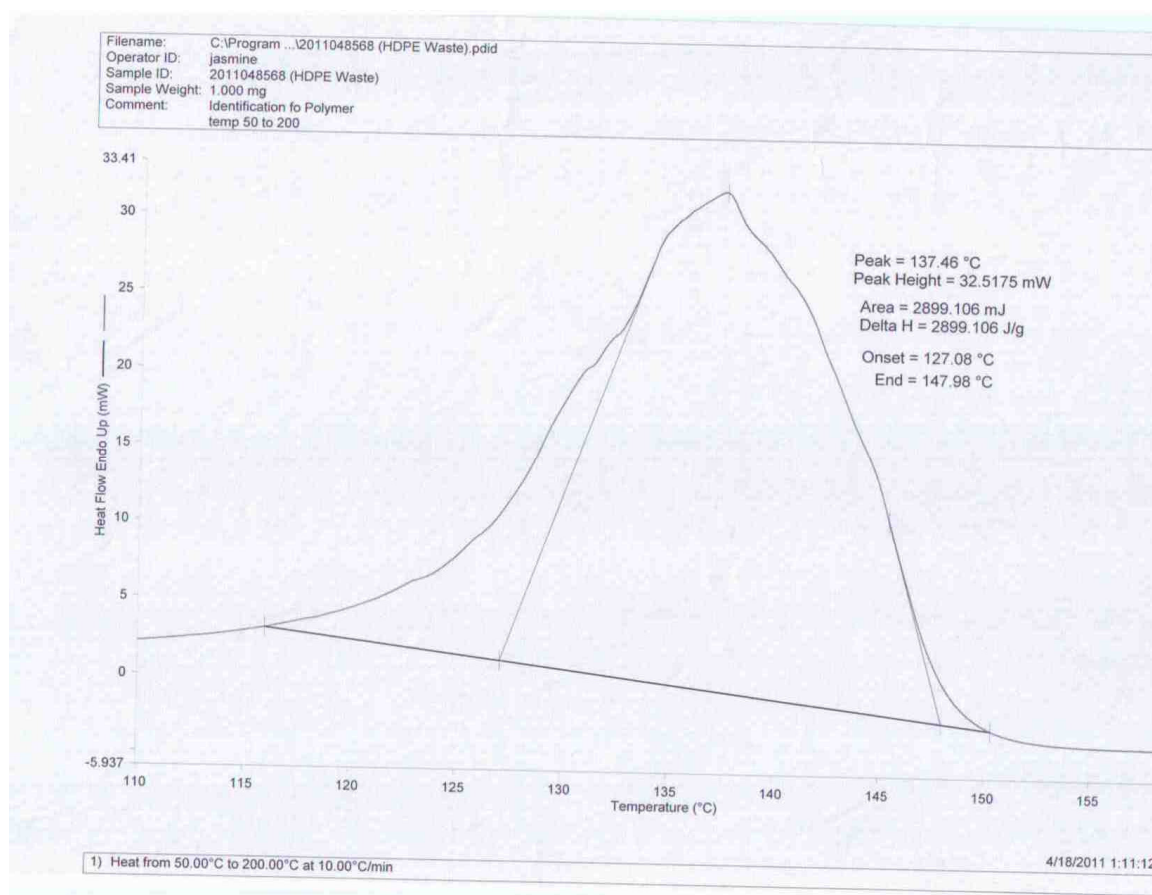


Figure 3.2 DSC of waste HDPE

3.1.2 Catalyst: Three types of catalysts were used in this experiment. They are kaolin, silica alumina and mordenite.

3.1.2.1 Kaolin: Commercial grade kaolin clay procured from Chemtex Corporation, Kolkata, India was used as catalyst in the pyrolysis reaction. The chemical composition of the kaolin sample was found to be SiO₂ 43.12 %, Al₂O₃ 46.07 %, Fe₂O₃ nil, MgO 0.027 %, CaO 0.030 %, ZnO 0.0064%, K₂O 0.01%, TiO₂ 0.74, LOI at 1000 °C 9.9%. The XRD of the sample (Figure 3.3) showed well defined reflections at 2 theta value of 12° and 25° corresponding to the d values of 7.154 Å. These peaks correspond to the reflections from [001], which are typical characteristic peaks of kaolinite. Again the peaks corresponding to the 2θ value 34–36°, 38–42°, 45–50°, and 54–63° may vary for kaolinites from different origin (Zhou Z et al. 2003). From the proximate analysis and

XRD report it could be concluded that the major component of the sample was kaolinite with Hinckley index of 0.4.

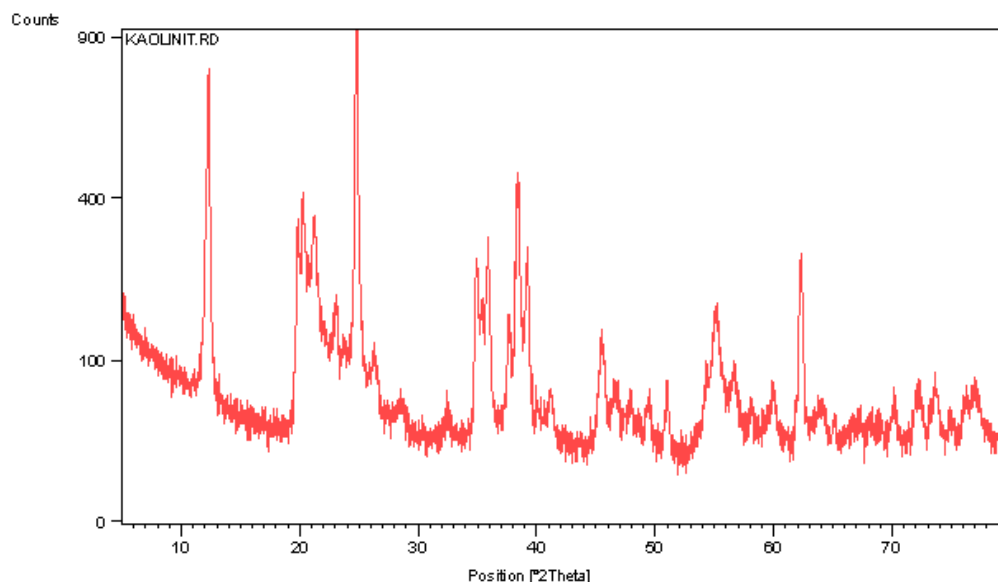


Figure 3.3 XRD of kaolin

Some traces of impurities (may be mica, quartz and feldspar which could not be traced in the XRD report) were also present which contribute the components other than SiO_2 and Al_2O_3 . The BET surface area of kaolin was found to be $23\text{m}^2/\text{g}$. The pore size distributions of kaolinite samples showed a sharp peak at a radius of 3.5nm , thus it is mesoporous. The acidity of the kaolin determined using ammonia-temperature programmed desorption method was $0.04\text{ mmol NH}_3/\text{g}$.

3.1.2.2 Silica Alumina: Commercial grade Silica Alumina was procured from Chemtex Corporation, Kolkata, India. The chemical composition of the Silica Alumina sample was found to be SiO_2 42.45%, Al_2O_3 35.1300%, Fe_2O_3 1.3100%, MgO 1.1060%, CaO 2.1430%, ZnO 0.0064%, K_2O 0.4410%, TiO_2 0.5600%, LOI at 1000°C 16.82%. The XRD (Figure 3.4) of the sample showed well defined reflections at 2 theta value of 12° , 20° , 25° , 27° , 35° , 38° , and 62° . The surface area and acidity of the sample was found to be $29\text{ m}^2/\text{g}$ and $0.214\text{mmol NH}_3/\text{g}$ respectively.

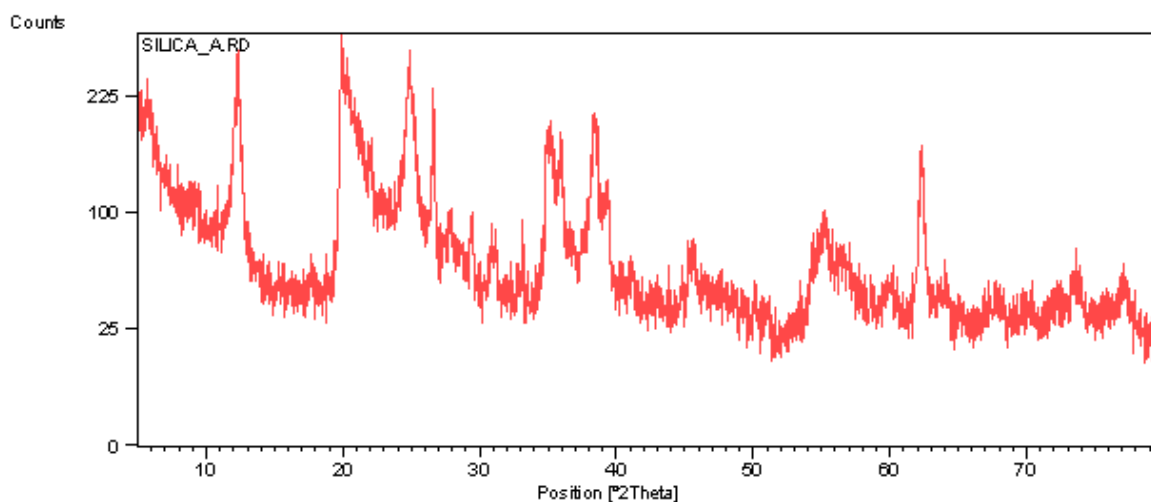


Figure 3.4 XRD of Silica Alumina

3.1.2.2 Mordenite: Commercial grade Mordenite was procured from Chemtex Corporation, Kolkata, India. The chemical composition of Mordenite sample was SiO_2 48.12%, Al_2O_3 34.54%, Fe_2O_3 2.48%, MgO 0.50%, CaO 0.83%, ZnO 0.0081%, K_2O 0.68%, TiO_2 0.40%, LOI at 1000 °C 12.44%. The XRD (Figure 3.5) of the sample showed well defined reflections at 2 theta value of 15°, 24°, 28°, 39°, 46° and 55°. The surface area and acidity of the sample was found to be 51 m^2/g and 1.121mmol NH_3/g respectively.

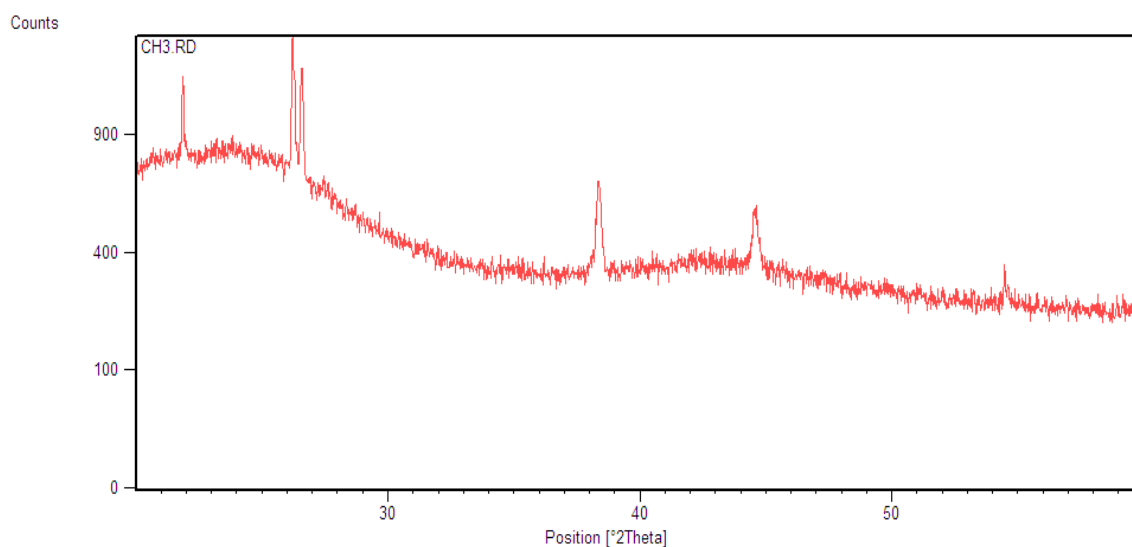


Figure 3.5 XRD of Mordenite

3.2 Methods

3.2.1 Catalyst modification: The thermo-chemical activation/modification was carried out by adding 50g of the kaolin clay to 500ml of four different acids (HNO_3 , HCl , H_3PO_4 and CH_3COOH) and a base (NaOH) of 3M concentration and refluxing at 110 °C under the atmospheric pressure in a round bottomed flask equipped with a reflux condenser for four hours. The resulting clay suspension was then rapidly quenched by adding 500ml ice cold water. The content was then filtered, repeatedly washed with distilled water to remove any unspent reagent, dried in an oven, calcined at 550 °C for four hours and ground in a mortar pastel to powder form. The untreated sample is referred to as K and treated samples are referred to as KHNO_3 , KHCl , KH_3PO_4 , KCH_3COOH , and KNaOH in the subsequent text where the name refers to the treated kaolin with different acid and base as indicated.

3.2.2 Catalyst characterization technique: The different acid treated kaolin clay materials were characterized by X-Ray Fluorescence spectroscopy (XRF), X-Ray Diffraction (XRD), Fourier Transformed Infrared Spectroscopy (FTIR), Thermogravimetric Analysis (TGA), Differential Thermal Analysis (DTA), sorptometric studies, Scanning Electron Microscope (SEM) and by temperature programme desorption ammonia methods.

3.2.2.1 X-Ray Fluorescence (XRF): XRF analyses of the samples were done using a Model-PW2400 of Phillips make, with X-ray tube of rhodium anode and scintillation detector with a current 40mA and voltage 40mV.

3.2.2.2 X-Ray Diffraction (XRD): The X-ray diffraction data was collected using a Philips Analytical X-ray Instrument, X'Pert-MPD (PW 3020 vertical goniometer and PW 3710 MPD control unit) employing Bragg–Brentano parafocusing optics. The XRD patterns were recorded in the range of 5–70° with a scanning rate of 2°/min.

3.2.2.3 Fourier Transformed Infrared Spectroscopy (FTIR): FTIR spectra were recorded on a Perkin-Elmer infrared spectrophotometer as KBr pellets with resolution of 4 cm^{-1} , in the range of 400–4000 cm^{-1} . The sample and analytical grade KBr were dried at 100 °C over-night prior to the FTIR analysis.

3.2.2.4 Thermogravimetric/Differential Thermal Analysis (TG/DTA):

Thermogravimetric analyses were carried out with a SHIMADZU DTG-60/60H instrument. A known weight of the sample was heated in a silica crucible at a constant heating rate of 10 °C/min operating in a stream of N₂ atmosphere with a flow rate of 40ml/min from 35 °C to 600 °C.

3.2.2.5 Sorptometric studies: Nitrogen adsorption–desorption measurements (BET method) were performed at liquid nitrogen temperature (–196 °C) with an autosorb BET apparatus from Quantachrome Corporation. The analysis procedure is automated and operates with the static volumetric technique. Before each measurement, the samples were outgassed first at 200 °C for 2 hours, at 5×10^{-3} torr and then at room temperature for 2 hours, at 0.75×10^{-6} torr. The isotherms were used to determine the specific surface areas using the BET equation.

3.2.2.6 Scanning Electron Microscope (SEM): Scanning electron micrographs were taken on a JEOL-JSM 5600 LV microscope, equipped with a 6587 EDS (energy dispersive X-ray spectrometry) detector, using an accelerating voltage of 15 kV. The samples were deposited on a sample holder with an adhesive carbon foil and sputtered with gold.

3.2.2.7 Temperature programmed desorption of ammonia method (NH₃-TPD): The acid properties of the catalysts were probed by ammonia TPD measurements in Micromeritics 2900 TPD equipment. Previously, the samples were outgassed under He flow (50Nml/min) by heating with a rate of 15 °C/min up to 560 °C and remaining at this temperature for 30 min. After cooling to 180 °C, the samples were treated with a 30Nml/min ammonia flow for 30 min. The physisorbed ammonia was removed by passing a He flow at 180 °C for 90 min. The chemically adsorbed ammonia was determined by increasing the temperature up to 550 °C with a heating rate of 15 °C/min, remaining at this temperature for 30 min, and monitoring the ammonia concentration in the effluent He stream with a thermal conductivity detector.

3.2.3 Pyrolysis experimental set up: The pyrolysis setup used in this experiment is a batch reactor shown in the Figure 3.6 and 3.7. It consists of a reactor made of stainless

steel tube (length- 145 mm, internal diameter- 37 mm and outer diameter- 41 mm) sealed at one end and an outlet tube at other end for obtaining the volatile/gas/oil products of the reaction.



Figure 3.6 Experimental set up



Figure 3.7 stainless steel reactor

The SS tube is heated externally by an electric furnace, with the temperature being measured by a Cr-Al: K type thermocouple fixed inside the reactor and temperature is controlled by external PID controller. Shimaden PID controller SR1 was used to control the temperature of the furnace. The accuracy of this PID controller is $\pm 0.3\%$ FS (FS = 1200°C). So the temperature can be measured with $\pm 3.6^\circ\text{C}$.

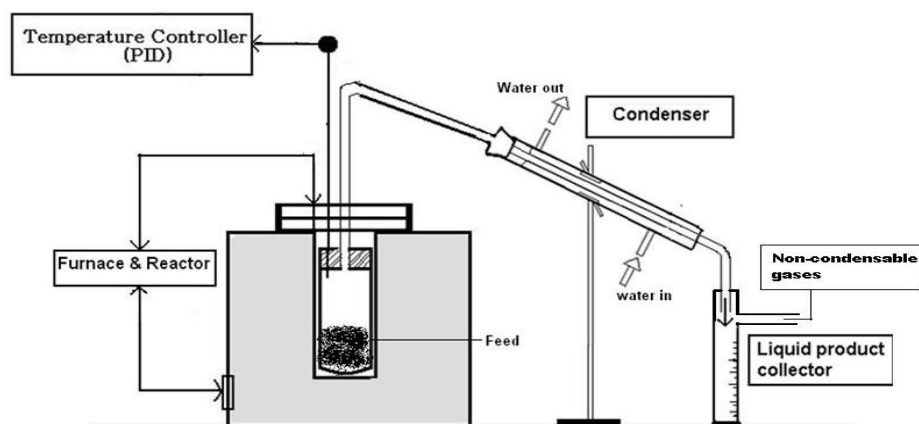


Figure 3.8 Schematic representation of pyrolysis set up

3.2.4 Pyrolysis experimental procedure: 20g. of plastics samples (virgin HDPE and waste HDPE) were loaded in each pyrolysis reaction. Precision balance of SHINKO DENSHI Co. LTD, JAPAN, Model: DJ 300S was used to measure the weight of the samples. This machine capacity is 200 gram and accuracy is 0.0001 gram and so the weight can be measured within ± 0.0001 g.

In the catalytic pyrolysis, a mixture of catalyst and the plastics samples in different catalyst to plastics proportion (1:4, 2:4, 3:4, 4:4) was subjected to pyrolysis in the reactor set up and heated at a rate of 20 °C/min up to the desired temperature. The condensable liquid products were collected through the condenser and weighed. After pyrolysis, the solid residue left out inside the reactor was weighed. Then the weight of gaseous product was calculated from the material balance. Reactions were carried out at different temperatures ranging from 400-550 °C.

3.2.5 Analysis of pyrolysis oil: The pyrolytic oil has been characterized for physical and chemical properties.

3.2.5.1 Physical properties of pyrolysis oil: All the fuel properties of the oil were tested by prescribed IS-1448 methods and summarized in the Table 3.1

Table 3.1 Test protocols

Properties	Test methods	Properties	Test methods
Specific Gravity	I.S.1448 P.16	Flash Point	I.S.1448: P:20
Density	I.S.1448 P.16	Fire Point	I.S. 1448 P:20
Kinematic Viscosity	I.S.,1448 P: 25	Gross Calorific Value	I.S. 1448: P:6
Pour Point	I.S.1448 P:10	Calculated Cetane Index	I.S.1448 :P:9
Cloud Point	I.S.1448: P:10	Distillation	I.S. 1448: P.18

The density and specific gravity measurement is done with accuracy of ± 0.0005 g/ml. and the other parameters such as pour point, cloud point, flash point and fire point is measured with $\pm 1^\circ\text{C}$ accuracy.

3.2.5.2 Chemical properties of pyrolysis oil

3.2.5.2.1 Fourier transformation infrared spectroscopy (FTIR): FTIR of the pyrolysis oil obtained at different temperatures were taken in a Perkin-Elmer Fourier transformed infrared spectrophotometer with resolution of 4 cm^{-1} , in the range of $400\text{--}4000\text{ cm}^{-1}$ using Nujol mull as reference to know the functional group composition.

3.2.5.2.2 Gas chromatography and mass spectroscopy (GC/MS): The GC/MS of the oil sample was carried out in Sargam laboratory, Chennai. The specification of GC/MS is summarized below.

Instrument: GC-MS-QP 2010 [SHIMADZU]

GC Condition

Column Oven Temperature: 70°C, Injector Temperature: 200°C, Injection Mode: Split

Split Ratio: 10, Flow Control Mode: Linear Velocity, Column Flow: 1.51ml/min,

Carrier Gas-Helium: 99.9995% purity

Column Oven Temperature Program

Rate	Temperature (°C)	Hold Time (min)
-	70.0	2.0
10	300.0	7.0 (32 mins total)

Column : DB-5

Length: 30.0m

Diameter: 0.25mm

Film Thickness: 0.25µm

MS Condition

Ion Source Temperature : 200 °C

Interface Temperature : 240 °C

Start m/z : 40

End m/z : 1000

Chapter 4

Virgin HDPE Pyrolysis

THERMAL DEGRADATION OF VIRGIN HIGH-DENSITY POLYETHYLENE TO LIQUID FUEL

4.1. Introduction

High-density polyethylene (HDPE) is a thermoplastic material composed of carbon and hydrogen atoms joined together forming high molecular weight products. Methane gas is converted into ethylene, then, with the application of heat and pressure, into polyethylene. The polymer chain may be 500,000 to 1,000,000 carbon units long. HDPE has a linear structure, with little or no branching. Short and/or long side chain molecules exist with the polymer's long main chain molecules. The longer the main chain, the greater the number of atoms, and consequently, the greater the molecular weight. The molecular weight, the molecular weight distribution and the amount of branching determine many of the mechanical and chemical properties of the end product. High-density polyethylene resin has a greater proportion of crystalline regions than low-density polyethylene. The size and size distribution of crystalline regions are determinants of the tensile strength and environmental stress crack resistance of the end product. Figure 4.1 is a schematic diagram of high density polyethylene structure.

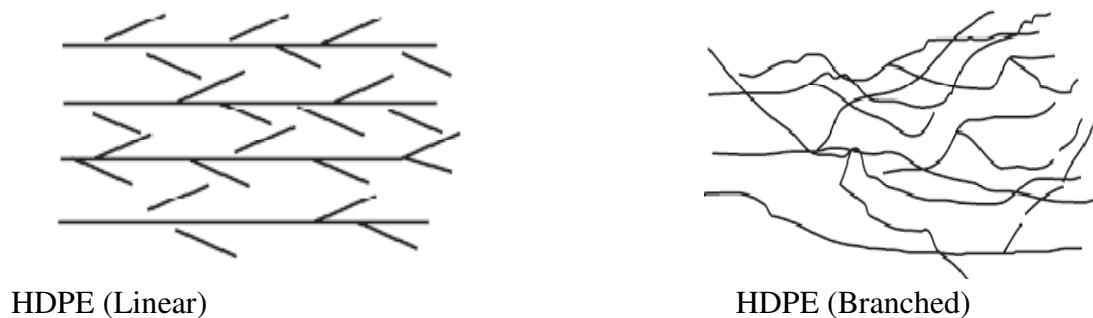


Figure 4.1. Schematic of linear and branched arrangements

HDPE has little branching, giving it stronger intermolecular forces and tensile strength than lower-density polyethylene. It is also harder and more opaque and can withstand somewhat higher temperature. High-density polyethylene, unlike polypropylene cannot

withstand normally-required autoclaving conditions. The lack of branching is ensured by an appropriate choice of catalyst. HDPE contains the chemical elements carbon and hydrogen.

High-density polyethylene (HDPE) is the third-largest commodity plastic material in the world, after polyvinyl chloride and polypropylene in terms of volume. According to a British market-research consulting agency, “Merchant Research & Consulting Ltd.” High density polyethylene (HDPE) has accounted for a major share of ethylene consumption structure over the recent years. The demand for HDPE has increased 4.4% in a year to 31.3 million MT in 2009 ([Plastics Production](#)).

Thermal pyrolysis of high-density polyethylene was reported in the literature review chapter. This work focuses on characterization of liquid fuel obtained from thermal pyrolysis of virgin high density polyethylene at different temperature range. Thermal pyrolysis of high density polyethylene pellets was done in a semi-batch reactor at a temperature range of 400 °C to 550 °C and at a heating rate of 20 °C/min. The effect of pyrolytic temperature on reaction time, liquid yield, and volatiles were also studied. The obtained liquid fuel was characterized for different physical and chemical properties using GC-MS, and FTIR.

4.2. Experimental programme

The details about the virgin high-density polyethylene used in this experiment, the experimental set up and procedure are summarized in the experimental section 3.

4.3. Result and discussion

4.3.1. Proximate and ultimate analysis of virgin HDPE

The proximate and ultimate analysis of virgin HDPE sample is shown in Table 4.1. The volatile matter is 100% in the proximate analysis, due to the negligible percentage of ash in virgin HDPE sample, its degradation occurs with minimal formation of residue. The oxygen is 2.51% in the ultimate analysis of virgin HDPE. The nitrogen and oxygen in the virgin HDPE sample may not be due to the fillers but due to the other ingredients which are added to resin during the manufacturing of HDPE.

Table 4.1. Proximate and ultimate analysis of virgin HDPE

Properties	Virgin HDPE
Proximate Analysis	
Moisture content	0.00
Volatile matter	100
Fixed carbon	0.00
Ash content	0.00
Ultimate Analysis	
Carbon (C)	82.69
Hydrogen (H)	13.93
Nitrogen (N)	0.80
Sulphur (S)	0.07
Oxygen (O)/Others	2.51
GCV (Mj/Kg)	47.64

4.3.2. TGA and DTG analysis of virgin HDPE sample

Thermogravimetric analysis (TGA) is a thermal analysis technique which measures the weight change in a material as a function of temperature and time, in a controlled environment. This can be very useful to investigate the thermal stability of a material, or to investigate its behavior in different atmospheres (e.g. inert or oxidizing). TGA applied in determination of the study of thermal stability/degradation of virgin HDPE in various ranges of temperature.

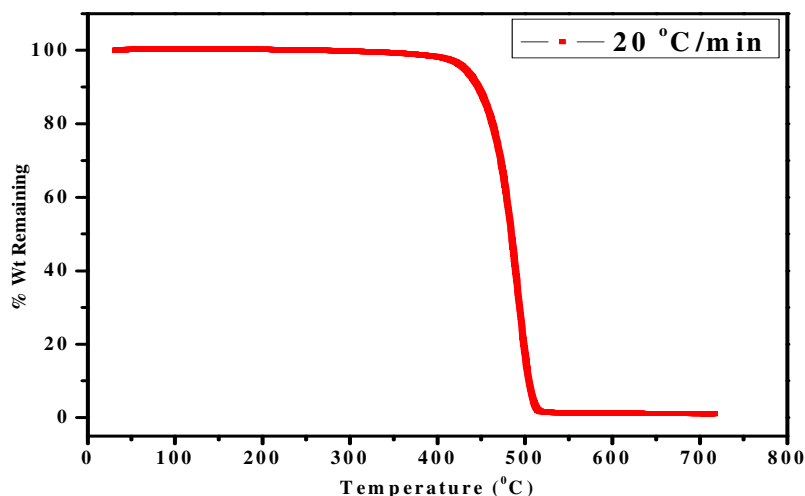


Figure 4.2. TGA curve of virgin HDPE

From the TGA curve as showed in figure 4.2, the virgin HDPE degradation started at 380 °C and was completed at 510 °C for a heating rate of 20 °C/min in nitrogen atmosphere. The degradation temperature at which weight loss of 50% (T_{50}) takes place was about 460 °C for virgin HDPE. The temperature range for waste HDPE was 390 °C to 490 °C and maximum weight loss occurred at temperature 440 °C as demonstrated (Kumar S et al. 2011). A similar trend of nature during the analysis of HDPE decomposition by TGA/DTG has reported by A. Aboulkas (Aboulkas A et al. 2007). Differential thermogravimetry (DTG) curve for virgin HDPE contains only one peak, this indicates that there is only one degradation step in figure 4.3 it has shown that the dominant peak over 390 °C to 510 °C where the conversion takes place.

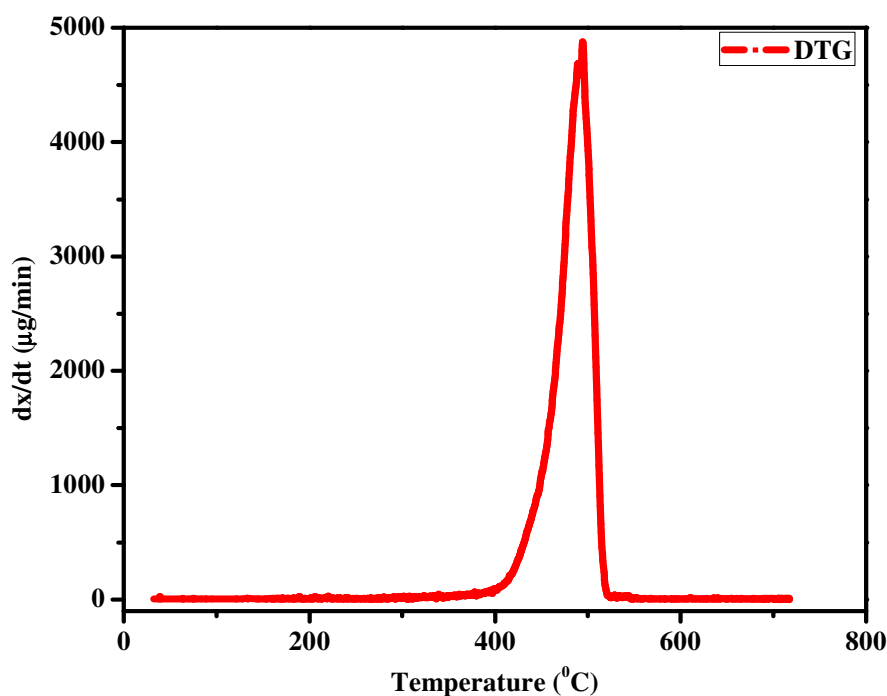


Figure 4.3. DTG curve of virgin HDPE

Though pyrolysis of individual polymers has attracted much attention, studies on pyrolysis behavior, particularly of mixed plastics, are rather scarce. Still, from the study reported by J. Chattopadhyay (Chattopadhyay J et al. 2008) it can be deduced that the mixture of HDPE, PP and PET starts decomposing at about 250 °C against 477 °C for pure HDPE (Zhou L et al. 2006). The decomposition of these two plastic samples ends at 521 °C and 700 °C, respectively. In the latter case, solid residue seems to have formed due the presence of PET. The addition of PP in HDPE has been reported by G. Hwang to improve the liquid yield during the degradation in supercritical acetone (450 °C to 470 °C, and 60 atm to 100 atm) (Hwang G et al. 2001). In case of catalytic decomposition, a reduction of 20 °C was reported when LDPE, PP and PS were present along with HDPE (Lee K et al. 2003).

4.4. Effect of temperature on product distribution

The pyrolysis of virgin HDPE yielded four different products i.e. oil, gas, wax, solid residue or coke. The distributions of these fractions are different at different temperatures and are shown in the Table 4.2.

Table 4.2. Distribution of different fractions at different temperatures in thermal pyrolysis of virgin HDPE

Temperature (°C)	Oil (wt%)	Residue (wt%)	Wax (wt%)	Gas/volatile (wt%)	Reaction time (min)
400	31.3	5.65	7.7	45.35	680
450	52.46	3.95	8.9	34.69	175
500	44.32	1.29	28.99	25.4	80
550	8.83	0.68	52.02	38.47	50

The condensable oil/wax (a mixture of alkanes that falls within the $20 \leq n \leq 40$ range; they are found in the solid state at room temperature and begin to enter the liquid phase past approximately 37 °C) and the non-condensable gas/volatiles fractions of the reaction

constituted major product as compared to the solid residue (coke) fractions. The condensable product obtained at low temperature (400 °C) was low viscous liquids. With increase in temperature, the liquid became viscous/wax at and above 450 °C. The hydrocarbon is continuously cracking; the wax may be representative of the intermediate molecular weight products. The recovery of condensable fraction was very low at low temperature i.e. at 400 °C and increased with gradual increase of temperature. From the Table 4.2, it is observed that at low temperature the reaction time was more, due to which secondary cracking of the pyrolysis product occurred inside the reactor and resulted in highly volatile product. The low temperature molecular weight changes without volatilization are principally due to the scission of weak links, such as oxygen, incorporated into the main chain as impurities. Similarly, the low liquid yield at high temperature was due to volatilizing higher molecular weight products before undergoing further cracking and more non-condensable gaseous/volatile fractions due to rigorous cracking.

4.5. Effect of temperature on reaction time

The effect of temperature on the reaction time of the reaction for the pyrolysis of virgin HDPE plastic is shown in Figure 4.4. The pyrolysis reaction rate increased and reaction time decreased with increase in temperature. High temperature supports the easy cleavage of bond and thus speeds up the reaction and lowers the reaction time. HDPE with long linear polymer chain with low branching and high degree of crystallinity led to high strength properties and thus required more time for decomposition. This shows that temperature has significant effect on reaction time and yield of liquid, wax and gaseous products. Similar effect of temperature on reaction time for waste HDPE has been demonstrated ([Kumar S et al. 2011](#)).

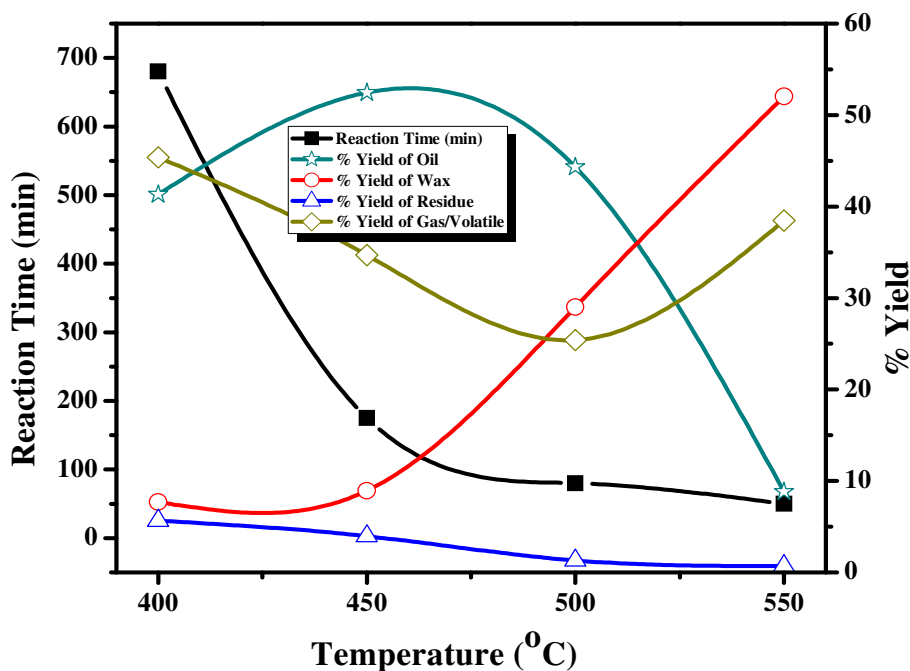


Figure 4.4. Effect of temperature on reaction time and product distribution

4.6. Characterization of the liquid product

4.6.1. FT-IR of the oil sample obtained at 450 °C

Fourier Transform Infrared spectroscopy (FTIR) is an important analysis technique which detects various characteristic functional groups present in oil. On interaction of an infrared light with oil, chemical bond will stretch, contract, and absorb infrared radiation in a specific wave length range regardless the structure of the rest of the molecules.

Figure 4.5 shows the FTIR spectra of virgin HDPE oil. The presence of alkanes is detected at 2918.68 cm^{-1} with C-H stretching vibrations. C=C stretching at 1647.39 cm^{-1} indicates the presence of alkenes. The presence of alkanes was detected by C-H scissoring and bending vibrations at 1440.22 cm^{-1} . The presence of alcohols, ethers, carboxylic acids, esters is detected by C-O stretching vibrations at 907.61 cm^{-1} and the C-H bending vibrations at frequency 719.92 indicates the presence of phenyl ring

substitution bands. The results were found consistent when compared with the results of GC-MS.

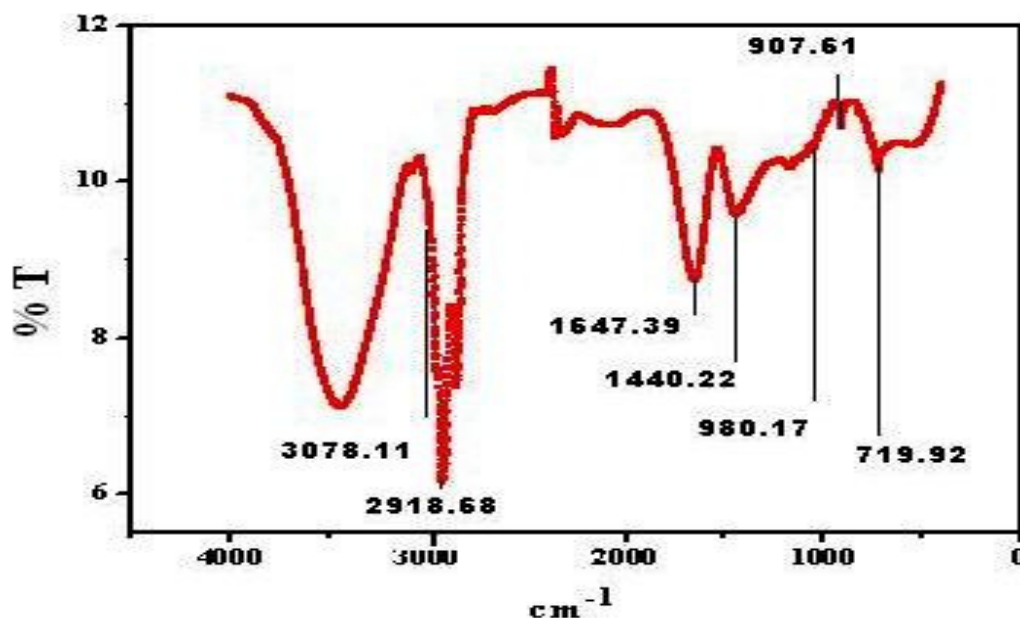


Figure 4.5. FT-IR spectrometry of virgin HDPE pyrolytic oil

4.6.2. GC-MS of the oil sample

The GC-MS analysis of the oil sample obtained by the thermal pyrolysis of virgin HDPE was carried out to know the compounds present in the oil (Figure 4.6) and is summarized in the Table 4.3. It has been observed that the pyrolytic oil contains around 25 compounds. Taking into account of area percentage, the highest peak areas of total ion chromatogram (TIC) of the compounds were n-Octadecane, n-Heptadecane, 1-Pentadecene, Octadecane, Pentadecane and 1-Nonadecene. The components present in HDPE are mostly the aliphatic hydrocarbons (alkanes and alkenes) with carbon number C₁₀-C₂₀.

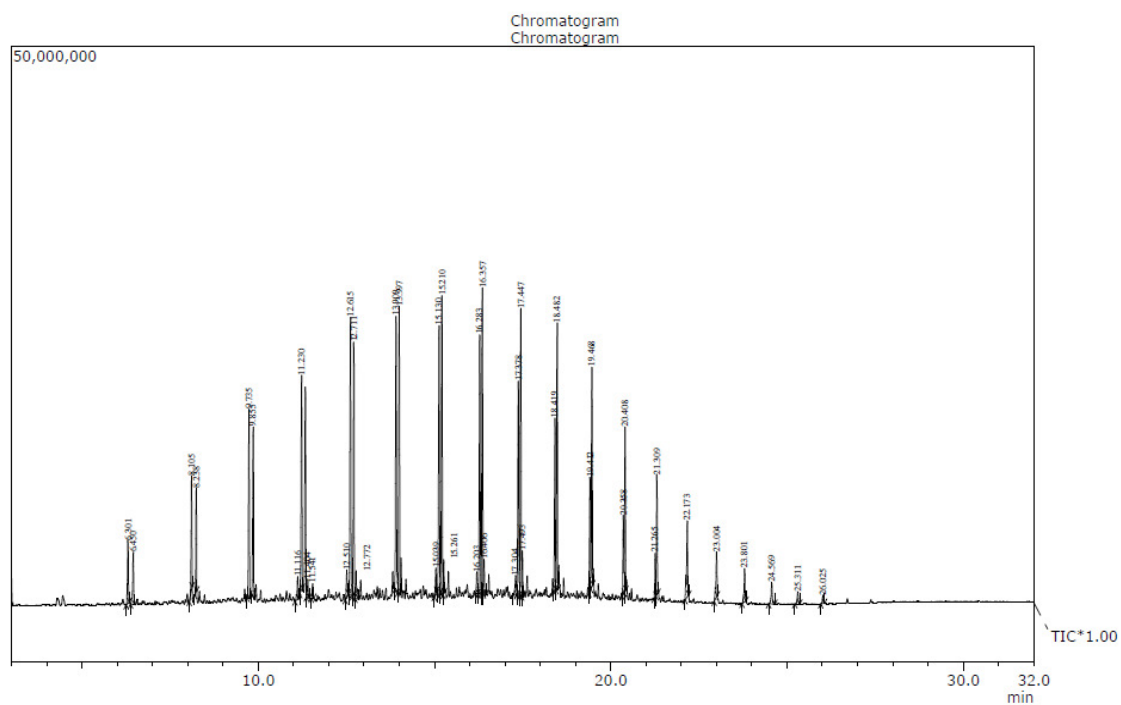


Figure 4.6. GC plot of oil obtained at 450 °C

Table 4.3. GC-MS Analysis of Virgin HDPE pyrolytic oil

R. Time (min)	Area%	Name of Compound	Molecular Formula
6.301	1.24	1-Decene	$C_{10}H_{20}$
6.450	1.12	Decane	$C_{10}H_{22}$
8.105	2.04	1-Undecene	$C_{11}H_{22}$
8.238	1.78	n-Undecane	$C_{11}H_{22}$
9.735	3.50	1-Dodecanol	$C_{12}H_{26}O$
9.855	3.19	n-Dodecane	$C_{12}H_{26}$
11.541	4.62	1-Tridecene	$C_{13}H_{26}$
12.615	5.30	1-Tetradecene	$C_{14}H_{28}$
12.711	4.82	Tetradecane	$C_{14}H_{30}$

12.772	0.65	7-Tetradecene	C ₁₄ H ₂₈
13.909	5.40	1-Pentadecene	C ₁₅ H ₃₀
13.997	5.13	Pentadecane	C ₁₅ H ₃₂
15.039	0.48	1,19-Eicosadiene	C ₂₀ H ₃₈
15.130	5.36	1-Hexadecene	C ₁₆ H ₃₂
15.210	5.60	n-Octadecane	C ₁₈ H ₃₆
15.261	0.51	Cyclohexadecane	C ₁₆ H ₃₂
16.203	0.49	1,19-Eicosadiene	C ₂₀ H ₃₈
16.283	5.09	1-Nonadecene	C ₁₉ H ₃₈
16.357	5.52	n-Heptadecane	C ₁₇ H ₃₆
16.406	0.51	1-Heptadecene	C ₁₇ H ₃₄
17.378	4.43	1-Octadecene	C ₁₈ H ₃₆
17.447	5.47	Octadecane	C ₁₈ H ₃₈
17.493	0.69	1-Octadecene	C ₁₈ H ₃₆
18.419	3.26	1-Nonadecene	C ₁₉ H ₃₈
18.482	4.67	Nonadecane	C ₁₉ H ₄₀

4.6.3. Physical properties of oil sample

Table 4.4 shows the results of physical property analysis of oil obtained from pyrolysis of virgin HDPE. The appearance of the oil is dark brownish free from visible sediments.

Table 4.4. Physical properties analysis of Virgin HDPE pyrolytic oil

Tests	Results Obtained	Test method
Specific Gravity @ 15°C/15°C	0.8013	IS:1448 P:16
Density @ 15°C in kg/cc	0.8006	IS:1448 P:16
Kinematic Viscosity @ 40°C in Cst	3.3	IS:1448 P:25
Kinematic Viscosity @ 100°C in Cst	1.4	IS:1448 P:25
Conradson Carbon Residue	<0.01%	IS:1448 P:122

Flash Point by Abel Method	10 °C	IS:1448 P:20
Fire Point	15 °C	IS:1448 P:20
Cloud Point	28 °C	IS:1448 P:10
Pour Point	18 °C	IS:1448 P:10
Gross Calorific Value in MJ/Kg	44.27	IS:1448 P:6
Sulphur Content	0.03%	IS:1448 P:33
Calculated Cetane Index (CCI)	70	IS:1448 P:9
<u>Distillation:</u>		IS:1448 P:18
Initial Boiling Point	72 °C	
Final Boiling Point	364 °C	

From comparison with other transportation fuels as shown in Table 4.5, the density and viscosity of liquid product can be modified by blending it with commercial transportation fuels. The flash point of the liquid product is in a comparable range and a pour point of 18 °C is acceptable for most geographic regions. HDPE pyrolytic oil has GCV of 44 MJ/Kg which is more as compared to that of gasoline and diesel; therefore this liquid product would perform relatively superior in engines. From the distillation report of the oil it is observed that, the boiling range of the oil is 72-364°C, which infers the presence of mixture of different oil components such as gasoline, kerosene and diesel in the oil. The liquid product contains substantial amount of volatiles as its initial boiling point is below 100°C. From this result, it is observed these could be possible feedstocks for further upgrading or use of lighter compounds as a diesel fuel.

Table 4.5. Fuel properties comparison of HDPE pyrolytic oil with commercial transportation fuels

Properties	Specific Gravity	Kinematic Viscosity	Flash Point	Pour Point	GCV (MJ/Kg)	IBP (°C)	FBP (°C)	Chemical Formula
	15°C/15°C	@40°C (cst)	(°C)	(°C)				
HDPE pyrolytic oil	0.8013	3.3	10	18	44.27	72	364	C ₁₀ -C ₂₀
Waste HDPE pyrolytic oil (Kumar S et al. 2011)	0.7835	1.63	1	-15	42.81	82	352	C ₁₉ -C ₂₄
Gasoline (Petroleum Product Surveys, 1986)	0.72-0.78	-	-43	-40	42-46	27	225	C ₄ -C ₁₂
Diesel (Tuttle J et al 2004)	0.82-0.85	2-5.5	53-80	-40 to -1	42-45	172	350	C ₈ -C ₂₅
Bio-Diesel (Tuttle J et al 2004)	0.88	4-6	100-170	-3 to 19	37-40	315	350	C ₁₂ -C ₂₂
Heavy Fuel Oil (Tuttle J et al 2004)	0.94-0.98	>200	90-180	-	- 40	-	-	-

4.7. Conclusion

Thermal pyrolysis of virgin HDPE was performed in a semi batch reactor made up of stainless steel at temperature range from 400 °C to 550 °C and at a heating rate of 20 °C/min. The liquid yield is highest at 450 °C, highly volatile products are obtained at low temperature, the products obtained 500 °C and 550 °C are viscous liquid and wax. Reaction time decreases with increase in temperature. The functional group present in the virgin HDPE pyrolytic oil is similar to the other plastic pyrolytic oils given in the several literatures. It was found that the pyrolytic oil contains around 25 types of compounds having carbon chain length in the range of C₁₀-C₂₀. The physical properties of pyrolytic oil obtained were in the range of other pyrolytic oils and moderate quality fuels. It has been shown that a simple batch pyrolysis method can convert virgin HDPE to liquid hydrocarbon products with a significant yield which varies with temperature.

Chapter 5

Waste HDPE Pyrolysis

THERMO-CATALYTIC DEGRADATION OF WASTE HIGH-DENSITY POLYETHYLENE TO LIQUID FUEL

5.1 Introduction

Plastics are one of the largely used materials due to its various advantages and numerous applications in our day today life. Plastics production has increased by an average of almost 10% every year on a global basis since 1950. The total global production of plastics has grown from around 1.3 million tonnes (MT) in 1950 to 230 MT in 2009 ([Plastic - The Facts 2010](#)). HDPE is the third-largest commodity plastic material in the world, after polyvinyl chloride and polypropylene in terms of volume. According to a British market-research consulting agency, “Merchant Research & Consulting Ltd.” High density polyethylene (HDPE) has accounted for a major share of ethylene consumption structure over the recent years. The demand for HDPE has increased 4.4% in a year to 31.3 million MT in 2009 ([Plastics Production](#)). The increased demand and production of waste HDPE led to the accumulation of large amount of its waste in the final waste stream due to its low life.

Recycling of plastics already occurs on a wide scale. Extensive recycling and reprocessing of plastics are performed on homogeneous and contaminant free plastic wastes. Most recycling schemes require a feedstock that is reasonably pure and contains only items made from a single polymer type, such as high density polyethylene (HDPE) commonly used to make milk bottles or polyethylene terephthalate (PET) soft drink bottles. However, a substantial fraction of the plastics in municipal waste still ends up in landfills. Realistically, most post-consumer wastes contain a mixture of plastic types, and are often contaminated with non-plastic items ([Hegberg BA et al. 1992](#)).

An alternative thermal approach to dealing with waste plastics is so-called chemical feedstock or chemical recycling. This term has been used to describe a diversity of techniques, including pyrolysis, hydrolysis, hydrogenation, methanolysis and gasification. Some of these techniques are suitable for use only with homogeneous polymer wastes but others can accept a feed of mixed wastes. The most attractive

technique of chemical feedstock recycling is pyrolysis. Thermal cracking or thermal pyrolysis involves the degradation of the polymeric materials by heating in the absence of oxygen. Unlike mechanical recycling techniques, in which the long polymeric chains of the plastic are preserved intact, pyrolysis produces lower molecular weight fragments. The process is usually conducted at temperatures between 500-800 °C and results in the formation of a carbonized char and a volatile fraction that may be separated into condensable hydrocarbon oil and a non-condensable high calorific value gas. The proportion of each fraction and their precise composition depends primarily on the nature of the plastic waste but also on process conditions. The effect of temperature and the type of reactor on the pyrolysis of waste HDPE studied by different researchers are summarized in literature review chapter.

The thermal degradation of waste HDPE can be improved by using suitable catalysts in order to obtain valuable products. The most common catalysts used in this process are; zeolite, alumina, silica–alumina, FCC catalyst, reforming catalyst etc. The effects of various catalysts on the pyrolysis of HDPE studied by different investigators are summarized in literature review chapter.

In the present study, waste high density poly ethylene was pyrolysed in a batch reactor at a temperature of 400 °C to 550 °C at a heating rate of 20 °C/min. The effect of pyrolytic temperature and holding time on the reaction time and yield of liquid product, char, and gaseous product were studied on. The fuel properties of the oil (obtained at temperature 450 °C from pyrolysis of waste HDPE) such as kinematic viscosity, flash point, fire point, cloud point, pour point, specific gravity, water content were determined using standard test methods. The chemical compositions of the waste HDPE pyrolytic oil were investigated using FTIR and GC/MS.

5.2. Materials and Methods

The details about the waste high-density polyethylene and catalysts used in this experiment, the experimental set up and procedure are summarized in the experimental section 3.

5.3. Results and Discussion

5.3.1. Characterization of raw material

5.3.1.1. Proximate and ultimate analysis of waste HDPE

The proximate and ultimate analysis of waste HDPE sample is shown in Table 5.1. The volatile matter is 99.92% in the proximate analysis, due to the negligible amount of ash in waste HDPE sample, its degradation occurs with minimal formation of residue. The oxygen is 5.19% in the ultimate analysis of waste HDPE. The oxygen in the waste HDPE sample may not be due to the fillers but due to the other ingredients which are added to resin in the manufacturing of HDPE.

Table 5.1. Proximate and ultimate analysis of waste HDPE:

Properties	Waste HDPE
Proximate analysis (wt%)	
Moisture content	0.00
Volatile matter	99.92
Fixed carbon	0.00
Ash content	0.08
Ultimate analysis (wt%)	
Carbon (C)	80.58
Hydrogen (H)	13.98
Nitrogen (N)	0.60
Sulphur (S)	0.080
Oxygen (O)/Others	5.19
GCV (MJ/Kg)	45.78

5.3.1.2. TGA and DTG analysis of waste HDPE sample

Thermogravimetric analysis (TGA) is a thermal analysis technique which measures the weight change in a material as a function of temperature and time, in a controlled environment. This can be very useful to investigate the thermal stability of a material, or to investigate its behavior in different atmospheres (e.g. inert or oxidizing). TGA applied in determination of the study of thermal stability/degradation of waste HDPE in various ranges of temperature. From the TGA curve as showed in figure 5.1, the waste HDPE degradation started at 390 °C and was completed at 490 °C for a heating rate of 20 °C/min. the degradation temperature at which weight loss of 50% (T_{50}) takes place was

about 440 °C for waste HDPE. A similar trend of nature during the analysis of HDPE decomposition by TGA/DTG has reported ([Aboulkas A et al. 2007](#)).

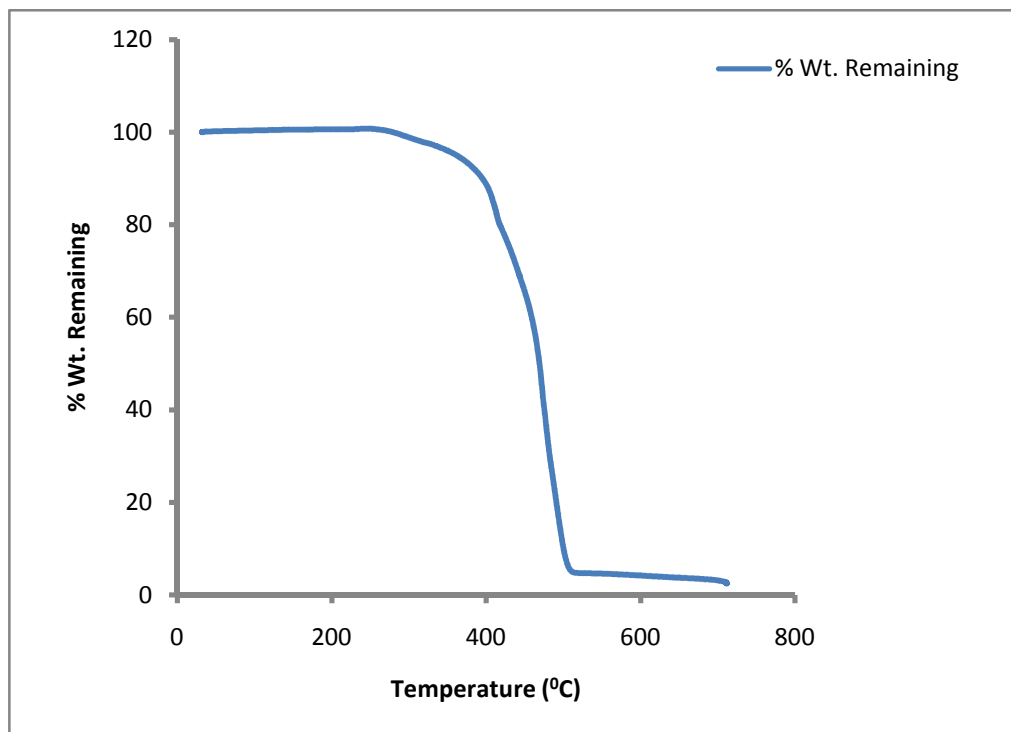


Figure 5.1. TGA curve of waste HDPE

Differential thermogravimetry (DTG) curve for waste HDPE contains only one peak, this indicates that there is only one degradation step in figure 5.2 it has shown that the dominant peak over 380 °C to 470 °C where the conversion takes place. Though pyrolysis of individual polymers has attracted much attention, studies on pyrolysis behavior, particularly of mixed plastics, are rather scarce. Still, from the study reported by Chattopadhyay et al. ([Chattopadhyay J et al. 2008](#)) it can be deduced that the mixture of HDPE, PP and PET starts decomposing at about 250 °C against 477 °C for pure HDPE (Zhou L et al. 2006). The decomposition of these two plastic samples ends at 521 °C and 700 °C, respectively. In the latter case, solid residue seems to have formed due the presence of PET. The addition of PP in HDPE has been reported by Hwang et al. ([Hwang G et al. 2001](#)) to improve the liquid yield during the degradation in supercritical acetone (450 °C to 470 °C, and 60 atm to 100 atm). In case of catalytic decomposition, a

reduction of 20 °C was reported by Lee et al. when LDPE, PP and PS were present along with HDPE (Lee KH et al. 2003)

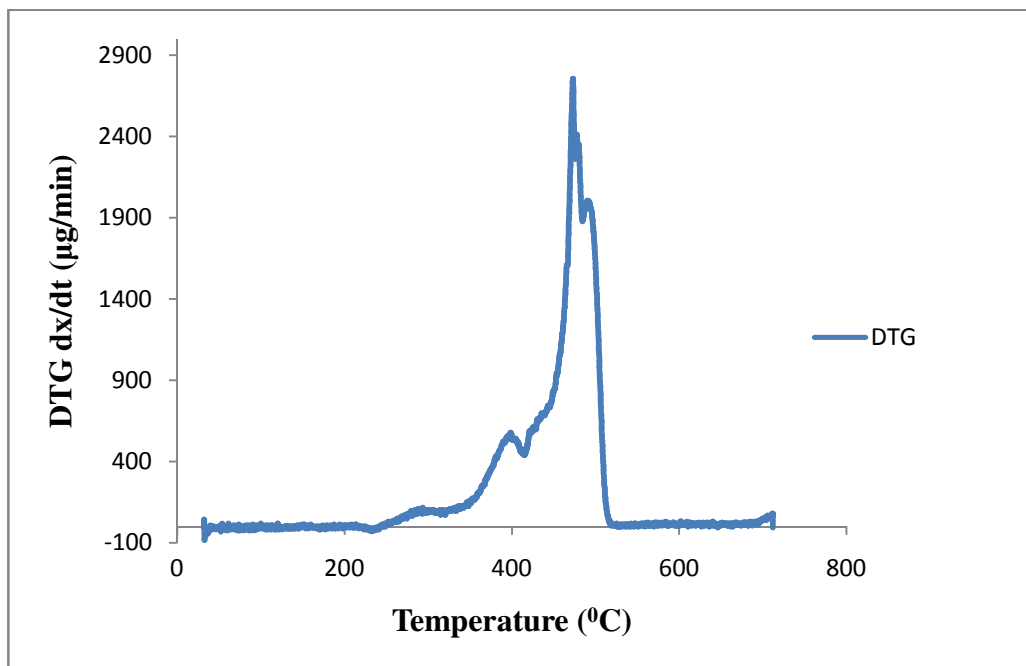


Figure 5.2. DTG curve of waste HDPE

5.3.2. Effect of temperature on product distribution

The pyrolysis of HDPE yielded four different products i.e. oil, wax, gas, and residue. The distributions of these fractions are different at different temperatures and are shown in the Table 5.2.

Table 5.2. Distribution of different fractions at different temperatures in the HDPE pyrolysis

Temperature (°C)	Oil (wt%)	Wax (wt%)	Gas/volatile (wt%)	Residue (wt%)	Reaction time (min)
400	11.2	1.3	67.6	19.9	760
450	23.96	2.7	61.31	12.04	100
500	21.87	44.69	24	9.45	50
550	7.86	51.15	37.2	3.79	40

The condensable oil/wax and the non-condensable gas/volatiles fractions of the reaction constituted major product as compared to the solid residue fractions. The condensable product obtained at low temperature (400 °C and 450 °C) was low viscous liquids. With increase in temperature, the liquid became viscous/wax at and above 475 °C. The formation of viscous and waxy product was due to improper cracking of plastic to high molecular mass hydrocarbon components. The recovery of condensable fraction was very low at low temperature i.e. at 400 °C and increased with gradual increase of temperature. From the table, it is observed that at low temperature the reaction time was more, due to which secondary cracking of the pyrolysis product occurred inside the reactor and resulted in highly volatile product. Similarly, the low liquid yield at high temperature was due to the formation less-cracked high molecular weight wax and more non-condensable gaseous/volatile fractions due to rigorous cracking.

5.3.3. Effect of temperature on reaction time and liquid yield

The effect of temperature on the reaction time of the reaction for the pyrolysis of waste HDPE plastic is shown in figure 5.3. The pyrolysis reaction rate increased and reaction time decreased with increase in temperature. High temperature supports the easy cleavage of bond and thus speeds up the reaction and lowers the reaction time. HDPE with long linear polymer chain with low branching and high degree of crystallinity led to high strength properties and thus required more time for decomposition. This shows that temperature has significant effect on reaction time and yield of liquid, wax and gaseous products.

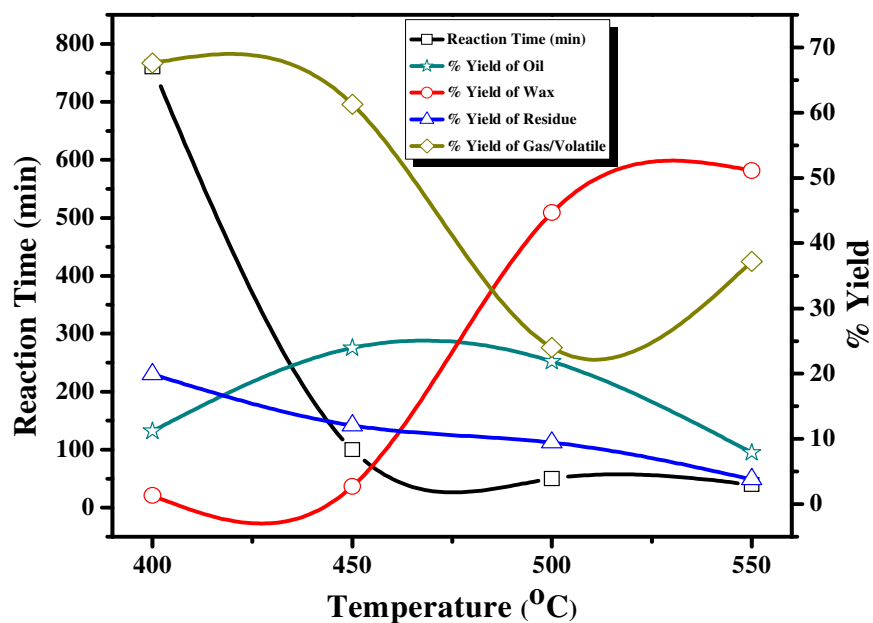


Figure 5.3. Effect of temperature on the reaction time and product distribution

5.3.4. Effect of holding time on yield of oil

The effect of holding time on the yield of the oil is shown in figure 5.4. The reaction was carried out by keeping the plastics in the reactor at 400 °C with different holding time from 1-6 hours followed by increase of the reaction temp to 450 °C. It was observed that this additional reaction phase increased the oil yield from 23% to 28% for 1 hour holding time and to 50.8% with 4 hour holding time and then decreased gradually with further increase in holding time. The introduction of this reaction phase loosens the polymer bonds which easily cleaved to liquid hydrocarbons and comes out through the out let at 450 °C without being converted to gas due to decrease in reaction time compared to 400 °C.

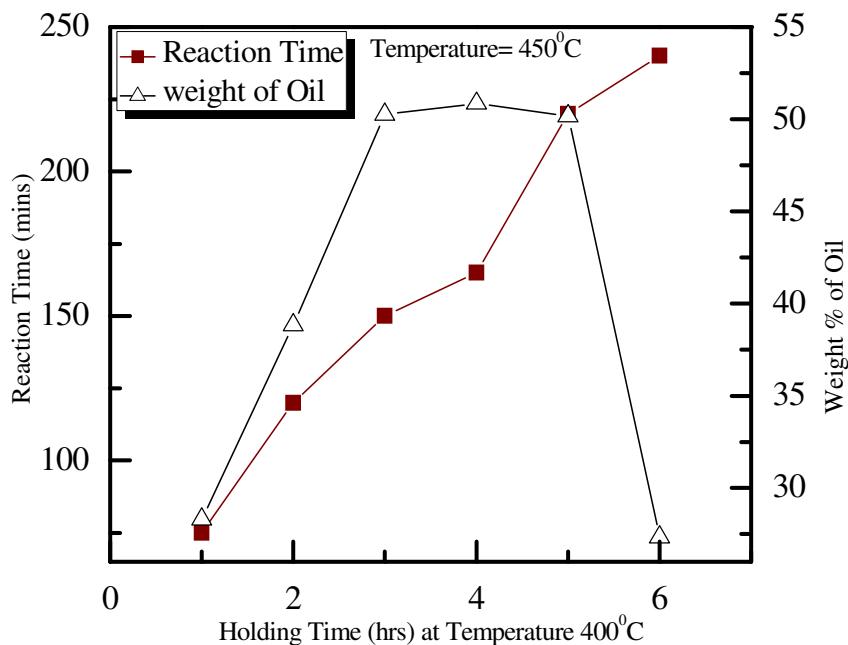


Figure 5.4. Effect of holding time on yield of the oil

5.3.5. Characterization of the liquid product

5.3.5.1. FTIR analysis of oil sample

Fourier Transform Infrared spectroscopy (FTIR) is an important analysis technique which detects various characteristic functional groups present in oil. On interaction of an infrared light with oil, chemical bond will stretch, contract, and absorb infrared radiation in a specific wave length range regardless the structure of the rest of the molecules. Figure 5.5 shows the FTIR spectra of waste HDPE oil, the different assignments of the FTIR spectra of waste HDPE oil are summarized in table 5.3 which shows the presence of mostly alkane and alkenes. The results were found consistent when compared with the results of GC-MS.

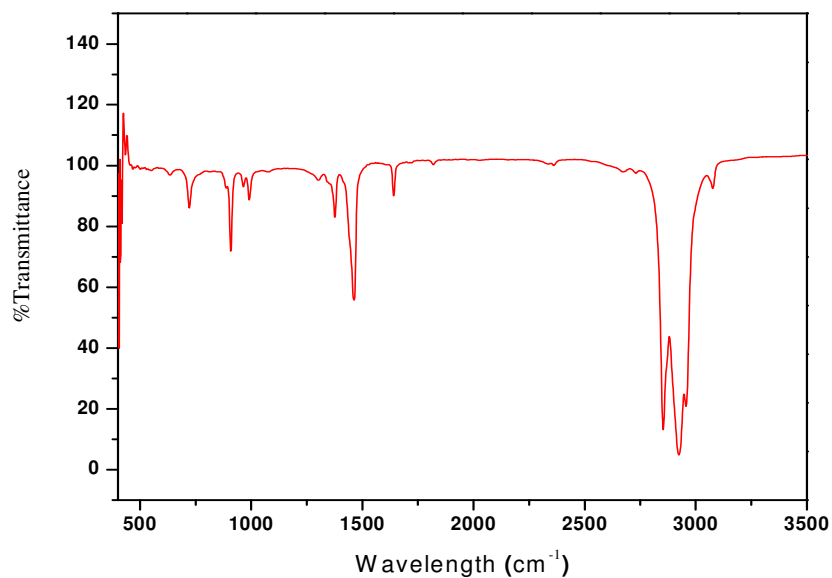


Figure 5.5. FTIR plot of oil obtained at 450 °C

Table 5.3. FTIR assignment of waste HDPE oil obtained at 450 °C

Wave number (cm ⁻¹)	Type of vibration	Nature of functional group
2955/2916	C-H stretching	Alkanes
1373	C-H Scissoring and Bending	Alkanes
2851	C-H stretching	Alkanes
1642	C=C stretching	Alkenes
1462	C=C stretching	Alkenes
991	C-H Bending	Alkenes
908	C-H out of plane bending	Alkenes
720	C-H bend	Phenyl Ring Substitution Bands

5.3.5.2. GC-MS of the oil sample

The GC-MS analysis of the oil sample obtained from waste HDPE was carried out to know the exact composition of the oil (figure 5.6) and is summarized in the table 5.4. The components present in HDPE are mostly the aliphatic hydrocarbons (alkane and alkenes) with carbon number C₉-C₂₄.

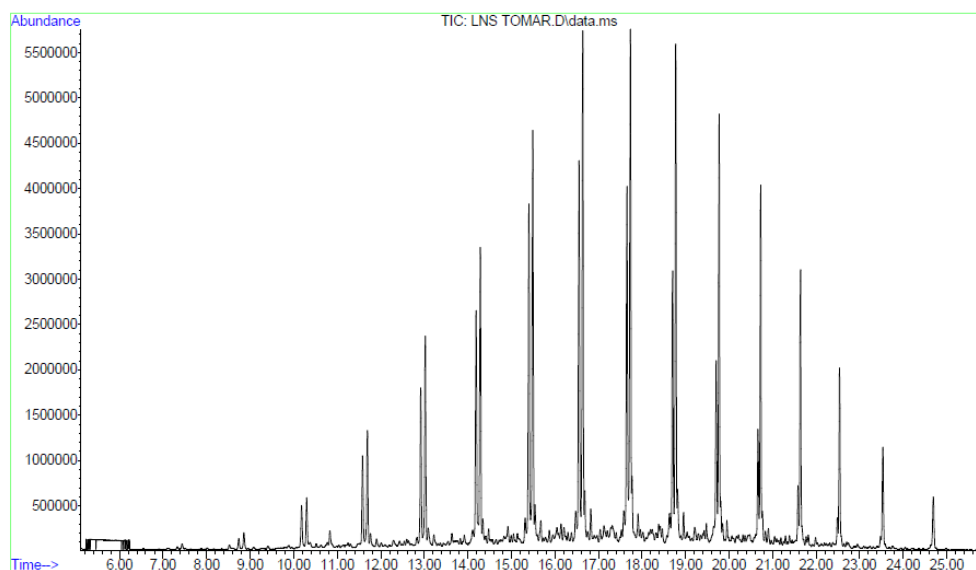


Figure 5.6. GC/MS of oil obtained at 450 °C

Table 5.4. GC-MS composition of oil obtained at 450 °C

R. Time	Area %	Name of compound	Molecular formula
3.051	1.55	1-Nonene	C ₉ H ₁₈
3.152	0.93	Nonane	C ₉ H ₂₀
4.435	2.63	1-Decene	C ₁₀ H ₂₀
4.463	1.23	Decane	C ₁₀ H ₂₂
5.974	3.02	1-Undecene	C ₁₁ H ₂₂
6.106	1.74	Undecane	C ₁₁ H ₂₄
7.505	3.34	1-Dodecene	C ₁₂ H ₂₄

7.629	2.27	Dodecane	$C_{12}H_{26}$
8.962	3.90	1-Tridecene	$C_{13}H_{26}$
9.076	2.51	Tridecane	$C_{13}H_{28}$
10.336	4.73	1-Tetradecene	$C_{14}H_{28}$
10.440	2.87	Tetradecane	$C_{14}H_{30}$
11.628	4.86	1-Pentadecene	$C_{15}H_{30}$
11.724	3.22	Pentadecane	$C_{15}H_{32}$
12.848	5.00	1-Octadecene	$C_{18}H_{36}$
12.934	3.70	Hexadecane	$C_{16}H_{34}$
14.001	4.94	1-Heptadecene	$C_{17}H_{34}$
14.082	3.65	Hexadecane	$C_{16}H_{34}$
15.098	4.71	1-Nonadecene	$C_{19}H_{38}$
15.170	3.74	Hexadeane	$C_{16}H_{34}$
16.141	4.38	1-Nonadecene	$C_{19}H_{38}$
16.207	3.65	Hexadecane	$C_{16}H_{34}$
17.133	3.79	1-Nonadecene	$C_{19}H_{38}$
17.194	3.21	Eicosane	$C_{20}H_{42}$
18.083	3.15	1-Nonadecene	$C_{19}H_{38}$
18.140	2.92	Heneicosane	$C_{21}H_{44}$
18.991	2.51	1-Nonadecene	$C_{19}H_{38}$
19.042	2.48	Docosane	$C_{22}H_{46}$
19.863	1.95	1-Nonadecene	$C_{19}H_{38}$
19.909	1.95	Tricosane	$C_{23}H_{48}$
20.699	1.26	1-Nonadecene	$C_{19}H_{38}$
20.740	1.29	Tetracosane	$C_{24}H_{50}$

21.502	0.92	1-Nonadecene	$C_{19}H_{38}$
21.539	0.64	Docosane	$C_{22}H_{46}$
22.275	0.47	N-Tetracosanol-1	$C_{24}H_{50}O$
22.308	0.37	Tetracosane	$C_{24}H_{50}$
23.019	0.28	1-Nonadecene	$C_{19}H_{38}$
25.051	0.22	4,6-Dimethyldodecane	$C_{14}H_{30}$

5.3.5.3. Physical properties analysis of oil sample

Table 5.5 shows the results of physical property analysis of oil obtained from pyrolysis of waste HDPE. The appearance of the oil is dark brownish free from visible sediments. From the distillation report of the oil it is observed that, the boiling range of the oil is 82-352 °C which infers the presence of mixture of different oil components such as gasoline, kerosene and diesel in the oil. The oil obtained from the pyrolysis was fractionated to two fractions by distillation and the fuel properties of the different fractions were studied. From this result, it is observed that the fuel properties of the thermal pyrolysis oil matches with the properties of petroleum fuels.

Table 5.5. Physical properties of HDPE pyrolytic oil sample

Tests	Results Obtained	Test method
Specific Gravity @ 15 °C/15 °C	0.7835	IS:1448 P:16
Density @ 15 °C in kg/cc	0.7828	IS:1448 P:16
Kinematic Viscosity @ 40 °C in Cst	1.63	IS:1448 P:25
Kinematic Viscosity @ 100 °C in Cst	0.89	IS:1448 P:25
Viscosity Index	Not Available	IS:1448 P:56
Conradson Carbon Residue	0.01%	IS:1448 P:122
Flash Point by Abel Method	1 °C	IS:1448 P:20

Fire Point	7 °C	IS:1448 P:20
Cloud Point	-4 °C	IS:1448 P:10
Pour Point	-15 °C	IS:1448 P:10
Gross Calorific Value in MJ/Kg	42.81	IS:1448 P:6
Sulphur Content	0.019%	IS:1448 P:33
Calculated Cetane Index (CCI)	61	IS:1448 P:9
<u>Distillation:</u>		IS:1448 P:18
Initial Boiling Point	82 °C	
10% Recovery	126 °C	
30% Recovery	188 °C	
50% Recovery	226 °C	
70% Recovery	278 °C	
90% Recovery	320 °C	
95% Recovery	340 °C	
Final Boiling Point	352 °C	
Residue	1.50 ml	
Loss	0.50%	

5.3.6. Effect of different catalysts on product yield and reaction time at a temperature 450 °C

5.3.6.1. Effect of kaolin catalyst on yield and reaction time at a temperature 450 °C:

Distribution of different products with kaolin catalyst to plastic ratio at a temperature 450 °C is shown table 5.6. The product distribution changed entirely when the same reaction was carried out in presence of catalyst in different feed ratios. The yield of liquid product was more and reaction time was less in presence of catalyst at an optimized temperature 450 °C as compared to thermal degradation.

Table 5.6. Distribution of different products with kaolin catalyst to plastic ratio at a temperature 450 °C

Catalyst to feed ratio	Oil (wt%)	Reaction time in min.
1:6	48.2	165
1:4	58.80	157
2:4	55.51	130
3:4	53.48	125
4:4	50.38	110

The feed ratio (catalyst: plastic) also affect on the yield of liquid product. The highest yield of liquid product at 450 °C was 58.8 wt.% with 1:4 catalyst to plastic ratio (figure 5.7). The liquid product decreased when amount of catalyst increased and the rate of reaction increased with increase in the amount of catalyst. Thus kaolin as a catalyst increased the liquid yield as well as lowered the reaction time. The mesoporous surface of kaolin facilitates the cracking reaction.

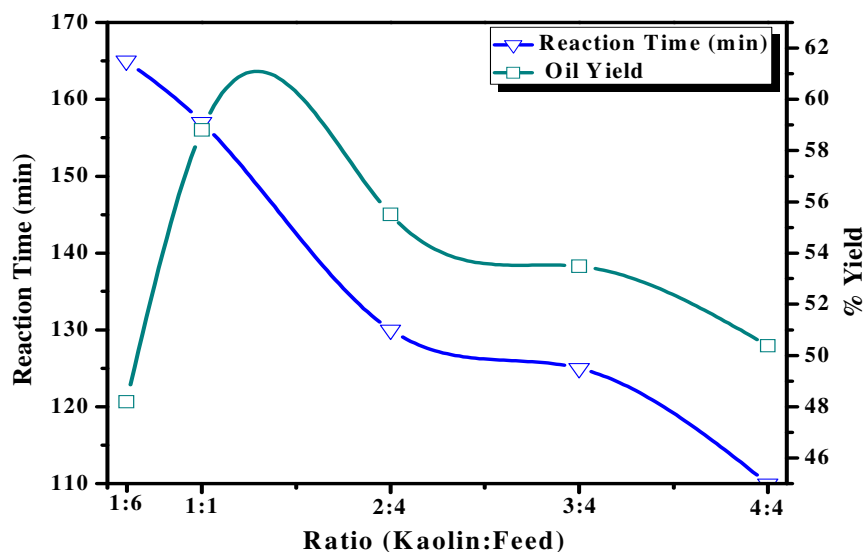


Figure 5.7. Effect of kaolin catalyst to plastic ratio on oil yield and reaction time

5.3.6.2. Effect of mordenite catalyst on yield and reaction time at a temperature 450 °C

Distribution of different products with mordenite catalyst to plastic ratio at a temperature 450 °C is shown table 5.7. The product distribution changed entirely when the same reaction was carried out in presence of catalyst in different feed ratios. The yield of liquid product was more and reaction time was less in presence of catalyst at an optimized temperature 450 °C as compared to thermal degradation.

Table 5.7. Distribution of products with mordenite catalyst to feed ratio at a temperature 450 °C

Catalyst to feed ratio	Oil (wt. %)	Reaction time in min.
1:6	47.4	195
1:4	58.47	175
2:4	56.34	160
3:4	53.44	150
4:4	51.44	140

The feed ratio (catalyst: plastic) also affect on the yield of liquid product. The highest yield of liquid product at 450 °C was 58.4 wt% with 1:4 catalyst to plastic ratio (figure 5.8). The liquid product decreased when amount of catalyst increased and the rate of reaction increased with increase in the amount of catalyst. Thus mordenite as a catalyst increased the liquid yield as well as lowered the reaction time.

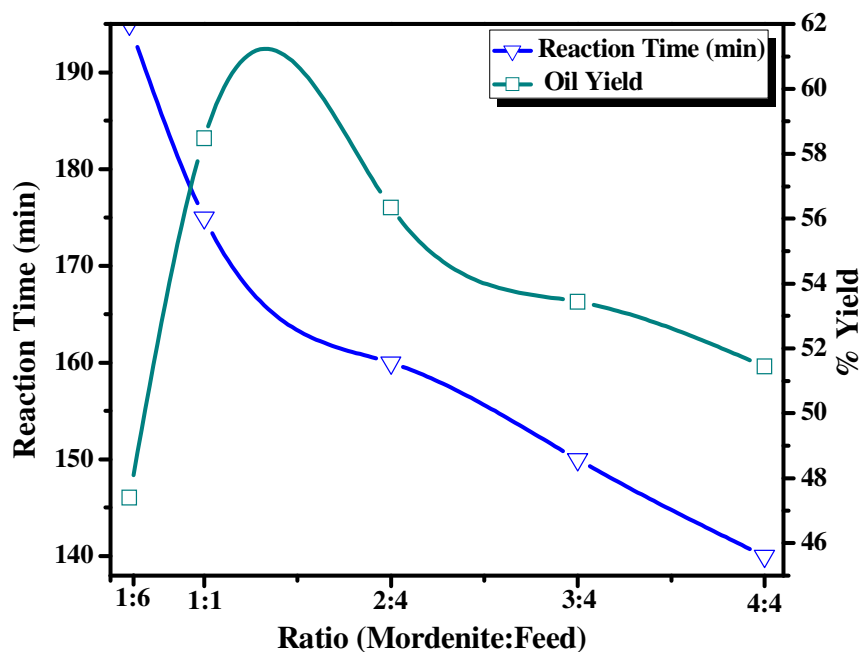


Figure 5.8. Effect of mordenite catalyst to plastic ratio on oil yield and reaction time

5.3.6.3. Effect of silica-alumina catalyst on yield and reaction time at a temperature 450 °C

Distribution of different products with mordenite catalyst to plastic ratio at a temperature 450 °C is shown table 5.8. The product distribution changed entirely when the same reaction was carried out in presence of catalyst in different feed ratios. The yield of liquid product was more and reaction time was less in presence of catalyst at an optimized temperature 450 °C as compared to thermal degradation.

Table 5.8. Distribution of products with silica-alumina catalyst to plastic ratio at a temperature 450 °C

Catalyst to feed ratio	Oil (wt.%)	Reaction time in min.
1:6	49.7	215
1:4	58.99	190
2:4	57.75	180
3:4	56.21	175
4:4	54.16	165

The feed ratio (catalyst: plastic) also affect on the yield of liquid product. The highest yield of liquid product at 450 °C was 58.9 wt% with 1:4 catalyst to plastic ratio (figure 5.9). The liquid product decreased when amount of catalyst increased and the rate of reaction increased with increase in the amount of catalyst. Thus silica-alumina as a catalyst increased the liquid yield as well as lowered the reaction time.

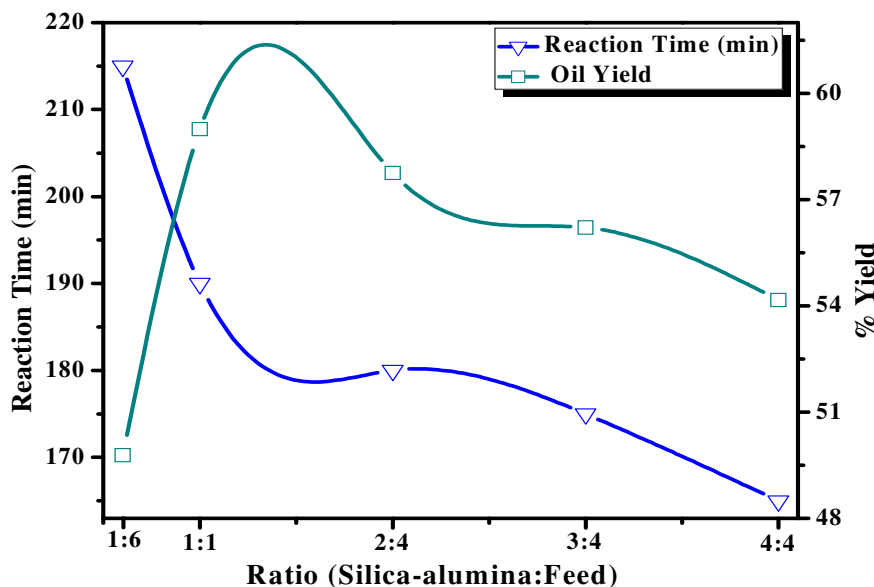


Figure 5.9. Effect of silica-alumina catalyst to plastic ratio on oil yield and reaction time

5.3.6.4. Effect of different catalysts on liquid product yield and reaction time at a temperature 450 °C and 1:4 catalyst to plastic ratio:

Effect of different catalysts (kaolin, mordenite and silica-alumina) on liquid product yield and reaction time at a temperature 450 °C and 1:4 catalysts to plastic ratio is shown in figure 5.10. The liquid product yield is almost similar i.e. 58.8 wt% with kaolin catalyst, 58.4 wt% with mordenite catalysts and 58.9 wt% with silica-alumina catalyst. But reaction time varies significantly with different catalysts. Reaction time is more 190 min in case of silica-alumina catalyst as compared to 175 min and 157 min with mordenite and kaolin catalysts respectively.

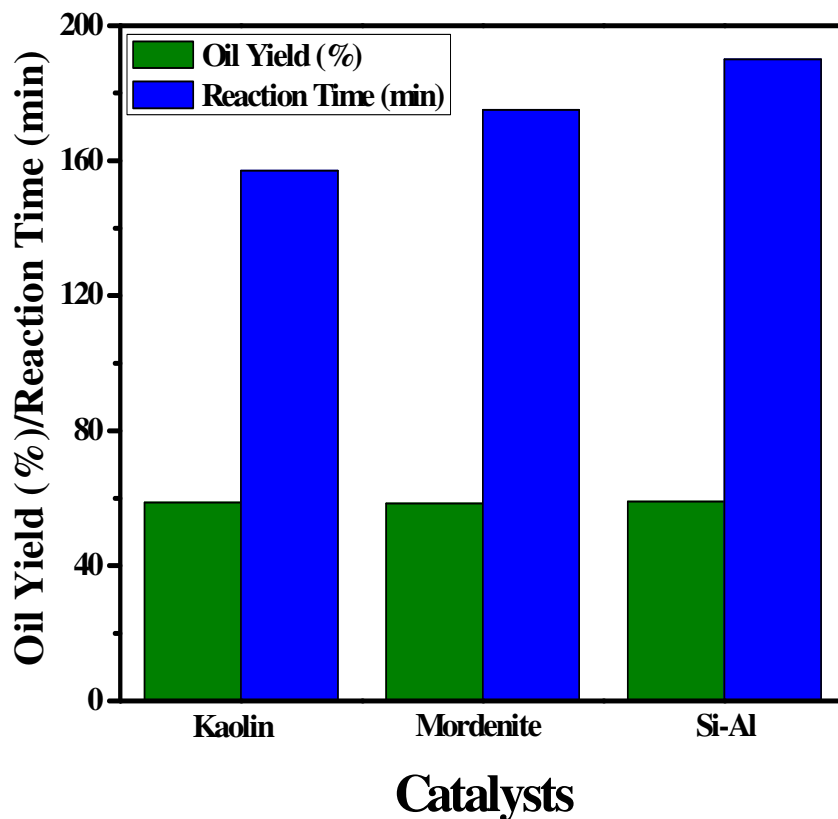


Figure 5.10. Effect of different catalysts on liquid yield and reaction time

5.4 Preparation and characterization of acid and alkali treated kaolin clay

5.4.1 Introduction

Physical and chemical behaviors of clay minerals have been studied by numerous researchers due to the adsorbing and catalytic properties of clay minerals. This behavior is governed by the extent and nature of their external surface which can be modified by suitable treatment techniques. There are broadly two different treatments or modification methods of clay minerals studied by different researchers such as (1) physical modification (thermal or microwave treatment) which involves alteration of chemical composition and crystalline structure by the effect of high temperature, (2) chemical modification (by acids, bases, organic compounds) which is usually by the alteration of structure, surface functional groups and surface area ([Hussin F et al. 2011](#)).

The most common physical modification is thermal treatment which involves the alteration of chemical composition and/or crystalline structure by the effect of temperature. The structure and composition of clay minerals can be modified by heating at high temperature ([Kallai LH 2006](#)). Some physicochemical properties such as swelling, strength, cation exchange capacity, particle size, specific surface area, surface acidity and catalytic activity as well as mineralogy can change considerably on the thermal treatment ([Onal M et al. 2007](#), [Sarıkaya Y et al. 2000](#)). In addition to thermal treatment, microwave heat treatment also plays an important role for modification of clay materials ([Korichi S et al. 2009](#)). Clark et al. has reported that the temperature and time required by microwave heating method for preparing adsorbents are far shorter than by the conventional thermal activation method and this method is simple, economic, time saving and energy efficient ([Clark DE et al. 2000](#)).

Acid treatment is one of the most common chemical treatments for clay minerals and has been used to increase the specific surface area and the number of acidic centers, modify the surface functional group and to obtain solids with high porosity. Numerous studies have been reported on the acid treatment of clays, especially on bentonite-smectite or montmorillonite, vermiculite, kaolin, palygorskite-sepiolite and glauconite ([Foletto EL et al. 2006](#), [Wu Z et al. 2006](#), [Ravichandran J et al. 1997](#), [Chmielarz L et al. 2010](#), [Lenarda](#)

M et al. 2007, Panda AK et al. 2010b, Belver C et al. 2002, Chitnis SR et al. 1997, Srasra E et al. 2000). The various types of acids used for acid treatment including inorganic acids such as hydrochloric, sulfuric, nitric and organic acids such as acetic, citric, oxalic and lactic. Among all of these, hydrochloric acid and sulfuric acid are probably the most widely used in acid activation, because it shows strong affection by the process parameters and superior results in specific surface area, porosity and adsorption capacity (Siddiqui MKH 1968).

Hussin et al has performed the basic treatment of clay and reported that the active centers increases and surface area decreases with NaOH treatment and cost of sodium hydroxide is much lesser than that of inorganic acids such as H_2SO_4 and HCl. However, the base treated clay materials are suitable only for some applications (Hussin F et al. 2011).

Several problems such as corrosion of the process vessels, increasing of free fatty acids, peroxide value in oil products and other environmental problems occur when acid treated clay is used. This led to modification of clay with cationic and anionic surfactants [Cetyl trimethyl ammonium bromide and linear alkyl benzene sulfonate] for the removal color pigment, free fatty acids and peroxide value (Gunawan NS et al. 2010). Intercalation or pillaring is also a clay treatment method that alters the properties of bleaching earth by using combination of chemical and physical treatments in which a layered compound is transformed in a thermally stable micro and/or mesoporous material with retention of the layer structure. Pillared clay minerals have magnetized much attention from the industry due to their microporous nature and catalytic potential (Caglayan MO et al. 2005, Gil A et al. 1994).

Recently, we have carried out the acid activation of kaolin with sulphuric acid of different concentrations under refluxed condition followed by a systematic analysis of the treated kaolin samples with wide characterization techniques to understand the changes in physico-chemical properties. It has been concluded that sulphuric acid treatment at and above 5M concentration almost destroys the crystalline structure and other properties to a considerable extent (Panda AK et al. 2010b). Therefore, in the present work, kaolin is treated with different other acids such as HNO_3 , HCl, H_3PO_4 , CH_3COOH , and base

NaOH of 3M concentration to compare their effects on modifications in physico-chemical properties of kaolin after treatment.

5.4.2 Experimental Programme

The details about the kaolin clay, acid and alkali activation process and different characterization technique are described in the experimental section 3.

5.4.3 Results and Discussion

5.4.3.1 XRF analysis

The XRF analysis was carried out to know the chemical compositions of the clay and the subsequent chemical changes that occurred due to treatment. Table 5.9 shows the results of chemical analysis of the parent and acid treated kaolinite clay. The parent clay contains alumina and silica which are in major quantities where as other oxides such as magnesium oxide, calcium oxide, potassium oxide, zinc oxide and titanium oxide are present in trace amounts.

Table 5.9. XRF analysis of acid and alkaline treated kaolin clay

Material	Chemical content (% weight)								Si/Al
	SiO ₂	Al ₂ O ₃	MgO	CaO	K ₂ O	ZnO	TiO ₂	V ₂ O ₅	
Kaolin	43.12	46.07	0.027	0.030	0.010	0.0064	0.74	0.003	0.82
KCH ₃ COOH	44.03	43.81	0.026	0.017	0.01	0.0062	0.40	0.003	0.885
KH ₃ PO ₄	45.83	41.51	Nil	0.018	0.007	0.0064	0.34	0.003	0.972
KHCl	48.80	37.61	0.016	0.017	0.01	0.0064	0.26	0.001	1.144
KHNO ₃	56.42	27.88	0.02	0.008	0.008	0.0064	0.23	0.002	1.782
KNaOH	56.14	29.30	0.030	0.186	0.017	0.0064	0.12	Nil	1.688

After the acid treatment, it was observed that the composition of the kaolin changes considerably. The Al₂O₃, MgO, CaO and K₂O contents decreases and SiO₂ content

increased in the treated kaolin progressively on treatment with different reagents (acids and base). The decrease in the alumina content in the treated sample can be ascribed to the leaching of the Al^{3+} ions from the octahedral layer due to hydrolysis under acidic/alkaline conditions. During treatment, it was observed that the concentration of CaO, MgO, K_2O , TiO_2 and V_2O_5 reduced, but that of ZnO remained almost unchanged with any types of reagent. The extent of leaching depends on the type of reagent and is in the order $\text{NaOH}=\text{HNO}_3>\text{HCl}>\text{H}_3\text{PO}_4>\text{CH}_3\text{COOH}$. For example, with 3M NaOH and HNO_3 treatment, the Al_2O_3 content decreases from 46.07 to 29.30% and 27.88% respectively, where as the SiO_2 content increases from 43.12 to 56.14% and 56.42% respectively. Thus the Si/Al ratio of the kaolin treated with different reagent increases in the same trend. The XRF study clearly indicates that leaching occurred in a sequential manner due to attack at tetrahedral layer resulting in the de-alumination of clay. This can be interpreted due to the increasing strength and leaching ability of the respective reagents.

5.4.3.2 XRD analysis

The structural changes that occurred in the clay material after the acid or alkali treatment were studied using X-ray diffraction technique. Figure 5.11 shows the XRD profiles of the untreated and treated kaolin samples. The parent clay shows well defined reflections at 2theta value of 12° , 25° (corresponding to the d values of 7.154 Å. These peaks correspond to the reflections from [001], which are typical characteristic peaks of kaolinite. After acid treatment, the peak intensity of the clay was found to decrease and extent of decrease follows the trend $\text{HNO}_3>\text{HCl}>\text{H}_3\text{PO}_4>\text{CH}_3\text{COOH}$, since leaching is quite severe with strong acids. This is attributed to the structural disorder that occurred owing to the acid leaching, which affects the crystalline character of the clay. With NaOH treatment the peak intensity increases and narrowed. The increase in intensity and/or narrowing of the peak may be related to the increase of crystallite size and/or the decrease of the mean lattice strain (Delhez R et al. 1982).

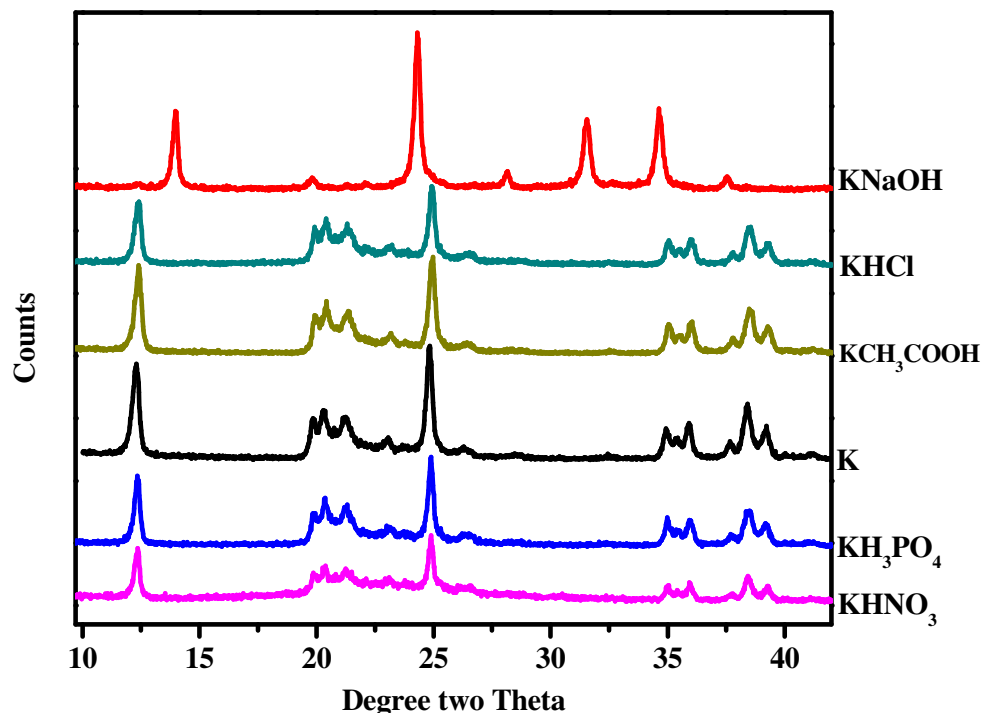


Figure 5.11. XRD analysis of acid and alkaline treated kaolin clay

5.4.3.3. FTIR analysis

The FTIR spectrums of kaolin and acid treated kaolinite clays are shown in Figure 5.12 and the corresponding band assignments are shown in Table 5.10. In the O-H stretching region, the parent and acid treated clay shows three prominent bands at 3620, 3653 and 3695 cm^{-1} corresponds to Al-OH stretching. Inner hydroxyl groups, lying between the tetrahedral and octahedral sheets give the absorption at 3620 cm^{-1} . A strong band at 3695 cm^{-1} is related to the in phase symmetric stretching and a weak absorption at 3653 cm^{-1} are assigned to out-of-plane stretching vibrations. The band observed at 3445 cm^{-1} , assigned to the high amount of water physisorbed on the surface of the clay (Dudkin BN et al. 2004, Suquet H 1989). There was not much variation in the peak pattern for 3M H_3PO_4 and CH_3COOH acid treated kaolin. However with HNO_3 and HCl treatment the peak intensity was found to decrease progressively indicating penetration of

protons into the clay mineral layers and attack to the structural hydroxyl groups resulted in the dehydroxylation and a successive leaching of the Al ions from the octahedral layer (Korichi S et al. 2009). For the NaOH treated kaolin the structural hydroxyl vibration band is extremely weak.

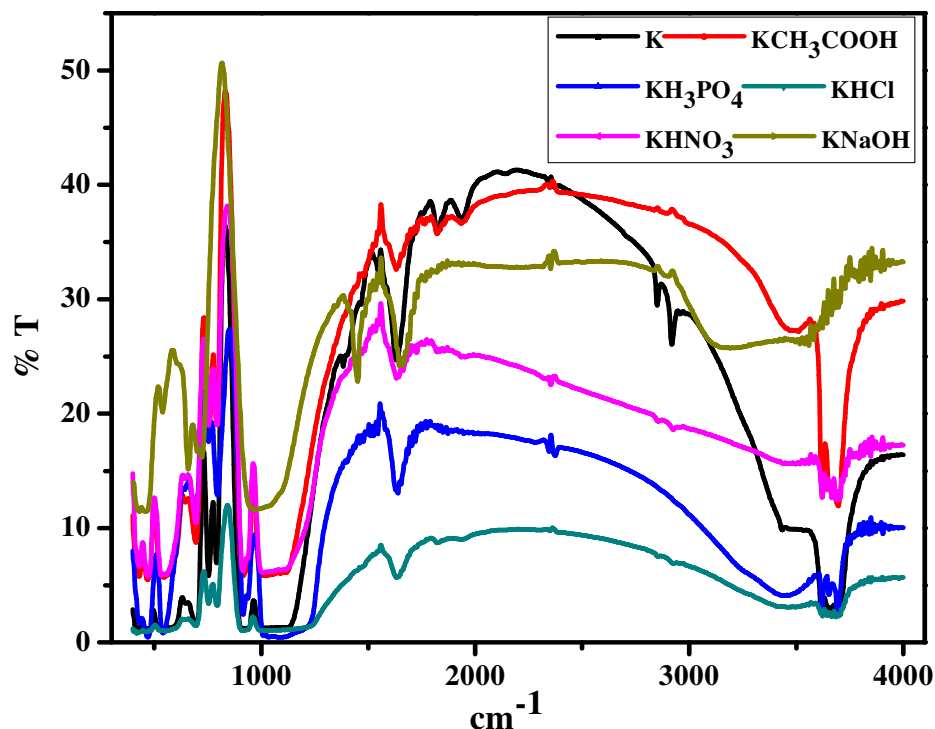


Figure 5.12. FTIR of acid and alkaline treated kaolin clay

In the bending region mode, the clay materials show a series of IR bands with peak maxima at 1634, 914, 795 and 755 cm^{-1} . The peak at 1634 cm^{-1} is quite intense is attributed to the bending vibration mode of physisorbed water on the surface of free silica produced due to leaching (Suquet H 1989). This peak was found to be absent in case of the HNO_3 treated clay due to structural disintegration. The IR peaks at 914, 795 and 755 cm^{-1} can be assigned to the Al–Al–OH, Al–Mg–OH and Si–O–Al vibration of the clay sheet. The high intense 914 cm^{-1} peak due to vibrations of inner OH groups was found to be drastically reduced for HCl and HNO_3 treated clay. This clearly points to the fact that

when the acid strength is more the de-alumination process is facilitated rapidly during acid treatment (Thorills CL et al. 1950).

Table 5.10. Important IR bands of acid and alkaline treated kaolin clay

Band cm^{-1}	Assignments
3445 3620, 3653 & 3695	Al--O-H _{str} (physisorbed and interlayer water) Al--O-H _{str} (structural hydroxyl groups, octahedral)
1634	H-O-H _{bending} (physisorbed)
912 1032, 1101 & 1114	Al-Al-OH _{str} , Si-O _{str}
795 755	Al-Mg-OH _{str} Si-O-Al _{str}
805	Si-O _{str}
693	Si-O _{str} , Si-O-Al _{str}
541	Si-O _{str} , Si-O-Al _{str}
472	Si-O _{str}

Again well resolved strong bands in the $1120\text{-}1000\text{cm}^{-1}$ region is due to Si-O stretching in untreated kaolinite which changed in shape and position due to structural changes in the tetrahedral cations. In addition, a new peak was observed at 805 cm^{-1} for the acid treated sample, which gained intensity with increase in the acid strength (Dudkin BN et al. 2004, Thorills CL et al. 1950). This peak is due to the formation of free amorphous silica. The FTIR result is in clear agreement with the XRF and XRD studies which indicates sequential degradation of the clay sheet upon acid treatment.

The FTIR of KNaOH showed wide water bands centered at about 3420 cm^{-1} , the asymmetric stretching of the tetrahedral units at 985 cm^{-1} with a shoulder at 1020 cm^{-1} , the symmetric stretching at 665 cm^{-1} , and the bending at 478 cm^{-1} . Moreover, the presence of carbonate groups was clearly shown by a wide band centered at 1440 cm^{-1} .

5.4.3.4. TG-DTA analysis

The TGA curves (Figure 5.13a) of the pure and treated kaolin show two well-defined weight loss regions due to the loss of physisorbed water (below $200\text{ }^{\circ}\text{C}$) and dehydroxylation of coordinated and structural water (above $450\text{ }^{\circ}\text{C}$). In general, clay materials contain three kinds of water molecules in their structure. The physisorbed and interlayer water is loosely bound and are mobile they can be removed by heat treatment below $200\text{ }^{\circ}\text{C}$. The water molecules present in the first coordination sphere of the interlayer ions are strongly bonded and they require higher temperature in the range of $300\text{--}500\text{ }^{\circ}\text{C}$ for their removal. Finally, the structural hydroxyl groups can condense and dehydrate in the temperature range of $500\text{--}800\text{ }^{\circ}\text{C}$. In the present study, the low temperature weight loss can be assigned to the physisorbed water, where as the high temperature weight loss is due to the dehydration and dehydroxylation of the clay sheet. Comparing the TGA profile of the parent and the acid treated clay it was observed that acid treatment increased the amount of physisorbed water and it increased with increased strength of the acid ($\text{HNO}_3 > \text{HCl} > \text{H}_3\text{PO}_4 > \text{CH}_3\text{COOH}$). It is extraordinarily high in case of sodium hydroxide treated kaolin. This may be due to the fact that chemical treatment increased the amount of amorphous silica and also the surface area which made the water adsorption higher. However, in the high temperature weight loss regions, the percentage loss is low for treated clay as compared to the parent clay due to the removal of octahedral Al ions along with the concurrent removal of structural hydroxyl groups after acid treatment.

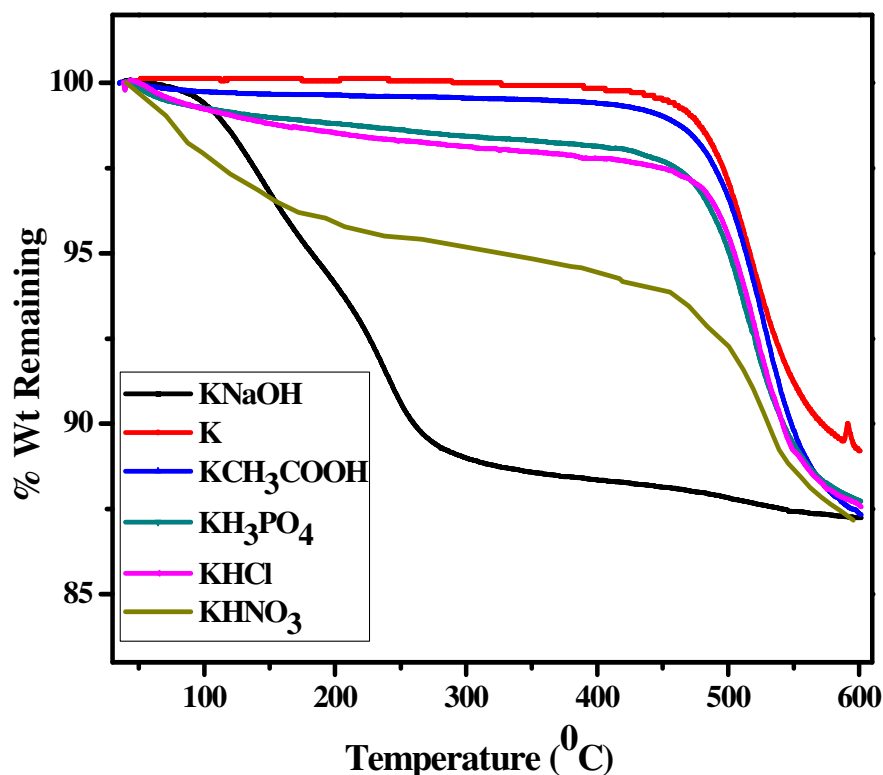


Figure 5.13a. TGA of acid and alkali treated kaolin clay

The DTA profiles of the clay and acid treated clay are shown in Figure 5.13b supports the weight loss pattern due to water removal in the TGA study. The DTA curve of untreated kaolin showed two endothermic peaks at 56 and 531 °C. The endothermic peak centered at around 56 °C may be due to physisorbed water and a large peak at 531 °C might be due to the liberation of water caused by dehydroxylation of co-ordinated and structural water molecules. Increase in acid strength due to change in type of acid increased the physisorbed water and decreased the structural and coordinated water leading to change in the endothermic peaks in treated samples. The thermal analyses of the alkali treated sample showed completely different curve as compared to acid treated kaolin samples. Thus, the weight loss is very high at low temperature, between room temperature and 250

°C. It may be considered that the fixed carbonate anions contributed in a small amount to the weight loss at high temperature.

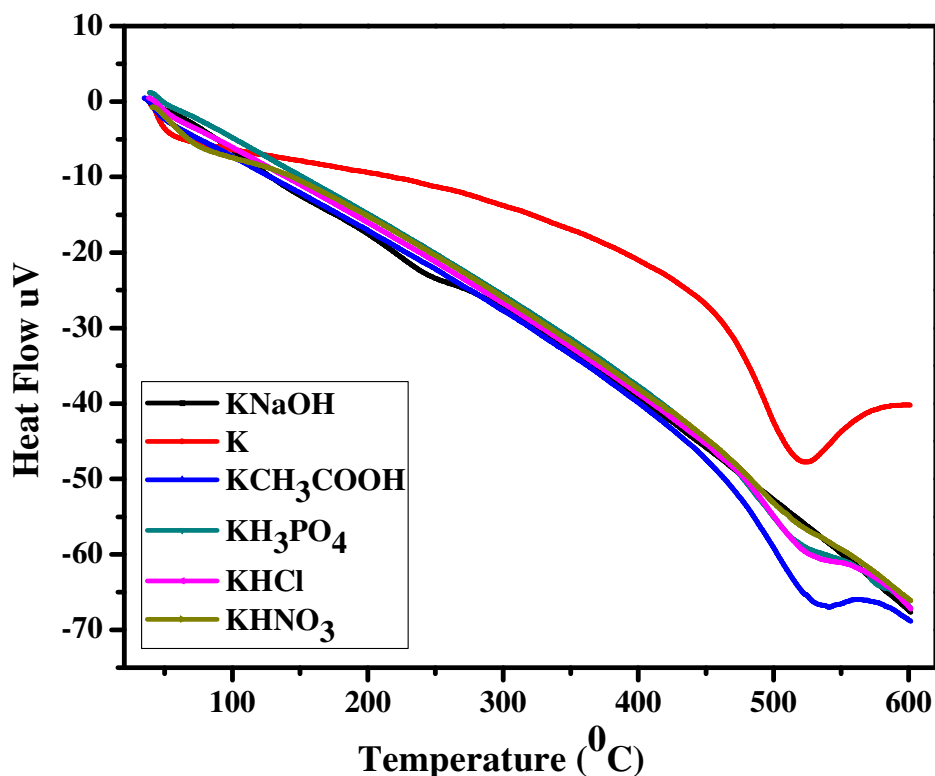


Figure 5.13b. DTA of acid and alkali treated kaolin clay

5.4.3.5. BET surface area and pore volume

The surface area and pore volume of the pure and treated kaolin obtained using N_2 adsorption-desorption isotherms summarized in table 5.11. The pore volume and BET surface area increased with increasing acid strength. Alkali treatment also increased the surface area and pore volume. This can be explained due to occurrence of the de-alumination process and thus surface disintegration.

The increase in pore volume due to acid treatment is more prominent as compared to alkali treatment. Production of finely dispersed Si oxides from destruction and leaching of kaolin, by removal of different cations plugging the surface pores or interlamellar spaces, by formation of surface pores and cracks as well as by decrease in mineral size

leading to increased pore volume due to acid treatment. Under alkaline treatment, similar processes may occur together with an accumulation of hydroxides of Mg and Ca (Jozefaciuk G et al. 2006).

Table 5.11. BET surface area and pore volume of acid and alkaline treated kaolin clay

Material	Surface Area (m ² /g)	Pore Volume (cc/g)
Kaolin	23	0.361
KCH ₃ COOH	38	0.504
KH ₃ PO ₄	42	0.658
KHCl	78	1.083
KHNO ₃	86	1.124
KNaOH	76	0.591

5.4.3.6. SEM analysis

The scanning electron micrographs of the different kaolin clay samples are presented in Figures 5.14(a-f) which shows the morphological features. The SEM micrograph of KC reveals the presence of large particles that appeared to have been formed by several flaky particles stacked together in form of agglomerates. The SEM images of treated kaolin show different particles morphology. The micrographs of KCH₃COOH and KH₃PO₄ indicate the disaggregation and decrease in size of clay structure on acid treatment and that of KHCl, KHNO₃ and KNaOH shows well-bonded aggregates rather than detached particles.

Figure 5.14. SEM images of acid and alkali treated kaolin clay, Figure 5.14a-Kaolin clay, Figure 5.14b-CH₃COOH treated, Figure 5.14c-H₃PO₄ treated, Figure 5.14d-HCl treated, Figure 5.14e-HNO₃ treated, Figure 5.14f-NaOH treated

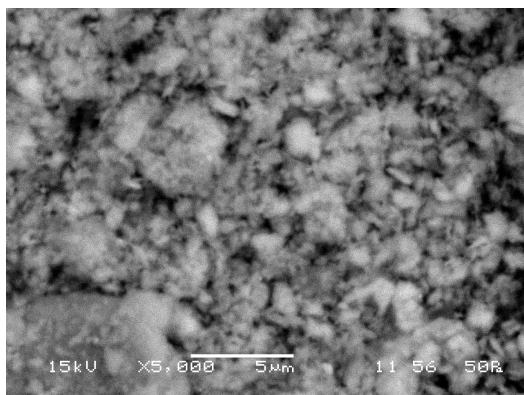


Figure 5.14a.-Kaolin clay

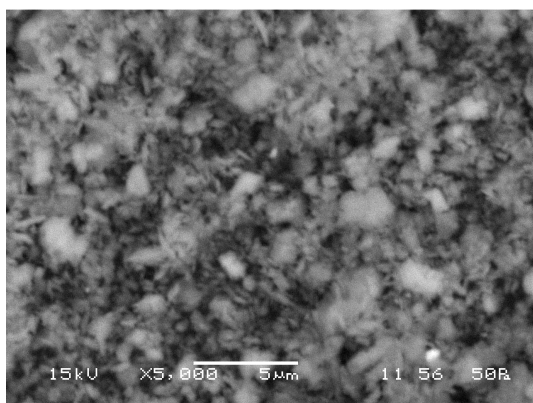


Figure 5.14b.- CH_3COOH treated

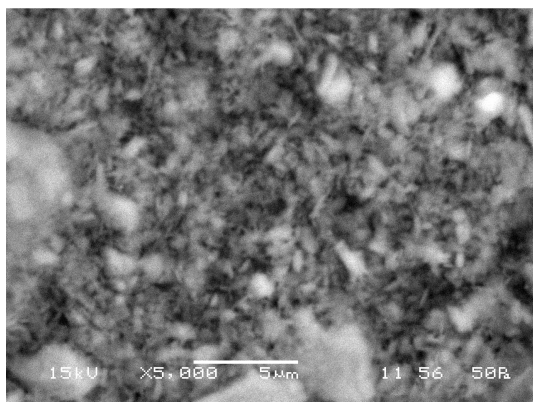


Figure 5.14c.- H_3PO_4 treated

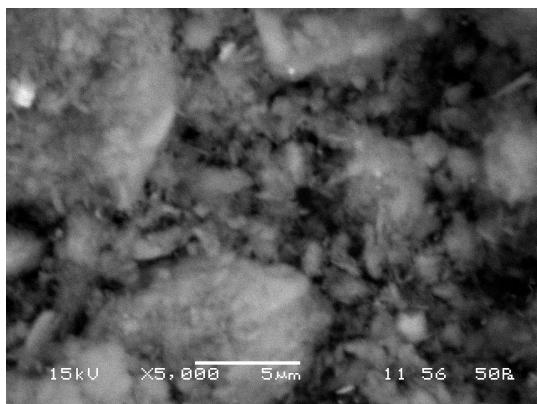


Figure 5.14d.-HCl treated

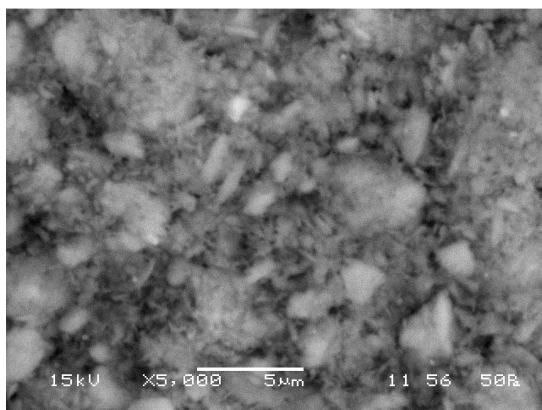


Figure 5.14e.-HNO₃ treated

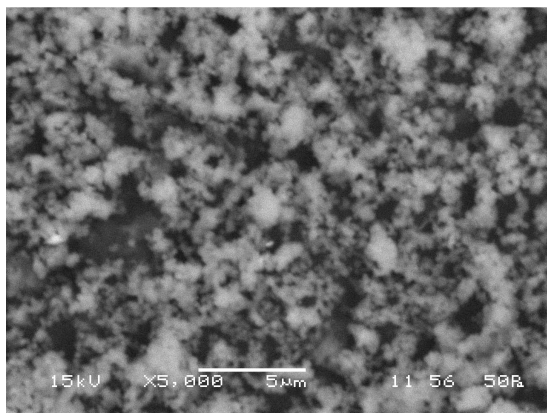


Figure 5.14f.-NaOH treated

5.4.3.7. TPD (ammonia) analysis

The acidity of aluminosilicates is characterized in terms of Bronsted and Lewis acid sites. Bronsted acid sites are formed by aluminum atoms connected to silicon by a so-called

“bridging hydroxyl” Al–(OH)–Si where the negative charge generated is compensated for by a proton. Lewis acid sites are composed of aluminum with low coordination or $\equiv\text{Si}^+$ ions formed from dehydroxylation. Therefore, the acidity of an aluminosilicate is related to its silica and aluminum contents, and increases linearly with increasing silica to aluminum ratio in the sample. Acidity values of pure kaolin and acid, alkaline treated kaolin is shown in table 5.12.

Table 5.12. Acidity Values

Materials	Acidity (mmol/g)
Kaolin	0.049
KCH_3COOH	0.109
KH_3PO_4	0.114
KHC	0.225
KHNO_3	0.341
KNaOH	0.112

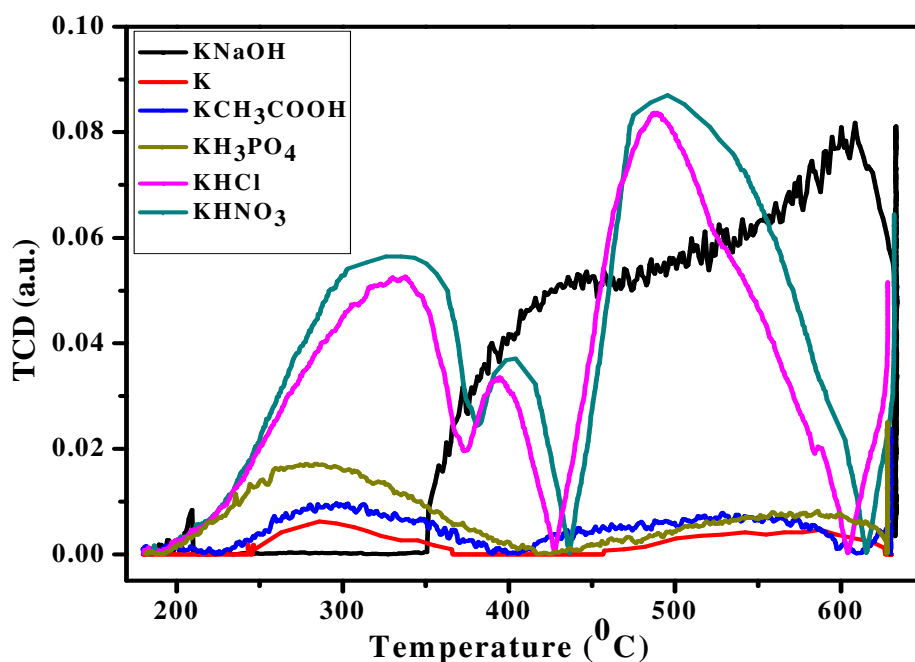


Figure 5.15. Acidity plot of acid treated catalyst

Figure 5.15 shows typical plots of ammonia desorption rates as a function of temperature for samples so treated. It can be seen from TPD plots that desorption of ammonia from all the samples starts at about 200 °C and ammonia desorption plots of samples KC, KCH_3COOH , KH_3PO_4 contain two peaks. In case of the first peak, that occurs at 200-300 °C is assigned to desorption of ammonia from Lewis acid sites as weak coordinate bond will break at low temperature. The second weak peaks at around 500-600 °C is due to desorption of Bronsted acid bound (strong ionic bond) ammonia molecules. Similarly, the plots of the ammonia desorption for samples KHCl and KHNO_3 contain three peaks out of which first one is due to Lewis acid sites which is at lower temperature and other two at higher temperature may be due to Bronsted acid sites. The lower ammonia desorption rate and as a result the less acidity were found to be on KC, KCH_3COOH , and KH_3PO_4 samples. Due to the low Si/Al-ratio of these kaolinite samples both SiOH and AlOH sites are center responsible for the ammonia adsorption. Slightly high acidity is due to dealumination. Other two samples KHCl and KHNO_3 have more acidity due to higher rate of desorption.

5.5 Catalytic conversion of waste high-density polyethylene to liquid fuel using acid and alkali treated kaolin clay

5.5.1 Introduction

Plastic materials encompass a gradually increasing share of the municipal and industrial waste going into landfill. Recycling of plastics has become a predominant subject in today's plastics industry due to the huge amount of plastic wastes and environmental pressures. Development of technologies for reducing plastic waste, which are acceptable from the environmental standpoint and are cost-effective, has proven to be a difficult challenge due to the complications innate in the reuse of polymers. Ascertaining most advantageous processes for the recycling of plastic materials thus leftovers a worldwide challenge in the new century. Plastic materials find applications in agriculture as well as in plastic packaging, which is a high-volume market owing to the many advantages of plastics over other traditional materials. High density polyethylene (HDPE) is the third largest commodity plastic material in the world, after polyvinyl chloride and polyethylene

in terms of volume ([Plastics Production](#)). The demand for HDPE is increasing day by day. The increased demand and production of HDPE has led to accumulation of large amount of its waste due to its low useful life. A thermal approach for dealing with waste plastics is the so-called chemical feedstock or chemical recycling. The most attractive technique for the chemical feed stock recycling is pyrolysis. A number of studies have been reported in which a range of catalysts and reaction conditions have been employed to convert waste plastics into the hydrocarbon liquid using pyrolysis during the past four decades. The most commonly used catalysts in the catalytic degradation of high-density polyethylene are solid acids (zeolite, silica-alumina) ([Lee KH et al. 2003](#), [Garforth AA et al. 1998](#), [Ali S et al. 2002](#), [Mastral JF et al. 2006](#), [Jan MR et al. 2013](#), [Takuma K et al. 2000](#)) and spent FCC ([Seo YH et al. 2003](#), [Manos G et al. 2000](#)).

The present work focuses on the pyrolysis of waste high-density polyethylene in a batch reactor in presence of 3M optimized concentration acid and alkaline treated kaolin clay catalysts at an optimum temperature of 450 °C and optimum catalyst to feed ratio 1:4 for enhanced yield of liquid fraction. This work also reports on the characterization of the liquid fraction using FTIR and GC-MS analysis for composition.

5.5.2 Experimental programme

The details about the materials used in this experiment such as waste HDPE, kaolin clay and acid and alkaline activation of kaolin clay and their characterization are given in experimental section chapter 3.

5.5.3 Results and Discussion

5.5.3.1 Effect of catalysts on reaction time and yield of liquid fuel

Table 5.13 shows the oil yield and reaction time for waste HDPE pyrolysis with no catalyst and using different acid and alkaline treated catalysts of 3M optimum concentration at an optimum temperature of 450 °C and optimum catalyst to feed ratio 1:4. The reaction time is higher (175 min) in thermal pyrolysis of waste HDPE which is decreased to 157 min, 135 min, 148 min, 90 min, 145 min, and 135 min in catalytic pyrolysis of waste HDPE using kaolin, HCl treated kaolin, CH₃COOH treated kaolin, HNO₃ treated kaolin, H₃PO₄ treated kaolin and NaOH treated kaolin catalysts

respectively. Similarly, the oil yield increased to 58.8%, 69.2%, 59.8%, 78.7%, 62.9% and 59.4% in catalytic pyrolysis of waste HDPE using kaolin, HCl treated kaolin, CH₃COOH treated kaolin, HNO₃ treated kaolin, H₃PO₄ treated kaolin and NaOH treated kaolin catalysts respectively as compared to oil yield of 51% in thermal pyrolysis of waste HDPE (figure 5.16). This may be due to fact that acid and alkaline treatment of kaolin clay increased the surface area, pore volume and acidity of pure kaolin. The acidic property of a catalyst is known to be closely related to the catalytic activity for the degradation of a polymer, since this acid site is necessary for the formation of carbonium ion which participates cracking reactions, strong acid sites are known to accelerate both the cracking and deactivation reactions, yielding higher amounts of liquid product. We believe that the initiation of polymer degradation will be at the external surface or at the pore margins of the pure kaolin since HDPE will be too large to diffuse into the internal sites. The decomposed fragments of appropriate sizes will then diffuse into the kaolin pores where further catalytic cracking occurs (Takuma K et al. 2000).

Table 5.13. Results of the waste HDPE pyrolysis (Temperature=450 °C, Catalyst: Feed=1:4) using different types of catalysts of optimum concentration (3M concentration)

Catalyst	Yield of oil in wt.%	Reaction time in minute
No catalyst (Thermal)	51	175
KC	58.8	157
KC (HCl)	69.2	135
KC (CH ₃ COOH)	59.8	148
KC(HNO ₃)	78.7	90
KC (H ₃ PO ₄)	62.9	145
KC (NaOH)	59.4	135

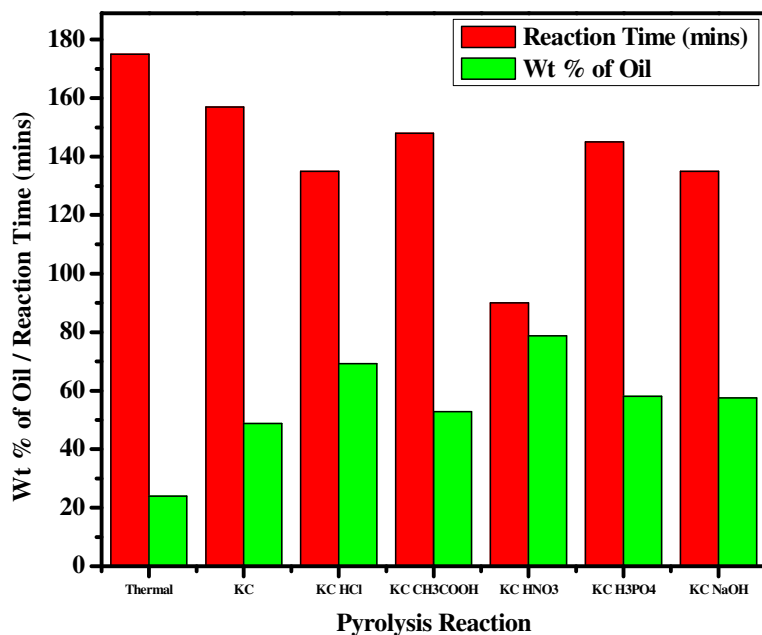


Figure 5.16. Effect of catalysts on reaction time and yield of liquid fuel

5.5.3.2 Compositional analysis of waste HDPE pyrolysis oil using acids and alkaline treated kaolin

5.5.3.1.2.1 FTIR analysis of waste HDPE pyrolysis oil using acids and alkaline treated kaolin

5.5.3.1.2.1.1 FTIR analysis of waste HDPE pyrolysis oil using hydrochloric acid treated kaolin

Figure 5.17 is the FTIR spectrum of the waste HDPE pyrolysis oil with some significant assignments. The presences of functional groups corresponding to different peaks in the spectra are summarized in Table 5.14. The table indicates that most of the components of the oil are aromatic in nature.

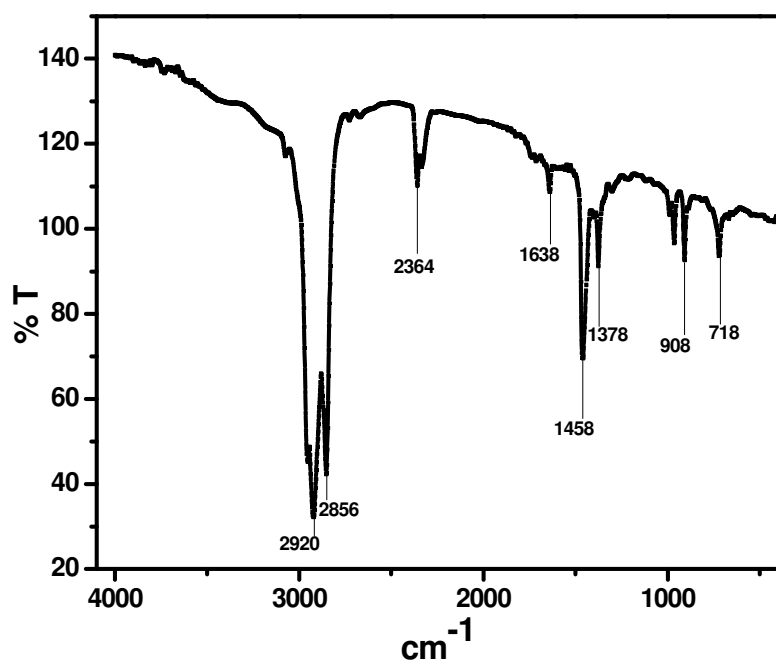


Figure 5.17. FTIR spectra of waste HDPE pyrolysis oil using hydrochloric acid treated kaolin

Table 5.14 FTIR assignments of hydrochloric acid treated kaolin catalyzed pyrolysis oil

Frequency	Type of Vibration	Name of the functional group
2920	C-H stretching	Alkanes
2856	C-H stretching	Alkanes
2364	C=O stretching	Aldehydes, Ketones, Carboxylic acids, Esters
1638	C=C stretching	Alkenes
1458	C-H scissoring and bending	Alkanes
1378	C-H scissoring and bending	Alkanes
908	C-H bending	Alkenes
718	C-H bending	Phenyl Ring Substitution Bands

5.5.3.1.2.1.2 FTIR analysis of waste HDPE pyrolysis oil using acetic acid treated kaolin

Figure 5.18 is the FTIR spectrum of waste HDPE pyrolysis oil with some significant assignments. The presences of functional groups corresponding to different peaks in the spectra are summarized in Table 5.15. The table indicates that most of the functional groups are alkanes and alkenes in the oil.

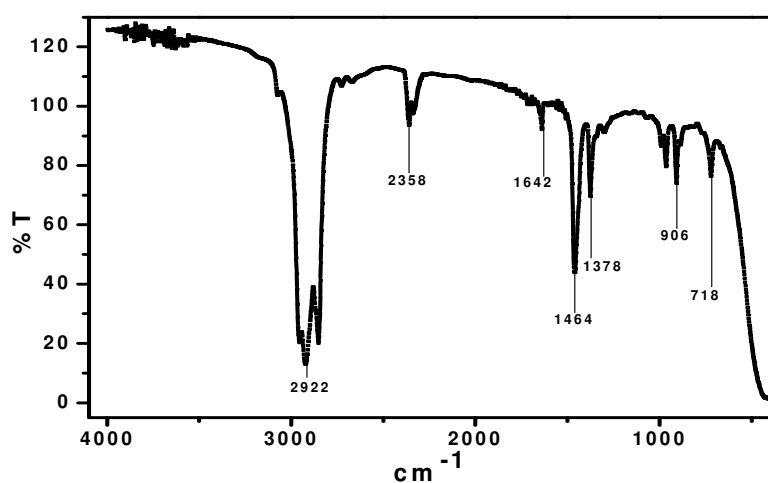


Figure 5.18. FTIR spectra of acetic acid treated kaolin catalyzed pyrolysis oil

Table 5.15. FTIR assignments of acetic acid treated kaolin catalyzed pyrolysis oil

Frequency	Type of Vibration	Name of the functional group
2922	C-H stretching	Alkanes
2358	C=O stretching	Aldehydes, Ketones, Carboxylic acids, Esters
1642	C=C stretching	Alkenes
1464	C-H scissoring and bending	Alkanes
1378	C-H scissoring and bending	Alkanes
906	C-H bending	Alkenes
718	C-H bending	Phenyl Ring Substitution Bands

5.5.3.1.2.1.3 FTIR analysis of waste HDPE pyrolysis oil using nitric acid treated kaolin

Figure 5.19 is the FTIR spectrum of waste HDPE pyrolysis oil with some significant assignments. The presences of functional groups corresponding to different peaks in the spectra are summarized in Table 5.16. The table indicates that most of the functional groups in the oil are alkanes, alkenes, phenol and hydroxyl group.

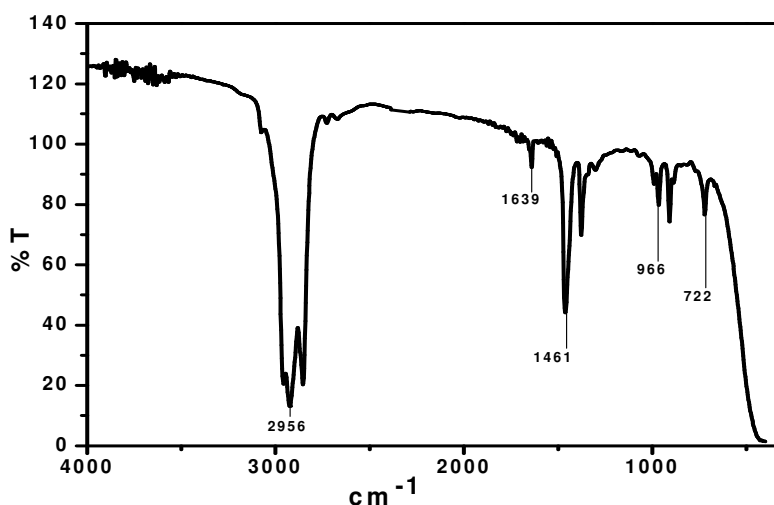


Figure 5.19. FTIR spectra of nitric acid treated kaolin catalyzed pyrolysis oil

Table 5.16. FTIR assignments of nitric acid treated kaolin catalyzed pyrolysis oil

Frequency	Type of Vibration	Name of the functional group
3675	C-H stretching	Alkynes
2956	C-H stretching	Alkanes
2360	C=O stretching	Aldehydes, Ketones, Carboxylic acids, Esters
1639	C=C stretching	Alkenes
1461	C-H scissoring and bending	Alkanes
966	C-H bending	Alkenes
722	C-H bending	Phenyl Ring Substitution Bands

5.5.3.1.2.1.4 FTIR analysis of waste HDPE pyrolysis oil using phosphoric acid treated kaolin

Figure 5.20 is the FTIR spectrum of waste HDPE pyrolysis oil with some significant assignments. The presences of functional groups corresponding to different peaks in the spectra are summarized in Table 5.17. The table indicates that most of the functional groups are alkanes and alkenes in the oil.

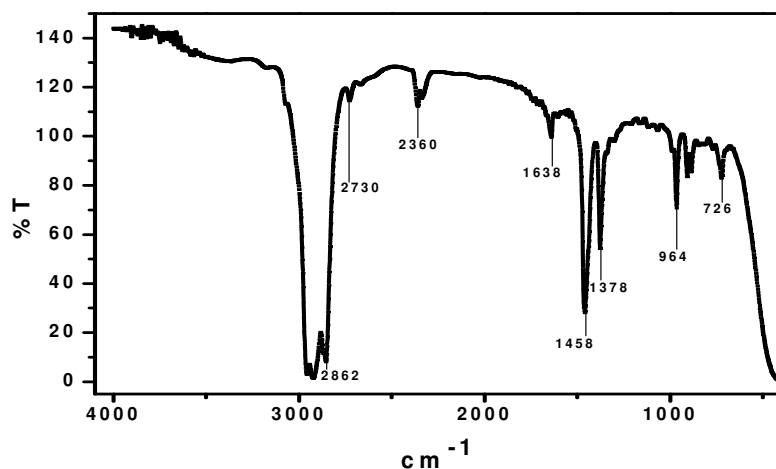


Figure 5.20. FTIR spectra of phosphoric acid treated kaolin catalyzed pyrolysis oil

Table 5.17. FTIR assignments of phosphoric acid treated kaolin catalyzed pyrolysis oil

Frequency	Type of Vibration	Name of the functional group
2862	C-H stretching	Alkanes
2730	C=O stretching	Aldehydes, Ketones, Carboxylic acids, Esters
2360	C=O stretching	Aldehydes, Ketones, Carboxylic acids, Esters
1638	C=C stretching	Alkenes
1458	C-H scissoring and bending	Alkanes
1378	C-H scissoring and bending	Alkanes
964	C-H bending	Alkenes
726	C-H bending	Phenyl Ring Substitution Bands

5.5.3.1.2.1.5 FTIR analysis of waste HDPE pyrolysis oil using sodium hydroxide treated kaolin

Figure 5.21 is the FTIR spectrum of waste HDPE pyrolysis oil with some significant assignments. The presences of functional groups corresponding to different peaks in the spectra are summarized in Table 5.18. The table indicates that most of the functional groups are alkanes and alkenes in the oil.

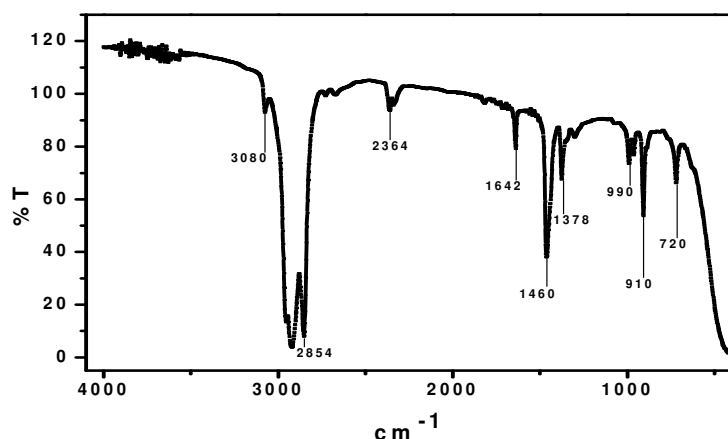


Figure 5.21. FTIR spectra of sodium hydroxide treated kaolin catalyzed pyrolysis oil

Table 5.18. FTIR assignments of sodium hydroxide treated kaolin catalyzed pyrolysis oil

Frequency	Type of Vibration	Name of the functional group
3080	C-H stretching	Alkenes
2854	C-H stretching	Alkanes
2364	C=O stretching	Aldehydes, Ketones, Carboxylic acids, Esters
1642	C=C stretching	Alkenes
1460	C-H scissoring and bending	Alkanes
1378	C-H scissoring and bending	Alkanes
990	C-H bending	Alkenes
910	C-H bending	Alkenes
720	C-H bending	Phenyl Ring Substitution Bands

5.5.3.1.2.2 GC-MS analysis of waste HDPE pyrolysis oil using acids and alkali treated kaolin

5.5.3.1.2.2.1 GC-MS analysis of waste HDPE pyrolysis oil using hydrochloric acid treated kaolin

The chemical composition of the waste HDPE pyrolysis oil was determined using GC-mass spectrometry (Figure 5.22). The compounds present in the oil were identified by comparing the chromatogram obtained with standard chromatogram data available. In chemical composition analysis (Table 5.19), it has been observed that the oil contains around 27 compounds. Taking into account of area percentage, the highest peak areas of total ion chromatogram (TIC) of the compounds were n-heptadecane, n-octadecane, 1-pentadecene and 1-nonadecene.

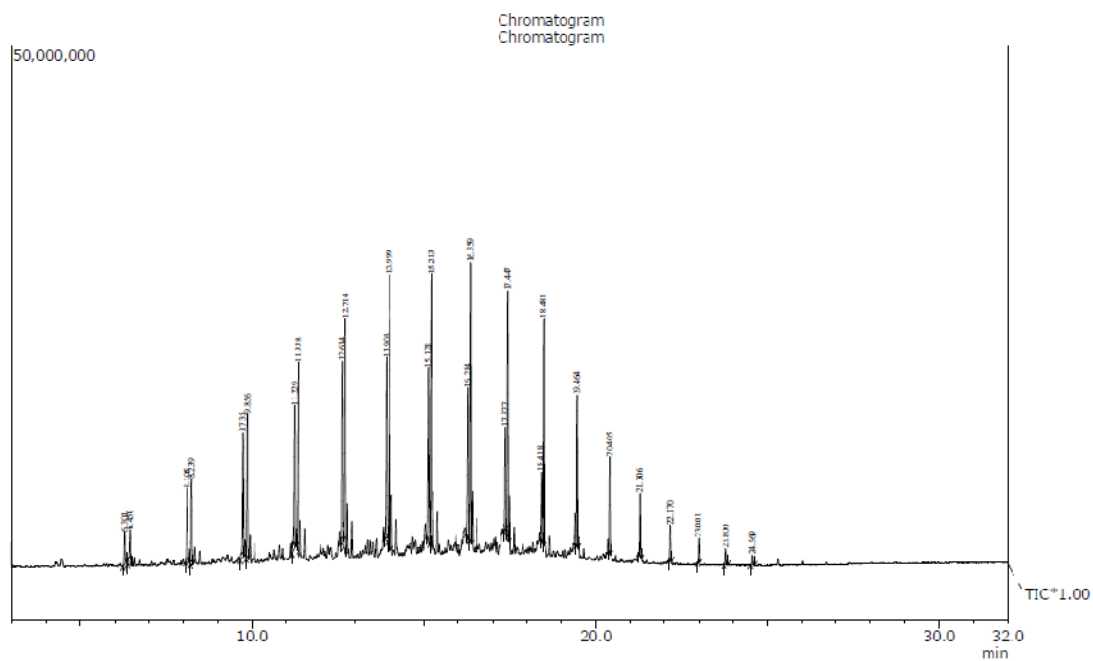


Figure 5.22. GC plot hydrochloric acid treated kaolin catalyzed pyrolysis oil

Table 5.19. GC-MS analysis of waste HDPE pyrolytic oil using hydrochloric acid treated kaolin

R. Time (min.)	Area%	Name of Compound	Molecular Formula
6.301	0.94	1-Decene	C ₁₀ H ₂₀
6.450	1.22	Decane	C ₁₀ H ₂₂
8.105	2.31	n-1-Undecene	C ₁₁ H ₂₂
8.239	2.47	Undecane	C ₁₁ H ₂₄
9.735	3.85	1-Dodecanol	C ₁₂ H ₂₆ O
9.856	4.10	n-Dodecane	C ₁₂ H ₂₆
11.229	4.53	1-Tridecene	C ₁₃ H ₂₆
11.338	4.99	Tridecane	C ₁₃ H ₂₈
12.614	5.20	1-Tetradecene	C ₁₄ H ₂₈
12.714	6.36	Tetradecane	C ₁₄ H ₃₀
13.908	5.41	1-Pentadecene	C ₁₅ H ₃₀
13.999	6.97	Pentadecane	C ₁₅ H ₃₂
15.128	5.49	1-Nonadecene	C ₁₉ H ₃₈
15.213	7.50	n-Heptadecane	C ₁₇ H ₃₆
16.284	4.60	1-Heptadecene	C ₁₇ H ₃₄
16.359	7.39	n-Octadecane	C ₁₈ H ₃₈
17.377	2.71	1-Octadecene	C ₁₈ H ₃₆
17.447	6.38	n-Octadecane	C ₁₈ H ₃₈

The chemical composition of the waste HDPE pyrolysis oil was determined using GC-mass spectrometry (Figure 5.23). The compounds present in the oil were identified by comparing the chromatogram obtained with standard chromatogram data available. In chemical composition analysis (Table 5.20), it has been observed that the oil contains around 31 compounds. Taking into account of area percentage, the highest peak areas of total ion chromatogram (TIC) of the compounds were tetradecane, pentadecane, tridecane, n-octadecane and n-heptadecane.



Table 5.20. GC-MS analysis of waste HDPE pyrolytic oil using acetic acid treated kaolin

R. Time (min.)	Area%	Name of Compound	Molecular Formula
6.291	0.95	1-Decene	C ₁₀ H ₂₀
6.445	0.78	Decane	C ₁₀ H ₂₂
8.106	2.51	1-Undecene	C ₁₁ H ₂₂
8.240	2.41	n-Undecane	C ₁₁ H ₂₄
9.739	4.56	1-Dodecanol	C ₁₂ H ₂₆ O
9.859	4.75	n-Dodecane	C ₁₂ H ₂₆
11.232	5.07	1-Tridecene	C ₁₃ H ₂₆
11.342	6.92	Tridecane	C ₁₃ H ₂₈
12.615	4.56	1-Tetradecene	C ₁₄ H ₂₈
12.716	7.89	Tetradecane	C ₁₄ H ₃₀
13.907	3.56	1-Pentadecene	C ₁₅ H ₃₀
14.000	7.11	Pentadecane	C ₁₅ H ₃₂
15.125	3.18	1-Heptadecene	C ₁₇ H ₃₄
15.209	6.97	n-Octadecane	C ₁₈ H ₃₈
16.279	2.61	1-Octadecene	C ₁₈ H ₃₆
16.355	5.99	n-Heptadecane	C ₁₇ H ₃₆
17.373	2.11	1-Octadecene	C ₁₈ H ₃₆
17.442	5.28	n-Octadecane	C ₁₈ H ₃₈
18.415	1.53	1-Nonadecene	C ₁₉ H ₃₈
18.477	4.48	Nonadecane	C ₁₉ H ₄₀
19.407	0.97	1-Docosanol	C ₂₂ H ₄₆ O
19.463	3.43	Eicosane	C ₂₀ H ₄₂
20.357	0.60	Eicosyl Trifluoroacetate	C ₂₂ H ₄₄ O ₂
20.405	2.63	n-Heneicosane	C ₂₁ H ₄₄
21.308	2.33	Docosane	C ₂₂ H ₄₆
22.173	1.67	n-Tetracosane	C ₂₄ H ₅₀
23.003	1.21	Pentacosane	C ₂₅ H ₅₂
23.801	1.03	Pentacosane	C ₂₅ H ₅₂
24.570	0.83	Hexacosane	C ₂₆ H ₅₄
25.310	1.14	n-Tetratriacontane	C ₃₄ H ₇₀
27.385	0.94	Tetracontane	C ₄₀ H ₈₂

5.5.3.1.2.2.3 GC-MS analysis of waste HDPE pyrolysis oil using nitric acid treated kaolin

The chemical composition of the waste HDPE pyrolysis oil was determined using GC-mass spectrometry (Figure 5.24). The compounds present in the oil were identified by comparing the chromatogram obtained with standard chromatogram data available. In chemical composition analysis (Table 5.21), it has been observed that the oil contains

around 25 compounds. Taking into account of area percentage, the highest peak areas of total ion chromatogram (TIC) of the compounds were eicosane, pentadecane, tridecane, n-octadecane, n-heptadecane and pentacosane.

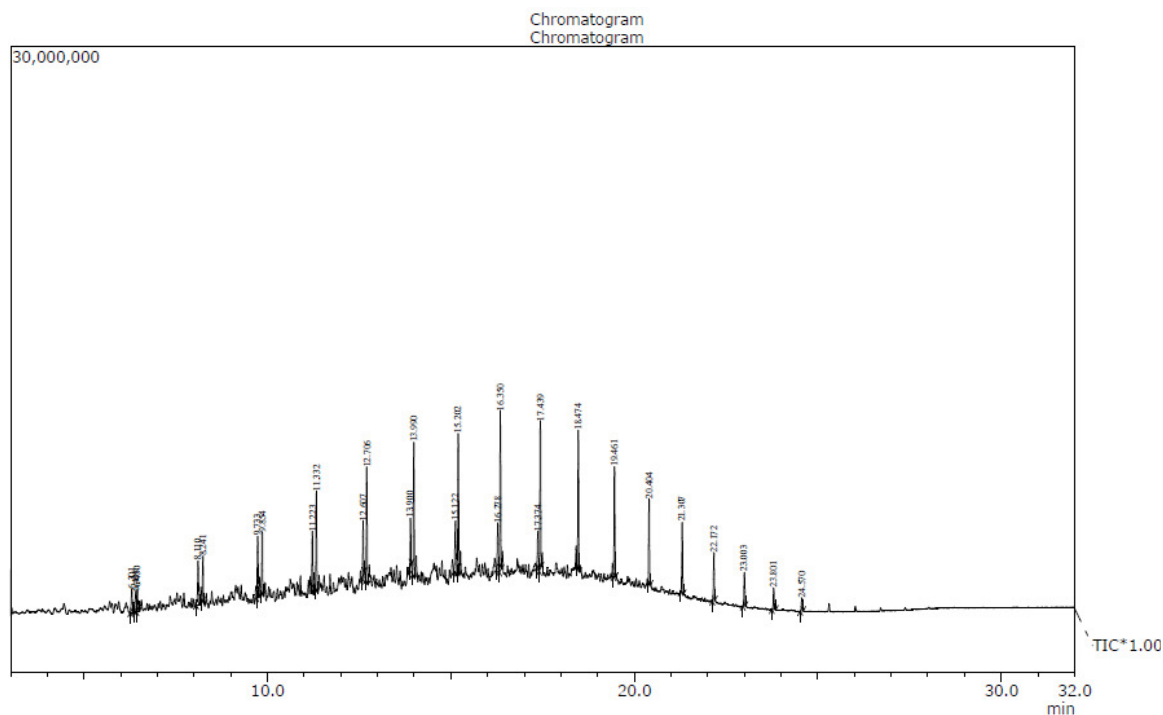


Figure 5.24. GC plot nitric acid treated kaolin catalyzed pyrolysis oil

Table 5.21. GC-MS analysis of waste HDPE pyrolytic oil using nitric acid treated kaolin

R. Time (min.)	Area%	Name of Compound	Molecular Formula
6.301	1.64	1-Decene	C ₁₀ H ₂₀
6.408	1.36	2-Methyl-2-Nonene	C ₁₀ H ₂₀
6.450	1.59	Decane	C ₁₀ H ₂₂
8.110	3.04	n-1-Undecene	C ₁₁ H ₂₂
8.241	2.22	n-Undecane	C ₁₁ H ₂₄
9.733	3.48	1-Dodecene	C ₁₂ H ₂₄
9.854	3.11	n-Dodecane	C ₁₂ H ₂₆
11.223	2.83	1-Tridecene	C ₁₃ H ₂₆
11.332	4.80	Tridecane	C ₁₃ H ₂₈
12.607	2.33	1-Tetradecene	C ₁₄ H ₂₈
12.706	5.79	Tetradecane	C ₁₄ H ₃₀
13.900	2.06	1-Pentadecene	C ₁₅ H ₃₀
13.990	6.52	Pentadecane	C ₁₅ H ₃₂
15.122	3.61	1-Hexadecene	C ₁₆ H ₃₂

15.202	7.44	n-Hexadecane	$C_{16}H_{34}$
16.278	2.73	1-Octadecene	$C_{18}H_{36}$
16.350	8.07	n-Heptadecane	$C_{17}H_{36}$
17.374	2.19	1-Octadecene	$C_{18}H_{36}$
17.439	7.87	n-Octadecane	$C_{18}H_{38}$
18.474	6.70	Nonadecane	$C_{19}H_{40}$
19.461	5.97	Eicosane	$C_{20}H_{42}$
20.404	4.54	n-Heneicosane	$C_{21}H_{44}$
21.307	3.64	Docosane	$C_{22}H_{46}$
23.003	1.84	n-Tetracosane	$C_{24}H_{50}$
23.801	4.62	Pentacosane	$C_{25}H_{52}$

5.5.3.1.2.2.4 GC-MS analysis of waste HDPE pyrolysis oil using phosphoric acid treated kaolin

The chemical composition of the waste HDPE pyrolysis oil was determined using GC-mass spectrometry (Figure 5.26). The compounds present in the oil were identified by comparing the chromatogram obtained with standard chromatogram data available. In chemical composition analysis (Table 5.22), it has been observed that the oil contains around 23 compounds. Taking into account of area percentage, the highest peak areas of total ion chromatogram (TIC) of the compounds were 1-dodecanol, pentadecane, tridecane, n-1-undecene, n-heptadecane and n-cetane.

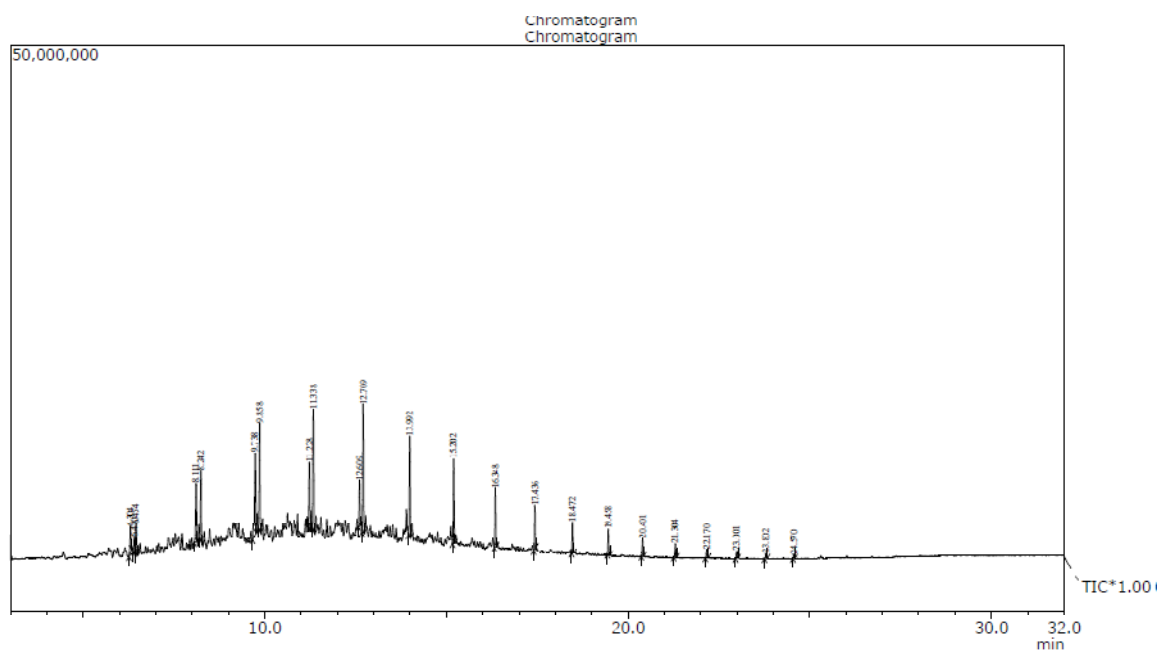


Figure 5.25. GC plot phosphoric acid treated kaolin catalyzed pyrolysis oil

Table 5.22. GC-MS analysis of waste HDPE pyrolytic oil using phosphoric acid treated kaolin

R. Time (min)	Area %	Name of Compound	Molecular Formula
6.304	2.59	1-Decene	C ₁₀ H ₂₀
6.410	1.33	2-Methyl-2-Nonene	C ₁₀ H ₂₀
6.454	3.06	Decane	C ₁₀ H ₂₂
8.111	6.18	n-1-Undecene	C ₁₁ H ₂₂
8.242	6.09	n-Undecane	C ₁₁ H ₂₄
9.738	9.87	1-Dodecanol	C ₁₂ H ₂₆ O
9.858	8.66	n-Dodecane	C ₁₂ H ₂₆
11.228	5.69	1-Tridecene	C ₁₃ H ₂₆
11.338	10.58	Tridecane	C ₁₃ H ₂₈
12.609	3.37	1-Tetradecene	C ₁₄ H ₂₈
12.709	10.21	Tetradecane	C ₁₄ H ₃₀
13.992	8.06	Pentadecane	C ₁₅ H ₃₂
15.202	6.81	n-Cetane	C ₁₆ H ₃₄
16.348	4.85	n-Heptadecane	C ₁₇ H ₃₆
17.436	3.46	n-Octadecane	C ₁₈ H ₃₈
18.472	2.62	Nonadecane	C ₁₉ H ₄₀
19.458	1.97	Eicosane	C ₂₀ H ₄₂
20.401	1.39	n-Heneicosane	C ₂₁ H ₄₄
21.304	1.12	Docosane	C ₂₂ H ₄₆
22.170	0.75	n-Tetracosane	C ₂₄ H ₅₀
23.001	0.60	Pentacosane	C ₂₅ H ₅₂
23.802	0.41	n-Pentacosane	C ₂₅ H ₅₂
24.570	0.31	Hexacosane	C ₂₆ H ₅₄

5.5.3.1.2.2.5 GC-MS analysis of waste HDPE pyrolysis oil using sodium hydroxide treated kaolin

The chemical composition of the waste HDPE pyrolysis oil was determined using GC-mass spectrometry (Figure 5.27). The compounds present in the oil were identified by comparing the chromatogram obtained with standard chromatogram data available. In chemical composition analysis (Table 5.23), it has been observed that the oil contains around 31 compounds. Taking into account of area percentage, the highest peak areas of total ion chromatogram (TIC) of the compounds were n-octadecane, 1-hexadecene, n-docosane, n-heptadecane, and tridecane.

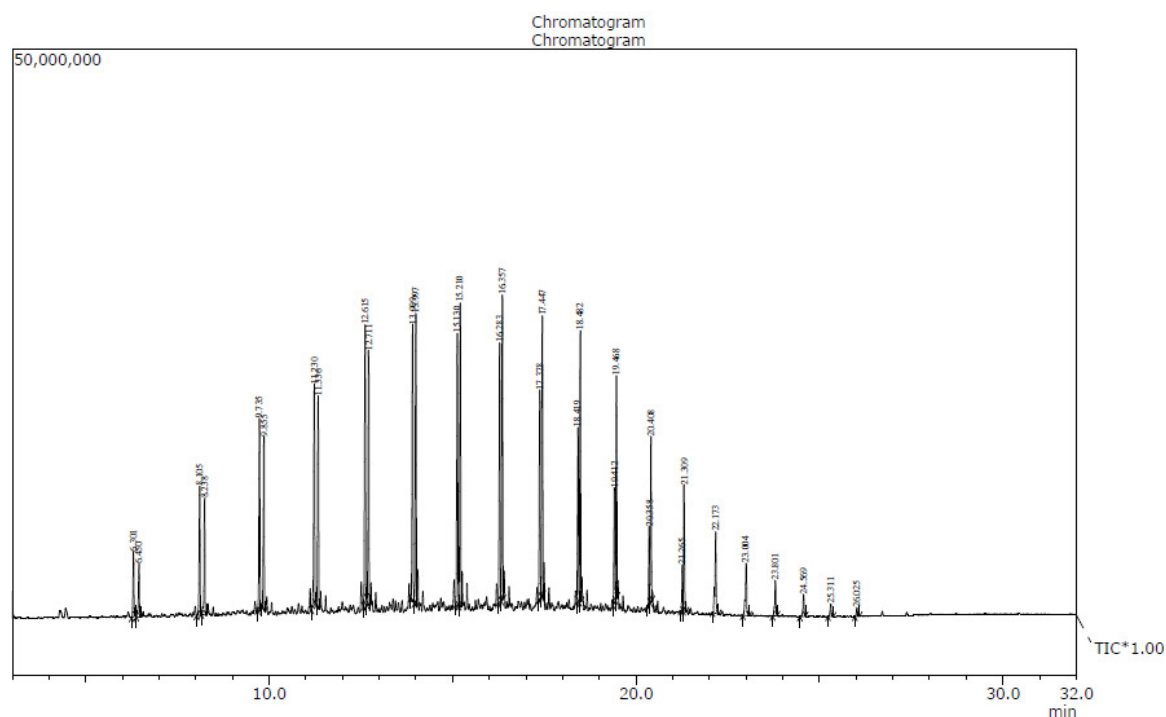


Figure 5.26. GC plot sodium hydroxide acid treated kaolin catalyzed pyrolysis oil

Table 5.23. GC-MS analysis of waste HDPE pyrolytic oil using sodium hydroxide treated kaolin

R. Time (min.)	Area %	Name of Compound	Molecular Formula
6.301	1.30	1-Decene	C ₁₀ H ₂₀
6.450	1.14	Decane	C ₁₀ H ₂₂
8.105	2.58	1-Undecene	C ₁₁ H ₂₂
8.238	2.39	n-Undecane	C ₁₁ H ₂₄
9.735	3.55	1-Dodecanol	C ₁₂ H ₂₆ O
9.855	3.25	n-Dodecane	C ₁₂ H ₂₆
11.230	4.32	1-Tridecene	C ₁₃ H ₂₆
11.336	4.01	Tridecane	C ₁₃ H ₂₈
12.615	5.05	1-Tetradecene	C ₁₄ H ₂₈
12.711	4.74	Tetradecane	C ₁₄ H ₃₀
13.909	5.30	1-Pentadecene	C ₁₅ H ₃₀
13.997	5.17	Pentadecane	C ₁₅ H ₃₂
15.130	5.44	1-Hexadecene	C ₁₆ H ₃₂
15.210	5.68	n-Octadecane	C ₁₈ H ₃₈
16.283	4.92	1-Nonadecene	C ₁₉ H ₃₈
16.357	5.35	n-Heptadecane	C ₁₇ H ₃₆
17.378	4.17	1-Octadecene	C ₁₈ H ₃₆

17.447	4.91	n-Octadecane	C ₁₈ H ₃₈
18.419	3.30	1-Nonadecene	C ₁₉ H ₃₈
18.482	4.73	Nonadecane	C ₁₉ H ₄₀
19.412	2.34	1-Docosanol	C ₂₂ H ₄₆ O
19.468	3.72	Eicosane	C ₂₀ H ₄₂
20.358	1.33	Heptacosan-1-ol	C ₂₇ H ₅₆ O
20.408	2.78	n-Heneicosane	C ₂₁ H ₄₄
21.265	0.86	EicosylTrifluoroacetate	C ₂₂ H ₄₄ O ₂
21.309	2.38	n-Docosane	C ₂₂ H ₄₆
22.173	2.06	Pentacosane	C ₂₅ H ₅₂
23.004	1.40	Pentacosane	C ₂₅ H ₅₂
23.801	0.81	n-Pentacosane	C ₂₅ H ₅₂
24.569	0.52	Hexacosane	C ₂₆ H ₅₄
25.311	0.51	Tetracontane	C ₄₀ H ₈₂

5.5.3.1.3.3 Physical properties of liquid fuel obtained by catalytic pyrolysis of waste HDPE using nitric acid treated kaolin clay

Table 5.24 shows the results of physical property analysis of liquid fuel obtained by catalytic pyrolysis of waste HDPE using nitric acid treated kaolin clay. The appearance of the oil is dark brownish free from visible sediments.

Table 5.24. Physical properties of liquid fuel obtained by catalytic pyrolysis of waste HDPE using nitric acid (3M concentration) treated kaolin clay

Tests	Results Obtained	Test method
Specific Gravity @ 15°C/15°C	0.7906	IS:1448 P:16
Density @ 15°C in kg/cc	0.7900	IS:1448 P:16
Kinematic Viscosity @ 40°C in Cst	2.1	IS:1448 P:25
Kinematic Viscosity @ 100°C in Cst	1.0	IS:1448 P:25
Conradson Carbon Residue	Less than 0.01%	IS:1448 P:122
Flash Point by Abel Method	-2°C	IS:1448 P:20
Fire Point	5°C	IS:1448 P:20
Cloud Point	12°C	IS:1448 P:10
Pour Point	-1°C	IS:1448 P:10

Gross Calorific Value in MJ/Kg	40.17	IS:1448 P:6
Sulphur Content	0.05%	IS:1448 P:33
Calculated Cetane Index (CCI)	66	IS:1448 P:9
<u>Distillation:</u>		IS:1448 P:18
Initial Boiling Point	58°C	
Final Boiling Point	376°C	

From comparison with other transportation fuels as shown in Table 5.25. The density and viscosity of liquid product can be modified by blending it with commercial transportation fuels. Flash point of the liquid fuel is in comparable range and hence will ensure safe storage but pour point is minus 1 °C which will not cause any trouble in most of the regions but in colder regions with sub-zero climates it may lead to freezing problems. Waste HDPE pyrolytic oil has GCV of 40 MJ/Kg which is less as compared to that of gasoline and diesel; therefore this liquid fuel can be used as blend with diesel or gasoline in engines. From the distillation report of the oil it is observed that, the boiling range of the oil is 58-376 °C, which infers the presence of mixture of different oil components such as gasoline, kerosene and diesel in the oil. The liquid fuel contains substantial amount of volatiles as its initial boiling point is below 100°C. From this result, it is observed the liquid fuel could be possible feedstocks for further upgrading or use of lighter compounds as a diesel fuel.

Table 5.25. Fuel properties comparison of waste HDPE oil obtained by catalytic pyrolysis with commercial transportation fuels

Properties	Specific Gravity	Kinematic Viscosity	Flash Point	Pour Point	GCV (MJ/Kg)	IBP (°C)	FBP (°C)	Chemical Formula
	15°C/15°C	@40°C (cst)	(°C)	(°C)				
Waste HDPE pyrolytic oil (Catalytic)	0.7906	2.1	-2	-1	40.17	58	376	C ₁₀ -C ₂₅

Virgin HDPE pyrolytic oil	0.8013	3.3	10	18	44.27	72	364	C ₁₀ -C ₂₀
Waste HDPE pyrolytic oil (Kumar S et al. 2011)	0.7835	1.63	1	-15	42.81	82	352	C ₁₉ -C ₂₄
Gasoline (Petroleum Product Surveys 1986)	0.72-0.78	-	-43	-40	42-46	27	225	C ₄ -C ₁₂
Diesel (Tuttle J et al. 2004)	0.82-0.85	2-5.5	53-80	-40 to -1	42-45	172	350	C ₈ -C ₂₅
Bio-Diesel (Tuttle J et al. 2004)	0.88	4-6	100-170	-3 to 19	37-40	315	350	C ₁₂ -C ₂₂
Heavy Fuel Oil (Tuttle J et al. 2004)	0.94-0.98	>200	90-180	-	- 40	-	-	-

5.6 Conclusion

The liquid yield is highest at 450 °C, highly volatile products are obtained at low temperature, the products obtained 500 °C and 550 °C are viscous liquid and wax and the product obtained at 600 °C is only wax. Liquid yield increases as the holding time increases from 1 hr to 4 hr at the increment of temperature from 400 °C to 450 °C but as the holding time increases from 4 hr to 6 hr, the liquid yield decreases. Reaction time decreases with increase in temperature. Different catalysts (kaolin, mordenite and silica-alumina) have the significant effect on liquid product yield and reaction time. Liquid yield is more 58.8 wt% with kaolin catalyst, 58.4 wt% with mordenite catalysts and 58.9 wt% with silica-alumina catalyst as compared to 51 wt% of liquid yield in thermal pyrolysis. Reaction time is very less 190 min with silica-alumina catalyst, 175 min with mordenite catalysts and 157 min with kaolin catalyst as compared to 290 min in thermal pyrolysis. It has been shown that a simple batch pyrolysis method can convert waste HDPE to liquid hydrocarbon products with a significant yield which varies with temperature and catalysts to plastic ratio.

The effect of the acid and alkali treatment on the structural and chemical properties of kaoline clay has been studied. The XRF and SEM study indicated clearly the leaching and disintegration of the clay sheet after treatment with different acid and alkali. The Al_2O_3 , MgO , CaO , K_2O , TiO_2 and ZnO contents in the treated material decreased progressively simultaneously increasing the SiO_2 content. XRD studies of the acid treated clay indicated the structural transformation of the clay sheet upon acid treatment. After acid treatment the peak intensity of the clay was found to decrease and extent of decrease follows the trend $\text{HNO}_3 > \text{HCl} > \text{H}_3\text{PO}_4 > \text{CH}_3\text{COOH}$. FTIR spectrum of the acid treated kaolinite clay shows that there is not much variation in the peak pattern for H_3PO_4 and CH_3COOH acid treated kaoline. The peak intensity is found to decrease progressively for HNO_3 and HCl acid treated kaoline and for NaOH treated kaolin, the structural hydroxyl vibration band is extremely weak. TGA profile of the parent and the acid treated clay shows that acid treatment increased the amount of physisorbed water and it increased with increased strength of the acid ($\text{HNO}_3 > \text{HCl} > \text{H}_3\text{PO}_4 > \text{CH}_3\text{COOH}$). It is extraordinarily high in case of sodium hydroxide treated kaolin. The DTA profiles of the clay and acid treated clay supports the weight loss pattern due to water removal in the TGA study. The increase in pore volume and BET surface area due to acid treatment is more prominent as compared to alkali treatment. The SEM micrograph of KC reveals the presence of large particles which are aggregated after treatment with HCl , HNO_3 , NaOH and disaggregated when treated with H_3PO_4 and CH_3COOH . The acidity was less in case of pure kaolin and after treatment with CH_3COOH and H_3PO_4 acids while HCl and HNO_3 acids treated kaolin have more acidity.

Reaction time decreased to 157 min, 135 min, 148 min, 90 min, 145 min, and 135 min in catalytic pyrolysis of waste HDPE using kaolin, HCl treated kaolin, CH_3COOH treated kaolin, HNO_3 treated kaolin, H_3PO_4 treated kaolin and NaOH treated kaolin catalysts respectively as compared to 175 min in thermal pyrolysis of waste HDPE. Similarly, the oil yield increased to 58.8%, 69.2%, 59.8%, 78.7%, 62.9% and 59.4% in catalytic pyrolysis of waste HDPE using kaolin, HCl treated kaolin, CH_3COOH treated kaolin, HNO_3 treated kaolin, H_3PO_4 treated kaolin and NaOH treated kaolin catalysts as compared to oil yield of 51% in thermal pyrolysis of waste HDPE. Reaction time is 90 min and oil yield is 79% in catalytic pyrolysis of waste HDPE using nitric acid treated kaolin clay. Study of FTIR and GC-MS confirmed the presence of different hydrocarbons (mostly alkanes and olefins) in the oil obtained by catalytic pyrolysis of waste HDPE using acids and alkaline treated kaolin clay.

Chapter 6

Optimization of Process Parameters by Response Surface Methodology (RSM)

OPTIMIZATION OF PROCESS PARAMETERS BY RESPONSE SURFACE METHODOLOGY (RSM) FOR CATALYTIC PYROLYSIS OF WASTE HIGH-DENSITY POLYETHYLENE TO LIQUID FUEL

6.1 Introduction

Plastic materials comprise a steadily increasing proportion of the municipal and industrial waste going into landfill. Owing to the huge amount of plastic wastes and environmental pressures, recycling of plastics has become a predominant subject in today's plastics industry (Kumar S et al. 2011b). HDPE is the third largest commodity plastic material in the world, after polyvinyl chloride and polypropylene in terms of volume. The demand for HDPE has increased 4.4% a year to 31.3 million MT in 2009 (Plastics Production). The increased demand and production of waste HDPE has led to the accumulation of large amount of its waste in the final waste stream due to its low useful life. Recycling of plastics already occurs on a wide scale. The most attractive technique of chemical feedstock recycling is pyrolysis (Kumar S et al. 2011a). Pyrolysis is known to be an environmentally friendly method because no wastes are produced during the process. The effect of temperature and the type of reactor on the pyrolysis of waste HDPE has been studied by different researchers (Walendziewski J et al. 2001, Marcilla A et al. 2001, Stefanis AD et al. 2001). The thermal degradation of waste HDPE can be improved by using suitable catalysts in order to obtain valuable products. The most common catalysts used in this process are: zeolite, alumina, silica–alumina, FCC catalyst, reforming catalyst (Venuto PB et al. 1979, Sharratt PN et al. 1997, Lee KH et al. 2003a, Lee KH et al. 2003b, Miskolczi N et al. 2008, Seo YH et al. 2003, Park JW et al. 2002, Manos G et al. 2000, Hernandez MR et al. 2006). A number of studies for liquid fuel production from pyrolysis of waste plastics have been reported at various scales and with varying success (Panda AK et al. 2011, Panda AK et al. 2012). The yield of liquid from thermal or catalytic pyrolysis depends on the relationship of parameters set in the process. In terms

of modeling and optimization in catalytic cracking process, there is only a few researcher focused on improving the process optimization. Most of previous researchers concerned on catalyst finding. Therefore, an optimization study was needed to adjust the parameters to maximize the production of liquid. One of the methods used to solve the optimization problem is to apply response surface methodology (RSM). In the present work, catalytic pyrolysis of waste high-density polyethylene was carried out to evaluate the yield and quality of liquid fuel produced. The mass ratio between modified catalysts to waste HDPE, temperature, and acidity of the modified catalysts were chosen as independent variables. The process was optimized by using response surface methodology with the aim of maximizing liquid yield. The liquid obtained was tested for physical properties, Gas chromatography-Mass spectrometry (GC-MS) and Fourier transform infrared (FTIR).

6.2 Experimental programme

The details about the characterization of raw material, preparation of catalysts, experimental setup and procedure and characterization of the liquid fuel are given in experimental section chapter 3. The detail about the optimization study is summarized below:

6.2.1 Optimization study

The responses and the corresponding factors are modeled and optimized using the response surface methodology. The RSM technique is aimed for: (a) designing of experiments to provide adequate and reliable measurements of the response, (b) developing a mathematical model having the best fit to the data obtained from the experimental design, and (c) determining the optimal value of the independent variables that produces maximum or minimum value of the response. Therefore, RSM was used to determine the optimum and experimental design matrix in this study specified according to the central composite design (CCD) method. Three effective parameters (temperature, catalysts to feed ratio and acidity of catalyst) were applied in this study with each parameter being evaluated at fifteen different points. Each point was investigated to

select the points that produced the largest volume of pyrolytic liquid. The variables and the experimental domain in this design are specified in Table 6.1.

Table 6.1. Range of independent variables and the experimental domain

Variables	Experimental domain		
	(-1)-level	0-level	(+1)-level
T: Temperature (°C)	400	450	500
A: Acidity of Catalysts	0.109	0.225	0.341
CR: Catalysts Ratio	2	4	6

The CCD consists of 8 cube points, 6 center points in cube, 6 axial points and 0 center points in axial. Thus, the CCD in this study, resulting in 20 experiments. The CCD matrix for varying 3 variables was constructed in Table 8.2.

Table 6.2: The CCD matrix of experimental and yield response

Run Order	Actual variables			Coded levels			Response
	Temperature (°C)	A (Acidity of catalysts)	CR (Catalysts to waste HDPE ratio)	T	A	CR	Liquid Yield 'Y' (wt%)
1	450	0.225	6	0	0	1	51.8
4	450	0.225	2	0	0	-1	56.4
6	450	0.109	4	0	-1	0	63.9
14	450	0.341	4	0	1	0	78.7
17	500	0.225	4	1	0	0	27.1
18	400	0.225	4	-1	0	0	28.8
2	450	0.225	4	0	0	0	70.6
5	450	0.225	4	0	0	0	69.9
7	450	0.225	4	0	0	0	71.2
9	450	0.225	4	0	0	0	68.5
13	450	0.225	4	0	0	0	67.9
19	450	0.225	4	0	0	0	67.0
3	500	0.109	6	1	-1	1	11.5
8	500	0.341	6	1	1	1	21.6
10	400	0.109	2	-1	-1	-1	18.9
11	400	0.341	2	-1	1	-1	29.9
12	400	0.109	6	-1	-1	1	17.8
15	500	0.341	2	1	1	-1	23.4
16	400	0.341	6	-1	1	1	27.2
20	500	0.109	2	1	-1	-1	12.8

All experiments were performed randomly to reduce the effect of unexplainable variance in the observed response caused by unrelated variables. After running the experiments, the results were fitted to a quadratic polynomial model to predict the system response as given in Eq. 1.

$$Y = \beta_0 + \sum_{i=1}^n \beta_i * X_i + \sum_{i=1}^n \beta_{ii} * X_i^2 + \sum_{i=1}^n \sum_{j>1}^n \beta_{ij} * X_i X_j \quad (1)$$

where Y is the predicted response; n is the number of experiments; β_0 , β_i , β_{ii} and β_{ij} are regression coefficients for the constant, linear, quadratic and interaction coefficients, respectively; and X_i and X_j are the coded independent factors. For each experimental factor the variance was partitioned into components, linear, quadratic and interaction, in order to assess the adequacy of the second order polynomial function and the relative importance or significance of the terms.

Minitab software Version 16.2.0 (Minitab Inc., Pennsylvania, USA) was used in this study. Three-dimensional response surfaces and contour plots were used for facilitating a straight forward examination of the influence of experimental variables on the responses. The individual response surface and the contour plots were created by holding both variables constant at their center points. Coefficients of the models for three responses were estimated with multiple regression analysis. The fit quality of the models was judged from their coefficients of correlation and determination. The adequacy of each model was also checked with the analysis of variance (ANOVA) using Fisher F -test (Montgomery DC 2001, Clarke GM et al. 1997, Cornell JA 1990, Box GEP et al. 1978). Significance of each equation parameter for each response was assessed by p -value and Student's t -test. The significance test is purposed to determine the relationship between the response variable and a subset of the independent variables.

6.3 Result and Discussion

6.3.1 Characterization of raw material and catalyst modification

The ultimate or elemental analysis of waste HDPE is shown in Table 6.3. The oxygen is 5.19% in the ultimate analysis of waste HDPE. The oxygen in the waste HDPE sample

may not be due to the fillers but rather to other ingredients that are added to the resin in the manufacturing of HDPE. Calorific value of waste HDPE was 45.78 MJ/Kg.

Table 6.3 Ultimate or elemental analysis of waste HDPE

Sample	C (wt%)	H (wt%)	N (wt%)	S (wt%)	O (wt%)	Cl (wt%)	GCV (MJ/kg)
Waste HDPE	80.58	13.98	0.60	0.080	5.19	-	45.78
Mixed Plastics (Cho MH et al. 2010)	79.9	12.6	-	-	5.10	1.13	44.40

From the comparison of waste HDPE with mixed plastic waste (Cho MH et al. 2010) in Table 6.3, it was found that the carbon and hydrogen percentage and gross calorific value (GCV) are more in waste HDPE as compared to mixed plastic waste. Mixed plastic waste contained 1.13% of chlorine which was not found in case of waste HDPE.

The chemical composition of the catalyst (kaolin clay and modified kaolin clay after acid treatment) was determined by the X-ray fluorescence (XRF) analysis. Table 6.4 shows the results of chemical analysis of the parent kaolin clay and acid treated kaolin clay.

Table 6.4 XRF analysis and acidity of parent and acid treated kaolin clay

Material	Chemical Content (% weight)								Si/Al Ratio	Acidity (mmol/g)
	SiO ₂	Al ₂ O ₃	MgO	CaO	K ₂ O	ZnO	TiO ₂	V ₂ O ₅		
KC	43.12	46.07	0.027	0.030	0.010	0.0064	0.74	0.003	0.82	0.049
KC (HCl)	48.80	37.61	0.016	0.017	0.01	0.0064	0.26	0.001	1.144	0.225
KC (HNO ₃)	56.42	27.88	0.02	0.008	0.008	0.0064	0.23	0.002	1.782	0.341
KC (H ₃ PO ₄)	45.83	41.51	Nil	0.01	0.007	0.0064	0.44	0.001	0.972	0.114
KC (CH ₃ COOH)	44.03	43.81	0.026	0.017	0.01	0.0065	0.20	0.003	0.885	0.109
KC (NaOH)	56.14	29.30	0.070	0.186	0.017	0.0064	0.12	Nil	1.688	0.112

The parent kaolin clay contains alumina and silica which are in major quantities where as other oxides such as magnesium oxide, calcium oxide, potassium oxide, zinc oxide and titanium oxide are present in trace amounts. After acid treatment, it was observed that the composition of the parent kaolin clay changes significantly. The Al_2O_3 , MgO , CaO and K_2O contents in the acid treated kaolin clay decreased progressively after the acid treatment of pure kaolin clay. Simultaneously, SiO_2 content increased after acid treatment of pure kaolin clay due to which the Si/Al ratio increased. The alumina content in the acid treated kaolin clay decreased due to the leaching of the Al^{3+} ions from the octahedral layer under acidic conditions by hydrolysis (Kumar S et al. 2013). The relative amount of the acid sites of the samples was evaluated by thermal desorption of ammonia. Ammonia is a strong base ($\text{pKb} \approx 5$) that reacts even with extremely weak acid sites, which therefore makes NH_3 -TPD a useful technique for evaluating the relative amount of acid sites present on a surface. The acidity of the acid treated kaolin clay is summarized in Table 8.4. The acidity of the kaolin clay is 0.049mmol/g which increases to 0.109mmol/g, 0.112mmol/g and 0.114mmol/g, 0.225mmol/g and 0.341mmol/g by treating it with 3M acetic acid, sodium hydroxide, phosphoric acid, hydrochloric acid and nitric acid respectively followed by calcination at 650 °C. The increase of acidity is due to creation of specific acid sites on the surface of silica generated due to leaching.

6.3.2 Optimization study of liquid fuel yield

Response Surface Methodology simulation focused on effect of reactor temperature, catalyst to feed ratio and acidity of catalysts on yields of liquid fuel in a semi batch reactor for present study. Three effective parameters (temperature, catalysts to feed ratio and acidity of catalyst) were selected in this study with each parameter being evaluated at five different points. Each point was investigated to select the points that produced the largest volume of pyrolytic liquid. The temperatures were varied in 25 °C increments from 400 °C to 500 °C, the acidities of catalysts were varied in range of 0.109, 0.112, 0.114, 0.225 and 0.341 and the ratios of different catalysts to waste HDPE were 1:2, 1:4 and 1:6 in this optimization study. A maximum liquid fuel yield response was obtained using RSM located at the instantaneous optimal factors. Coefficients of the liquid fuel

yield model proposed in Eq. (1) were estimated using multiple regression analysis in the RSM. The coded factor model developed to fit a polynomial model is represented in Eq. 2, where Y is yield of pyrolytic liquid, T is temperature, A is acidity, and CR is catalyst to feed ratio.

$$Y = -3133.19 + 14.07 (T) - 86.69 (A) + 25.52 (CR) - 0.015 (T^2) + 303.34 (A^2) - 3.27 (CR^2) + 0.006 (T*A) + 0.0008 (T*CR) - 1.13 (A*CR) \quad (2)$$

The results of analysis of variance (ANOVA) for yield 'Y' were summarized in Table 6.5.

Table 6.5 ANOVA for liquid fuel yield model

Source	Degree of freedom (df)	Sum of Squares (SS)	Mean Square (MS)	F-Value	p-value	% Contribution
Regression	9	10856.4	1206.27	264.00	0.000	99.58
Linear	3	394.4	131.45	28.77	0.000	3.62
T	1	68.6	68.64	15.02	0.003	0.63
A	1	312.5	312.48	68.39	0.000	2.87
CR	1	13.2	13.22	2.89	0.120*	0.12
Square	3	10461.5	3487.15	763.18	0.000	95.96
T*T	1	9986.0	4240.47	928.05	0.000	91.60
A*A	1	2.2	45.82	10.03	0.010	0.02
CR*CR	1	473.2	473.24	103.57	0.000	4.34
Interaction	3	0.6	0.21	0.05	0.986*	0.01
T*A	1	0.0	0.01	0.00	0.961*	0.00
T*CR	1	0.1	0.06	0.01	0.910*	0.00
A*CR	1	0.6	0.55	0.12	0.736*	0.01
Residual Error	10	45.7	4.57			0.42
Lack-of-Fit	5	32.2	6.44	2.39	0.180*	0.30
Pure Error	5	13.5	2.69			0.12
Total	19	10902.1				100.00

S = 2.13758 R-Sq = 99.58% R-Sq (adj) = 99.20% *insignificant (p -value > 0.05)

The analysis showed that the p -value (less than 0.05) as a statistic test indicated that the model terms are significant. In this case, T, A, T^2 , A^2 and CR^2 are significant model terms while linear CR and interaction (T*A, T*CR, A*CR) are insignificant. The parameter having the most significant effect on pyrolytic liquid yield is the acidity (A)

since the p -value of A is the smallest in value compared to other conditions. Liquid fuel yield increased from 63.9 wt% at the 0.109 acidity value to 78.7 wt% at the 0.341 acidity value. Similar result has been obtained in catalytic pyrolysis of waste polypropylene with sulphuric acid treated kaolin clay (Panda AK 2011). Furthermore, the model developed also shows a high determination coefficient of R^2 (0.995), indicating a close fit of the model to the actual data. R^2 can be calculated using Eq. 3. The actual value represents the response data from the experiment; the predicted value represents the value obtained from the model.

$$R^2 = 1 - SS_{resid}/(SS_{model} - SS_{resid}) \quad (3)$$

6.3.3 Residual plots of optimization

The residual plot for means of this process is shown in figure 6.1. This layout is useful to determine whether the model meets the assumptions of the analysis.

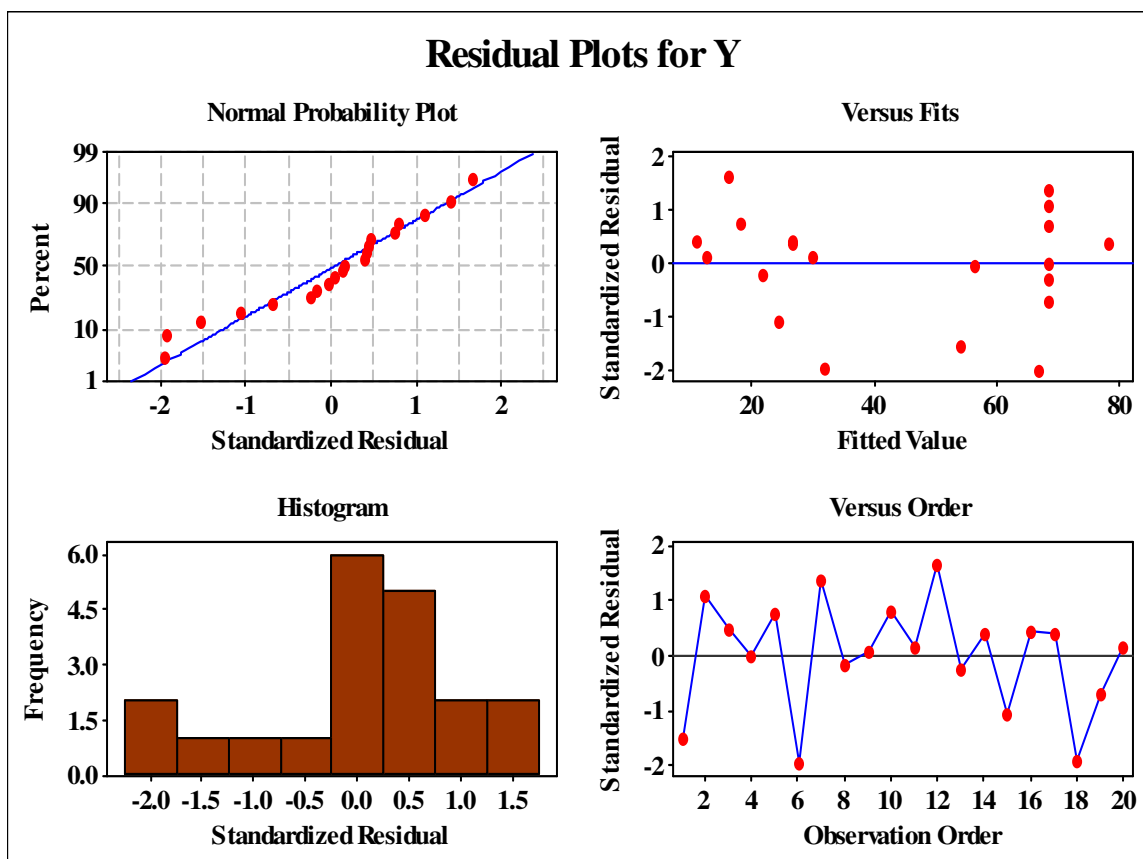


Figure 6.1 Residual plots for adequacy of the proposed model

The residuals are the deviations of the observed data values from the predicted value \hat{Y} and estimate the error terms (e_i) in the model (Mendenhall W et al. 1989). The e_i are assumed to be random and normally distributed with mean equal to zero and constant standard deviation. If the error terms follow a normal distribution, they will fall on a straight line on the normal probability plot. Because they are estimates of the error terms, the residuals should exhibit similar properties. If the assumptions are valid, plots of the residuals versus run sequence, predicted values, and other independent variables should be random and structure less. If structure remains in the residuals, residual plots may suggest modifications to the model that will remove the structure. Investigation of residuals has been used to evaluate the model adequacy. Residuals are found to be scattered and without any definite pattern which prove the adequacy of the model. The interpretation of each residual plot for the present experiment states that the R^2 is very good for fitting stress, the lack-of-fit test is not significant (very small " $P < 0.05$ " would indicate a lack of fit), normal probability plot indicates the data are normally distributed and the variables are influencing the response, residuals versus fitted values indicate the variance is constant and a non-linear relationship exists, histogram proves the data are not skewed and no outliers exist, residuals versus order of the data indicate that there are systematic effects in the data due to time or data collection order, the residual plots do not reveal any major violations of the underlying assumptions.

6.3.4 Surface plots and Contour plots of optimization

The interaction effects were analyzed using 3D response surface plots. From the figure 6.2 (a), it has been observed that yield of liquid fuel increases with increase in temperature from 400 °C to 450 °C and decreases with further increase in temperature from 450 °C to 500 °C due to the formation of more non condensable gaseous/volatile fractions by rigorous cracking at higher temperature. Yield of liquid fuel increases with use of different catalyst of increasing acidity due to the increase in the acid centers which is mainly responsible for cracking process.

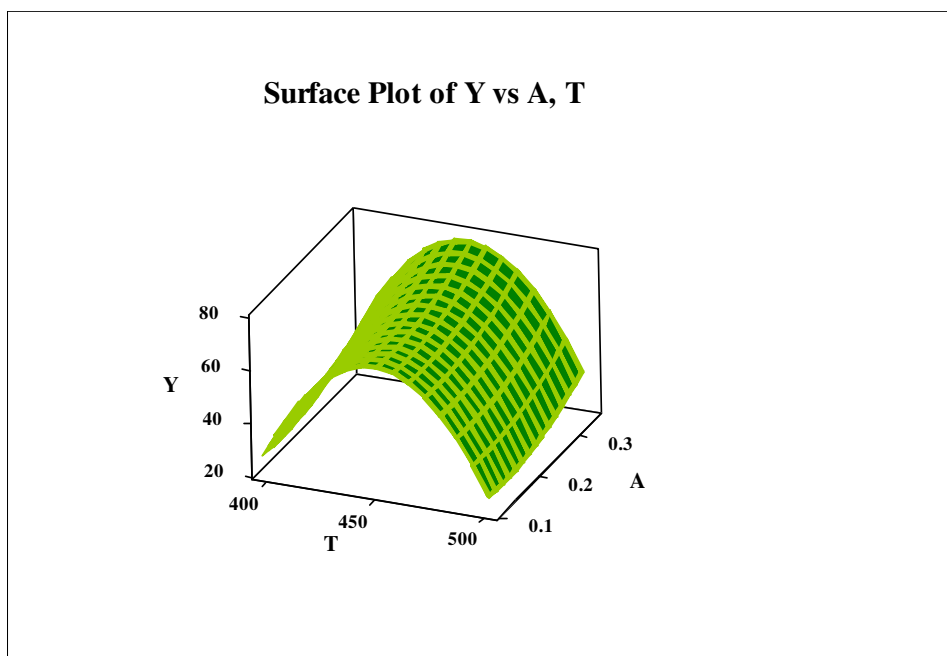


Figure 6.2 (a) Response surface plot showing the effect of acidity and reaction temperature on liquid yield

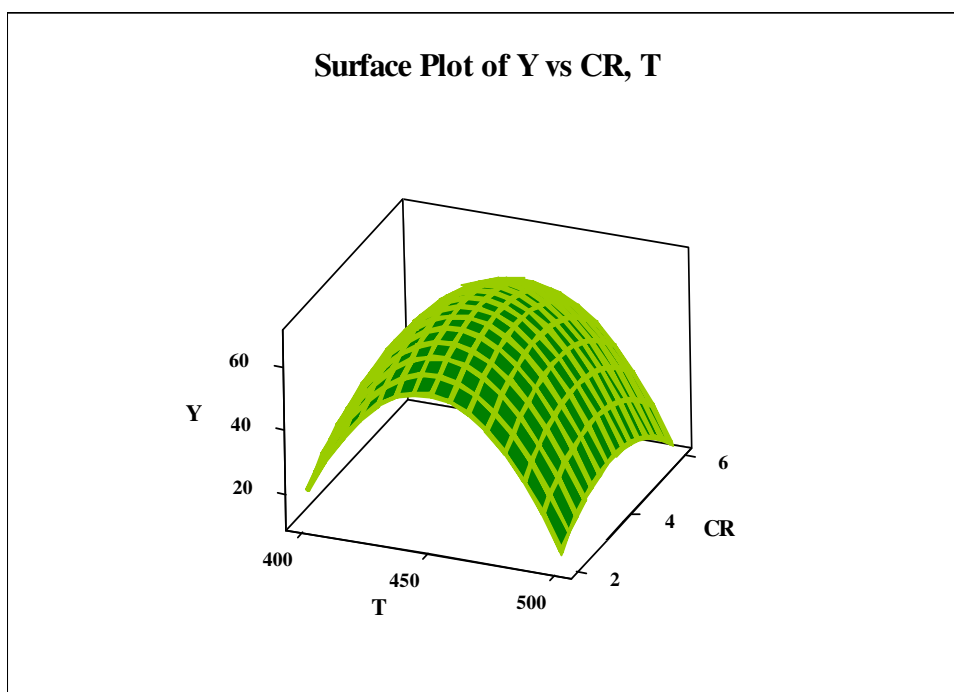


Figure 6.2 (b) Response surface plot showing the effect of catalyst ratio and reaction temperature on liquid yield

Figure 6.2 (b) shows that yield of liquid fuel increases with increase in catalyst to feed ratio from 1:2 to 1:4 and decreases with further increase in ratio from 1:4 to 1:6 due to increase in rate of reaction and formation of wax like product.

Figure 6.3 (a) and 6.3 (b) show 2D contour plots for effect of catalyst ratio 'CR' and temperature 'T' on liquid yield 'Y' and effect of acidity 'A' and temperature 'T' on liquid yield 'Y' respectively.

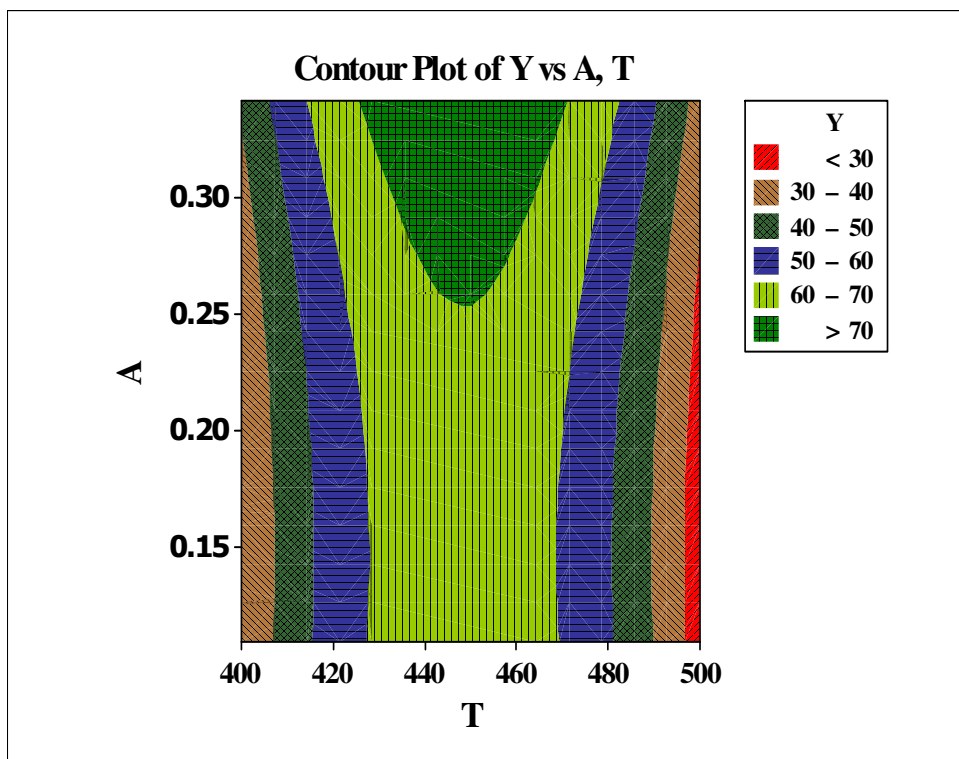


Figure 6.3 (a) Contour plot showing the effect of acidity and reaction temperature on liquid yield

The contour plots are the graphical representation of the regression equation used to visualize the relationship between the response and experimental levels of each factor. The liquid yield is maximum in temperature range 440 °C to 460 °C and acidity greater than 0.3 as shown in figure 6.3 (a) and from figure 6.3 (b), it is shown that liquid yield is maximum in temperature range 440 °C to 460 °C and catalyst to feed ration in between 3 to 5.

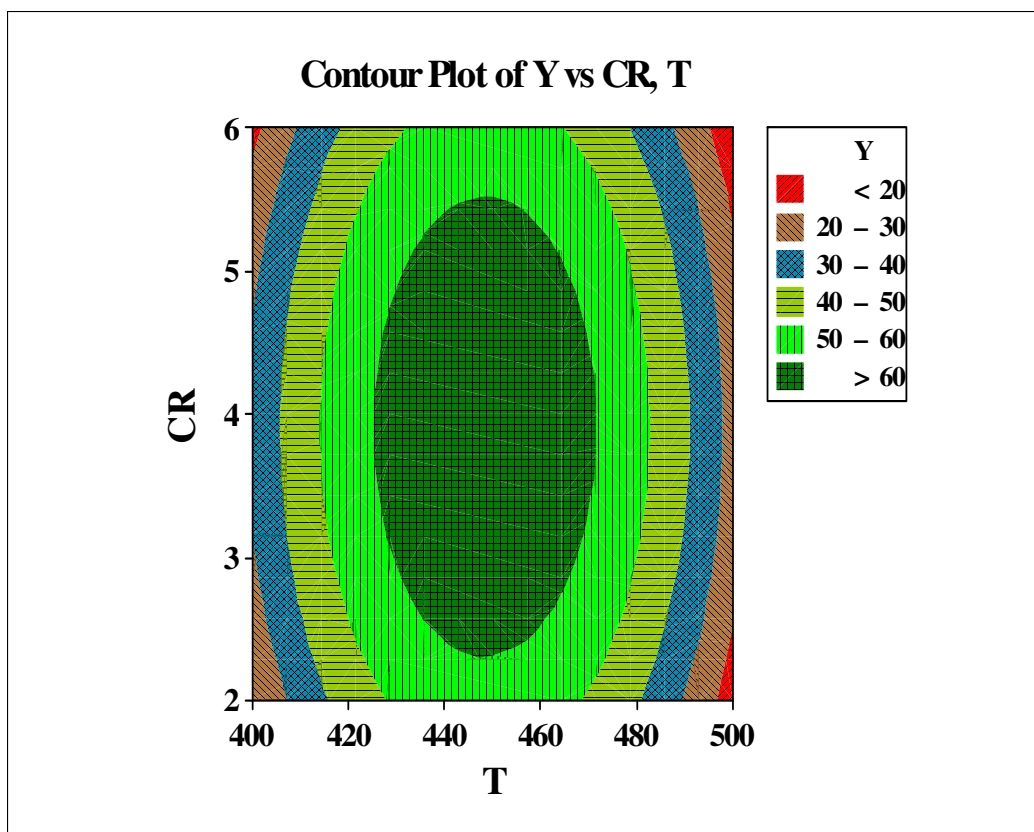


Figure 6.3 (b) Contour plot showing the effect of catalyst ratio and reaction temperature on liquid yield

6.3.5 Characterization of liquid fuel

6.3.5.1 FT-IR of the oil sample

Fourier Transform Infrared spectroscopy (FTIR) is an important analysis technique which detects various characteristic functional groups present in oil. On interaction of an infrared light with oil, chemical bond will stretch, contract, and absorb infrared radiation in a specific wave length range regardless the structure of the rest of the molecules.

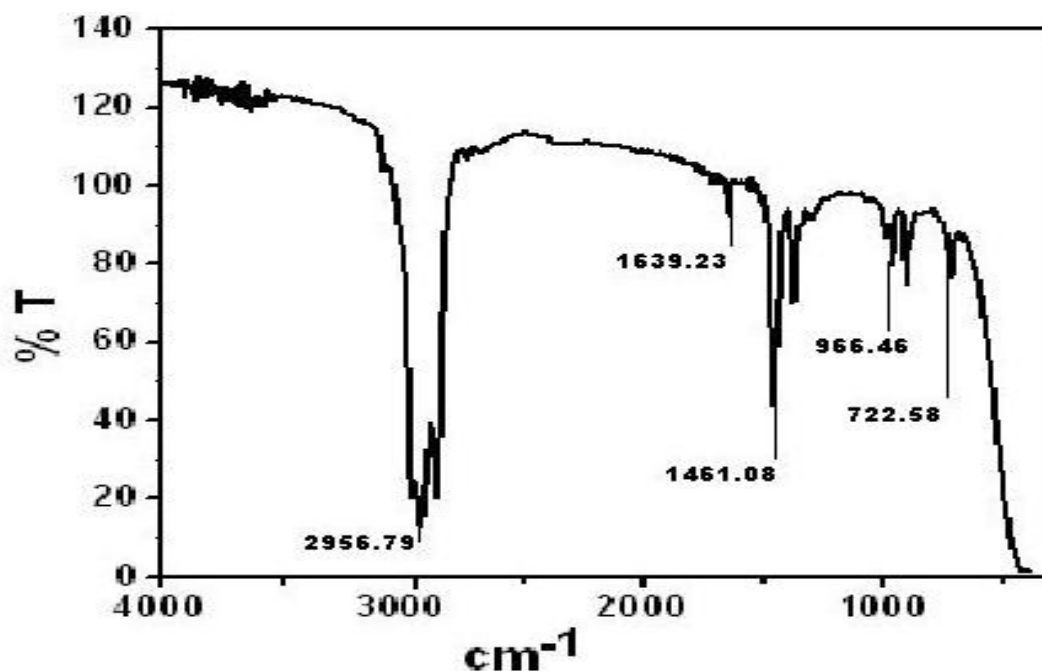


Figure 6.4 FT-IR spectrum of liquid fuel obtained at optimized condition by catalytic pyrolysis of waste HDPE

Figure 6.4 shows the FTIR spectra of liquid fuel obtained at optimized condition by catalytic pyrolysis of waste HDPE. The presence of alkanes is detected at 2956.79 cm^{-1} with C-H stretching vibrations. C=C stretching vibrations at 1639.23 cm^{-1} indicates the presence of alkenes/fingerprint region. The presence of alkanes is detected by C-H scissoring and bending vibrations at 1461.08 cm^{-1} . C-H bending vibrations at 966.46 cm^{-1} indicate the presence of alkenes and the C-H bending vibrations at frequency 722.58 cm^{-1} indicates the presence of phenyl ring substitution bands. The results were found consistent when compared with the results of GC-MS.

6.3.5.2 GC-MS of the oil sample

The GC-MS analysis of the liquid fuel sample obtained by catalytic pyrolysis of waste HDPE was carried out to know the compounds present in the fuel (figure 6.5) and is summarized in the Table 6.6.

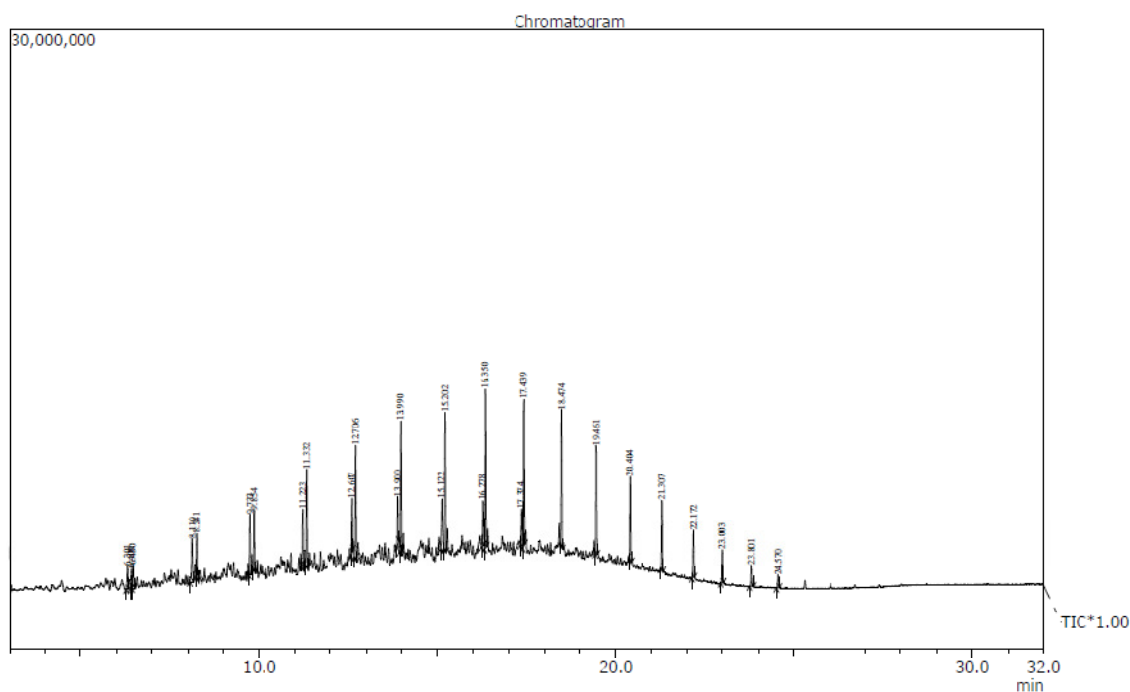


Figure 6.5 GC plot of liquid fuel obtained at optimized condition by catalytic pyrolysis of waste HDPE

It has been observed that the pyrolytic oil contains around 25 compounds. Taking into account of area percentage, the highest peak areas of total ion chromatogram (TIC) of the compounds were n-heptadecane, n-octadecane, n-hexadecane, nonadecane, pentadecane, eicosane, tetradecane and tridecane. The components present in waste HDPE liquid fuel are mostly the aliphatic hydrocarbons (alkanes and alkenes) with carbon number C_{10} - C_{25} .

Table 6.6 GC-MS analysis of liquid fuel obtained at optimized condition by catalytic pyrolysis of waste HDPE

R. Time (min.)	Area %	Name of Compound	Molecular Formula
6.301	1.64	1-Decene	$C_{10}H_{20}$
6.408	1.36	2-Methyl-2-Nonene	$C_{10}H_{20}$
6.450	1.59	Decane	$C_{10}H_{22}$
8.110	3.04	n-1-Undecene	$C_{11}H_{22}$
8.241	2.22	n-Undecane	$C_{11}H_{24}$
9.733	3.48	1-Dodecene	$C_{12}H_{24}$
9.854	3.11	n-Dodecane	$C_{12}H_{26}$
11.223	2.83	1-Tridecene	$C_{13}H_{26}$
11.332	4.80	Tridecane	$C_{13}H_{28}$
12.607	2.33	1-Tetradecene	$C_{14}H_{28}$

12.706	5.79	Tetradecane	$C_{14}H_{30}$
13.900	2.06	1-Pentadecene	$C_{15}H_{30}$
13.990	6.52	Pentadecane	$C_{15}H_{32}$
15.122	3.61	1-Hexadecene	$C_{16}H_{32}$
15.202	7.44	n-Hexadecane	$C_{16}H_{34}$
16.278	2.73	1-Octadecene	$C_{18}H_{36}$
16.350	8.07	n-Heptadecane	$C_{17}H_{36}$
17.374	2.19	1-Octadecene	$C_{18}H_{36}$
17.439	7.87	n-Octadecane	$C_{18}H_{38}$
18.474	6.70	Nonadecane	$C_{19}H_{40}$
19.461	5.97	Eicosane	$C_{20}H_{42}$
20.404	4.54	n-Heneicosane	$C_{21}H_{44}$
21.307	3.64	Docosane	$C_{22}H_{46}$
23.003	1.84	n-Tetracosane	$C_{24}H_{50}$
23.801	4.62	Pentacosane	$C_{25}H_{52}$

6.3.5.3 Physical properties of oil sample

Table 6.7 shows the results of physical property analysis of liquid fuel obtained from catalytic pyrolysis of waste HDPE at optimized condition.

Table 6.7 Physical properties of liquid fuel obtained by catalytic pyrolysis of waste HDPE at optimized condition

Tests	Results Obtained	Test method
Specific Gravity @ 15°C/15°C	0.7906	IS:1448 P:16
Density @ 15°C in kg/cc	0.7900	IS:1448 P:16
Kinematic Viscosity @ 40°C in Cst	2.1	IS:1448 P:25
Kinematic Viscosity @ 100°C in Cst	1.0	IS:1448 P:25
Conradson Carbon Residue	Less than 0.01%	IS:1448 P:122
Flash Point by Abel Method	Minus 2°C	IS:1448 P:20
Fire Point	Plus 5°C	IS:1448 P:20
Cloud Point	Plus 12°C	IS:1448 P:10
Pour Point	Minus 1°C	IS:1448 P:10
Gross Calorific Value in MJ/Kg	40.17	IS:1448 P:6
Sulphur Content	0.05%	IS:1448 P:33

Calculated Cetane Index (CCI)	66	IS:1448 P:9
<u>Distillation:</u>		IS:1448 P:18
Initial Boiling Point	58°C	
Final Boiling Point	376°C	

The appearance of the oil is dark yellowish free from visible sediments. From comparison with other transportation fuels as shown in table 6.8, the density and viscosity of liquid product can be modified by blending it with commercial transportation fuels. The flash point of the liquid product is in a comparable range and a pour point is minus 1 °C which will not cause any trouble in most of the regions but in colder regions with sub-zero climates it may lead to freezing problems. Liquid fuel obtained by catalytic pyrolysis of waste HDPE has GCV of 40 MJ/Kg which is in the range of gasoline and diesel; therefore this liquid product would perform relatively well in engines. From the distillation report of the oil it is observed that, the boiling range of the liquid fuel is 58-376°C, which infers the presence of mixture of different oil components such as gasoline, kerosene and diesel in the oil. From this result, it is observed these could be possible feedstock for further upgrading or use of lighter compounds as a diesel fuel.

Table 6.8 Fuel properties comparison of waste HDPE catalytic pyrolytic oil with commercial transportation fuels

Liquid Fuel	Specific Gravity	Kinematic Viscosity	Flash Point	Pour Point	GCV (MJ/Kg)	IBP (°C)	FB P (°C)	Chemical Formula
	15°C/15°C	@40°C (cst)	(°C)	(°C)				
Waste HDPE catalytic pyrolytic liquid fuel	0.7906	2.1	-2	-1	40.17	58	376	C ₁₀ -C ₂₅

Gasoline (Petroleum Product Surveys 1986)	0.72-0.78	-	-43	-40	42-46	27	225	C ₄ -C ₁₂
Diesel (Tuttle J et al. 2004)	0.82-0.85	2-5.5	53-80	-40 to -1	42-45	172	350	C ₈ -C ₂₅
Bio-Diesel (Tuttle J et al. 2004)	0.88	4-6	100-170	-3 to 19	37-40	315	350	C ₁₂ -C ₂₂
Heavy Fuel Oil (Tuttle J et al. 2004)	0.94-0.98	>200	90-180	-	- 40	-	-	-

6.4 Conclusion

From Response Surface Methodology method, optimum operating parameters of reaction temperature, acidity of catalysts and catalyst to waste plastic ratio were achieved with respect to maximum liquid fuel yield. The results were showed that the high liquid yields was obtained in the range temperature of 440 to 460 °C, acidity of catalysts greater than 0.3 and catalyst to waste HDPE ratios of 1:3 to 1:5. The polynomial model obtained fits well to predict the response with a high determination coefficient of R^2 (0.995). Optimum operating conditions of reaction temperature 450 °C, acidity of catalyst 0.341 and catalyst to waste HDPE ratio 1:4 were produced with respect to maximum liquid product yield of 78.7 %. The liquid fuel by obtained catalytic pyrolysis of waste HDPE at optimized condition consists of petroleum products range hydrocarbons (C₁₀-C₂₅) with high heating value (40.17 MJ/Kg).

Nomenclature

DF Degree of freedom

SS Sum of squares

MS Mean of squares

S/N Signal to noise ratio

R-Sq Regression squared

R-Sq (adj) Adjusted regression

Chapter 7

Performance and Emission Analysis of Waste HDPE Pyrolysis Oil in CI Diesel Engine

PERFORMANCE AND EMISSION ANALYSIS OF BLENDS OF WASTE PLASTIC OIL OBTAINED BY CATALYTIC PYROLYSIS OF WASTE HDPE WITH DIESEL IN A CI ENGINE

7.1 Introduction

Plastics materials have proved their reputation and have gained popularity as they are light in weight, does not rust or rot, low in cost, reusable and conserve natural resources. There are a numerous of ways that plastic is being used nowadays/will be used in the years to come. Hence plastics have become essential materials and their applications in the industrial field are continually increasing. At the same time, waste plastics have created a very serious environmental challenge because of their huge quantities and their disposal problems. Plastics are produced from petroleum derivatives and are composed primarily of hydrocarbons but also contain additives such as antioxidants, colorants, and other stabilizers. HDPE is the third largest commodity plastic material in the world, after polyvinyl chloride and polypropylene in terms of volume. The demand for HDPE has increased 4.4% a year to 31.3 million MT in 2009 ([Kumar S et al. 2011b](#)). The increased demand and production of waste HDPE has led to the accumulation of large amount of its waste in the final waste stream due to its low useful life. Recycling of plastics already occurs on a wide scale. The most attractive technique of chemical feedstock recycling is pyrolysis ([Kumar S et al. 2011a](#)). Thermal cracking or thermal pyrolysis involves the degradation of the polymeric materials by heating in the absence of oxygen. The effect of temperature and the type of reactor on the pyrolysis of waste HDPE has been studied by different researchers ([Walendziewski J et al. 2001](#), [Marcilla A et al. 2001](#), [Stefanis AD et al. 2001](#)). The thermal degradation of waste HDPE can be improved by using suitable catalysts in order to obtain valuable products. The most common catalysts used in this process are: zeolite, alumina, silica–alumina, FCC catalyst, reforming catalyst ([Venuto PB et al. 1979](#), [Sharratt PN et al. 1997](#), [Lee KH et al. 2003a](#), [Lee KH et al. 2003b](#), [Miskolczi N et al. 2008](#), [Seo YH et al. 2003](#), [Park JW et al. 2002](#), [Manos G et al. 2000](#), [Hernandez MR et al. 2006](#)). Pyrolysis is useful to break down the waste plastics into

three products; wax, liquid and gas in an inert environment. The liquid is attractive because its properties show its potential for use as chemical feedstock or fuel. A number of studies of waste plastic oil production have been reported at various scales and with varying success (Panda AK et al. 2011, Panda AK et al. 2012). The waste plastic oil was compared with the petroleum products and found that it can also be used as fuel in compression ignition engines (Mani M et al. 2009b). Compression ignition engines or diesel engines are most preferred power plants due to their excellent driveability and higher thermal efficiency. Despite their advantages, they emit high levels of NO_x and smoke which will have an effect on human health. Hence, stringent emission norms and the depletion of petroleum fuels have necessitated the search for alternate fuels for diesel engines. On the other hand, due to the rapid growth of automotive vehicles in transportation sector, the consumption of oil keeps increasing. Most of the research work has been done by mixing oil developed from waste plastic disposal with heavy oil for marine application. The results showed that waste plastic disposal oil when mixed with heavy oils reduces the viscosity significantly and improves the engine performance. However, very little has been done to test their use in high-speed diesel engines (Mani M et al. 2009a). In this work, different proportions of waste plastic oil obtained by catalytic pyrolysis of waste high-density polyethylene, viz, 10%, 20%, 30% and 40% are mixed with 90%, 80%, 70% and 60% respectively with diesel fuel on mass basis and investigate its suitability as a fuel in the diesel engine.

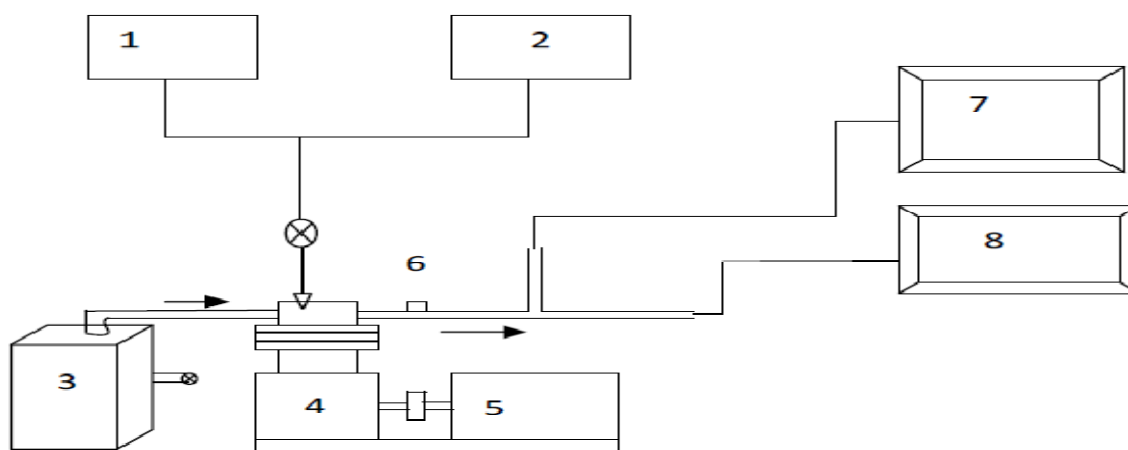
7.2 Experimental programme

The detail about the raw material, characterization of raw material, preparation of catalysts, pyrolysis experimental setup and procedure is summarized in chapter 3. Preparation of waste plastic oil obtained by catalytic pyrolysis of waste HDPE is given in chapter 5. The detail about the experimental setup of CI engine and test detail is summarized below:

7.2.1 Experimental set up of CI engine and test detail

The schematic representation of the experimental set up is shown in figure 7.1. The research engine specifications are given in table 7.1. The engine was coupled to an

electrical dynamometer to provide the engine load. An air box with U-tube manometer connected to the intake of the engine. The air consumption of the engine was measured with the help of U-tube manometer. Fuel consumption was measured with the help of a burette fitted with a three way cock. One side of three way cock is connected with fuel line from fuel tank and the second end is connected to the burette and the third way is connected to the fuel supply system. The fuel flow rate was measured on volumetric basis using a stopwatch. Chromel alumel thermocouple in conjunction with a digital temperature indicator was used to measure the exhaust gas temperature. Exhaust emissions from the engine were measured with the help of AVL digas analyzer and smoke density was measured by AVL 437 C diesel smoke meter. A probe was used to receive sample of exhaust gas from the engine. All the experiments were conducted at the rated engine speed of 1500 rpm. WPO- Diesel blends of 10%, 20% 30% and 40% were used to test in the engine. These blends are denoted as 10% B WPO, 20% B WPO, 30% B WPO, and 40% B WPO, where the numbers indicate the percentage of WPO in the blend. Higher blends were not used due to detonation in the engine. All the tests were conducted by starting the engine with diesel only and then switched over to run with waste plastic oil blend. At the end of the test, the engine was run for some time with diesel to flush out the waste plastic oil from the fuel line and the injection system.



- | | | |
|-----------------|-----------------------------|---|
| 1. Diesel Tank | 2. Alternative Fuel Tank | 3. Air Box |
| 4. Engine | 5. Eddy current dynamometer | 6. Exhaust gas temperature thermocouple |
| 7. Gas Analyzer | 8. Smoke meter | |

Figure 7.1 Schematic representation of the CI engine

Table 7.1 Engine specification

Make of model	CometVCT-10
Engine type	Four-stroke, CI, direct injection, water cooled twin cylinder, constant Speed engine
Bore (mm)	80
Stroke (mm)	110
Compression ratio	17.5:1
Rated power@ 1500 rpm(kW)	7.4
Nozzle opening pressure (bar)	200
Injection timing (CA)	23° BTDC

7.3 Result and Discussion

7.3.1 Characterization of raw material and catalyst preparation

The ultimate or elemental analysis of waste HDPE is shown in Table 7.2. The oxygen is 5.19% in the ultimate analysis of waste HDPE. The oxygen in the waste HDPE sample may not be due to the fillers but rather to other ingredients that are added to the resin in the manufacturing of HDPE. Calorific value of waste HDPE was 45.78 MJ/kg. From the comparison of waste HDPE with mixed plastic waste (Cho MH et al. 2010) in Table 7.2, it was found that the carbon and hydrogen percentage and gross calorific value (GCV) are more in waste HDPE as compared to mixed plastic waste. Mixed plastic waste contained 1.13% of chlorine which was not found in case of waste HDPE.

Table 7.2 Ultimate or elemental analysis of waste HDPE

Sample	C (wt %)	H (wt %)	N (wt %)	S (wt %)	O (wt %)	Cl (wt %)	GCV (MJ/kg)
Waste HDPE	80.58	13.98	0.60	0.080	5.19	-	45.78
Mixed Plastics (Cho MH et al. 2010)	79.9	12.6	-	-	5.10	1.13	44.40

The chemical composition of nitric acid treated kaolin catalyst was determined by the X-ray fluorescence (XRF) analysis. Table 7.3 shows the results of chemical analysis of the parent kaolin clay and nitric acid treated kaolin clay. The parent kaolin clay contains alumina and silica which are in major quantities where as other oxides such as magnesium oxide, calcium oxide, potassium oxide, zinc oxide and titanium oxide are present in trace amounts. After acid treatment, it was observed that the composition of the parent kaolin clay changes significantly. The Al_2O_3 , MgO , CaO and K_2O contents in the acid treated kaolin clay decreased progressively after nitric acid treatment of pure kaolin clay. Simultaneously, SiO_2 content increased after nitric acid treatment of pure kaolin clay due to which the Si/Al ratio increased. The alumina content in the acid treated kaolin clay decreased due to the leaching of the Al^{3+} ions from the octahedral layer under acidic conditions by hydrolysis (Kumar S et al. 2013). The relative amount of the acid sites of the samples was evaluated by thermal desorption of ammonia. Ammonia is a strong base ($\text{pK}_b \approx 5$) that reacts even with extremely weak acid sites, which therefore makes NH_3 -TPD a useful technique for evaluating the relative amount of acid sites present on a surface. The acidity of parent kaolin clay and nitric acid treated kaolin clay is summarized in Table 7.3. The acidity of the kaolin clay is 0.049mmol/g which increases to 0.341mmol/g by treating it with 3M nitric acid followed by calcination at 650 °C. The increase of acidity is due to creation of specific acid sites on the surface of silica generated due to leaching.

Table 7.3 XRF analysis and acidity of parent and acid treated kaolin clay

Material	Chemical Content (% weight)								Si/Al Ratio	Acidity (mmol/g)
	SiO ₂	Al ₂ O ₃	MgO	CaO	K ₂ O	ZnO	TiO ₂	V ₂ O ₅		
KC	43.12	46.07	0.027	0.030	0.010	0.0064	0.74	0.003	0.82	0.049
KC (HNO ₃)	56.42	27.88	0.02	0.008	0.008	0.0064	0.23	0.002	1.782	0.341

7.3.2 Characterization of waste plastic oil

7.3.2.1 FT-IR of the oil sample

Fourier Transform Infrared spectroscopy (FTIR) is an important analysis technique which detects various characteristic functional groups present in oil. On interaction of an infrared light with oil, chemical bond will stretch, contract, and absorb infrared radiation in a specific wave length range regardless the structure of the rest of the molecules.

Figure 7.2 shows the FTIR spectra of liquid fuel obtained at 450 °C by catalytic pyrolysis of waste HDPE. The presence of alkanes is detected at 2956.79 cm⁻¹ with C-H stretching vibrations. C=C stretching vibrations at 1639.23 cm⁻¹ indicates the presence of alkenes. The presence of alkanes is detected by C-H scissoring and bending vibrations at 1461.08 cm⁻¹. C-H bending vibrations at 966.46 cm⁻¹ indicate the presence of alkenes and the C-H bending vibrations at frequency 722.58 cm⁻¹ indicates the presence of phenyl ring substitution bands. The results were found consistent when compared with the results of GC-MS.

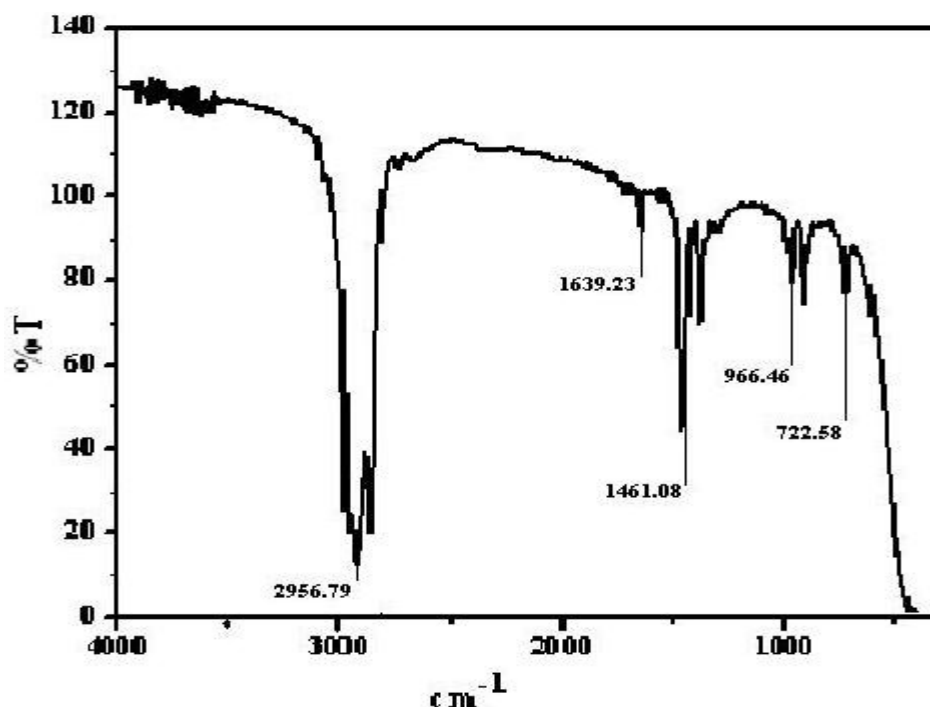


Figure 7.2 FT-IR spectrometry of oil sample obtained at 450 °C by catalytic pyrolysis of waste HDPE

7.3.2.2. GC-MS of the oil sample

The GC-MS analysis of the liquid fuel sample obtained by catalytic pyrolysis of waste HDPE was carried out to know the compounds present in the fuel (Figure 7.3) and is summarized in the table 7.4. It has been observed that the pyrolytic oil contains around 25 compounds. Taking into account of area percentage, the highest peak areas of total ion chromatogram (TIC) of the compounds were n-heptadecane, n-octadecane, n-hexadecane, nonadecane, pentadecane, eicosane, tetradecane and tridecane. The components present in waste HDPE liquid fuel are mostly the aliphatic hydrocarbons (alkanes and alkenes) with carbon number C_{10} - C_{25} .

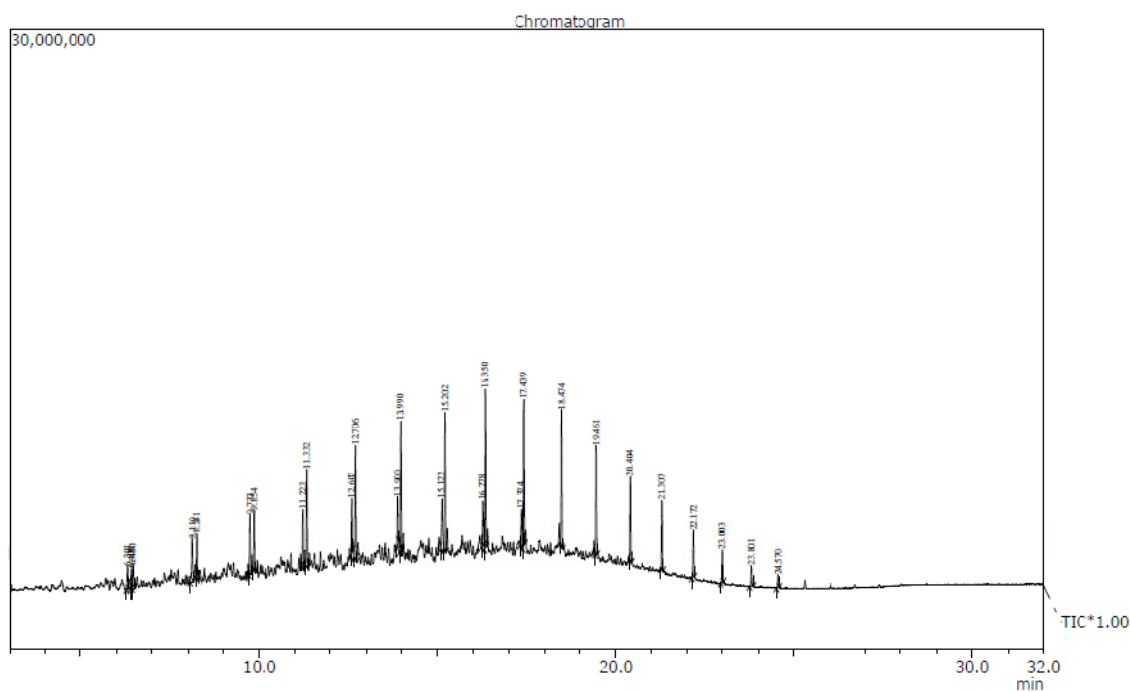


Figure 7.3 GC plot of oil sample obtained at 450 °C by catalytic pyrolysis of waste HDPE

Table 7.4 GC-MS analysis of oil sample obtained at 450 °C by catalytic pyrolysis of waste HDPE

R. Time (min.)	Area%	Name of Compound	Molecular Formula
6.301	1.64	1-Decene	C ₁₀ H ₂₀
6.408	1.36	2-Methyl-2-Nonene	C ₁₀ H ₂₀
6.450	1.59	Decane	C ₁₀ H ₂₂
8.110	3.04	n-1-Undecene	C ₁₁ H ₂₂
8.241	2.22	n-Undecane	C ₁₁ H ₂₄
9.733	3.48	1-Dodecene	C ₁₂ H ₂₄
9.854	3.11	n-Dodecane	C ₁₂ H ₂₆
11.223	2.83	1-Tridecene	C ₁₃ H ₂₆
11.332	4.80	Tridecane	C ₁₃ H ₂₈
12.607	2.33	1-Tetradecene	C ₁₄ H ₂₈
12.706	5.79	Tetradecane	C ₁₄ H ₃₀

13.900	2.06	1-Pentadecene	$C_{15}H_{30}$
13.990	6.52	Pentadecane	$C_{15}H_{32}$
15.122	3.61	1-Hexadecene	$C_{16}H_{32}$
15.202	7.44	n-Hexadecane	$C_{16}H_{34}$
16.278	2.73	1-Octadecene	$C_{18}H_{36}$
16.350	8.07	n-Heptadecane	$C_{17}H_{36}$
17.374	2.19	1-Octadecene	$C_{18}H_{36}$
17.439	7.87	n-Octadecane	$C_{18}H_{38}$
18.474	6.70	Nonadecane	$C_{19}H_{40}$
19.461	5.97	Eicosane	$C_{20}H_{42}$
20.404	4.54	n-Heneicosane	$C_{21}H_{44}$
21.307	3.64	Docosane	$C_{22}H_{46}$
23.003	1.84	n-Tetracosane	$C_{24}H_{50}$
23.801	4.62	Pentacosane	$C_{25}H_{52}$

7.3.2.3 Physical properties of oil sample

Table 7.5 shows the results of physical property analysis of liquid fuel obtained from catalytic pyrolysis of waste HDPE at optimized condition. The appearance of the oil is dark yellowish free from visible sediments. The flash point of the liquid product is minus 2 °C and a pour point is minus 1 °C which will not cause any trouble in most of the regions but in colder regions with sub-zero climates it may lead to freezing problems. Liquid fuel obtained by catalytic pyrolysis of waste HDPE has GCV of 40 MJ/Kg which is in the range of gasoline and diesel; therefore this liquid product would perform relatively well in engines. From the distillation report of the oil it is observed that, the boiling range of the liquid fuel is 58-376 °C, which infers the presence of mixture of different oil components such as gasoline, kerosene and diesel in the oil. From this result, it is observed these could be possible feedstock for further upgrading or use of lighter compounds as a diesel fuel.

Table 7.5 Physical properties of oil sample obtained by catalytic pyrolysis of waste HDPE at 450 °C

Tests	Results Obtained	Test method
Specific Gravity @ 15°C/15°C	0.7906	IS:1448 P:16
Density @ 15°C in gm/cc	0.7900	IS:1448 P:16
Kinematic Viscosity @ 40°C in Cst	2.1	IS:1448 P:25
Kinematic Viscosity @ 100°C in Cst	1.0	IS:1448 P:25
Conradson Carbon Residue	Less than 0.01%	IS:1448 P:122
Flash Point by Abel Method	-2 °C	IS:1448 P:20
Fire Point	5 °C	IS:1448 P:20
Cloud Point	12 °C	IS:1448 P:10
Pour Point	-1 °C	IS:1448 P:10
Gross Calorific Value in MJ/Kg	40.17	IS:1448 P:6
Sulphur Content	0.05%	IS:1448 P:33
Calculated Cetane Index (CCI)	66	IS:1448 P:9
<u>Distillation:</u>		IS:1448 P:18
Initial Boiling Point	58 °C	
Final Boiling Point	376 °C	

7.3.3 Performance analysis of blends of waste plastic oil with diesel

7.3.3.1 Brake thermal efficiency

Figure 7.4 shows the variation of the brake thermal efficiency with respect to load for diesel fuel and waste plastic oil blends. It can be observed from the figure that, waste plastic oil blends show lower brake thermal efficiencies at all load conditions compared to that of diesel fuel. The brake thermal efficiency is 23.12% at full load for diesel, however when the engine is fueled with WPO-diesel blends such as 10% B WPO, 20% B WPO, 30% B WPO and 40% B WPO, it gives lower thermal efficiencies of 19.98%, 19.13%, 20.1% and 19.25% respectively at full load. This may be due to lower calorific

value of WPO-diesel blend than diesel as the calorific value of WPO is lower than diesel. Again at full load, the exhaust gas temperature and the heat release rate are marginally higher for waste plastic oil compared to diesel. This may result in higher heat losses and lower brake thermal efficiency in the case of waste plastic oil blend. Raheman et al. also reported lower values of BTE from blends of karanja methyl ester and diesel in a diesel engine due to low calorific value and higher fuel consumption (Raheman H et al. 2004).

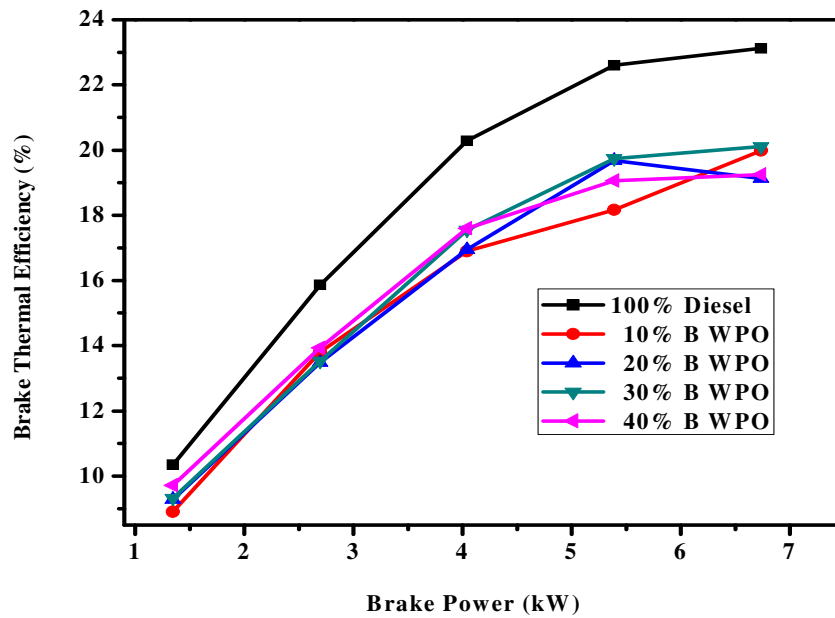


Figure 7.4 Variation of brake thermal efficiency with brake power

7.3.3.2 Exhaust gas temperature

The variation of exhaust gas temperature with brake power is shown in figure 7.5. The exhaust gas temperature varies from 310 °C at zero load to 490 °C at full load for diesel whereas in the case of WPO-diesel blends it varies from 320 °C to 510 °C for 10% B WPO, 320 °C to 500 °C for 20% B WPO, 310 °C to 515 °C for 30% B WPO, 340 °C to 520 °C for 40% B WPO, as the load increased from 0kW to 6.7kW. The reason for increase in exhaust gas temperature with engine load from the simple fact that more amount of fuel was required by the engine to generate the extra power needed to take up the additional loading (Kim D et al. 2002, Lucas N et al. 2008). It is observed that, the

exhaust gas temperature in the case of different blends is marginally higher compared to diesel. The increased exhaust gas temperature may be due to higher heat release or may be due to the lower thermal efficiencies of the engine. At lower thermal efficiency, less of the energy input in the fuel is converted to work, thereby increasing exhaust temperature (Nagarajan G et al. 2002). In addition to high oxygen content, waste plastic oil usually contains constituents that have higher boiling points than diesel. These relatively higher boiling point constituents were not adequately evaporated during the main combustion phase, and continued to burn in the late combustion phase (Bari S et al. 2004). This resulted in higher exhaust temperatures.

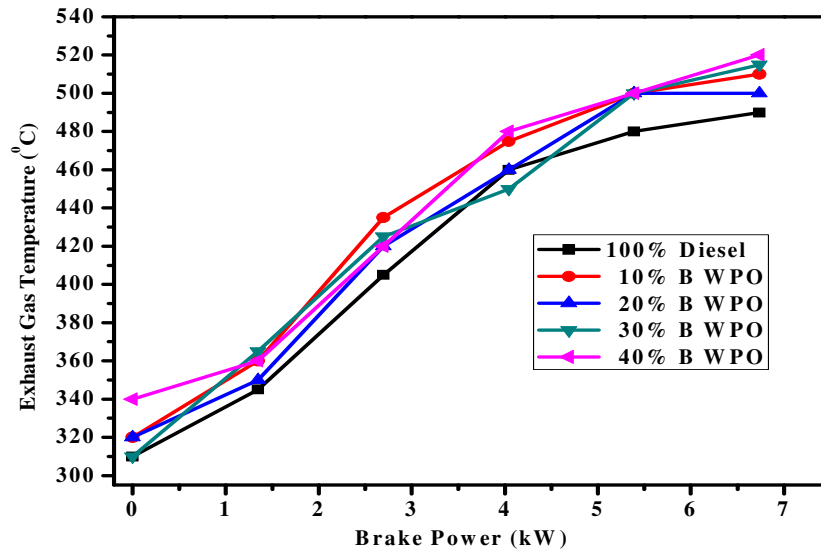


Figure 7.5 Variation of exhaust gas temperature with brake power

7.3.3.3 Brake specific energy consumption

The brake specific energy consumption (BSEC) will give more reliable value, when two different fuels of different heating values and densities are blended together. Figure 7.6 shows the comparison of the brake specific energy consumption of WPO-diesel blend with diesel. The brake specific energy consumption varies from 34.80 MJ/kWh at low load to 17.28 MJ/kWh at full load for diesel, and it varies from 40.43 MJ/kWh to 18.01 MJ/kWh for 10% B WPO, 38.73 MJ/kWh to 18.81 MJ/kWh for 20% B WPO, 38.61

MJ/kWh to 17.90 MJ/kWh for 30% B WPO, 37.04 MJ/kWh to 18.69 MJ/kWh for 40% B WPO. It is clear from the graph that as the load increases the BSEC decreases for all fuels as expected. At the same time, it can be seen that BSEC is higher with increase in the concentration of WPO in WPO-Diesel blend. This behavior is obvious since the engine will consume more fuel with blends due to low calorific value of WPO (Kidoguchi Y et al. 2000, Soloiu A et al. 2000).

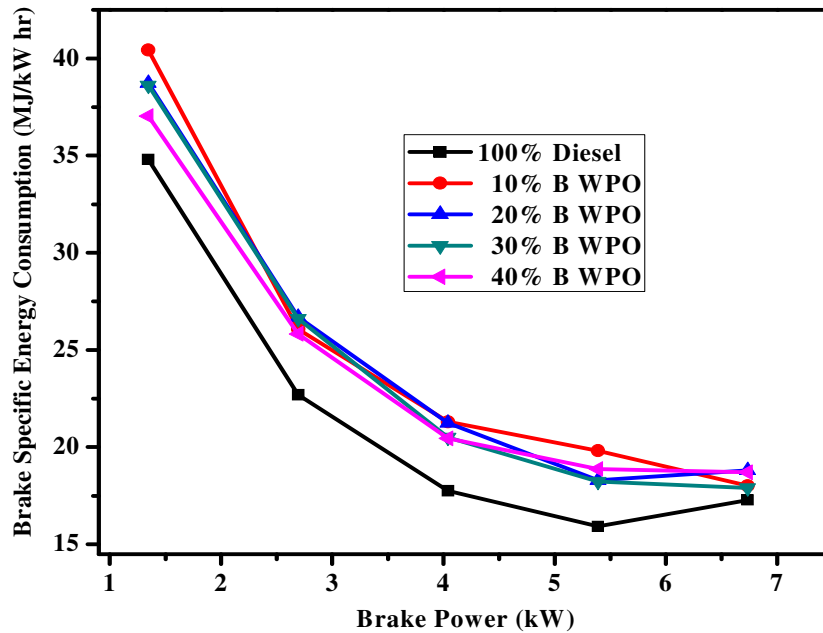


Figure 7.6 Variation of BSEC with brake power

7.3.3.4 Mechanical Efficiency

Mechanical efficiency is the rating that shows how much of the power developed by the expansion of the fuels in the cylinder is actually delivered as useful power. The factor which has the greatest effect on mechanical efficiency is friction within the engine. The friction between moving parts in an engine remains practically constant throughout the engine's speed range. Therefore, the mechanical efficiency of an engine will be highest when the engine is running at the speed at which maximum BHP is developed. The variation in mechanical efficiency of fuel blends with load is shown in figure 7.7.

Mechanical efficiency increases with increasing brake power for all fuel blends. It can be seen that the mechanical efficiency for 10% B WPO (10% blend of waste plastic oil) is better than diesel fuel at all load conditions and there was no significant deviation in mechanical efficiency for 40% B WPO than pure diesel. Rath et al. has obtained the similar result of mechanical efficiency in compression ignition engine fueled with karanja methyl ester and diesel blends (Rath S et al. 2011).

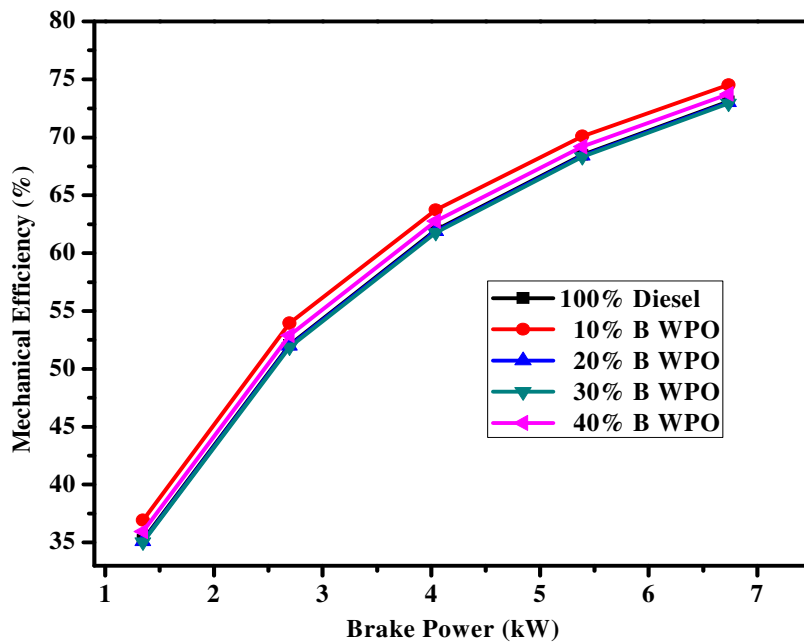


Figure 7.7 Variation of mechanical efficiency with brake power

7.3.4 Emission analysis of blends of waste plastic oil with diesel

7.3.4.1 Oxides of nitrogen

The oxides of nitrogen in the emissions contain nitric oxide (NO) and nitrogen dioxide (NO₂). Nitrogen oxide is formed as a result of the oxidation of nitrogen in the air during burning of the air-fuel mixture in the combustion chamber. In the formation of nitrogen oxides, the predominant factors are the air/fuel ratio and the environment temperature. In the case of adequate burning the temperature rises and, consequently, more free oxygen

atoms combine nitrogen; this, in turn, increases the formation rate of nitrogen oxide (Zhu L et al. 2011).

Figure 7.8 shows the comparison of nitrogen oxides with load. It can be observed that the NO_x emission increases with increase in percentage of waste plastic oil in blends. NO_x emission decreases with increase in load from 2.14 g/kWh at low load to 1.39 g/kWh at full load condition for diesel and from 4.2 g/kWh at low load to 2.79 g/kWh at full load for 40% B WPO. It varies from 2.98 g/kWh to 1.97 g/kWh for 10% B WPO, 3.1 g/kWh to 1.99 g/kWh for 20% B WPO and 3.52 g/kWh to 2.16 g/kWh for 30% B WPO with low and full load. The reason for the increased NO_x in WPO blends compared to diesel may be plastic oil contains some oxygenated hydrocarbons which promote better combustion and thus the formation of NO_x in exhaust. It was observed that the NO_x emission decreases with increase in load for all the blends. This is due to the less amount of oxygen available for combustion and hence reduction in NO_x emission due to late combustion of fuel. Mani et al. also reported decrease in NO_x emission with increase in load in DI diesel engine (Mani M et al. 2009b).

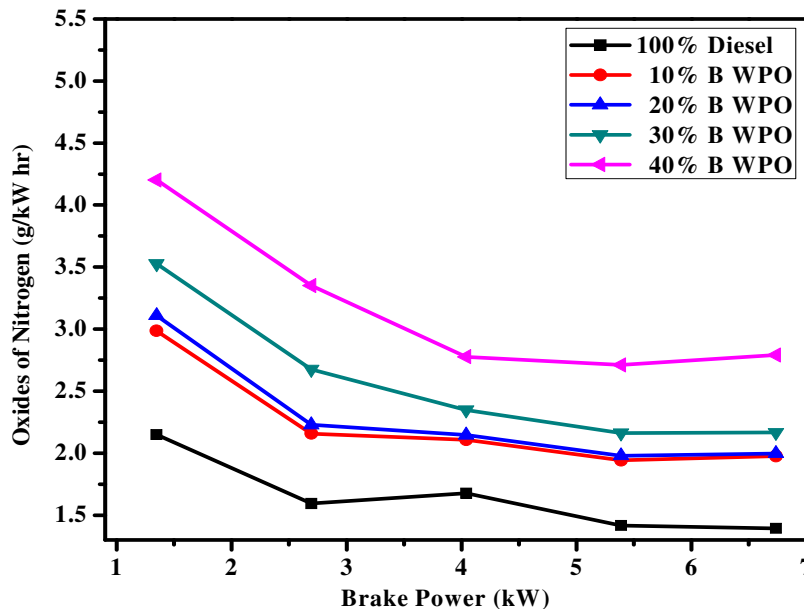


Figure 7.8 Variation of NO_x with brake power

7.3.4.2 Unburned hydrocarbon

HC's emissions are mainly the result of flame extinction in the cold regions of the combustion chamber along the walls of the cylinder, and are also related with fuel volatility and viscosity. High viscosities lead to larger droplet sizes and reduce the vapor pressure. Unburned hydrocarbon is a useful measure of combustion inefficiency. Unburned hydrocarbon consists of fuel that is incompletely burned. At light load, large amounts of excess air and low exhaust temperature and lean fuel air mixture regions may survive to escape into the exhaust. The variation of unburned hydrocarbon with load for tested fuels is shown in figure 7.9.

The hydrocarbon emission is decreasing with increase in the load. HC varies from 0.749 g/kWh at low load to 0.010 g/kWh at full load for diesel fuel, and it varies from 1.016 g/kWh at low load to 0.141 g/kWh at full load for 40% B WPO. Similarly for 10% B WPO, it varies from 0.681 g/kWh at low load to 0.028 g/kWh at full load, for 20% B WPO it varies from 0.718 g/kWh to 0.070 g/kWh and for 30% B WPO it varies from 0.899 g/kWh to 0.090 g/kWh from low load to full load. At low load high fuel supply lead to higher hydrocarbon, at lighter loads due to charge homogeneity and higher oxygen availability, the unburned hydrocarbon level is less, whereas at higher load ranges due to higher quantity of fuel admission, unburned hydrocarbon increases (Zhu L et al. 2011). The higher HC emission in blend compared to diesel may be attributed to two reasons. One is that the fuel spray does not propagate deeper into the combustion chamber and gaseous hydrocarbons remain along the cylinder wall and the crevice volume and left unburned (Muralidharan K et al. 2011). The other one is unsaturated hydrocarbons present in the WPO which are unbreakable during the combustion process (Kidoguchi Y et al. 2000).

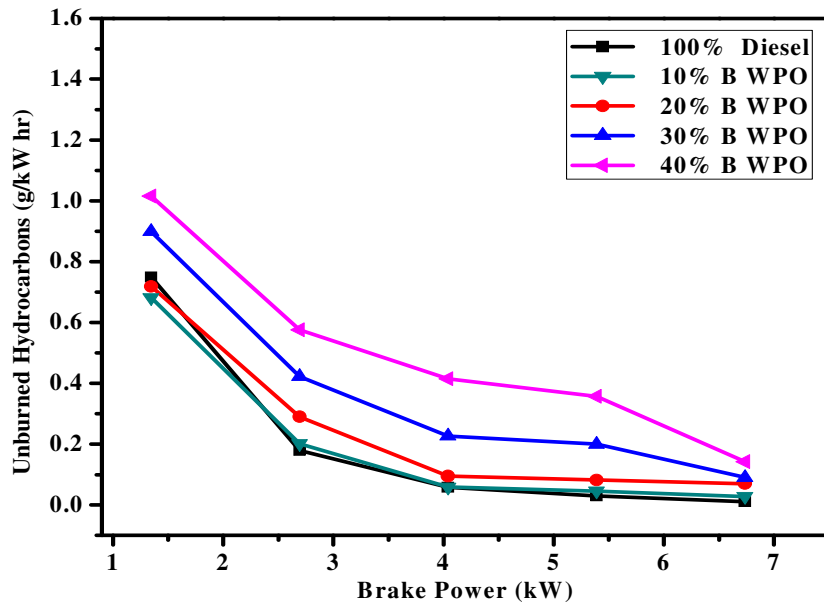


Figure 7.9 Variation of unburned hydrocarbon with brake power

7.3.4.3 Carbon monoxide

Carbon monoxide emission is mainly due to the lack of oxygen, poor air entrainment, mixture preparation and incomplete combustion during the combustion process. CO emission is toxic and must be controlled. It is an intermediate product in the combustion of a hydrocarbon fuel, so its emission results from incomplete combustion (Ilkilic C 2012). The variation of carbon monoxide with load is shown in figure 7.10. The CO emission varies from 0.046 g/kWh at low load to 0.86 g/kWh at full load for diesel. For 10% B WPO, it varies from 0.22 g/kWh at low load to 1.34 g/kWh for full load, for 20% B WPO it is 0.21 g/kWh at low load to 1.19 g/kWh at full load, from 0.177 g/kWh at low load to 1.30 g/kWh at full load for 30% B WPO and 0.241 g/kWh at low load to 2.26 g/kWh at high load for 40% B WPO. The results show that CO emission of waste plastic oil is higher than diesel especially at higher load and higher blend. The reason behind increased CO emission is incomplete combustion due to absence of oxygenated compounds in waste plastic oil (Mani et al. 2009a).

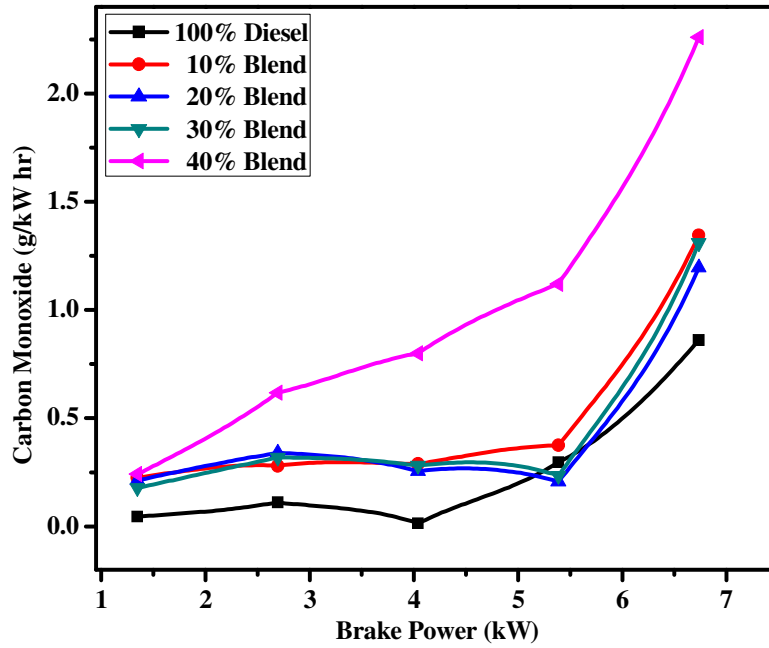


Fig 7.10 Variation of CO with brake power

7.3.4.4 Carbon Dioxide

Figure 7.11 illustrates the variation of carbon dioxide emission for various blends of waste plastic oil and diesel fuel at varying loads. The CO_2 emission varies from 9.83 g/kWh at low load to 1.98 g/kWh at full load for diesel fuel. For 10% blend, it varies from 8.54 g/kWh at low load to 1.74 g/kWh at full load, from 8.05 g/kWh at low load to 1.14 g/kWh at full load for 20% blend. For 30% blend, it varies from 7.97 g/kWh at low load to 1.04 g/kWh at full load and from 7.4 g/kWh at low load to 1.15 g/kWh at full load for 40% blend. The carbon dioxide emission for the blends is lower than diesel for almost all loads and all blends. The carbon dioxide emission for the blends is lower than diesel for almost all loads and all blends. This may be due to late burning of fuel leading to incomplete oxidation of CO (Mani et al. 2009a).

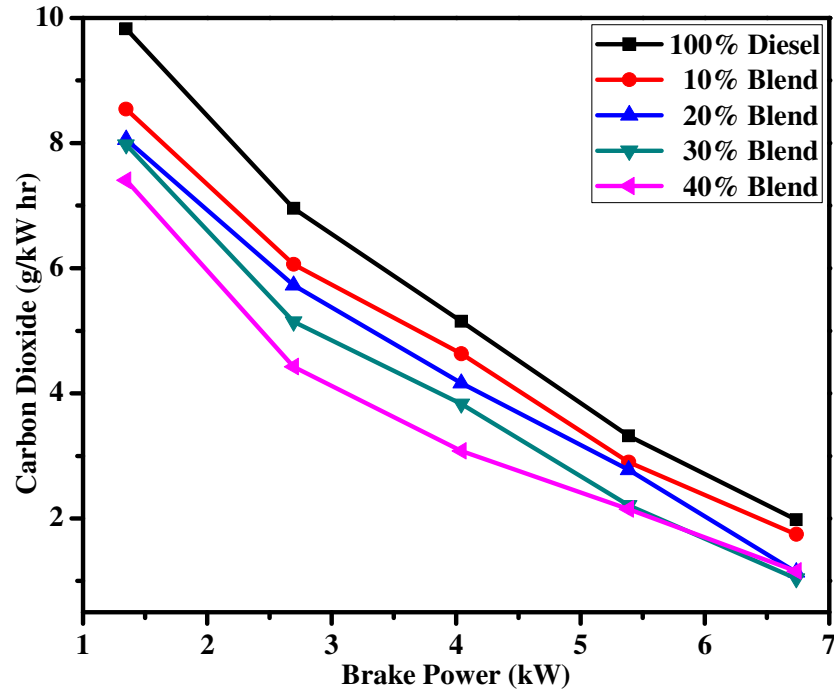


Figure 7.11 Variation of CO₂ with brake power

7.4 Conclusion

In this study, the experiments were conducted using diesel, waste plastic oil obtained by catalytic pyrolysis of waste HDPE and their blends under different loads to investigate the impact of waste plastic oil on the performance and emission characteristics of compression ignition engine at varying load conditions. Based on the experimental results, the following major conclusions have been drawn.

Brake thermal efficiencies at all load conditions are lower as compared to that of diesel fuel due to the lower calorific value of waste plastic oil, exhaust gas temperature increases with increase in engine load. The BSEC increases with the increasing WPO blend ratio at all engine loads and decreases with increase in engine load. The largest increase in BSEC is found to be 40.43 MJ/kWh at low load and 18.01 MJ/kWh at full

load for 10% B WPO. Mechanical efficiency increases with increasing brake power for all fuel blends. It can be seen that the mechanical efficiency for 10% B WPO is better than diesel fuel at all load conditions

The blends of WPO with diesel fuel and varying engine load are found to have significant influences on the NO_x, HC, CO and CO₂ emissions. The NO_x emission increases with increase in percentage of waste plastic oil in blends and decreases with increase in engine load. The unburnt hydrocarbon emission is decreasing with increase in the engine load and increases with increase in percentage of waste plastic oil in blends. The CO emission increases with the increasing WPO blend ratio and engine load. CO emission is higher 0.241 g/kWh at low load to 2.26 g/kWh at high load for 40% B WPO as compared to 0.046 g/kWh at low load to 0.86 g/kWh at full load for diesel. The carbon dioxide emission for the blends is lower than diesel for almost all loads and all blends.

Chapter 8

Kinetic Study of Waste HDPE Pyrolysis

KINETIC STUDY OF WASTE HIGH-DENSITY POLYETHYLENE PYROLYSIS USING THERMOGRAVIMETRIC ANALYSIS

8.1 Introduction

Plastic materials have become very useful commodities in many aspects of human life due to their diversity, relatively low cost, easy processing and light properties. Therefore, the amount of waste plastics is increasing continuously and this situation causes serious environmental issues. Waste plastics are not suitable either for composting or landfilling, because they are essentially nonbiodegradable. The recycling of waste plastics has attracted much interest as an alternative method for their disposal and management over the last few decades. Waste plastic recycling is mainly divided into two routes: mechanical reprocessing of waste plastics, and thermal or catalytic degradation of waste plastics into gas and liquid products, which can subsequently be utilized as fuels and valuable chemicals. Pyrolysis is the most attractive technique of chemical feed stock recycling. Valuable products can be produced from waste plastics by using pyrolysis technology. However, there are many serious problems to be solved in the near future. The present issues are the necessary scale-up of the industry, minimization of production cost and optimization of higher-valued products for a wide range of plastic mixtures (Panda AK et al. 2010a). Especially, the lack of kinetic data hampers the optimal design of pyrolysis process and the design of commercial pyrolysis reactors. Therefore, the kinetics of thermal degradation of waste plastics must be analyzed to provide the apparent kinetic parameters that are useful for the optimal design and operation of pyrolysis process. Thermal behavior of plastics can be improved by knowing thermal degradation kinetics. Thermogravimetric analysis (TGA) technique is an excellent way for studying the kinetics of thermal degradation. It provides information on pre-exponential factor and activation energy. Many studies on pyrolysis kinetics of plastic wastes have been carried out, and also various reaction kinetic models are available to estimate plastic degradation, including integral method (Coats AW et al. 1964, Petrovic ZS et al. 1986, Westerhout RWJ et al. 1997).

High-density polyethylene (HDPE) is the third-largest commodity plastic material in the world, after polyvinyl chloride and polypropylene in terms of volume (Kumar S et al. 2011a). The demand for HDPE has increased 4.4% a year to 31.3 million MT in 2009. The increased demand and production of waste HDPE has led to the accumulation of large amount of its waste in the final waste stream due to its low useful life (Kumar S et al. 2011b). Some researchers studied the pyrolysis kinetics of HDPE using different conditions, different methods and different heating rates (Ceamanos J et al. 2002, Kayacan I et al. 2008, Khaghanikavkani E et al. 2011, Kim HT et al. 2005)[167-170]. In the present work, the kinetics of the thermal degradation of waste HDPE was studied using the thermo-gravimetric analysis (TGA) and integral method. The values of activation energy and the pre-exponential factor for waste HDPE have been obtained in non isothermal condition assuming first order reaction kinetic. Heating rates of 10, 20, and 40 °C/min were employed in TGA experiments.

8.2 Experimental programme

The detail about the raw material, characterization of raw material is summarized in chapter 3. Thermo-gravimetric analysis (TGA) of waste HDPE sample was done using a DTG60 instrument made by Shimadzu Scientific Instruments, North America. Around 10-15 milligrams of waste HDPE sample was taken and heated from room temperature to a final temperature of 600 °C and a residence time of 1 minute at 600 °C was allowed. TGA was performed in nitrogen atmosphere at the heating rates of 10 °C/min, 20 °C/min and 40 °C/min under the 45ml/min gas flow rate. Thermo-gravimetric weight loss curve was plotted against temperature. It provides a range of temperature in which maximum thermal degradation of waste HDPE takes place.

8.2.1 Non-isothermal kinetic study using TGA

Thermo gravimetric analysis (TGA) is one of the most commonly used methods to study the kinetics of thermal decomposition reactions. The kinetic parameters, activation energy and pre-exponential factor of waste HDPE pyrolysis were determined by the integral method (Westerhout RWJ et al. 1997). The approach adopted by many researchers in kinetic analysis of TGA data for solid fuel pyrolysis is to assume first order

reaction for devolatilization (Mustafa VK et al. 1998, Solomon PR et al. 1986, Ying GP et al. 1996). So the first order reaction of waste HDPE pyrolysis with respect to the amount of undecomposed material states that,



For 1st order reaction, we have:

$$dx/dt = k(1 - \alpha) \quad (2)$$

$$k = k_0 * e^{(-E_a/RT)} \quad (3)$$

The extent of conversion or fraction of material pyrolysed, α was defined by expression

$$\alpha = (W_0 - W_t)/(W_0 - W_\infty)$$

Where W_0 is the initial weight (mg), W_t is the weight after “t” minutes (mg), and W_∞ is the final weight after pyrolysis (mg).

Where R = Universal gas constant, $8.314 \text{ J K}^{-1} \text{ mol}^{-1}$

k_0 = Pre-exponential factor (min^{-1})

E_a = Activation energy (kJ/mol)

For a constant heating rate ‘A’ during pyrolysis,

$$A = dT/dt \quad (4)$$

Rearranging and Integrating Eq. (2) results in

$$\ln[-\ln(1 - \alpha)] = \ln \left[\left(\frac{k_0 RT^2}{AE_a} \right) \left(1 - \frac{2RT}{E_a} \right) \right] - E_a/RT \quad (5)$$

Since it may be shown that for most values of E_a and for the temperature range of the pyrolysis, the expression $\ln[RT^2 k_0 / AE_a (1 - 2RT/E_a)]$ in Eq. (5) is essentially constant, if the left side of Eq. (5) is plotted versus $1/T$, a straight line may be obtained when the process is assumed as a first order reaction. From the slope, $-E_a/R$, the activation energy E_a can be determined, and by taking the temperature at which $W_t = (W_0 + W_f)/2$ in the place of T in the intercept term of Eq. (5), the pre-exponential factor k_0 can also be determined.

8.3 Result and Discussion

8.3.1 Characterization of waste HDPE sample

The ultimate or elemental analysis of waste HDPE is shown in Table 8.1. The oxygen is 5.19% in the ultimate analysis of waste HDPE. The oxygen in the waste HDPE sample may not be due to the fillers but rather to other ingredients that are added to the resin in

the manufacturing of HDPE. Calorific value of waste HDPE was 45.78 MJ/kg. From the comparison of waste HDPE with mixed plastic waste (Cho MH et al. 2010) in table 8.1, it was found that the carbon and hydrogen percentage and gross calorific value (GCV) are more in waste HDPE as compared to mixed plastic waste. Mixed plastic waste contained 1.13% of chlorine which was not found in case of waste HDPE.

Table 8.1 Ultimate or elemental analysis of waste HDPE

Sample	C (wt %)	H (wt %)	N (wt %)	S (wt %)	O (wt %)	Cl (wt %)	GCV (MJ/kg)
Waste HDPE	80.58	13.98	0.60	0.080	5.19	-	45.78
Mixed Plastics (Cho MH et al. 2010)	79.9	12.6	-	-	5.10	1.13	44.40

8.3.2 TGA and DTG analysis

The thermal stability of the polymeric materials plays a crucial role in determining the limit of their working temperature and the environmental conditions for uses, which are related to their thermal decomposition temperature and decomposition rate. TGA applied in determination of the study of thermal stability/degradation of waste HDPE in various ranges of temperature. Figure 8.1 shows the TGA results of waste HDPE at the heating rates of 10 °C/min, 20 °C/min and 40 °C/min in nitrogen atmosphere. The initial temperature at which the degradation started and final temperature at which the degradation completed for waste HDPE was 385 °C and 490 °C, 400 °C and 505 °C, 410 °C and 510 °C at the heating rates of 10 °C/min, 20 °C/min and 40 °C/min respectively. As the heating rates increased, the initial and final degradation temperature for waste HDPE also increased due to the fact that polymer molecules does not have enough time to exhaust the heat with increasing heating rate, leading to slower decomposition rate and higher decomposition temperature due to slow diffusion of heat (Malek J 1992). Similarly, when the heating rate increases, the decomposition temperature of the plastics

samples also increases for raw and waste HDPE at 5, 10, 20 and 50 K/min heating rates (Kayacan I et al. 2008).

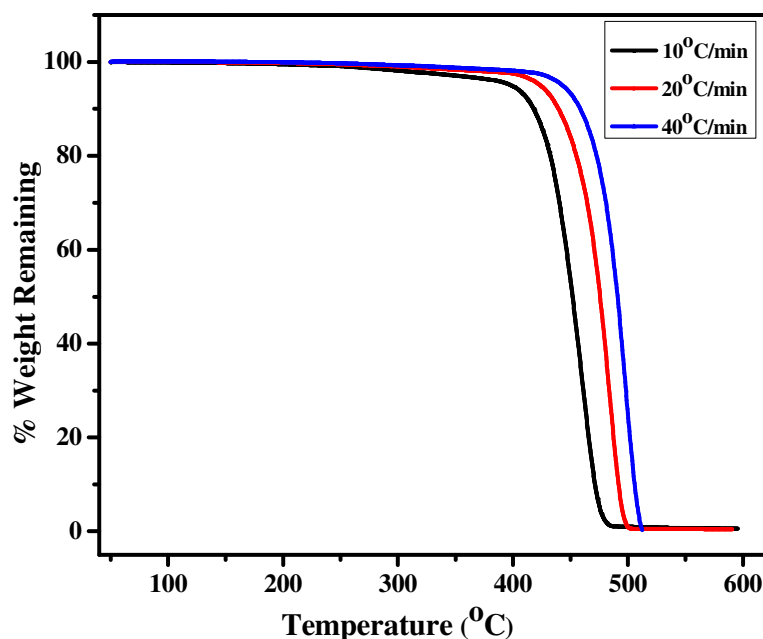


Figure 8.1 TGA plot of waste HDPE at different heating rates in N₂ atmosphere

Differential thermogravimetry (DTG) curve for waste HDPE at 10 °C/min, 20 °C/min and 40 °C/min heating rates contains only one peak, this indicates that there is only one degradation step in figure 8.2 for different heating rates. The degradation temperatures for waste HDPE at which the maximum weight losses (T_{max}) take place were about 465 °C, 485 °C and 500 °C at the heating rates of 10, 20 and 40 °C/min respectively. DTG curves at different heating rates were shifted to higher temperature due to the heat transfer enlarging with increasing heating rate. Similar effect of various heating rates on DTG curves for HDPE pyrolysis has been obtained by A. Aboulkas (Aboulkas A et al. 2007).

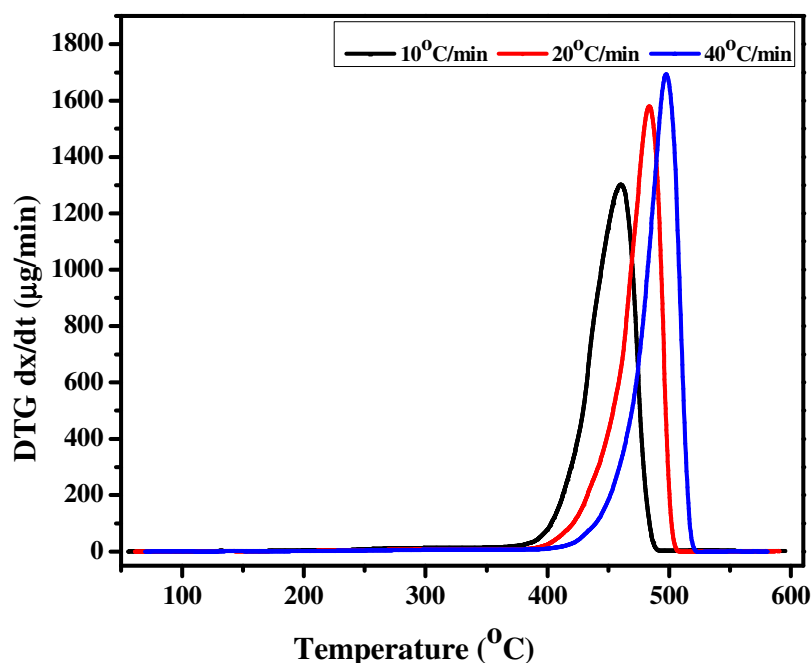


Figure 8.2 DTG plot of waste HDPE at different heating rates in N₂ atmosphere

8.3.3 Kinetic study using TGA under non-isothermal conditions

Pyrolysis kinetic analysis is valuable for the in-depth exploration of process mechanisms. On the basis of thermo gravimetric analysis of different kinds of polymeric materials, thermal kinetics analysis was performed to analyze the pyrolysis behavior of waste HDPE. With the apparent kinetic parameters derived, a kinetic model was proposed for the main reaction section of waste HDPE pyrolysis process. Figure 8.3 shows the plot of the integral method for waste HDPE under non-isothermal conditions. In this figure, as the entire range of $\ln(-\ln(1-x))$ as a function of $1/T$, data could be represented by a single straight line ($R^2=0.99$) for all three heating rates. Reasonable fits of data to straight lines in this figure indicate that the assumption of first-order kinetics for thermal decomposition of waste HDPE is acceptable. The activation energy values of waste HDPE have been calculated as 207.43, 268.22 and 473.05 kJ/mol at 10, 20 and 40 °C/min heating rates (see table 8.2) under nitrogen atmosphere. Activation energy

increased with increase in heating rate due to very low thermal conductivity of polymeric material and hence the temperature distribution in the waste HDPE sample will be significant at a high heating rate. Reported values in literature are 268 kJ/mol by H. Bockhorn (Bockhorn H et al. 1999), 396-493 kJ/mol by I. Kayacan (Kayacan I et al. 2008), 146.5 kJ/mol by N. A. Khalturinskii (Khalturinskii et al. 1987), 126-275 kJ/mol by F. S. M. Sinfronio (Sinfronio FSM et al. 2005), 243.8 kJ/mol by J. M. Encinar (Encinar JM et al. 2008), 238.4 kJ/mol by L. Ballice (Ballice et al. 2001) and 233.2 kJ/mol by C. H. Wu (Wu CH et al. 1993). The reason for the wide discrepancy in the measured values of activation energy (apart from the characteristics of the sample) could be attributed to a defective heat transfer and a complex mechanism of decomposition due to diverse operating conditions in the literature (Khaghanikavkani E et al. 2011).

Table 8.2 Activation energy and pre-exponential factor determined by integral method for waste HDPE pyrolysis

Heating rate A, °C/min	Activation Energy (E_a) kJ/mol	Pre-exponential factor (k_0) min ⁻¹
10	207.43	1.37×10^{11}
20	268.22	5.21×10^{13}
40	473.05	1.68×10^{30}

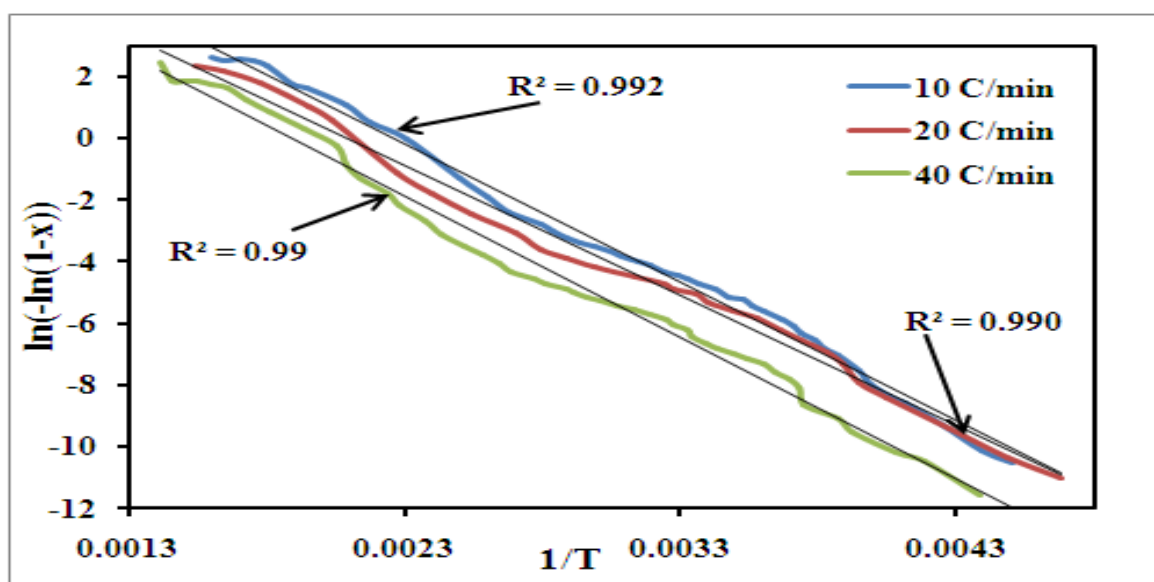


Figure 8.3 Kinetic study plot at different heating rates in N₂ atmosphere

8.4 Conclusion

The kinetic parameters of waste HDPE pyrolysis under non isothermal conditions using TGA were determined. Determining the kinetic parameters also provides information to design more effective conversion systems and optimum pyrolysis regimes. The TGA experiment showed that the heating rate has an important role on the degradation reaction. When the heating rate increases, the activation energy and degradation temperature of the waste HDPE also increases. The degradation temperatures for waste HDPE at which the maximum weight losses (T_{\max}) take place were about 465 °C, 485 °C and 500 °C at the heating rates of 10, 20 and 40 °C/min respectively. The activation energy values of waste HDPE have been calculated as 207.43, 268.22 and 473.05 kJ/mol at 10, 20 and 40 °C/min heating rates respectively. Reasonable fits of data to straight lines in kinetic study plot indicate that the assumption of first-order kinetics for thermal degradation of waste HDPE is acceptable.

Chapter 9

Conclusions and Future Recommendations

CONCLUSIONS AND FUTURE RECOMMENDATIONS

9.1 Summary and conclusions

The pyrolysis of waste plastics using different catalysts and reactor set ups at different reaction parameters has been studied by a number of researchers as revealed from the literature review. A number of process industries have come up based on these research results. However, there are many problems that have to be solved in the near future. The present challenges include the need for scale up, minimization of waste handling costs, production cost and optimization of gasoline range products for a wide range of plastic waste. One of the ways to reduce the cost of the process is to develop a novel and more efficient catalyst for the pyrolysis process which would be cheaper, available on commercial scale and should be reusable. Therefore, the present study deals with the pyrolysis of high-density polyethylene (HDPE) using a commonly available material i.e. kaolin clay to know its suitability as a catalyst for this process.

Thermal and catalytic pyrolysis of high-density polyethylene using kaolin, silica-alumina and mordenite as catalysts in a batch reactor has been studied. From the comparison of the results obtained with these catalysts, kaolin showed the promising result for HDPE pyrolysis. Therefore, the kaolin has been treated with 3M concentration of four different acids and one base (acetic acid, phosphoric acid, nitric acid, hydrochloric acid and sodium hydroxide) to enhance the catalytic activity of the resultant clay in the HDPE pyrolysis process. The acid and alkali treated kaolin clays are characterized for studying the effect of acid and alkali treatment on the different physico-chemical properties. Catalytic pyrolysis of waste HDPE using acid and alkali treated kaolin has been carried out and the properties of liquid fuel obtained by catalytic pyrolysis have been determined. Response surface methodology (RSM) was used to optimize the process parameters involved in decomposition of waste HDPE. The liquid fuel obtained by the catalytic pyrolysis of waste HDPE using nitric acid treated kaolin catalyst has been tested for engine performance and emission analysis in a CI engine. The thermo gravimetric analysis of waste HDPE at heating rate of 10 °C/min, 20 °C/min and 40 °C/min in the N₂

atmosphere was studied and kinetic parameter (activation energy) was determined by using thermogravimetric plots.

The major findings of present work are as follows:

Maximum oil yield in thermal pyrolysis of waste HDPE was 50.8 wt. % at optimum condition of temperature, which was improved to 58.8 wt. %, in kaolin catalyzed degradation under optimum condition of temperature and feed ratio. Reaction time decreased with increased in temperature. The maximum yield of oil in the acid treated kaolin catalyzed pyrolysis of waste HDPE was 79% under optimum conditions. The fuel properties of the oil obtained from the catalytic pyrolysis of waste HDPE is similar with that of petro-fuels. Optimum operating conditions of reaction temperature (450 °C), acidity of catalyst (0.341) and catalyst to waste HDPE ratio (1:4) were produced with respect to maximum liquid product yield of 78.7% from optimization by response surface methodology (RSM). The polynomial model obtained fits well to predict the response with a high determination coefficient of R^2 (0.995). The diesel blended plastic oil obtained by the catalytic pyrolysis of waste HDPE has been tested for its performance and emission in a CI diesel engine. Engine was able to run with maximum 40% waste plastic oil-diesel blends. The activation energy values by the thermo gravimetric analysis of waste HDPE have been calculated as 207.43, 268.22 and 473.05 kJ/mol at 10, 20 and 40 °C/min heating rates respectively. When the heating rate increases, the activation energy and degradation temperature of the waste HDPE also increases.

9.2 Recommendations for future

From the above results, it can be concluded that kaolin work very well in the pyrolysis of waste high-density polyethylene and further studies are required to materialize the process. The followings are the recommendations for the future work.

- Modification in the design of reactor used in pyrolysis process.
- The non-condensable gases were gone off in the experiment. It would be valuable to collect some of the gases and investigate their composition.
- Better and effective distillation columns should be applied for refining of the pyrolysis products.
- Hydrogenation can significantly improve the liquid product quality by converting alkenes into alkanes to get higher stability liquid fuel for the transportation purpose.
- Study of high-density polyethylene pyrolysis using other clay materials such as bentonite, dickite, nacrite, and halloysite, silica gel, alumina gel and Kieselguhr etc.
- Activation of clay using other methods such as intercalation, mechanical grinding, etc to increase the catalytic activity and its study in HDPE pyrolysis.
- Synthesis of nano clay catalyst and its use in HDPE pyrolysis.
- Kinetic study of high-density polyethylene pyrolysis with different kinetic models for better reactor design.
- Develop a continuous process for HDPE pyrolysis using suitable catalyst.

References

REFERENCES

- Aboulkas A**, Harfi KE, Bouadili AE, Benchanaa M, Mokhlisse A, Outzourit, A. (2007) Kinetics of co-pyrolysis of tarfaya (Morocco) oil shale with high-density polyethylene. *Oil Shale*, 24(1):15-33.
- Ali S**, Garforth AA, Harris DH, Rawlence DJ, Uemichi Y. (2002) Polymer waste recycling over used catalysts. *Catalysis Today*, 75:247-255.
- Bagri R**, Williams PT. (2002) Catalytic pyrolysis of polyethylene. *Journal of Analytical and Applied Pyrolysis*, 63:29–41.
- Ballice L**. (2001) A Kinetic approach to the temperature programmed pyrolysis of low and high-density polyethylene in a fixed bed reactor: Determination of kinetic parameters for the evolution of n-paraffins and 1-olefins. *Fuel*, 80(13):1923-1935.
- Ballice L**, Reimert R. (2002) Classification of volatile products from the temperature programmed pyrolysis of polypropylene (PP), atactic-polypropylene (APP) and thermogravimetrically derived kinetics of pyrolysis. *Chemical Engineering and Processing: Process Intensification*, 41:289–296.
- Bari S**, Yu CW, Lim TH. (2004) Effect of fuel injection timing with waste cooking oil as a fuel in a direct injection diesel engine. *Proceedings of the Institution of Mechanical Engineers, Part D: Journal of Automobile Engineering*. 218:93–104.
- Bate DM**, Lehrle RS. (1996) Kinetic measurements by pyrolysis-gas chromatography, and examples of their use in deducing mechanisms, *Polymer Degradation and Stability*, 53:39–44.
- Beltrame PL**, Carniti P, Audisio G, Bertini F. (1989) Catalytic Degradation of Polymers: Part II-Degradation of Polyethylene. *Polymer Degradation and Stability*, 26:209–220.
- Belver C**, Munoz MAB, Vicente MA. (2002) Chemical activation of a kaolinite under acid and alkaline conditions. *Chemistry of Materials*, 14:2033–2043.
- Bockhorn H**, Hornung A, Hornung U, Schawaller D. (1999) Kinetic study on the thermal degradation of polypropylene and polyethylene. *Journal of Analytical and Applied Pyrolysis*, 48:93–109.

- Box GEP**, Hunter WG, Hunter JS. (1978) Statistics for experimenters: An Introduction to Design, Data Analysis, and Model Building, John Wiley & Sons, New York.
- Breen C**, Last PM, Taylor S, Komadel P. (2000) Synergic chemical analysis – the coupling of TG with FTIR, MS and GC-MS 2. Catalytic transformation of the gases evolved during the thermal decomposition of HDPE using acid-activated clays. *Thermochimica Acta*, 363:93–104.
- Buekens G**, Huang H. (1998) Catalytic plastics cracking for recovery of gasoline-range hydrocarbons from municipal plastic wastes. *Resources, Conservation and Recycling*, 23:163–181.
- Burkle D**. (1992) Proceedings of Recycle, Davos, Switzerland, 11/1.1.
- Caffrey WCM**, Kamal MR, Cooper DG. (1995) Thermolysis of polyethylene, *Polymer Degradation and Stability*, 47:133–139.
- Caglayan MO**, Kafa S, Yigit N. (2005) Al-pillared clay for cottonseed oil bleaching: an optimization study. *Journal of American Oil Chemists' Society*, 82:599–602.
- Ceamanos J**, Mastral JF, Millera A, Aldea ME. (2002) Kinetics of pyrolysis of high density polyethylene, Comparison of isothermal and dynamic experiments. *Journal of Analytical and Applied Pyrolysis*, 65(2):93–110.
- CEH report on high density polyethylene resins**
<http://www.sriconsulting.com/CEH/Public/Reports/580.1340/>
- Chan JH**, Balke ST. (1997a) The thermal degradation kinetics of polypropylene: Part II. Time–temperature superposition. *Polymer Degradation and Stability*, 57:113–125.
- Chan JH**, Balke ST. (1997b) The thermal degradation kinetics of polypropylene: Part III. Thermogravimetric analyses, *Polymer Degradation and Stability*, 57:135–149.
- Chan JH**, Balke ST. (1997c) The thermal degradation kinetics of polypropylene: Part I. Time–temperature superposition. *Polymer Degradation and Stability*, 57:127–134.
- Chattopadhyay J**, Kim C, Kim R, Pak D.(2008) Thermogravimetric characteristics and kinetic study of biomass co-pyrolysis with plastic. *Korean Journal of Chemical Engineering*, 25(5):1047-1053.

- Chitnis SR**, Sharma MM. (1997) Industrial applications of acid-treated clays as catalysts. *Reactive and Functional Polymers*, 32:93–115.
- Chmielarz L**, Kowalczyk A, Michalik M, Dudek B, Piwowarska Z, Matusiewicz A. (2010) Acid-activated vermiculites and phlogophites as catalysts for the DeNO_x process. *Applied Clay Science*, 49:156–162.
- Cho YS**, Shim MJ, Kim SW. (1998) Thermal degradation kinetics of PE by Kissinger equation, *Materials Chemistry and Physics*, 52:94–97.
- Clark DE**, Folz DC, West JK. (2000) Processing materials with microwave energy. *Material Science and Engineering*, 287:153–158.
- Clarke GM**, Kempson RE. (1997) Introduction to the design and analysis of experiments, Arnold, London.
- Coats AW**, Redfern J.P. (1964) Kinetic parameters from thermogravimetric data. *Nature*, 201:68-69.
- Cornell JA**. (1990) How to apply response surface methodology, American Society for Quality Control, Wisconsin.
- Cho MH**, Jung SH, Kim JS. (2010) Pyrolysis of mixed plastic wastes for the recovery of benzene, toluene and xylene (BTX) aromatics in a fluidized bed and chlorine removal by applying various additives, *Energy and Fuels*, 24:1389-1395.
- Consea JA**, Font R, Marcilla A, Garcia AN. (1994) Pyrolysis of polyethylene in a fluidized bed reactor. *Energy and Fuels*, 8:1238-1246.
- Delhez R**, Keijser TH, Mittemeijer EJ, Fresenius Z. (1982) Determination of crystallite size and lattice distortions through X-ray diffraction line profile analysis. *Analytical Chemistry*, 312:1–10.
- Dudkin BN**, Loukhina IV, Avvakumov EG, Isupov VP. (2004) Application of mechanochemical treatment of disintegration of kaolinite with sulphuric acid. *Chemical and Sustainable Development*, 12: 327–330.
- Encinar JM**, Gonzalez JF. (2008) Pyrolysis of synthetic polymers and plastic wastes., Kinetic study. *Fuel Processing Technology*, 89(7):678-686.

- Fernandes VJ**, Araujo AS, Frenandes GJT. (1997) Catalytic degradation of polyethylene evaluated by GC, *Journal of Thermal Analysis*, 49:255–260.
- Foletto EL**, Volzone C, Porto LM. (2006) Clarification of cottonseed oil: how structural properties of treated bentonites by acid affect bleaching efficiency. *Latin America Applied Research*, 36:37–40.
- Gao Z**, Amasaki I, Nakada M. (2003) A thermogravimetric study on thermal degradation of polyethylene. *Journal of Analytical and Applied Pyrolysis*, 67:1–9.
- Garforth A**, Fiddy S, Lin YH, Siakhali AG, Sharratt PN, Dwyer J. (1997) Catalytic degradation of high density polyethylene: an evaluation of mesoporous and microporous catalysts using thermal analysis. *Thermochimica Acta*, 294:65–69.
- Garforth AA**, Lin YH, Sharratt PN, Dwyer J. (1998) Production of hydrocarbons by catalytic degradation of high density polyethylene in a laboratory fluidised-bed reactor. *Applied catalysis A: General*, 169:331–342.
- Garforth AA**, Jesus SA, Martinez H, Akhan A. (2004) Feedstock recycling of polymer wastes. *Current Opinion in Solid State Material*, 8:419–425.
- Gil A**, Montes M. (1994) Effect of thermal treatment on microporous accessibility in aluminium pillared clays. *Journal of Materials Chemistry*, 4:1491–1496.
- Gonzalez J**, Albano C, Ichazo M, Hernandez M, Sciamanna R. (2001) Analysis of thermogravimetric data of blends of polyolefins with calcium carbonate treated with Lica 12. *Polymer Degradation and Stability*, 73:211–224.
- Grieken RV**, Serrano DP, Aguado J, Garcya R, Rojo C. (2001) Thermal and catalytic cracking of polyethylene under mild conditions. *Journal of Analytical and Applied Pyrolysis*, 58–59:127–142.
- Gunawan NS**, Indraswati N, Ju YH, Soetaredjo FE, Ayucitra A, Ismadji S. (2010) Bentonites modified with anionic and cationic surfactants for bleaching of crude palm oil. *Applied Clay Science*, 47:462–464.

HDPE

http://en.wikipedia.org/wiki/High-density_polyethylene

- Hernandez MR**, Garcia AR, Gomez A, Agullo J, Marcilla A. (2006) Effect of residence time on volatile products obtained in the HDPE pyrolysis in the presence and absence of HZSM-5. *Industrial & Engineering Chemistry Research*, 45:8770-8778.
- Horvat N**, Ng FTT. (1999) Tertiary polymer recycling: study of polyethylene thermolysis as a first step to synthetic diesel fuel. *Fuel*, 78:459–470.
- Hujuri U**, Ghoshal AK, Gumma S. (2011) Temperature-Dependent Pyrolytic Product Evolution Profile for Polypropylene. *Journal of Applied Polymer Science*, 119(4):2318–2325.
- Hussin F**, Aroua MK, Daud WMAW.(2011) Textural characteristics, surface chemistry and activation of bleaching earth: A review. *Chemical Engineering Journal*, 170:90–106.
- Hwang G**, Kim K, Bae S, Yi S, Kumazawa H. (2001) Degradation of high density polyethylene, polypropylene and their mixtures in supercritical acetone. *Korean Journal of Chemical Engineering*, 18(3):396-401.
- Hwang EY**, Kim JR, Choi JK, H. Woo HC, Park DW. (2002) Performance of acid treated natural zeolites in catalytic degradation of polypropylene. *Journal of Analytical and Applied Pyrolysis*, 62:351–364.
- Ilkilic, C.** (2012) The emission characteristics of a CI engine fueled with a bio-fuel blend. *Energy Sources, Part A: Recovery, Utilization, and Environmental Effects*, 34:1901–1912.
- Jalil PA.** (2002) Investigations on polyethylene degradation into fuel oil over tungstophosphoric acid supported on MCM-41 mesoporous silica. *Journal of Analytical and Applied Pyrolysis*, 65:185–195.
- Jan MR**, Shah J, Gulab H. (2010a) Degradation of waste high-density polyethylene into fuel oil using basic catalyst. *Fuel*, 89:474-480.
- Jan MR**, Shah J, Gulab H. (2010b) Catalytic degradation of waste high-density polyethylene into fuel products using BaCO₃ as a catalyst. *Fuel Processing Technology*, 91:1428-1437.
- Jan MR**, Shah J, Gulab H. (2013) Catalytic conversion of waste high-density polyethylene into useful hydrocarbons. *Fuel*, 105:595-602.

- Jozefaciuk G**, Sarzynska DM. (2006) Effect of acid treatment and alkali treatment on nanopore properties of selected minerals. *Clays and Clay Minerals*, 54(2):220-229.
- Kallai LH**. (2006) Developments in clay science: handbook of clay science, in: L. Heller-Kallai (Ed.), *Thermally Modified Clay Minerals*, Elsevier, Oxford.
- Karagoz S**, Yanik J , Uçar S , Saglam M, Song C (2003) Catalytic and thermal degradation of high-density polyethylene in vacuum gas oil over non-acidic and acidic catalysts. *Applied Catalysis A: General*, 242:51-62.
- Kayacan I**, Dogan OM. (2008) Pyrolysis of low and high density polyethylene. Part I: non-isothermal pyrolysis kinetics. *Energy Sources, Part A: Recovery, Utilization, and Environmental Effects*, 30(5):385–391.
- Khaghanikavkani E**, Farid MM. (2011) Thermal pyrolysis of polyethylene: Kinetic study. *Energy Science and Technology*, 2(1):1-10
- Khalturinskii NA**. (1987) High-temperature pyrolysis of polymers. *Journal of Thermal Analysis and Calorimetry*, 32(6):1675-1682.
- Kidoguchi Y**, Yang C, Kato R, Miwa K. (2000) Effects of fuel cetane number and aromatics on combustion process and emissions of a direct injection diesel engine. *JSAE Review*, 21(4):469–475.
- Kim D**, Shin S, Sohn S, Choi J, Ban B. (2002) Waste plastics as supplemental fuel in the blast furnace process: improving combustion efficiencies. *Journal of Hazardous Materials*, 94(3):213–222.
- Kim HT**, Oh SC. (2005) Kinetics of thermal degradation of waste polypropylene and high-density polyethylene. *Journal of Industrial and Engineering Chemistry*, 11(5):648-656.
- Kim JS**, Lee WY, Lee SB, Kim SB, Choi KJ. (2003) Degradation of polystyrene waste over base promoted Fe catalysts. *Catalysis Today*, 87:59–68.
- Kiran E**, Gillham JK. (1976) Pyrolysis-molecular weight chromatography: a new on-line system for analysis of polymers. II. Thermal decomposition of polyolefins: polyethylene, polypropylene, polyisobutylene. *Journal of Applied Polymer Science*, 20:2045-2068.

- Korichi S**, Elias A, Mefti A. (2009) Characterization of smectite after acid activation with microwave irradiation. *Applied Clay Science*, 42:432–438.
- Kumar S**, Singh RK. (2011a) Recovery of hydrocarbon liquid from waste high density polyethylene by thermal pyrolysis. *Brazilian Journal of Chemical Engineering*, 28:659-667.
- Kumar S**, Panda AK, Singh RK. (2011b) A review on tertiary recycling of high-density polyethylene to fuel, *Resources, Conservation and Recycling*. 55(11):893-910.
- Kumar S**, Panda AK, Singh RK. (2013) Preparation and characterization of acid and alkali treated kaolin clay, *Bulletin of Chemical Reaction Engineering and Catalysis*, 8(1):61-69.
- Lehrle RS**. (1987) Polymer pyrolysis mechanisms: experimental Approaches for investigating them. *Journal of Analytical and Applied Pyrolysis*, 11:55-64.
- Lee K**, Shin D. (2003) Catalytic degradation of waste HDPE over acidic catalysts with different pore sizes. *Journal of Industrial and Engineering Chemistry*, 9(5):584-589.
- Lee KH**, Shin DH. (2003a) Catalytic degradation of waste polyolefinic polymers using spent FCC catalyst with various experimental variables. *Korean Journal of Chemical Engineering*, 20(1):89–92.
- Lee KH**, Jeon SG, Kim KH, Noh NS, Shin DH, Park J, Seo YH, Yee JJ, Kim GT. (2003b) Thermal and catalytic degradation of waste high-density polyethylene using spent FCC catalyst. *Korean Journal of Chemical Engineering*, 20(4):693–697.
- Lenarda M**, Storaro L, Talona A, Moretti E, Riello P. (2007) Solid acid catalysts from clays: preparation of mesoporous catalysts by chemical activation of metakaolin under acid conditions. *Journal of Colloid and Interfacial Science*, 311:537–543.
- Lin YH**, Sharratt PN, Garfohrt AA, Dwyer J. (1997) Deactivation of US-Y zeolite by coke formation during the catalytic pyrolysis of high density polyethylene. *Thermochimica Acta*, 294:45–50.
- Lin YH**, Hwu WH, Ger MD, Yeh TF, Dwyer J. (2001) A combined kinetic and mechanistic modelling of the catalytic degradation of polymers. *Journal of Molecular Catalysis A: Chemical*, 171:143–151.

- Lin YH**, Yang MH, Yeh TF, Ger MD. (2004) Catalytic degradation of high density polyethylene over mesoporous and microporous catalysts in a fluidized-bed reactor. *Polymer and Degradation Stability*, 86:121-128.
- Lucas N**, Bieniaime C, Belloy C, Queneudec M, Silvestre F, Saucedo JEN. (2008) Polymer biodegradation: mechanisms and estimation techniques – a review. *Chemosphere*, 73(4):429–442.
- Malek J**. (1992) The kinetic-analysis of nonisothermal data. *Thermochimica Acta*, 200:257-269.
- Manchado ML**, Torre L, Kenny JM. (2002) Kinetic analysis of the thermal degradation of PP-EPDM blends. *Rubber Chemistry and Technology*, 23:73–84.
- Manos G**, Garforth A, Dwyer J. (2000) Catalytic degradation of high-density polyethylene over different zeolitic structures. *Industrial & Engineering Chemistry Research*, 39:1198-1202.
- Mani M**, Subash C, Nagarajan G. (2009a) Performance, emission and combustion characteristics of a DI diesel engine using waste plastic oil. *Applied Thermal Engineering*, 29:2738-2744.
- Mani M**, Nagarajan G. (2009b) Influence of injection timing on performance, emission and combustion characteristics of a DI diesel engine running on waste plastic oil. *Energy*, 34:1617-1623.
- Maraghi R**. (1993) Disposal, recycling and reuse. In: Mostafa N, Dekker M, editors. *Plastics Waste Management*, New York, USA; 223-226.
- Marcilla A**, Beltran M, Conesa JA. (2001) Catalyst addition in polyethylene pyrolysis thermogravimetric study. *Journal of Analytical and Applied Pyrolysis*, 58–59: 117–126.
- Marcilla A**, Gomez A, Reyes-Labarta GA, Giner A, Hernandez F. (2003) Kinetic study of polypropylene pyrolysis using ZSM-5 and an equilibrium fluid catalytic cracking catalysts. *Journal of Analytical and Applied Pyrolysis*, 68–69:467–480.
- Marcilla A**, Gomez A, Reyes-Labarta JA, Giner A, Hernandez F. (2003a) Kinetic study of polypropylene pyrolysis using ZSM-5 and an equilibrium fluid catalytic cracking catalyst. *Journal of Analytical and Applied Pyrolysis*, 68–69:467–480.

- Marcilla A**, Gomez A, Labarta JAR, Giner A. (2003b) Catalytic pyrolysis of polypropylene using MCM-4: kinetic model, *Polymer Degradation and Stability*, 80:233–240.
- Mastral JF**, Esperanza E, Berrueco C, Juste M, Ceamanos J. (2003) Fluidized bed thermal degradation products of HDPE in an inert atmosphere and in air–nitrogen mixture. *Journal of Analytical and Applied Pyrolysis*, 70:1–17.
- Mastral JF**, Berrueco C, Gea M, Ceamanos J. (2006) Catalytic degradation of high density polyethylene over nanocrystalline HZSM-5 zeolite. *Polymer Degradation and Stability*, 91:3330–3338.
- Masuda T**, Kuwahara H, Mukai SR, Hashimoto K. (1999) Production of high quality gasoline from waste polyethylene derived heavy oil over Ni-REY catalyst in steam atmosphere. *Chemical Engineering Science*, 54:2773–2779.
- Mendenhall W**, Sincich T. (1989) *Statistics for the engineering and computer sciences*, second ed. Maxwall Macmillan, Singapore.
- Miranda R**, Yang J, Roy C, Vasile C. (2001) Vacuum pyrolysis of commingled plastics containing PVC I. Kinetic study. *Polymer Degradation and Stability*, 72:469–449.
- Miskolczi N**, Bartha L, Deak G, Jover B, Kalló D. (2004) Kinetic model of the chemical recycling of waste polyethylene into fuels. *Process safety and environmental Protection*, 82:223–29.
- Miskolczi N**, Bartha L. (2008) Investigation of hydrocarbon fractions from waste plastic recycling by FTIR, GC, EDX-RFS and SEC techniques. *Journal of Biochemical and Biophysical Methods*, 70:1247–1253.
- Montgomery DC**. (2001) *Design and analysis of experiments*, John Wiley & Sons, New York.
- Moriya T**, Enomoto H. (1999) Characteristics of polyethylene cracking in supercritical water compared to thermal cracking. *Polymer Degradation and Stability*, 65:373–386.
- Muralidharan K**, Vasudevan D. (2011) Performance, emission and combustion characteristics of a variable compression ratio engine using methyl esters of waste cooking oil and diesel blends. *Applied Energy*, 88(11):3959–3968.

- Murata K**, Hirano Y, Sakata Y. (2002) Basic study on a continuous flow reactor for thermal degradation of polymers. *Journal of Analytical and Applied Pyrolysis*, 65:71-90.
- Murata K**, Sato K, Sakata Y. (2004) Effect of pressure on thermal degradation of polyethylene. *Journal of Analytical and Applied Pyrolysis*, 71:569-89.
- Mustafa VK**, Esber O, Ozgen K, Cahit H. (1998) Effect of particle size on coal pyrolysis. *Journal of Analytical and Applied Pyrolysis*, 45:103–110.
- Nagarajan G**, Rao AN, Renganarayanan S. (2002) Emission and performance characteristics of neat ethanol fuelled DI diesel engine. *International Journal of Ambient Energy*, 23(3):149–158.
- Navarro R**, Torre L, Kenny JM, Jimenez A. (2003) Thermal degradation of recycled polypropylene toughened with elastomers. *Polymer Degradation and Stability*, 82:279–290.
- Onal M**, Sarikaya Y. (2007) Preparation and characterization of acid-activated bentonite powders. *Powder Technology*, 172:14–18.
- Ono Y**. (2003) A survey of the mechanism in catalytic isomerization of alkanes. *Catalysis Today*, 81:3–16.
- Panda AK**, Singh RK, Mishra DK. (2010a) Thermolysis of waste plastics to liquid fuel; A suitable method for plastic waste management and manufacture of value added products- A world prospective. *Renewal and Sustainable Energy Review*, 14:233–248.
- Panda AK**, Mishra BG, Mishra DK, Singh RK. (2010b) Effect of sulphuric acid treatment on the physico-chemical characteristics of kaolin clay. *Colloids and Surfaces A: Physicochemical and Engineering Aspects*, 363:98-104.
- Panda AK**. (2011) Studies on process optimization for production of liquid fuels from waste plastics. PhD Thesis, <http://ethesis.nitrkl.ac.in/3850/>
- Panda AK**, Singh RK. (2011) Catalytic performances of kaoline and silica alumina in the thermal degradation of polypropylene. *Journal of Fuel Chemistry and Technology*, 39(3):198-202.
- Panda AK**, Singh RK, Mishra DK. (2012) Thermo-catalytic degradation of thermocol waste to value added liquid products. *Asian Journal of Chemistry*. 24(12): 5539-5542.

Park JW, Kim JH, Seo G. (2002) The effect of pore shape on the catalytic performance of zeolites in the liquid-phase degradation of HDPE. *Polymer Degradation and Stability*, 76:495–501.

Petroleum Product Surveys, Motor Gasoline, Summer, Winter 1986/1987, National Institute for Petroleum and Energy Research (1986).

Petrovic ZS, Zavargo ZZ. (1986) Reliability of methods for determination of kinetic parameters from thermogravimetric and DSC measurements. *Journal of Applied Polymer Science*, 32(4):4353–4367.

Pielichowski K, Njuguna J. (2005) *Thermal Degradation of Polymeric Materials*, UK: Rapra Technology Limited, 1st chapter.

Pinto F, Costa P, Gulyurtulu I, Cabrita I. (1999) Pyrolysis of plastic waste: 2. Effect of catalyst on product yield. *Journal of Analytical and Applied Pyrolysis*, 51:57–71.

Plastics Data

<http://k-mac-plastics.net/data%20sheets/hdpe.htm>

Plastics Production

<http://www.plastemart.com/upload/Literature/India-petrochemical-production-to-double.asp>

Plastic - The Facts 2010

(www.plasticseurope.org/.../20101006091310-final_plasticsthefacts_28092010_lr.pdf)

Puente DLG, Klocker C, Sedran U. (2002) Conversion of waste plastics into fuels recycling polyethylene in FCC. *Applied Catalysis B-Environmental*, 36(4):279–285.

Raheman H, Phadatare AG. (2004) Diesel engine emissions and performance from blends of karanja methyl ester and diesel. *Biomass & Bioenergy*, 27:393-397.

Ravichandran J, Sivasankar B. (1997) Properties and catalytic activity of acid modified montmorillonite and vermiculite. *Clays and Clay Minerals*, 45:854–858.

Rath S, Kumar S, Singh RK. (2011) Performance and emission analysis of blends of karanja methyl ester with diesel in a compression ignition engine. *International Journal of Ambient Energy*, 32(3):161-166.

- Sakata Y**, Uddin MA, Muto A, Kanada Y, Koizumi K, Murata K.(1997) Catalytic degradation of polyethylene into fuel oil over mesoporous silica (KFS-16) catalyst. *Journal of Analytical and Applied Pyrolysis*, 43:15–25.
- Sakata Y**, Uddin MA, Muto A. (1999) Degradation of polyethylene and polypropylene into fuel oil by using solid acid and non-acid catalysts. *Journal of Analytical and Applied Pyrolysis*, 51:135–155.
- Sarikaya Y**, Onal M, Baran B, Alemdaroglu T. (2000) The effect of thermal treatment on some of the physicochemical properties of a bentonite. *Clays and Clay Minerals*, 48:557–562.
- Schirmer J**, Kim JS, Klemm E.(2001) Catalytic degradation of polyethylene using thermal gravimetric analysis and a cycled-spheres-reactor. *Journal of Analytical and Applied Pyrolysis*, 60:205–217.
- Seddegi ZS**, Budrthumal U, Arfaj AAA, Amer AMA, Barri SAI. (2002) Catalytic cracking of polyethylene over all-silica MCM-41 molecular sieve. *Applied Catalysis A: General*, 225:167–176.
- Seeger M**, Cantow HJ. (1975) Thermische spaltungsmechanismen in homo-und copolymeren aus α -olefinen. *Makromolekulare Chemie-Macromolecular Chemistry and Physics*, 176:1411-1425.
- Seeger M**, Gritter RJ. (1977) Thermal decomposition and volatilization of poly (α -olefines). *Journal of Polymer Science*, 15:1393-1402.
- Seo YH**, Lee KH, Shin DH. (2003) Investigation of catalytic degradation of high-density polyethylene by hydrocarbon group type analysis. *Journal of Analytical and Applied Pyrolysis*, 70:383-398.
- Serrano DP**, Aguado J, Escola JM. (2000) Catalytic conversion of polystyrene over HMMCM 41, HZSM-5 and amorphous $\text{SiO}_2\text{-Al}_2\text{O}_3$: comparison with thermal cracking. *Applied Catalysis B-Environmental*, 25:181–189.
- Sharratt PN**, Lin YH, Garforth AA, Dwyer J. (1997) Investigation of the catalytic pyrolysis of high-density polyethylene over a HZSM-5 catalyst in a laboratory fluidized-bed reactor. *Industrial & Engineering Chemistry Research*, 36:5118–5124.

- Siddiqui MKH.** (1968) Bleaching Earths, 1st ed., Pergamon Press, London.
- Sinfronio FSM,** Santos JCO, Pereira LG, Souza AG, Conceicao MM, Fernandes VJJ. (2005) Kinetic of thermal degradation of low-density and high-density polyethylene by non-isothermal thermogravimetry. *Journal of Thermal Analysis and Calorimetry*, 79:393-399.
- Singh B,** Sharma N. (2008) Mechanistic implications of plastic degradation. *Polymer Degradation and Stability*, 93:561-584.
- Soloiu A,** Yoshinobu Y, Masakatsu H, Kazuie N, Yasuhito M, Yasufumi A. (2000) The investigation of a new diesel produced from waste plastics ISME.
- Solomon PR,** Serio MA, Carangelo RM, Markham JR. (1986) Very rapid coal pyrolysis. *Fuel*, 65:182–194.
- Srasra E,** Ayedi MT. (2000) Textural properties of acid activated glauconite. *Applied Clay Science*, 17:71–84.
- Stefanis AD,** Perez G, Lilla E, Ursini O, Tomlinson AAG. (2001) Conversion of resins and asphaltene in porous catalysts. *Journal of Analytical and Applied Pyrolysis*, 57:37–44.
- Suquet H.** (1989) Effects of dry grinding and leaching on the crystal structure of chrysotile. *Clays and Clay Minerals*, 37:439–445.
- Takuma K,** Uemichi Y, Ayame A. (2000) Product distribution from catalytic degradation of polyethylene over H-gallosilicate. *Applied Catalysis A: General*, 192:273–280.
- Thorills CL,** Hickey J, Stecker G. (1950) Chemistry of clay racking catalysts. *Journal of Industrial and Engineering Chemistry*, 42:866–871.
- Tuttle J,** Kuegelgen TV. (2004) Biodiesel handling and use guidelines, Third Edition in National Renewable Energy Laboratory.
<http://www.afdc.energy.gov/afdc/pdfs/fueltable.pdf>
- Uddin MA,** Koizumi K, Murata K, Sakata Y. (1997) Thermal and catalytic degradation of structurally different types of polyethylene into fuel oil. *Polymer Degradation and Stability*, 56:37–44.

- Ueno T**, Nakashima E, Takeda K. (2010) Quantitative analysis of random scission and chain-end scission in the thermal degradation of polyethylene. *Polymer Degradation and Stability*, 95:1862-1869.
- Ullmann F.** (2003a) ULLMANN's Encyclopedia of Industrial Chemistry, 6th edition. Germany: Wiley-VCH Verlag GmbH & Co, 27:607-615.
- Ullmann F.** (2003b) ULLMANN's Encyclopedia of Industrial Chemistry, 6th edition. Germany: Wiley-VCH Verlag GmbH & Co., 27:616-623
- Venuto PB**, Habib ET. (1979) Fluid catalytic cracking with zeolite catalysts, New York: Marcel Dekker Inc.
- Yang J**, Mirand R, Roy C. (2001) Using the DTG curve fitting method to determine the apparent kinetic parameters of thermal decomposition of polymers. *Polymer Degradation and Stability*, 73:455–461.
- Ying GP**, Enrique V, Luis P. (1996) Pyrolysis of blends of biomass with poor coals. *Fuel*, 75:412–418.
- Zhou L**, Wang Y, Huang Q. (2006) Thermogravimetric characteristics and kinetic of plastic and biomass blends co-pyrolysis. *Fuel Processing Technology*, 87(11):963-969.
- Zhou Z**, Zhang Y, Tierney JW, Wender I. (2003) Hybrid zirconia catalysts for conversion of Fischer-Tropsch waxy products to transportation fuels. *Fuel Processing Technology*, 83:67–80.
- Zhu L**, Cheung CS, Zhang WG, Huang Z. (2011) Combustion, performance and emission characteristics of a DI diesel engine fueled with ethanol-biodiesel blends. *Fuel*. 90:1743–1750.
- Walendziewski J**, Steininger M. (2001) Thermal and catalytic conversion of waste polyolefins. *Catalysis Today*, 65:323–330.
- Wallis MD**, Bhatia SK. (2007) Thermal degradation of high density polyethylene in a reactive extruder. *Polymer Degradation and Stability*, 92:1721-1729.
- Warren LM**, Burns R. (1988) Processors Make a Go of Mixed-Waste Recycling. *Plastics Technology*, 6:41-63.

Waste Care

<http://www.wastecare.com/>

What are plastics

<http://composite.about.com/od/Plastics/a/What-Are-Plastics.htm>

Westerhout RWJ, Waanders J, Kuipers JAM, Swaaij WPMV.(1997) Kinetics of the low-temperature pyrolysis of polyethylene, polypropylene and polystyrene modeling: Experimental determination and comparison with literature models and data. *Industrial & Engineering Chemistry Research* 36(6):1955–1964.

Wiley J. (1966) *Encyclopedia of Polymer Science and Technology*, New York.

Wu CH, Chang CY, Hor JL, Shih SM, Chen LW, Chang FW. (1993) On the thermal treatment of plastic mixtures of MSW: Pyrolysis kinetics. *Waste Management*, 13(3):221-235.

Wu Z, Li C. (2009) Kinetics and thermodynamics of carotene and chlorophyll adsorption onto acid-activated bentonite from Xinjiang in xylene solution. *Journal of Hazardous Materials*, 171:582–587.

LIST OF FIGURES

Figure No.	Caption	Page No.
Figure 2.1	Schematic of linear and branched arrangements	10
Figure 2.2	The different routes of chemical recycling	16
Figure 2.3	Most probable reactions involved in thermal degradation of polymers	45
Figure 3.1	Virgin HDPE, Used mobil oil containers, Small pieces of used mobil oil containers	58
Figure 3.2	DSC of waste HDPE	59
Figure 3.3	XRD of kaolin	60
Figure 3.4	XRD of silica-alumina	61
Figure 3.5	XRD of mordenite	61
Figure 3.6	Experimental set up	64
Figure 3.7	Stainless steel reactor	64
Figure 3.8	Schematic representation of pyrolysis set up	64
Figure 4.1	Schematic of linear and branched arrangements	67
Figure 4.2	TGA curve of virgin HDPE	69
Figure 4.3	DTG curve of virgin HDPE	70
Figure 4.4	Effect of temperature on reaction time and product distribution	73
Figure 4.5	FT-IR spectrometry of virgin HDPE pyrolytic oil	74
Figure 4.6	GC plot of oil obtained at 450 °C	75
Figure 5.1	TGA curve of waste HDPE	83
Figure 5.2	DTG curve of waste HDPE	84
Figure 5.3	Effect of temperature on the reaction time and product distribution	86
Figure 5.4	Effect of holding time on yield of oil	87
Figure 5.5	FTIR plot of oil obtained at 450 °C	88
Figure 5.6	GC/MS of oil obtained at 450 °C	89

Figure 5.7	Effect of kaolin catalyst to plastic ratio on oil yield and reaction time	93
Figure 5.8	Effect of mordenite catalyst to plastic ratio on oil yield and reaction time	95
Figure 5.9	Effect of silica-alumina catalyst to plastic ratio on oil yield and reaction time	96
Figure 5.10	Effect of different catalysts on liquid yield and reaction time	97
Figure 5.11	XRD analysis of acid and alkaline treated kaolin clay	102
Figure 5.12	FTIR of acid and alkaline treated kaolin clay	103
Figure 5.13a	TGA of acid and alkali treated kaolin clay	106
Figure 5.13b	DTA of acid and alkali treated kaolin clay	107
Figure 5.14	SEM images of acid and alkali treated kaolin clay	108
Figure 5.15	Acidity Plot of acid treated catalyst	111
Figure 5.16	Effect of catalysts on reaction time and yield of liquid fuel	115
Figure 5.17	FTIR spectra of waste HDPE pyrolysis oil using hydrochloric acid treated kaolin	116
Figure 5.18	FTIR spectra of acetic acid treated kaolin catalyzed pyrolysis oil	117
Figure 5.19	FTIR spectra of nitric acid treated kaolin catalyzed pyrolysis oil	118
Figure 5.20	FTIR spectra of phosphoric acid treated kaolin catalyzed pyrolysis oil	119
Figure 5.21	FTIR spectra of sodium hydroxide treated kaolin catalyzed pyrolysis oil	120
Figure 5.22	GC plot hydrochloric acid treated kaolin catalyzed pyrolysis oil	122
Figure 5.23	GC plot acetic acid treated kaolin catalyzed pyrolysis oil	123
Figure 5.24	GC plot nitric acid treated kaolin catalyzed pyrolysis oil	125
Figure 5.25	GC plot phosphoric acid treated kaolin catalyzed pyrolysis oil	126
Figure 5.26	GC plot sodium hydroxide acid treated kaolin catalyzed pyrolysis oil	128
Figure 6.1	Residual plots for adequacy of the proposed model	140

Figure 6.2a	Response surface plot showing the effect of acidity and reaction temperature on liquid yield	142
Figure 6.2b	Response surface plot showing the effect of catalyst ratio and reaction temperature on liquid yield	142
Figure 6.3a	Contour plot showing the effect of acidity and reaction temperature on liquid yield	143
Figure 6.3b	Contour plot showing the effect of catalyst ratio and reaction temperature on liquid yield	144
Figure 6.4	FT-IR spectrum of liquid fuel obtained at optimized condition by catalytic pyrolysis of waste HDPE	145
Figure 6.5	GC plot of liquid fuel obtained at optimized condition by catalytic pyrolysis of waste HDPE	146
Figure 7.1	Schematic representation of the CI engine	152
Figure 7.2	FT-IR spectrometry of oil sample obtained at 450 °C by catalytic pyrolysis of waste HDPE	156
Figure 7.3	GC plot of oil sample obtained at 450 °C by catalytic pyrolysis of waste HDPE	157
Figure 7.4	Variation of brake thermal efficiency with brake power	160
Figure 7.5	Variation of exhaust gas temperature with brake power	161
Figure 7.6	Variation of BSEC with brake power	162
Figure 7.7	Variation of mechanical efficiency with brake power	163
Figure 7.8	Variation of NO _x with brake power	164
Figure 7.9	Variation of unburned hydrocarbon with brake power	165
Figure 7.10	Variation of CO with brake power	166
Figure 7.11	Variation of CO ₂ with brake power	168
Figure 8.1	TGA plot of waste HDPE at different heating rates in N ₂ atmosphere	174
Figure 8.2	DTG plot of waste HDPE at different heating rates in N ₂ atmosphere	175
Figure 8.3	Kinetic study plot at different heating rates in N ₂ atmosphere	176

LIST OF TABLES

Table No.	Caption	Page No.
Table 2.1	Physical properties of HDPE	11
Table 2.2	Mechanical properties of HDPE	11
Table 2.3	Electrical properties of HDPE	11
Table 2.4	Thermal properties of HDPE	12
Table 2.5	Composition of gas products obtained from pyrolysis of polyethylene at 400 °C	24
Table 2.6	Yields of gas, liquid and residue obtained from thermal and catalytic degradation of waste HDPE at 430 °C	27
Table 2.7a	The distribution of gas, liquid and residue fractions from thermal and catalytic degradation of HDPE with various catalysts at 450 °C	30
Table 2.7b	PONA distribution in oil products from thermal and catalytic degradation of HDPE with various catalysts at 450 °C	31
Table 2.8	Energies of elementary steps in polymer degradation	48
Table 2.9	Summary of approaches for the determination of kinetic parameters	54
Table 2.10	The reaction rates and other reaction kinetic parameters of degradation of waste polyethylene	56
Table 3.1	Test protocols	65
Table 4.1	Proximate and ultimate analysis of virgin HDPE	69
Table 4.2	Distribution of different fractions at different temperatures in thermal pyrolysis of virgin HDPE	71
Table 4.3	GC-MS Analysis of Virgin HDPE pyrolytic oil	75
Table 4.4	Physical properties analysis of Virgin HDPE pyrolytic oil	76
Table 4.5	Fuel properties comparison of HDPE pyrolytic oil with commercial transportation fuels	78
Table 5.1	Proximate and ultimate analysis of waste HDPE	82

Table 5.2	Distribution of different fractions at different temperatures in the HDPE pyrolysis	84
Table 5.3	FTIR assignment of waste HDPE oil obtained at 450 °C	88
Table 5.4	GC-MS composition of oil obtained at 450 °C	89
Table 5.5	Physical properties of HDPE pyrolytic oil sample	91
Table 5.6	Distribution of different products with kaolin catalyst to plastic ratio at a temperature 450 °C	93
Table 5.7	Distribution of products with mordenite catalyst to feed ratio at a temperature 450 °C	94
Table 5.8	Distribution of products with silica-alumina catalyst to plastic ratio at a temperature 450 °C	96
Table 5.9	XRF analysis of acid and alkaline treated kaolin clay	100
Table 5.10	Important IR bands of acid and alkaline treated kaolin clay	104
Table 5.11	BET surface area and pore volume of acid and alkaline treated kaolin clay	108
Table 5.12	Acidity Values	111
Table 5.13	Results of the waste HDPE pyrolysis (Temperature=450 °C, Catalyst: Feed=1:4) using different types of catalysts of optimum concentration (3M concentration)	114
Table 5.14	FTIR assignments of hydrochloric acid treated kaolin catalyzed pyrolysis oil	117
Table 5.15	FTIR assignments of acetic acid treated kaolin catalyzed pyrolysis oil	118
Table 5.16	FTIR assignments of nitric acid treated kaolin catalyzed pyrolysis oil	119
Table 5.17	FTIR assignments of phosphoric acid treated kaolin catalyzed pyrolysis oil	120
Table 5.18	FTIR assignments of sodium hydroxide treated kaolin catalyzed pyrolysis oil	121

Table 5.19	GC-MS analysis of waste HDPE pyrolytic oil using hydrochloric acid treated kaolin	122
Table 5.20	GC-MS analysis of waste HDPE pyrolytic oil using acetic acid treated kaolin	124
Table 5.21	GC-MS analysis of waste HDPE pyrolytic oil using nitric acid treated kaolin	125
Table 5.22	GC-MS analysis of waste HDPE pyrolytic oil using phosphoric acid treated kaolin	127
Table 5.23	GC-MS analysis of waste HDPE pyrolytic oil using sodium hydroxide treated kaolin	128
Table 5.24	Physical properties of liquid fuel obtained by catalytic pyrolysis of waste HDPE using nitric acid (3M concentration) treated kaolin clay	129
Table 5.25	Fuel properties comparison of waste HDPE oil obtained by catalytic pyrolysis with commercial transportation fuels	130
Table 6.1	Range of independent variables and the experimental domain	135
Table 6.2	The CCD matrix of experimental and yield response	135
Table 6.3	Ultimate or elemental analysis of waste HDPE	137
Table 6.4	XRF analysis and acidity of parent and acid treated kaolin clay	137
Table 6.5	ANOVA for liquid fuel yield model	139
Table 6.6	GC-MS analysis of liquid fuel obtained at optimized condition by catalytic pyrolysis of waste HDPE	146
Table 6.7	Physical properties of liquid fuel obtained by catalytic pyrolysis of waste HDPE at optimized condition	147
Table 6.8	Fuel properties comparison of waste HDPE catalytic pyrolytic oil with commercial transportation fuels	148
Table 7.1	Engine specification	153
Table 7.2	Ultimate or elemental analysis of waste HDPE	153
Table 7.3	XRF analysis and acidity of parent and acid treated kaolin clay	155

Table 7.4	GC-MS analysis of oil sample obtained at 450 °C by catalytic pyrolysis of waste HDPE	157
Table 7.5	Physical properties of oil sample obtained by catalytic pyrolysis of waste HDPE at 450 °C	159
Table 8.1	Ultimate or elemental analysis of waste HDPE	173
Table 8.2	Activation energy and pre-exponential factor determined by integral method for waste HDPE pyrolysis	176

LIST OF PUBLICATIONS

Patent

1). R. K. Singh, **Sachin Kumar**, 'Catalytic Conversion of Waste High Density Polyethylene to liquid fuel' applied for Indian patent, Application No.- 8/KOL/2013 publication date 08/03/2013 Journal No.- 10/2013.

Journals (PhD Work)

1). **Sachin Kumar**, Achyut K. Panda, R. K. Singh, A review on tertiary recycling of high density polyethylene to fuel, **Resources, Conservation & Recycling** 55 (2011) 893-910.

2). **Sachin Kumar**, R. K. Singh, 'Recovery of hydrocarbon liquids from waste high density poly ethylene by thermal pyrolysis' **Brazilian Journal of Chemical Engineering** 28 (04) (2011) 659 - 667.

3). **Sachin Kumar**, Achyut K. Panda, R. K. Singh, 'Preparation and characterization of acid and alkali treated kaolin clay' **Bulletin of Chemical Reaction Engineering & Catalysis** 8 (1) (2013) 61-69.

4). **Sachin Kumar**, R. Prakash, S. Murugan, R. K. Singh, 'Performance and emission analysis of blends of waste plastic oil obtained by catalytic pyrolysis of waste HDPE with diesel in a CI engine' **Energy Conversion and Management** 74 (2013) 323-331.

5). **Sachin Kumar**, R. K. Singh, 'Thermolysis of high-density polyethylene to petroleum products' **Journal of Petroleum Engineering** Volume 2013 (2013) Article ID 987568, 7 pages.

6). **Sachin Kumar, R. K. Singh**, 'Pyrolysis kinetics of waste high-density polyethylene using thermogravimetric analysis' **International Journal of ChemTech Research** 6 (1) (2014) 131-137.

7). **Sachin Kumar, R. K. Singh**, 'Optimization of process parameters by response surface methodology (RSM) for catalytic pyrolysis of waste high-density polyethylene to liquid fuel' **Journal of Environmental Chemical Engineering** 2 (1) (2014) 115-122.

Other Related Publications

- 8). **Sachin Kumar**, Ankit Agrawalla, R. K. Singh, 'Thermogravimetric analysis of groundnut cake' **International Journal of Chemical Engineering and Applications** 02 (04) (2011) 268-271.
- 9). Ankit Agrawalla, **Sachin Kumar**, R. K. Singh, 'Pyrolysis of groundnut de-oiled cake and characterization of the liquid product' **Bioresource Technology** 102 (2011) 10711–10716.
- 10). Saswat Rath, **Sachin Kumar**, R. K. Singh, 'Performance & emission analysis of blends of karanja methyl ester with diesel in a compression ignition engine' **International Journal of Ambient Energy** 32 (03) (2011), 161–166.
- 11). Niraj K. Nayan, **Sachin Kumar**, R. K. Singh, 'Characterization of the liquid product obtained by thermal pyrolysis of karanja seed' **Bioresource Technology** 124 (2012) 186-189.
- 12). Niraj K. Nayan, **Sachin Kumar**, R. K. Singh, 'Production of the liquid fuel by thermal pyrolysis of neem seed' **Fuel** 103 (2013) 437-443.
- 13). Bijayani Biswal, **Sachin Kumar**, R. K. Singh, 'Production of hydrocarbon liquid by thermal pyrolysis of paper cup waste' **Journal of Waste Management** Volume 2013 (2013) Article ID 731858, 7 pages.
- 14). R. K. Singh, Bijayani Biswal, **Sachin Kumar**, 'Determination of activation energy from pyrolysis of paper cup waste using thermogravimetric analysis' **Research Journal of Recent Sciences** Vol. 2 (ISC-2012) (2013) 177-182.
- 15). Rahul Sinha, **Sachin Kumar**, R. K. Singh, 'Determination of activation energy of linseed pyrolysis using thermogravimetry' **International Journal of Ambient Energy** 34 (4) (2013) 195-199.
- 16). Rahul Sinha, **Sachin Kumar**, R. K. Singh, 'Production of bio-fuel and bio-char by thermal pyrolysis of linseed seed' **Biomass Conversion and Biorefinery** 3 (4) 2013, 327-335.

17). V. K. Singh, A. B. Soni, **Sachin Kumar**, R. K. Singh, ‘Pyrolysis of sal seed to liquid product’ **Bioresource Technology** 151 (2014) 432-435.

18). **Sachin Kumar**, Niraj K. Nayan, R. K. Singh, ‘Kinetics of pyrolysis and combustion characteristics of non-edible oilseeds (karanja and neem seed) using thermogravimetric analysis’ accepted in **Energy Sources, Part A: Recovery, Utilization and Environmental Effects** (DOI:10.1080/15567036.2012.748106).

Conferences

1). Achyut K. Panda, **Sachin Kumar**, R. K. Singh, “Thermolytic conversion of waste plastics to fuels and chemicals”, National conference on Smart materials and 25th annual seminar of Orissa Chemical Society, from 25-26 Dec. 2010, organized by Apex Institute of Technology and Management Bhubaneswar.

2). **Sachin Kumar**, R. K. Singh, “Thermolytic conversion of waste HDPE into fuels and chemicals”, International Conference on Recent Advances in Chemical Engineering and Technology (RACET 2011) held from 10-12 March 2011 at Cochin India.

3). R. K. Singh, Bijayani Biswal, **Sachin Kumar**, ‘Determination of activation energy from pyrolysis of paper cup waste using thermogravimetric analysis’ 2nd International Science Congress (ISC-2012) held from 8th to 9th December 2012 at Bon Maharaj Engineering College, Raman Reti, Vrindavan (Mathura), UP, India.

4). **Sachin Kumar**, R. K. Singh, “Non-isothermal kinetic study of waste high-density polyethylene pyrolysis using thermogravimetric analysis”, 2nd International Science Congress (ISC-2012) held from 8th to 9th December 2012 at Bon Maharaj Engineering College, Raman Reti, Vrindavan (Mathura), UP, India.

BIOGRAPHY

Sachin Kumar was born at Pilibhit (Uttar Pradesh), India on 10th November. He completed his schooling from D. G. Inter College, Pilibhit. He obtained his B. Tech. degree in Chemical Engineering from M. J. P. Rohilkhand University, Bareilly with 62% marks. He obtained his M. Tech. degree in Fuel Engineering from Indian School of Mines, Dhanbad with 74% marks. He has been awarded MHRD Fellowship for pursuing master degree in engineering after qualifying GATE exam. He has been also awarded MHRD Fellowship for pursuing doctorate degree in engineering. His research interests focus on liquid fuels from Biomass and Waste Plastics. He has published research papers in the peer-reviewed international scientific journals based on liquid fuels from Biomass and Waste Plastics. He has also got 'Best Paper Award' in an International Conference organised by Indian Institute of Chemical Engineers, Kochi Chapter.